Regulation of Central Carbon Metabolism in *Enterococcus faecalis*

By Erica C. Keffeler

B.Sc., Missouri Western State University, 2016

Submitted to the graduate degree program in Molecular Biosciences and the Graduate Faculty of the University of Kansas in partial fulfillment of the requirements for the degree of Doctor of Philosophy.

_____

Chair: Dr. Lynn Hancock

_____

Dr. P. Scott Hefty

_____

Dr. Susan Egan

_____

Dr. David Davido

_____

Dr. Mark Farrell

Date Defended: 10 September 2021

The dissertation committee for Erica C. Keffeler certifies that this is the approved version of the following dissertation:

Regulation of Central Carbon Metabolism in *Enterococcus faecalis*

Chair Person: Dr. Lynn Hancock

Date Approved: 10 September 2021

Abstract

Enterococcus faecalis has emerged as a multidrug-resistant (MDR) nosocomial pathogen that causes life-threatening healthcare-associated infections at various host anatomic sites. Enterococcal colonization of these biological niches is, in part, dependent on its adaptive response to host conditions. Some important strategies to adapt to varying host environments include biofilm formation, immune evasion, and the utilization of secondary nutrients in the absence of preferred carbon sources, which are often host limited. The regulation of these factors is governed by environmental or metabolic cues that influence alterations of a bacterium's transcriptome, often orchestrated by alternative sigma factors or other transcriptional regulators. Investigating the role of various transcriptional regulators and identifying the genes and cellular processes that these factors regulate may lead to new treatments against multidrug resistant enterococcal infections.

In this study, we show that the alternative sigma factor 54 (σ^{54}; RpoN) and its cognate enhancer binding protein MptR are essential for mannose utilization and principally responsible for glucose uptake by directly regulating the expression of the Mpt phosphotransferase system in *Enterococcus faecalis*. We performed a microarray transcriptional analysis of the parental strain V583 and an isogenic *rpoN* mutant grown in a chemically defined medium supplemented with glucose as the sole carbon source to gain further insight into how the disruption of RpoN-mediated glucose utilization influences global transcriptional changes. Transcripts of approximately 340 genes were differentially affected in the *rpoN* mutant. Predicted functions of these differentially affected genes were primarily related to nutrient acquisition. Predicted catabolite responsive element (*cre*) sites were identified in 42.74% of the differentially upregulated genes in the *rpoN* mutant, consistent with loss of repression by the transcriptional regulator Carbon Catabolite Protein A (CcpA).

Three gene clusters (*ef0114, ef0362-61,* and *ef2863*) that encode the respective enterococcal endoglycosyl hydrolases were highly upregulated in the *rpoN* mutant with identified putative *cre* sites within their promoter regions. These glycosyl hydrolases possess putative signal peptide sequences and signal peptide cleavage sites, suggesting that these glycosidases are secreted into the surrounding environment and may contribute to the survival of this bacterium in nutrient limited environments. We confirmed that CcpA negatively regulates the expression of *ef0114, ef0362-61,* and *ef2863* in a CCR-dependent manner. Further characterization of the enzymatic function of EF0362-61, EF0114, and EF2863 revealed that they target the β1,4-linked N-acetylglucosamine glycosidic bond present in chitinous substrates, complex-type glycoproteins, and high-mannose type glycoproteins, respectively. The amino sugar, N-acetylglucosamine (GlcNAc) is among the most abundant natural sugars and provides bacteria with a source of carbon and nitrogen when metabolized. Here, we propose a model of the metabolic pathway by which *E. faecalis* utilizes poly-β-1,4-linked N-acetylglucosamine (i.e. chitinous substrates) as a valuable carbon and nitrogen source.

Acknowledgements

I would like to express my sincere gratitude to my research adviser, Dr. Lynn Hancock for providing me the opportunity to conduct research and providing valuable guidance throughout this research. His scientific vision, integrity, and motivation have immensely shaped me into the scientist and person I am today. It has been a great privilege and honor to work alongside him and study under his guidance. I am extremely grateful for his mentorship and support during my graduate studies. I would also like to thank my committee members, Dr. Scott Hefty, Dr. Susan Egan, Dr. David Davido, Dr. Mark Farrell, and the late Dr. Steven Benedict for their insightful suggestions and advice throughout all of the stages of completing my dissertation. A special thank you to Dr. Mark Farrell for providing various experimental materials and the many insightful discussions related to my project.

I am also sincerely thankful for the numerous of friends I have made throughout the years for their stimulating scientific conversations, friendship, and being by my side during the happy and hard moments graduate school has to offer.

I would like to express my deepest gratitude to my parents, Dale Keffeler and Carol Keffeler for their love, unconditional support, and sacrifices for educating me and preparing me for my future. I am thankful for my brother, Jake Keffeler for teaching me the importance of friendly competition and always providing a source of humor. Last but not least, I would like to thank my fiancé, David Lassley for the unwavering love and support he has provided me during my pursuit of this Ph.D. degree. I deeply appreciate his belief in me and for always motivating me to be the best version of myself.

Table of Contents

Chapter 1: Introduction 1
Enterococcus faecalis 2
Gene regulation in *Enterococcus faecalis* 3
Sigma factors in *Enterococcus faecalis* 6
Alternative sigma factor-54 9
The role of σ^{54} in other bacteria 12
The role of σ^{54} in Enterococcus faecalis 12
Central carbon metabolism in *Enterococcus faecalis* 15
Catabolite control protein A (CcpA) 21
Glycosyl hydrolases 22
Glycosyl hydrolase family 18 (GH18) 23
Glycosyl hydrolase family 18 chitinases 24
Glycosyl hydrolase family 18 ENGases 25
Glycosyl hydrolase family 20 (GH20) 27
Scope of dissertation 27
References 30
Author Contributions 39

Chapter 2: Influence of the alternative sigma factor RpoN on global gene expression and carbon catabolism in *Enterococcus faecalis* V583 40
Abstract 41
Importance 42
Introduction 43
Materials and Methods 46
Bacterial strains and growth conditions: 46
Construction of in-frame markerless deletion: 46
Construction of in-frame markerless complement: 47
Growth assessment in nutrient limiting conditions: 47
Microarray analysis: 48
In silico analysis of identified proteins: 49
Quantitative real time (q-RT) PCR: 49
Biofilm formation assessment using a drip-flow biofilm reactor (DFBR): 50
Animal models: 50
Experimental endocarditis and determination of bacterial burden: 51
Murine model for catheter associated urinary tract infection (CAUTI): 51
Bioinformatics and statistical analysis: 52
Results 53
RpoN and MptR regulate glucose uptake and are essential for mannose utilization 53
Transcriptional Analysis of *E. faecalis* V583Δ*rpoN* 58
Catabolite repression elements (*cre*) in differentially expressed genes in V583Δ*rpoN* 60
Identification of cell-envelope associated or secreted gene products among the differentially expressed genes in the *rpoN* mutant that contain *cre* sites 61
Quantitative real time PCR of differentially expressed genes in the *rpoN* mutant that are CcpA-dependent and -independent 64

The EF2223-21 ABC transporter contributes to glucose importation 68
Role of RpoN and CcpA in enterococcal biofilm formation 70
Role of RpoN and CcpA in enterococcal virulence 74
Discussion 76
Supplemental Figures 86
Supplemental Tables 89
References 107

Chapter 3: Activity of CcpA-regulated GH18 family glycosyl hydrolases that contribute to nutrient acquisition and fitness in *Enterococcus faecalis* 111
Abstract 112
Importance 113
Introduction 114
Materials and Methods 117
Bacterial strains and growth conditions: 117
Construction of in-frame markerless deletion strains: 117
Construction of in-frame markerless complement strains: 118
Construction of the CcpA Phase-Lock mutant strain: 118
5' rapid amplification of cDNA ends (RACE) analysis: 120
Quantitative reverse transcriptase (q-RT) PCR: 120
Cloning, expression, and purification of EndoE (EF0114) and EfEndo18A (EF2863): 121
RNase B assays: 122
Growth assessment in nutrient-limiting conditions supplemented with RNase B or IgG: . 123
IgG lectin blot analysis: 123
Biofilm assays on polystyrene microtiter plates: 123
High-mannose IgG Fc (HM-Fc) assays: 124
Animal models: 125
Murine model for catheter associated urinary tract infection (CAUTI) 125
Bioinformatics and statistical analyses 125
Results 126
Genetic organization and transcriptional start site of *ef0114, ef0362-61,* and *ef2863* in *E. faecalis* V583 126
CcpA negatively regulates *ef0114, ef0362-61,* and *ef2863* expression 128
CcpA phase-lock mutant (PLM) represses the expression of *ef0114, ef0362-61,* and *ef2863* irrespective of glucose concentrations 129
Culture supernatant from the *ccpA* mutant results in the removal of glycans from RNase B, a model high-mannose type glycoprotein 131
Culture supernatant from the constitutively active CcpA PLM variant attenuates glycosidase activity towards RNase B 132
The deletion of *ef2863* results in a loss of glycosidase activity towards the high-mannose type glycoprotein, RNase B 133
The ability to utilize the glycans from high-mannose type glycoproteins as a carbon source is dependent on the activity of EfEndo18A and the Mpt PTS complex 134
Dose-dependent analysis of EfEndo18A and EndoE hydrolase activity against the high-mannose type glycoprotein, RNase B 136
Analysis of EndoE and EfEndo18A hydrolase activity on the complex glycoprotein, IgG 138
EndoE does not contribute to the dispersal of bacterial biofilms 141

Analysis of glycosidase activity against a synthetic high-mannose IgG Fc glycoform (HM-Fc) 142
Glycosyl hydrolase activity contributes to enterococcal virulence 145
Discussion 146
Supplemental Figures 152
Supplemental Tables 153
References 158

Chapter 4: Metabolism of poly-β1,4-N-acetylglucosamine substrates and importation of N-acetylglucosamine and glucosamine by *Enterococcus faecalis* 163
Abstract 164
Importance 165
Introduction 166
Materials and Methods 168
Bacterial strains and growth conditions: 168
Construction of in-frame markerless deletion strains: 168
Construction of in-frame markerless complement strains: 169
Growth assessment in nutrient limiting conditions: 170
Expression and purification of EF0114 variants 170
Chitinolytic assays: 171
Statistical analyses 171
Results 172
The deletion of the enterococcal chitinase and chitin-binding protein, *ef0362-61,* impacts growth on a poly-β1,4-N-acetylglucosamine substrate 172
EF0114 is responsible for degrading β1,4-$GlcNAc_2$ into GlcNAc prior to importation into the bacterial cell 173
The GH20 domain of EF0114 is responsible for degrading β1,4-$GlcNAc_2$ into GlcNAc monomers 176
Importation of GlcNAc is mediated through the Mpt PTS complex and EF1516 177
The Mpt PTS system is the primary glucosamine (GlcN) transporter in *E. faecalis* 179
Growth on N-acetylglucosamine is dependent on EF1317, an N-acetylglucosamine-6-phosphate deacetylase (NagA) homolog 180
Growth on glucosamine is dependent on the activity of EF0466, a glucosamine-6-phosphate deaminase (NagB) homolog 182
Discussion 184
References 191

Chapter 5: Concluding Remarks and Future Directions 195
References 219

Chapter 1: Introduction

Enterococcus faecalis

Enterococcus faecalis is a Gram-positive cocci, low G-C rich (i.e. 37% of GC in the chromosome) commensal that inhabits mammalian gastrointestinal (GI) tracts and oral cavities. This bacterium was first discovered in 1899 by Thiercelin (1, 2) as an intestinal commensal. MacCallum and Hastings (3) in the same year isolated *Enterococcus faecalis* from a lethal case of endocarditis, highlighting the opportunistic nature of the organism. Based on morphological features, enterococci were originally classified as members of the streptococcal genus, and were classified by Lancefield (4) as members of the Group D streptococci. With the advent of DNA hybridization studies, they were reclassified as a unique genus (5). Based on phylogenetic similarity, enterococci are formally classified under the phylum of Firmicutes, class: Bacilli, order: Lactobacillales, family: Enterococcaceae, genus: *Enterococcus*. As members of the mammalian gut consortium, enterococci help in the digestion of certain foods and, therefore, has been amended for use as a probiotic (6-8). In addition to inhabiting mammalian hosts, members of the *Enterococcus* genus can also be isolated from the GI tracts of insects (9-11), traditional fermented foods and dairy products (12, 13), and can be found in various environments including soil (14) and water (15, 16). Additional beneficial effects of *E. faecalis* as a commensal include, modulating the host immune responses, promoting the function of the epithelial barrier, and preventing the colonization and invasion of intestinal pathogens (17, 18). Specifically, native commensal strains of *E. faecalis* produce a bacteriocin capable of killing pathogenic *E. faecalis* V583 (19), therefore competing for the biological niche and preventing colonization of multi-drug resistant hospital-adapted pathogenic isolates, typified by *E. faecalis* V583.

Apart from their beneficial role, enterococci have emerged as a hospital-adapted, opportunistic pathogen that now rank second on the list of causative agents of disease in healthcare settings in

the United States (20-24). This nosocomial pathogen causes a variety of infections, including endocarditis, bacteremia associated with central-line catheters, surgical site infections, and catheter associated urinary tract infections (CAUTI) (20, 23, 24). How enterococci have emerged as prominent nosocomial pathogens is in part due to their ability to adapt and survive in a variety of host environments, the ability to form biofilms on biotic and abiotic surfaces, as well as their intrinsic and acquired antibiotic resistance (21, 25, 26). The extensive use of antibiotics to treat enterococcal infections and horizontal gene transfer have heavily contributed to this bacterium's emergence as a multidrug resistant (MDR) pathogen (27-29), thus strengthening the need for finding alternative therapies to combat such infections. Although strains of *Enterococcus faecium* are associated with higher mortality rates than *E. faecalis* due to its more frequent resistance to ampicillin and vancomycin, antibiotic-resistant CAUTI and hospital-associated infections caused by *Enterococcus faecalis* are seen at higher rates than *E. faecium* (24, 27). In addition, 94% of all enterococcal infective endocarditis is caused by *E. faecalis*, which is dependent on its ability to adhere to collagen (30).

Gene regulation in *Enterococcus faecalis*

Enterococci are capable of surviving in a variety of habitats, ranging from the gastrointestinal tract of mammals to the environment (i.e. soil, water, food supplies) (31). Colonizing these diverse niches requires enterococci to be resilient against drastic changes within their environments, including temperature, pH, salinity, and nutrient availability (31). The ability of enterococci to rapidly adapt to varying environmental conditions is largely achieved by the regulation of gene expression. In bacteria, gene regulation can occur on multiple levels. The most common type of regulation occurs at the transcriptional level (32), where transcriptional regulators bind to the promoter region of their effector genes and either positively or negatively affect their transcription,

which subsequently alters the amount of specific mRNA produced. There are at least 15 different families of transcriptional regulators (33).

The regulation of gene expression at the transcriptional level can also occur via regulation machinery referred to as two-component systems (TCS). A typical two-component system consists of a membrane-bound histidine sensor kinase, responsible for sensing extracellular signals, and a cognate response regulator which functions as a transcription factor (34, 35). Upon sensing a specific environmental stimuli, the histidine kinase will phosphorylate the response regulator, which alters its ability to bind to the target DNA, thus affecting gene expression (34, 35). Although the outcome of two-component system gene regulation is modulating gene expression at the transcriptional level, the phosphorylation of the sensor kinase and response regulator is an example of posttranslational regulation. Currently in the *E. faecalis* V583 genome, there are 17 annotated two-component systems that sense a variety of stimuli, including quorum signals, antimicrobials, and nutrients (36, 37). The best characterized two-component systems of *E. faecalis* are the vancomycin-resistant VanRS TCS system and the quorum-sensing related Fsr TCS system (38, 39). The *fsr* system activates the expression of two extracellular proteases, gelatinase (GelE) and serine protease (SprE). These two proteases have been linked to enterococcal virulence by contributing to bacterial migration and invasion, as well as biofilm formation (36, 37, 40).

Besides the types of bacterial transcriptional regulation, the modulation of gene expression can also occur post-transcriptionally. Mechanisms of post-transcriptional regulation include mRNA processing, regulation via riboswitches, or by small regulatory RNA (sRNA). The 18 gene operon involved in ethanolamine utilization is one of the best-studied examples of post-transcriptional regulation in *E. faecalis* (41). Although such post-transcriptional regulation exists in *E. faecalis*, transcriptional gene regulation will be a major component of this dissertation.

In the *E. faecalis* V583 genome, there are 145 genes that encode putative transcriptional regulators belonging to various protein families, including but not limited to, GntR, LacI/GalR, and the various families of sigma factors (36, 42). In bacteria, the GntR family of transcriptional regulators is one of the most widespread family of transcription factors that regulate the transcription of effector genes via allosteric binding to metabolites (43, 44). This family was named after the gluconate operon repressor in *Bacillus subtilis* (45), but GntR transcriptional regulators have been found to modulate the expression of a variety of other cellular processes, including motility, metabolism, and virulence (44). Members of this family possess two domains, a highly conserved N-terminal DNA-binding domain and a C-terminal effector binding/oligomerization domain (43, 44). The DNA-binding domain has a helix-turn-helix (HTH) motif for binding to the A/T rich palindromic sequences of DNA in the promoter region(s) of effector genes (43). The C-terminal effector binding/oligomerization domain is the signal sensing module responsible for binding the particular metabolites/ligands (43, 44). The C-terminal domain possesses low homogeneity among the family members, therefore the GntR family is further subdivided into seven major subfamilies (FadR, HutC, MocR, YtrA, AraR, DevA, and PlmA) based on effector binding domain similarities (43). Currently, there are 14 annotated GntR regulators in the *E. faecalis* V583 genome. Among these GntR regulators in *E. faecalis*, only one has been characterized, thus far. In *E. faecalis*, the GntR transcriptional regulator CitO (EF3328) positively regulates the expression of the citrate metabolism operons (46).

An additional family of bacterial global regulators is the LacI/GalR family of transcription factors, a family of more than 1000 members divided into approximately 33 subfamilies (47). The founder of this family is the lactose repressor protein (LacI), however LacI/GalR family members regulate the transcription of a wide variety of cellular processes. This family possesses a small N-terminal

HTH DNA-binding domain and a large C-terminal effector binding domain (48). Additionally, majority of the LacI/GalR members are transcriptional repressors (47). There are two members of the LacI/GalR family that are referred to as "master" regulators, the catabolite repressor/activator (Cra) protein and the carbon catabolite repressor protein A (CcpA), that regulate a variety of central carbon metabolic pathways, as well as genes involved in bacterial virulence (47).

Sigma factors in *Enterococcus faecalis*

The central component in transcriptional regulation in bacteria is the multi-subunit RNA polymerase. The core enzyme of the RNA polymerase consists of five subunits: two identical α subunits, two large β subunits (β and β'), and the ω subunit (32, 49). All of the core RNA polymerase subunits are essential for transcription to occur with the exception of the ω subunit, which aids in the assembly of the RNA polymerase (50). The core enzyme is responsible for all bacterial transcription, but perplexingly not directly involved in the initiation of transcription (50, 51). For the RNA polymerase to begin transcription at a given promoter, it must interact with the sixth RNA polymerase subunit, the sigma factor (σ), to form the holoenzyme (52). The sigma factor is required only for transcription initiation and will be released from the core enzyme once the RNA polymerase leaves the promoter (32, 51). Bacterial sigma factors have three main functions: (i) to ensure the recognition of specific promoter sequences, (ii) to position the RNA polymerase holoenzyme at a given promoter, and (iii) to facilitate the unwinding of the DNA near the transcriptional start site (32, 52, 53). Sigma-70 (σ^{70}) is the housekeeping sigma factor in bacteria and initiates the expression of "housekeeping" genes during the exponential growth phase, that are required for basic survival (54), by directing the RNA polymerase to the -10 and -35 promoter elements in DNA (33). However, bacteria typically encode multiple sigma factors, most of which are non-essential for cell viability under optimum growth conditions and are referred to

as alternative sigma factors. The function of alternative sigma factors generally entails the recognition of a distinct subset of promoters that become activated in response to a specific environmental stimuli, such as various stress conditions, lack of nutrients, or entrance into stationary growth phase (32, 53). The number of alternative sigma factors present in a bacteria can vary. For example, the Gram-positive pathogen, *Streptococcus pyogenes* possesses two alternative sigma factors, but the soil bacterium, *Streptomyces coelicolor* encodes more than 60 alternative sigma factors (55). In the *E. faecalis* V583 genome, there are eight functionally annotated alternative sigma factors, which are summarized in table 1 of this chapter. Included in table 1 is the enterococcal housekeeping sigma factor (σ^{70}) encoded by *ef1522*.

Bacterial sigma factors are classified into two families based on structural similarities and function. These distinct families are designated as σ^{70} and σ^{54} (55, 56). Sigma factors belonging to the σ^{54} family are structurally similar to the 54kDa sigma factor produced by *Escherichia coli* that is required for metabolizing nitrogen (55). On the other hand, the family of σ^{70} sigma factors are all structurally similar to the 70kDa housekeeping sigma factor. Of the eight alternative sigma factors encoded in *E. faecalis* V583, only one belongs to the sigma^{54} family, while the other seven belong to the sigma^{70} family (Table 1).

Table 1: Sigma factors annotated in *E. faecalis* V583

Gene locus	Name	Anti-Sigma Factor	Size (aa)	σ Domain Regions	Sigma Factor Group	Cellular Processes	Reference
EF0049	SigH		188	R2.1-2.4, R3.0-3.2, R4.1-4.2	Sigma^{70}-family Group III	Heat shock response$^{\#}$	(57)
EF0482*			133	R2.1-2.4, R4.1-4.2	Sigma^{70}-family Group IV	ECF$^{\#}$ Virulence$^{\#}$	
EF0782	RpoN		443		Sigma^{54}	Carbon PTS systems	(58-60) Chapter 3
EF1522	RpoD		368	R1.1-1.2, R2.1-2.4, R3.0-3.2, R4.1-4.2	Sigma^{70}-family Group 1	Housekeeping	

EF1850			133	R2.1-2.4, R4.1-4.2	Sigma^{70}-family Group IV	ECF# Virulence#	
EF2244			152	R2.1-2.4, R4.1-4.2	Sigma^{70}-family Group IV	ECF# Virulence#	
EF2290			126	R2.1-2.4, R4.1-4.2	Sigma^{70}-family Group IV	ECF# Virulence#	
EF3020		EF3019	154	R2.1-2.4, R4.1-4.2	Sigma^{70}- family Group IV	ECF# Virulence#	
EF3180	SigV	RsiV	165	R2.1-2.4, R4.1-4.2	Sigma^{70}- family Group IV	Heat shock response Ethanol tolerance Acid stress response Lysozyme tolerance	(61-64)

Group characterization were determined using InterPro
Group 1: R1.1-1.2, R2.1-2.4, R3.0-3.2, R4.1-4.2
Group 2: R1.2, R2.1-2.4, R3.0-3.2, R4.1-4.2
Group 3: R2.1-2.4, R3.0-3.2, R4.1-4.2
Group 4: R2.1-2.4, R4.1-4.2

Extracytoplasmic functions (ECFs) include modulating the expression of genes whose products carry various functions in the bacterial response to specific environmental stimuli, including presence of denatured proteins or toxic molecules, osmolarity, nutrient limitation, and oxidative stresses (55). Members of this group also regulate the expression of bacterial virulence genes (55).

*EF0482 is absent in commonly used laboratory lab strain *E. faecalis* OG1RF because it is present in the V583 PAI.
Indication that the cellular process listed is a putative cellular function based on experimentally determined functions of members belonging to that particular group.

The sigma^{70} family of sigma factors are further classified into four major classifications based on the presence or absence of four structural conserved domains (i.e. σ region domains) (56). These conserved domains are further divided into subregions (σ R1.1-1.2, σ 2.1–2.4, σ R3.0–3.2, σ R4.1–4.2) (54, 65). The σ region 1 is located at the N-terminus of the protein and comprises of subregions 1.1 and 1.2 (55). Subregion 1.1 is only present among the bacterial σ^{70} housekeeping sigma factors. Region 2 is comprised on four subregions, with subregion 2.3 being responsible for forming the transcription bubble, while 2.4 is required for -10 promoter element recognition (55). Region 3 consists of three subregions and, lastly, region 4 includes subregions 4.1 and 4.2. Subregion 4.2 interacts with transcriptional activator proteins and is also required for -35 promoter element recognition (55). The classifications of the four σ^{70} family groups with respect to their associated

σ domain regions is summarized in the footnote of table 1 in this chapter. Also depicted in table 1, sigma factor group designations and experimentally determined/putative sigma factor-associated cellular processes are listed for all enterococcal sigma factors encoded in the *E. faecalis* V583 strain.

Regulating the activity of alternative sigma factors can be quite complicated and may sometimes involve transcriptional, translational, or posttranslational control (32, 53). Posttranslational regulation of an alternative sigma factor is dependent on the action of an anti-sigma factor (55, 56). The function of anti-sigma factors is to prevent their cognate sigma factor from binding to the core RNA polymerase, therefore inhibiting the expression of the alternative sigma factor's target genes (55, 56). The C-terminal region of anti-sigma factors protrudes into the periplasm of Gram-negative bacteria or outside the cytoplasmic membrane for Gram-positives where it can interact with a sensory protein or signal (55, 56). Upon receiving a specific environmental signal, the sensor protein alters the C-terminal region of the anti-sigma factor, or the anti-sigma factor undergoes a structural conformation change enabling a site-1 and site-2 protease to cleave the anti-sigma factor (55, 56). Once cleaved, the N-terminal region of the anti-sigma factor releases the cognate sigma factor (55, 56), allowing transcription of the target genes to occur. There are two sigma factor/anti-sigma factor pairs annotated in the enterococcal genome, EF3020/EF3019 and SigV/RsiV. The alternative sigma factor, SigV has been shown to play a role in the heat shock response, ethanol tolerance, acid stress response, and tolerance to lysozyme (63, 64). The alternative sigma factor/anti-sigma factor pair encoded by *ef3020-19* is currently uncharacterized.

Alternative sigma factor-54

Among the various alternative sigma factors, the alternative sigma factor-54 (σ^{54}) is a unique sigma factor that is structurally and functionally different from the σ^{70} family (66). For Gram-positive

bacteria, the first σ^{54} described was in *Bacillus subtilis* (67). Sigma-54 has no significant sequence similarity with σ^{70} (68) and recognizes the distinct -24/-12 promoter element (TTGGCACNNNNNTTGCT) (58, 66, 69, 70). In contrast to other sigma factors, the mode of transcription initiation by σ^{54} is unique as it is unable to initiate open complex formation upon association with the core RNA polymerase and target DNA (71, 72). In order to activate transcription, sigma-54 requires the assistance of an ATP-dependent activator protein, termed bacterial enhancer biding proteins (bEBPs) (72, 73). bEBPs interact with upstream DNA from the promoter site of certain genes and typically consist of three domains: a DNA-binding domain, a central AAA+ ATPase/transcriptional activation domain, and a regulatory domain (74-76). The regulatory domain is responsive to cellular signals and has been shown to function as a response-regulator domain of two-component systems (TCS), a ligand-binding domain, or as a phosphotransferase regulation domain (PRD) (71, 76). Upon receiving an internal or external environmental signal, the bEBP becomes active and will bind to an enhancer sequence, or upstream activation sequence (UAS), located approximately 100-150 bp upstream of the promoter region (72, 74, 76) (Figure 1). Through DNA looping, the bEBP becomes in contact with σ^{54} and hydrolyzes ATP to promote open complex formation, allowing transcription to occur (76).

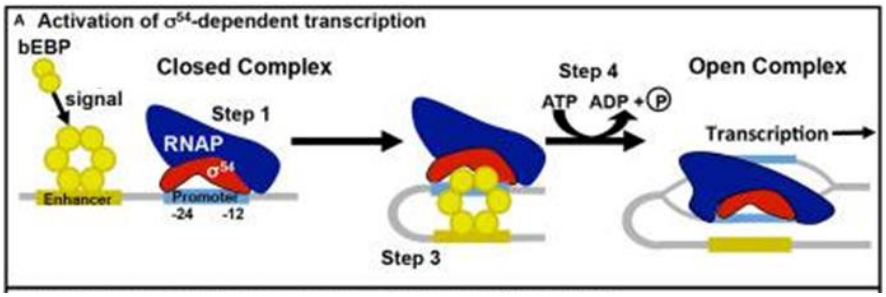

Figure 1: Bacterial enhancer-binding protein (bEBP) activation of σ^{54}-dependent transcription adapted from Hartman et al 2016. Step 1: σ^{54} binds to the core RNA polymerase and the σ^{54} binding site (-24/-12 promoter element) in a stable closed complex formation. Step 2: Upon sensing of an environmental signal, the bEBP is activated and binds to an upstream activation sequence (UAS). Step 3: DNA looping brings the bEBP in proximity with σ^{54}. Step 4: To promote open complex formation, the bEBP hydrolyzes ATP via its AAA+ ATPase domain.

Based on amino acid sequence similarity of all sigma-54 factors in bacteria, this sigma factor is divided into three regions (66, 77). Region I is located on the N-terminus of the protein and comprises of a glutamine and leucine rich domain that is responsible for interacting with the bEBP to initiate transcription (78, 79). This particular domain is approximately 50 amino acids long (77). Region II varies in amino acid length, is comprised of predominately acidic amino acids, and is responsible for binding to the RNA polymerase (77, 79). Lastly, region III is located at the C-terminus of the protein and is designated as the DNA binding domain (77, 80). The DNA binding domain contains three highly conserved motifs: the DNA crosslink motif, followed by the helix-turn-helix motif, and lastly the motif which has been termed the RpoN box (77, 80). The RpoN box is conserved across all bacterial sigma-54 proteins with the conserved 10-amino acid sequence of ARRTVAKYRE (77). The RpoN box is the portion of the sigma factor that binds to the distinct -24/-12 consensus sequence in the promoter of sigma-54-dependent genes (80). The helix-turn-helix motif of region III that precedes the RpoN box enhances the interaction between the RpoN box and -24/-12 consensus sequence (80). As for the cross-linking motif, its function is not defined.

The role of σ^{54} in other bacteria

Sigma-54 is found widely distributed among the bacterial kingdom, although some phyla lack the sigma-54 protein family (71, 81). Even before the protein was recognized as a sigma factor, σ^{54} was linked to the regulation of nitrogen metabolism (82, 83) and the expression of glutamine synthetase in *Salmonella* (84). It is now well established that sigma-54 directly regulates a wide variety of cellular processes across the bacterial kingdom. Some of the sigma-54 dependent cellular processes include, but are not limited to, cold shock adaptation in *Bacillus subtilis* (85), osmotolerance in *Listeria* (86), flagellar biosynthesis in *Escherichia coli* (87), lipoprotein biosynthesis and virulence in *Borrelia burgdorferi* (88), biofilm formation in *Burkholderia* (89), acid resistance of pathogenic *E. coli* O157 (90), biofilm formation, motility, luminescence, and colonization in *Vibrio fischeri* (91, 92), and phosphotransferase system-mediated carbohydrate uptake in various Gram-negative and Gram-positive bacteria (93-95). Others have sought to identify a unifying biological theme for the wide range of sigma-54 and bEBP-mediated regulated cellular processes (71, 96, 97). A recent extensive comparative genomic analysis performed by Francke et al. proposed that σ^{54} is a central player in the control of cellular processes that are involved in the physical interaction of an organism with its environment (host colonization, motility, biofilm, nitrogen and carbohydrate uptake, etc.) (98).

The role of σ^{54} in Enterococcus faecalis

In *E. faecalis* V583, the alternative sigma factor-54 is encoded by *rpoN* (*ef0782*) and is 443 amino acid long (~51kDa). RpoN of *E. faecalis* possesses all domain and region features of the sigma-54 family of transcriptional regulators (99). The first study conducted on RpoN in *E. faecalis* revealed that sigma-54 was involved in the sensitivity to class IIa bacteriocins (mesentericin Y105, pediocin PA-1, and enterocin A), as the *rpoN* mutant was resistant to the class IIa bacteriocins used in the

study (99). Bacteriocins are secreted antibacterial proteins produced by bacteria that will inhibit the growth of similar or closely related bacteria (100). Mesentericin Y105 is produced by *Leuconostoc mesenteroides* Y105 (101), while pediocin PA-1 is produced by *Pediococcus acidilactici* PAC1.0. (102), and the enterocin A bacteriocin is produced by *Enterococcus faecium* (103-105). Because RpoN from *E. faecalis* is involved in the sensitivity to class IIa bactericins, Hechard et al. sought to identify the associated bEBPs and RpoN-dependent genes involved in *E. faecalis* sensitivity to mesentericin Y105. Using the highly conserved central domain of the bEBPs as a query, Hechard et al. identified four bEBPs encoded in the *E. faecalis* V583 genome (MptR (*ef0018*), LpoR (*ef1010*), MphR (*ef1955*), and MpoR (*ef2981*)), with a fifth (XpoR (*ef3214* and *ef3216*)) disrupted by a natural insertion of an IS256 element (*ef3215*) (58). The mesentericin Y105 sensitivity of the various bEBP knockout strains revealed that only the deletion of *mptR* resulted in full resistance to the class IIa bacteriocin (58), indicating that RpoN and one of its bEBPs, MptR, control the expression of protein(s) involved in *E. faecalis* sensitivity to mesenteric Y105. One of the common features of bEBPs is that they are often encoded directly upstream or in close proximity to the σ^{54}-dependent genes that they help regulate (70). When Hechard et al. scanned the DNA regions near the *E. faecalis* bEBPs using the -24/-12 consensus sequence, they identified six putative σ^{54}-depenent operons encoding putative sugar PTS system (MptBACD (*ef0019-22*), MpoABCD (*ef2980-77*), MphABCD (*ef1954-52*), LpoBAC (*ef1012-13*), LptBAC (*ef1017-19*), and XpoABCD (*ef3210-13*)) (Figure 2) (58).

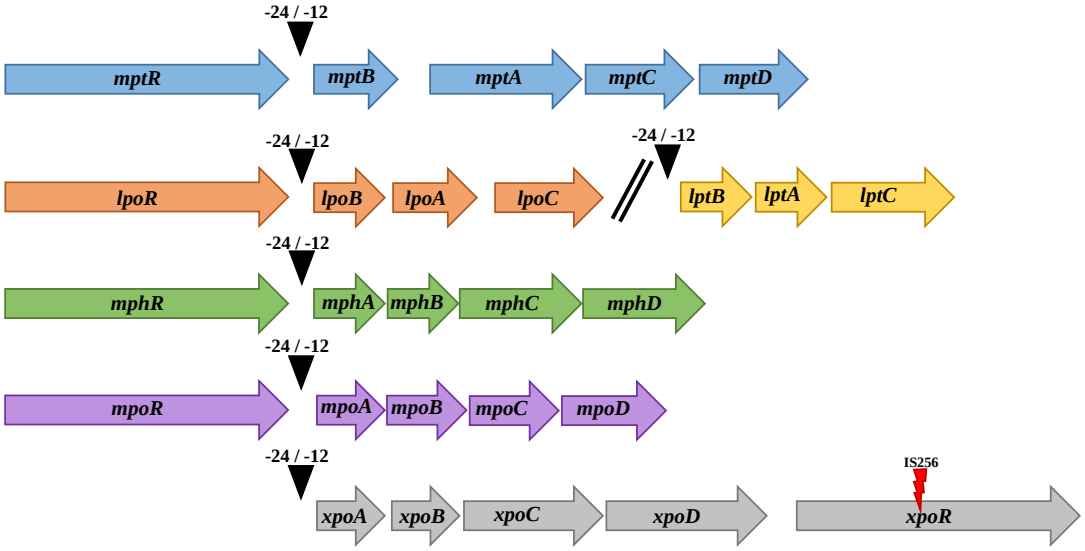

Figure 2: The genetic organization of RpoN-associated bEBPs and RpoN-dependent PTS operons adapted from Hechard et al. 2001.

These six PTS systems are the only genes/operons in the *E. faecalis* genome that possess a RpoN-binding site within their promoter region. Upon further analysis, the MptBACD PTS complex was identified as the cell surface receptor that confers *E. faecalis* susceptibility to mesentericin Y105 and is likely the receptor for various other subclass IIa bacteriocins (58). The expression of PTS systems is often induced in the presence of its transporter sugar (106). Hechard et al. observed that growing *E. faecalis* in the presence of glucose or mannose increased its susceptibility to mesentericin Y105 (58), suggesting that the Mpt PTS system imports glucose and mannose into the bacterial cell.

Besides RpoN directly regulating the cellular target of a class IIa bacteriocin, RpoN has previously been shown to play a role in extracellular DNA (eDNA) release, autolysis, and static biofilm formation in *E. faecalis*. As observed in Iyer et al., the deletion of *rpoN* from the *E. faecalis* V583 genome resulted in a significant decrease in autolysis, likely attributing to the decrease in eDNA release into the surrounding environment (59). eDNA has been extensively characterized as an

important biofilm matrix component in *E. faecalis* (107, 108). Although there is less eDNA released with respect to the *rpoN* mutant, this mutant perplexingly has a more robust static biofilm formation phenotype relative to the parental strain, represented by an increase in adherence to polystyrene plates and overall biofilm biomass (59). The authors propose that RpoN-dependent factors likely play a role in *E. faecalis* biofilm matrix composition that is unrelated to eDNA (59). Nonetheless, with the observation that RpoN-binding sites are located directly upstream of six PTS operons, this suggests that RpoN may influence a larger regulatory network of genes associated with carbon metabolism and overall enterococcal pathogenesis.

Central carbon metabolism in *Enterococcus faecalis*

The ability of *Enterococcus faecalis* to colonize various host anatomic sites is, in part, dependent on its adaptive response to host conditions and governed by its ability to metabolize secondary carbon sources in nutrient poor host environments (22, 25, 109). The three routes of intermediary carbohydrate metabolism in *E. faecalis*; (i) the Embdem-Meyerhof-Parnas (glycolysis) pathway, (ii) the Entner-Doudoroff pathway, and (iii) the pentose phosphate shunt (110). Although, *E. faecalis* is capable of metabolizing approximately 70 different carbon sources (109), little is known of how this bacterium acquires them in the host. The plethora of functionally encoded sugar transport systems in the *E. faecalis* genome emphasizes the importance of carbohydrate utilization and confers an advantage to survive in nutrient varying host environments. The carbohydrates commonly metabolized by enterococci are substrates for phosphotransferase systems (PTS) (110), which are transport complexes that sense sugars outside the bacterial cell and couples their uptake with phosphorylation (111) (Figure 3). A bacterial PTS complex consist of three main components: (i) cytoplasmic enzyme I (EI), (ii) cytoplasmic histidine-containing phosphocarrier protein (HPr), and (iii) carbohydrate specific enzymes II (EIIs). The sugar specific EII enzymes create a single

membrane-bound transport module composed of three, but in some cases, four domains (EIIA, EIIB, EIIC, and ± EIID) (111, 112). On the other hand, the cytoplasmic EI and HPr proteins participate in the phosphorylation of all PTS carbohydrate systems in a given organism (111, 112). The transport and simultaneous phosphorylation of a PTS sugar is initiated through a phosphotransfer cascade that begins with a phosphoryl group from the phosphoryl donor, phosphoenolpyruvate (PEP), being transferred to EI (111-113). Phosphorylated EI simultaneously transfers its phosphate to the histidine-15 amino acid residue of HPr (Figure 3) (111-113). Hpr [His-15-P] donates the phosphoryl group to the EIIA domain of the sugar specific PTS complex, followed by phosphoryl transfer to the sugar upon uptake into the bacterial cell (Figure 3) (111-113).

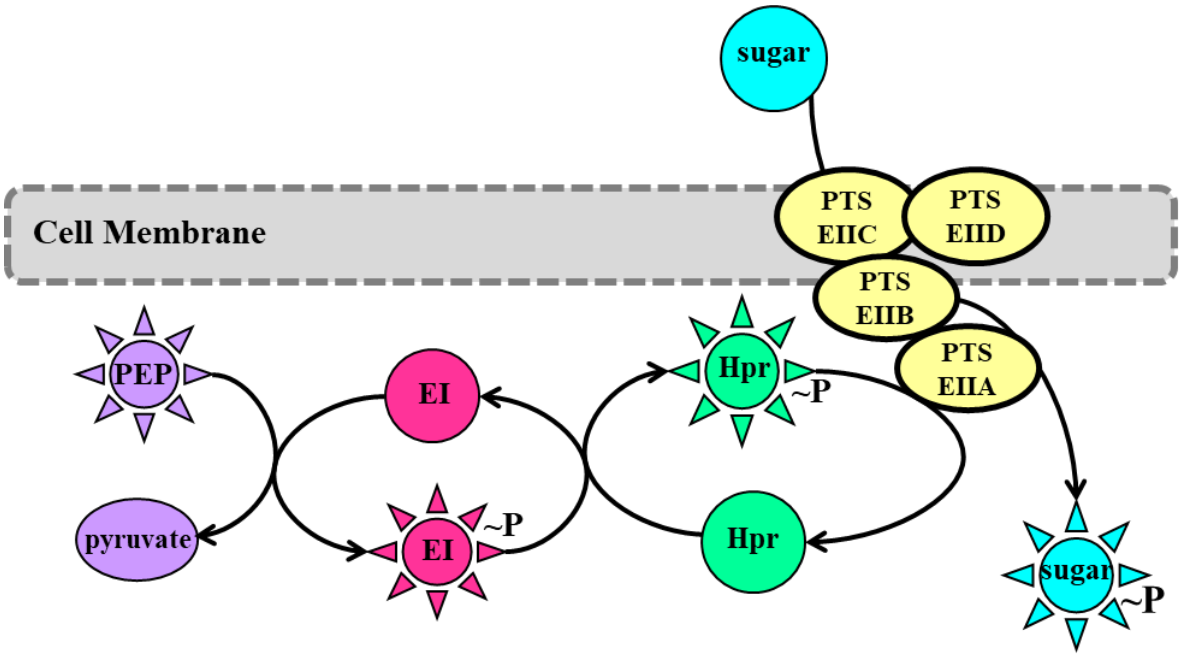

Figure 3: Bacterial phosphotransferase system (PTS) for sugar uptake in Gram-positive bacteria adapted from Postma et al. 1993 and Gorke et al. 2008. PTS components EIIA-D; Hpr = histidine-containing phosphocarrier protein; EI = enzyme I; PEP = phosphoenolpyruvate

Coupling sugar transport with its phosphorylation via bacterial PTS complexes is more efficient than sugar uptake with non-PTS systems, as non-PTS systems consume more than one adenosine

triphosphate (ATP) per imported carbohydrate versus the utilization of a single phosphoenolpyruvate (PEP) (110, 111). There are currently 46 different PTS systems encoded in the *E. faecalis* V583 genome, which are summarized in table 2 of this chapter. Among these PTS system, a novel PTS system (EF0552-55) resides within a known pathogenicity island in the multidrug-resistant, hospital-adapted *E. faecalis* strain V583 (42, 114), potentially linking sugar metabolism with pathogenesis or increased competitive fitness in complex human ecologies.

Table 2: Phosphotransferase systems encoded in the *E. faecalis* V583 genome

PTS System	Protein	PTS EII Component	Experimentally Determined Substrate	Operon	Reference
Mpt	EF0019	PTS EIIB	glucose, mannose, glucosamine, N-acetylglucosamine	*ef0019-22*	(58, 60) Chapter 2 Chapter 3 Chapter 4
	EF0020	PTS EIIA			
	EF0021	PTS EIIC			
	EF0022	PTS EIID			
MalX	EF0028	PTS EIIBC	N/A	*ef0028-29*	
	EF0097	PTS EIIC	N/A	*ef0097-ef0100*	
	EF0270	PTS EIIABC	N/A	*ef0269-73*	
GenB	EF0292	PTS EIIC	gentiobiose, amygdalin	*ef0292-91*	(115)
	EF0406	PTS EIIBC	N/A	*ef0406-08*	
	EF0408	PTS EIIA			
	EF0411	PTS EIICB	N/A	*ef0411-13*	
	EF0412	PTS EIIA			
	EF0455	PTS EIIC	N/A	*ef0455-61*	
	EF0456	PTS EIID			
	EF0457	PTS EIIB			
	EF0461	PTS EIIA			
	EF0516	PTS EIIC	N/A	*ef0517-16*	
	EF0541	PTS EIIBC	N/A	*ef0540-41*	
	EF0552	PTS EIIC	N/A	*ef0551-55*	
	EF0553	PTS EIID			
	EF0554	PTS EIIB			
	EF0555	PTS EIIA			
	EF0628	PTS EIIA	N/A		
	EF0694	PTS EIIBC	N/A	*ef0693-96*	
	EF0695	PTS EIIA			
	EF0717	PTS EIIABC	N/A	*ef0719-17*	
	EF0815	PTS EIIAB	N/A	*ef0815-17*	
	EF0816	PTS EIIC			
	EF0817	PTS EIID			
	EF0834	PTS EIIC	N/A	*ef0834-40*	
MalP	EF0958	PTS EIIBCA	maltose		(116)
Lpo	EF1012	PTS EIIB	N/A	*ef1012-13*	(58)

	EF1013	PTS EIIC			
Lpt	EF1017	PTS EIIB	N/A	*ef1017-19*	(58)
	EF1018	PTS EIIA			
	EF1019	PTS EIIC			
	EF1126	PTS EIIA	N/A	*ef1125-31*	
	EF1127	PTS EIIC			
	EF1128	PTS EIIB			
	EF1159	PTS EIIB	N/A	*ef1158-64*	
	EF1160	PTS EIIC			
NagE	EF1516	PTS EIICBA	N-acetylglucosamine, glucosamine (low-affinity)	*ef1515-16*	Chapter 4
	EF1529	PTS EIIC	N/A	*ef1528-29*	
	EF1601	PTS EIIBCA	N/A	*ef1602-01*	
	EF1607	PTS EIIA	N/A	*ef1607-06*	
	EF1657	PTS EIIC	N/A		
	EF1769	PTS EIIB	N/A		
	EF1801	PTS EIIA	N/A	*ef1809-01*	
	EF1802	PTS EIID			
	EF1803	PTS EIIC			
	EF1804	PTS EIIB			
	EF1829	PTS EIID	N/A	*ef1832-29*	
	EF1830	PTS EIIC			
	EF1831	PTS EIIB			
	EF1832	PTS EIIA			
	EF1836	PTS EIIA	N/A	*ef1836-38*	
	EF1837	PTS EIIB			
	EF1838	PTS EIIC			
	EF1852	PTS EIIC	N/A		
Mph	EF1952	PTS EIID	N/A	*ef1955-49*	(58)
	EF1953	PTS EIIC			
	EF1954	PTS EIIAB			
TreP	EF2213	PTS EIIBC	trehalose		(110)
	EF2257	PTS EIIC	N/A	*ef2258-57*	
	EF2267	PTS EIIA	N/A	*ef2268-67*	
	EF2269	PTS EIID		*ef2272-69*	
	EF2270	PTS EIIC			
	EF2271	PTS EIIB			
	EF2435	PTS EIIBC	N/A	*ef2437-34*	
	EF2438	PTS EIIA			
	EF2598	PTS EIIABC	N/A	*ef2598-97*	
	EF2603	PTS EIIA	N/A	*ef2603-02*	
	EF2964	PTS EIIC	N/A	*ef2966-64*	
	EF2965	PTS EIIB			
Mpo	EF2977	PTS EIID	N/A	*ef2980-75*	(58)
	EF2978	PTS EIIC			
	EF2979	PTS EIIB			
	EF2980	PTS EIIA			

	EF3029	PTS EIID	N/A	*ef3034-29*	
	EF3030	PTS EIIC			
	EF3031	PTS EIIB			
	EF3033	PTS EIIA			
	EF3042	PTS EIID	N/A	*ef3046-42*	
	EF3043	PTS EIIC			
	EF3045	PTS EIIB			
	EF3046	PTS EIIA			
	EF3136	PTS EIIA	N/A	*ef3142-34*	
	EF3137	PTS EIIB			
	EF3138	PTS EIID			
	EF3139	PTS EIIC			
Xpo	EF3210	PTS EIIA	N/A	*ef3210-13*	(58)
	EF3211	PTS EIIB			
	EF3212	PTS EIIC			
	EF3213	PTS EID			
	EF3285	PTS EIIC	N/A	*ef3285-84*	
	EF3305	PTS EIIA	N/A	*ef3310-05*	
	EF3306	PTS EIIB			
	EF3307	PTS EIIC			
Universal PTS Components					
Protein	**Characterized Name**	**Alternative Name**		**Operon**	**Reference**
EF0709	HPr	phosphocarrier protein		*ef0709-10*	(110)
EF0710	EI ; PtsP	phosphoenolpyruvate--protein phosphotransferase			

Bacteria, including enterococci, will repress alternative carbon source metabolism in the presence of preferred, rapidly fermentable carbon sources, such as glucose, via the regulatory phenomenon referred to as carbon catabolite repression (CCR) (117-119). CCR has been extensively studied in the model bacteria *Escherichia coli* and *Bacillus subtilis*. With the exception of mycoplasmas, all Firmicutes use the same elements of CCR (i.e. CcpA, HPr, and HPrK/P) (120). As a CCR-mechanism in low G-C Gram-positive bacteria, *cis*-acting nucleotide sequences termed catabolite responsive element (*cre*) sites in DNA are bound by a protein complex consisting of the *trans*-acting transcription factor catabolite repression protein A (CcpA) and HPr [Ser-46-P] to inhibit the transcription of target secondary nutrient acquisition genes under glucose-replete conditions (121-123) (Figure 4). As depicted in figure 4, in the presence of glucose or another rapidly metabolizable

carbon source, HPr is phosphorylated at a conserved secondary regulatory site, serine-46, by the HPr kinase/phosphorylase, HPrK/P (120, 124). The kinase activity of HPrK/P is triggered by the availability of glucose-6-phosphate and fructose-6-phosphate as indicators of high glycolytic activity (120). Hpr [Ser-46-P] serves as the effector for CcpA to form a protein complex that stimulates the activity of CcpA by reorientating CcpA's DNA binding domain. This reorientation event repositions the DNA-binding domain into a more favorable conformation for binding to *cre* sequences in DNA (125).

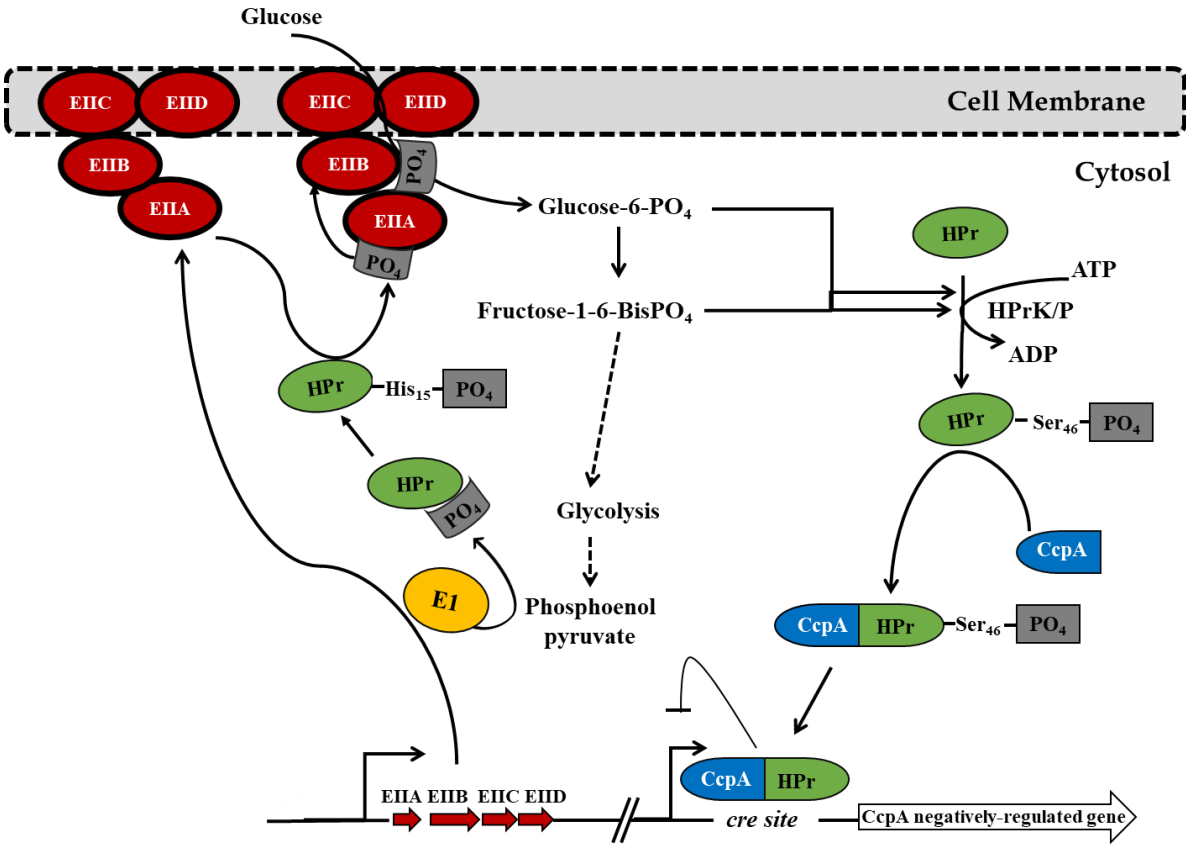

Figure 4: Carbon catabolite repression (CCR) in low G-C Gram-positive bacteria adapted from Keffeler et al. 2021 PTS components EIIA-D; Hpr = histidine-containing phosphocarrier protein; EI = enzyme I; PEP = phosphoenolpyruvate; CcpA = catabolite control protein A; *cre* = catabolite-responsive element; HprK/P = bifunctional ATP-dependent Hpr kinase/phosphatase

In contrast, under nutrient-limiting conditions, the CcpA and HPr [Ser-46-P] complex disassociates leading to derepression of CcpA negatively-regulated genes (120, 122, 126). Dephosphorylation of HPr [Ser-46-P] is catalyzed by the phosphorylase activity of HPrK/P as a consequence of low concentrations of glycolytic intermediates, glucose-6-phosphate and fructose-6-phosphate (127). These derepressed CcpA negatively-regulated genes may allow the bacterium to survive in an unfavorable environment and/or provide a competitive advantage in complex microbial niches.

Catabolite control protein A (CcpA)

The catabolite control protein A (CcpA) is a member of the LacI/GalR family of transcriptional regulators (128). Each member of the LacI/GalR family possesses an N-terminal DNA binding domain, followed by several regions involved in effector recognition and oligomerization (128, 129). Additionally, the LacI/GalR family of protein regulates transcription through binding as a dimer of identical subunits (125, 128). For binding to DNA, the N-terminal DNA binding domain will undertake the form of a helix-turn-helix motif. Unlike most members of the LacI/GalR family of bacterial regulators, CcpA requires a corepressor (i.e. HPr [Ser-46-P]) in order to regulate the transcription of its target genes (128, 130). Although CcpA is constitutively synthesized regardless of nutrient availability (131), the activity of this transcription factor is modulated by the availability of its corepressor, HPr [Ser-46-P] (Figure 4).

The binding sites for CcpA are referred to as catabolite responsive element (*cre*) sites. These DNA elements are pseudopalindromes and are considered a low-conservation consensus sequence of WTGNNARCGNWWWCAW (strongly conserved residues are underlined; W= A or T; R= A or G; N= any base) (132-134). As a general rule, the location of the *cre* site within a given promoter determines whether CcpA acts as an activator or repressor (129, 132, 135, 136). For instance,

promoters with a *cre* site overlapping or located near the transcriptional start site (TSS; +1) and the -10 or -35 promoter elements are repressed by CcpA (135, 137), whereas *cre* sites located further upstream in a given promoter are activated by CcpA (132, 135). Because the *cre* consensus sequence is considered to be a highly degenerate pseudopalindrome with only a few strongly conserved nucleotide residues, CcpA is thought to be capable of binding to its *cre* sites with different binding affinities (138).

Glycosyl hydrolases

Glycosyl hydrolases (synonyms: glycoside hydrolases, glycosidases) are a widespread group of enzymes which hydrolyze the glycosidic bond between two carbohydrates or between a carbohydrate and a non-carbohydrate. These enzymes are found in essentially all domains of life and are the major catalytic machinery for the breakage of glycosidic bonds (139, 140). Currently, there are 171 different families of glycosidases categorized by their amino acid sequence similarity, substrate specificity, and catalytic mechanism (Carbohydrate Active Enzymes database; http://www.cazy.org) (139, 140). The catalytic mechanism for hydrolysis by glycosidases is catalyzed by two amino acid residues: an acidic amino acid, referred to as the proton donor, and a deprotonated dibasic or basic amino acid (141). In bacteria, glycosyl hydrolase are found both as cytosolic and secreted enzymes and are largely involved in nutrient acquisition and, in some instances, involved in anti-bacterial defense strategies (142, 143). One example of a well characterized glycosyl hydrolase in bacteria is the bifunctional enzyme β-galactosidase (LacZ), which is involved in degrading lactose and the regulation of the *lac* operon for lactose utilization in *E. coli* (144). The β-galactosidase enzyme from *E. coli* belongs to the family 2 of glycosyl hydrolases (http://www.cazy.org). The glycosidase activity of β-galactosidase is responsible for cleaving the disaccharide lactose into glucose and galactose (144, 145), which can then be used by

other metabolic pathways, whereas its transgalactosylation activity catalyzes the conversion of lactose into allolactose, the natural inducer of the *lac* operon (146).

In mammals, glycosidases are commonly found within the endoplasmic reticulum (ER) and Golgi where they are involved in the synthesis and processing of N-linked glycoproteins (147). Interestingly, bacteria have evolved to secrete glycosyl hydrolases that degrade these mammalian N-linked glycoproteins as a nutrient source (148). Bacterial utilization of N-linked glycans as a nutrient source enables an advantage for bacteria to survive in host environments where preferred nutrients are host-limiting. Disrupting the function of these microbial enzymes may lead to new treatments against multidrug resistant bacterial infections.

Glycosyl hydrolase family 18 (GH18)

Glycosyl hydrolases belonging to the glycosyl hydrolase family 18 (GH18) are comprised of chitinases and endo-β-N-acetylglucosaminidases (ENGases) based on amino acid sequence similarity, possession of a conserved DXXDXDXE motif, and conserved catalytic mechanisms (149). Although their catalytic mechanisms are conserved, the substrates for chitinases and ENGases somewhat differ. For example, the catalytic mechanism for all GH18 family glycosidases involves the cleavage of two adjoining β-1,4-linked-N-acetylglucosamine (GlcNAc) moieties (synonym: chitobiose). Chitinases cleave β-1,4-linked GlcNAc within complex carbohydrates, such as chitin (a linear polymer of β-1,4-linked GlcNAc) (149-151), whereas ENGases target the diacetylchitobiose core (GlcNAc-β1,4-GlcNAc) of N-linked glycoproteins (149, 152, 153). *Enterococcus faecalis* chromosomally encodes three GH18 containing glycosyl hydrolases, EF0114 (EndoE), EF0361 (EfChi18A), and EF2863 (EfEndo18A). EF0114 and EF2863 are classified as GH18 ENGases (154, 155), whereas EF0361 has been characterized as a GH18 chitinase (156, 157).

Glycosyl hydrolase family 18 chitinases

Glycosyl hydrolase family 18 chitinases can be found across all kingdoms of life and are primarily associated with cleaving chitinous substrates that are composed of β-1,4-linked N-acetylglucosamine (158). Chitinases often work synergistically with chitin-binding proteins (CBPs), which help facilitate the accessibility of chitinases to chitinous substrates by creating breaks in the chitin chains (151, 159). Although chitin is the second most abundant natural polysaccharide, this complex carbohydrate is not synthesized by mammals (158, 160). Instead, chitin is predominately found in the cell wall of filamentous fungi, as well as in the exoskeletons of arthropods, including crustaceans and insects (158, 161). Although chitin is not naturally present in mammalian hosts, chitinases have been identified in various bacterial species (150, 151) and in some cases have a biological role in bacterial virulence (162-164). The biological role of bacterial chitinases during infection suggests that additional substrates for chitinases likely exist in mammalian hosts. Recent observations indicate that chitinases produced by *Salmonella* and *Listeria* have specificity towards LacNac (Galβ1–4GlcNAc) and LacdiNAc (GalNAcβ1–4GlcNAc) sugar linkages present in mammalian N and O-linked glycans, glycolipids and glycosaminoglycans (151, 165). These LacNAc and LacdiNAc containing substrates present in a mammalian host are likely an additional substrate for bacterial chitinases and chitinolytic cleavage of these substrates may contribute to bacterial pathogenesis in a host.

As previously mentioned, chitinases often work in a coordinated fashion with a chitin-binding protein (CBP). Interestingly, the chitinase encoded in the *E. faecalis* genome EfChi18A (EF0361) is encoded in the same operon as its cognate chitin-binding protein, EfCBM33A (EF0362). Figure 5 illustrates the protein organization of the enterococcal chitinase and chitin-binding protein.

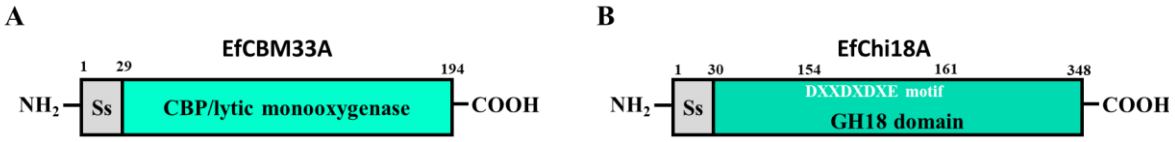

Figure 5: (A) Representation of EfCBM33A (EF0362) domain structure. The putative signal peptide sequence is located between amino acid residues 1 and 29. (B) Representation of EfChi18A (EF0361) domain structure. The putative signal peptide sequence is located between amino acid residues 1 and 30. The GH18 DXXDXDXE catalytic motif is located between amino acid residues 154 and 161.

The enterococcal chitinase (EF0361) and chitin-binding protein (EF0362) has previously been characterized for depolymerizing chitinous substrates (i.e. chitin (poly-β1,4-GlcNAc), chitohexaose (β1,4-$GlcNAc_6$), chitopentaose (β1,4-$GlcNAc_5$), chitotetraose (β1,4-$GlcNAc_4$), or chitotriose (β1,4-$GlcNAc_3$) into dimers of β-1,4-linked N-acetylglucosamine (β1,4-$GlcNAc_2$; chitobiose), however little is known of how these enzymes contribute to enterococcal metabolism in a mammalian host and overall pathogenesis.

Glycosyl hydrolase family 18 ENGases

Protein glycosylation, the act of adding sugar moieties to the backbone of a protein, is a key component of many biological processes, including cell-cell signaling and eliciting an immune response (166). The predominant form of protein glycosylation is N-linked glycosylation which entails oligosaccharides or glycans being attached to the amide nitrogen of a particular asparagine residue of a protein (166). N-linked glycoproteins are also classified into three groups: high-mannose, complex, or hybrid (a combination of high-mannose and complex sugar moieties), all of which possess a core consisting of an asparagine-attached diacetylchitobiose (Asn-GlcNAc-β1,4-GlcNAc) followed by three mannose moieties (Asn-GlcNAc-β1,4-GlcNAc-Man_3) (166). Depending on the host glycosylation machinery, the first GlcNAc residue of the diacetylchitobiose is also fucosylated in complex and hydrid N-linked glycoforms (151, 166). Glycosyl hydrolases

belonging to the GH18 family of endo-β-N-acetylglucosaminidases (ENGases; endoglycosidases) are capable of cleaving the diacetylchitobiose of N-linked glycoproteins (149, 152, 154, 155, 166-169). Although the catalytic activity of all GH18 ENGases is the same, they may have different specificities towards the precise structure of the N-linked glycoprotein that they can hydrolyze (166).

The observations from Roberts et al. (170) where a model high-mannose type glycoprotein, RNase B, can support growth of *E. faecalis* under nutrient-limiting conditions, suggests that this bacterium secretes an ENGase that is responsible for removing the glycans from RNase B. There are two GH18 ENGases encoded in the *E. faecalis* genome, EndoE (EF0114) and EfEndo18A (EF2863), however it is unclear which of these enterococcal ENGases targets high-mannose type glycoprotein as a nutrient acquisition mechanism. Figure 6 illustrates the protein organization of EndoE and EfEndo18A.

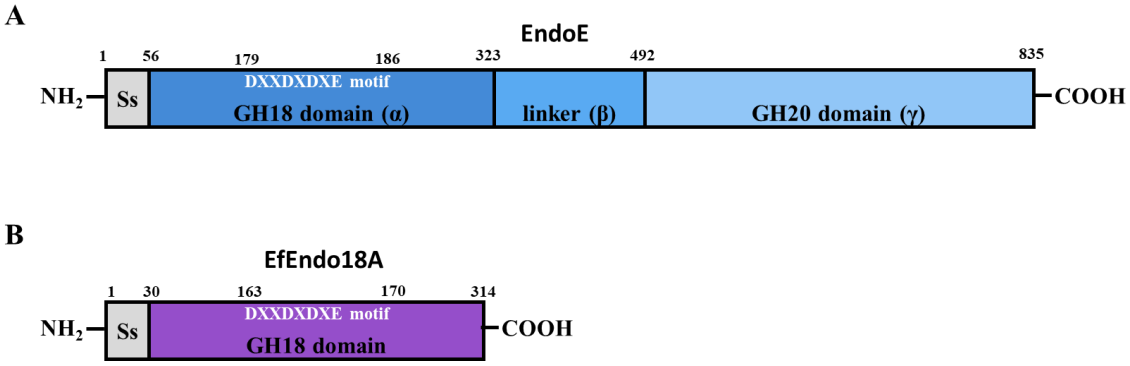

Figure 6: (A) Representation of EndoE (EF0114) domain structure. The putative signal peptide sequence is located between amino acid residues 1 and 56. The GH18 catalytic domain, described as α, is located between amino acid residues 56-323, with the GH18 DXXDXDXE catalytic motif located between amino acid residues 179-186. The uncharacterized linker region is described as the β domain (amino acid residues 323-492). The GH20 domain (γ) is located between amino acid residues 492-835. (B) Representation of EfEndo18A (EF2863) domain structure. The putative signal peptide sequence is located between amino acid residues 1 and 30. The GH18 DXXDXDXE catalytic motif is located between amino acid residues 163 and 170.

Glycosyl hydrolase family 20 (GH20)

Interestingly, the enterococcal glycosyl hydrolase, EndoE (EF0114), is a dual catalytic domain containing glycosyl hydrolase. The N-terminal catalytic domain of EndoE belongs to the aforementioned GH18 family of glycosidases. The second catalytic domain is located at the C-terminal end of the protein and is annotated as a GH20 catalytic domain, therefore belonging to the family 20 β-N-acetylhexosaminidases. GH20 hexoaminidases in bacteria are involved in the catabolism of oligosaccharides that serve as nitrogen and carbon sources by cleaving non-reducing β-1,4- and/or β-1,6- glycosidic bonds between two adjacent N-acetylglucosamine moieties (171). The oral pathogen, *Aggregatibacter actinomycetemcomitans*, which causes periodontitis, uses its GH20 family glycosidase (Dispersin B) to disaggregate self-produced biofilms, as well as biofilms produced by several bacterial species including *Staphylococcus epidermidis, Escherichia coli, Yersinia pestis,* and *Pseudomonas fluorescens* (172-174). The role of the GH20 catalytic domain of EndoE in *E. faecalis* is still to be elucidated. Whether it has specificity towards non-reducing β-1,4-linked GlcNAc or β-1,6 GlcNAc remains undefined. Additionally, the potential of EndoE being a biofilm dispersing enzyme is intriguing and would require experimental assessment.

Scope of dissertation

Enterococci have emerged as one of the leading causes of healthcare-associated infections, in part due to its intrinsic and acquired resistance to common antibiotics, and now rank second as causative agents of disease in healthcare settings in the United States. Nutrient acquisition systems and immune evasions strategies are key factors that contribute to enterococcal colonization and influences the overall pathogenic potential of this organism. The regulation of these factors is governed by metabolic cues, specifically the availability of glucose as a preferred carbon source. The alternative sigma factor 54 has been shown to regulate the expression of various genes

involved in metabolism and virulence in other bacteria and likely directly regulates the expression of a PTS system (MptBACD) responsible for glucose and mannose uptake in *E. faecalis*. After confirming that the Mpt PTS system is the primary glucose transporter in *E. faecalis,* we hypothesized that RpoN influences a larger regulatory network when RpoN-regulated glucose uptake is disrupted. We therefore performed a microarray transcriptional analysis on the *rpoN* mutant to identify genes that may enable the bacterium to cope in glucose-limited environments. Overall, chapter two of this dissertation provides important evidence that links central carbon metabolism with *in vivo* growth and provides the rationale for several distinct pathways that could be targeted as a potential therapeutic for treating enterococcal infections.

Among the differentially expressed genes in the transcriptomic study of *E. faecalis* strain V583 and the isogeneic *rpoN* mutant, *cre* sites were present in the promoter regions of a subset of the upregulated genes present in the *rpoN* mutant, suggesting that they are under CcpA secondary catabolite control. Three gene clusters (*ef0114*, *ef0362-61*, and *ef2863*) that encode the respective endoglycosyl hydrolases (EndoE (155), EfChi18A (157), and EfEndo18A (154)) and cognate chitin binding protein of EfChi18A (EfCBM33A (157)), were highly upregulated in the *rpoN* mutant with identified putative *cre* sites within their promoter regions. These enzymes also possess putative signal peptide sequences and signal peptide cleavage sites. Chapter 3 of this dissertation provides insight into how these secreted enterococcal glycosidases may contribute to the survival of *E. faecalis* in nutrient limited environments.

Metabolism of alternative carbon sources enables bacteria to colonize various biologically unique anatomic sites. Although *E. faecalis* can metabolize an enormous range of carbon sources, little is known of how this bacterium acquires these secondary nutrient sources in mammalian hosts. We sought to understand how *E. faecalis* metabolizes N-acetylglucosamine containing substrates.

Described in chapter 4 of this dissertation, we identified the machinery for which *E. faecalis* extracellular degrades chitinous substrates, the PTS system(s) required for the uptake of N-acetylglucosamine and glucosamine, and the cytosolic enzymes responsible for preparing the amino sugar for glycolysis.

Collectively, this dissertation provides insight into the regulation of central carbon metabolism in *E. faecalis* and highlight alternative nutrient acquisition mechanisms that may facilitate this bacterium's survival in nutrient-limiting host environments.

References

1. Thiercelin ME. 1899. Morphologie et modes de reproduction de l'enterocoque. . Comptes Rendus des Seances de la Societe de Biologie et des ses Filiales 11:551-553.
2. Thiercelin ME, Jouhaud L. 1899. Sur un diplococque saprophyte de l'intestin susceptible de devenir pathogene. CR Soc Biol 5:269-271.
3. Maccallum WG, Hastings TW. 1899. A Case of Acute Endocarditis Caused by Micrococcus Zymogenes (Nov. Spec.), with a Description of the Microorganism. J Exp Med 4:521-34.
4. Lancefield RC. 1933. A Serological Differentiation of Human and Other Groups of Hemolytic Streptococci. J Exp Med 57:571-95.
5. Schleifer KH, Kilpper-Bälz R. 1984. Transfer of Streptococcus faecalis and Streptococcus faecium to the Genus Enterococcus nom. rev. as Enterococcus faecalis comb. nov. and Enterococcus faecium comb. nov. International Journal of Systematic Bacteriology 34:31-34.
6. Christoffersen TE, Jensen H, Kleiveland CR, Dorum G, Jacobsen M, Lea T. 2012. In vitro comparison of commensal, probiotic and pathogenic strains of Enterococcus faecalis. Br J Nutr 108:2043-53.
7. Domann E, Hain T, Ghai R, Billion A, Kuenne C, Zimmermann K, Chakraborty T. 2007. Comparative genomic analysis for the presence of potential enterococcal virulence factors in the probiotic Enterococcus faecalis strain Symbioflor 1. Int J Med Microbiol 297:533-9.
8. Franz CM, Huch M, Abriouel H, Holzapfel W, Galvez A. 2011. Enterococci as probiotics and their implications in food safety. Int J Food Microbiol 151:125-40.
9. Chandler JA, Lang JM, Bhatnagar S, Eisen JA, Kopp A. 2011. Bacterial communities of diverse Drosophila species: ecological context of a host-microbe model system. PLoS Genet 7:e1002272.
10. Chapman JR, Dowell MA, Chan R, Unckless RL. 2020. The Genetic Basis of Natural Variation in Drosophila melanogaster Immune Defense against Enterococcus faecalis. Genes (Basel) 11.
11. Martin JD, Mundt JO. 1972. Enterococci in insects. Appl Microbiol 24:575-80.
12. Suvorov A. 2020. What Is Wrong with Enterococcal Probiotics? Probiotics Antimicrob Proteins 12:1-4.
13. Yu J, Wang WH, Menghe BL, Jiri MT, Wang HM, Liu WJ, Bao QH, Lu Q, Zhang JC, Wang F, Xu HY, Sun TS, Zhang HP. 2011. Diversity of lactic acid bacteria associated with traditional fermented dairy products in Mongolia. J Dairy Sci 94:3229-41.
14. Mundt JO. 1961. Occurrence of Enterococci: Bud, Blossom, and Soil Studies. Appl Microbiol 9:541-4.
15. Ator LL, Starzyk MJ. 1976. Distribution of group D streptococci in rivers and streams. Microbios 16:91-104.
16. Mundt JO, Larsen SA, McCarty IE. 1966. Growth of lactic acid bacteria in waste waters of vegetable-processing plants. Appl Microbiol 14:115-8.
17. Kao PHN, Kline KA. 2019. Dr. Jekyll and Mr. Hide: How Enterococcus faecalis Subverts the Host Immune Response to Cause Infection. J Mol Biol 431:2932-2945.
18. Martin R, Miquel S, Ulmer J, Kechaou N, Langella P, Bermudez-Humaran LG. 2013. Role of commensal and probiotic bacteria in human health: a focus on inflammatory bowel disease. Microb Cell Fact 12:71.
19. Gilmore MS, Rauch M, Ramsey MM, Himes PR, Varahan S, Manson JM, Lebreton F, Hancock LE. 2015. Pheromone killing of multidrug-resistant Enterococcus faecalis V583 by native commensal strains. Proc Natl Acad Sci U S A 112:7273-8.
20. Garcia-Solache M, Rice LB. 2019. The Enterococcus: a Model of Adaptability to Its Environment. Clin Microbiol Rev 32.
21. Gilmore MS, Lebreton F, van Schaik W. 2013. Genomic transition of enterococci from gut commensals to leading causes of multidrug-resistant hospital infection in the antibiotic era. Curr Opin Microbiol 16:10-6.

22. Lebreton F, Manson AL, Saavedra JT, Straub TJ, Earl AM, Gilmore MS. 2017. Tracing the Enterococci from Paleozoic Origins to the Hospital. Cell 169:849-861 e13.
23. Van Tyne D, Gilmore MS. 2014. Friend turned foe: evolution of enterococcal virulence and antibiotic resistance. Annu Rev Microbiol 68:337-56.
24. Weiner-Lastinger LM, Abner S, Edwards JR, Kallen AJ, Karlsson M, Magill SS, Pollock D, See I, Soe MM, Walters MS, Dudeck MA. 2020. Antimicrobial-resistant pathogens associated with adult healthcare-associated infections: Summary of data reported to the National Healthcare Safety Network, 2015-2017. Infect Control Hosp Epidemiol 41:1-18.
25. Fiore E, Van Tyne D, Gilmore MS. 2019. Pathogenicity of Enterococci. Microbiol Spectr 7.
26. Giridhara Upadhyaya PM, Ravikumar KL, Umapathy BL. 2009. Review of virulence factors of enterococcus: an emerging nosocomial pathogen. Indian J Med Microbiol 27:301-5.
27. Arias CA, Murray BE. 2012. The rise of the Enterococcus: beyond vancomycin resistance. Nature Reviews Microbiology 10:266-278.
28. Coburn PS, Baghdayan AS, Dolan GT, Shankar N. 2007. Horizontal transfer of virulence genes encoded on the Enterococcus faecalis pathogenicity island. Molecular Microbiology 63:530-544.
29. Hollenbeck BL, Rice LB. 2012. Intrinsic and acquired resistance mechanisms in enterococcus. Virulence 3:421-433.
30. Anderson DJ, Olaison L, McDonald JR, Miro JM, Hoen B, Selton-Suty C, Doco-Lecompte T, Abrutyn E, Habib G, Eykyn S, Pappas PA, Fowler VG, Sexton DJ, Almela M, Corey GR, Cabell CH. 2005. Enterococcal prosthetic valve infective endocarditis: report of 45 episodes from the International Collaboration on Endocarditis-merged database. Eur J Clin Microbiol Infect Dis 24:665-70.
31. Klare I, Werner G, Witte W. 2001. Enterococci. Habitats, infections, virulence factors, resistances to antibiotics, transfer of resistance determinants. Contrib Microbiol 8:108-22.
32. Browning DF, Busby SJ. 2004. The regulation of bacterial transcription initiation. Nat Rev Microbiol 2:57-65.
33. Snyder L. 2005. Molecular Genetics of Bacteria, 4th ed. ASM Press.
34. Stock AM, Robinson VL, Goudreau PN. 2000. Two-component signal transduction. Annu Rev Biochem 69:183-215.
35. Stock AM, Zhulin IB. 2017. Two-Component Signal Transduction: a Special Issue in the Journal of Bacteriology. J Bacteriol 199.
36. DebRoy S, Gao P, Garsin DA, Harvey BR, Kos V, Nes IF, Solheim M. 2014. Transcriptional and Post Transcriptional Control of Enterococcal Gene Regulation. *In* Gilmore MS, Clewell DB, Ike Y, Shankar N (ed), Enterococci: From Commensals to Leading Causes of Drug Resistant Infection, Boston.
37. Hancock L, Perego M. 2002. Two-component signal transduction in Enterococcus faecalis. J Bacteriol 184:5819-25.
38. Evers S, Courvalin P. 1996. Regulation of VanB-type vancomycin resistance gene expression by the VanS(B)-VanR (B) two-component regulatory system in Enterococcus faecalis V583. J Bacteriol 178:1302-9.
39. Qin X, Singh KV, Weinstock GM, Murray BE. 2000. Effects of Enterococcus faecalis fsr genes on production of gelatinase and a serine protease and virulence. Infect Immun 68:2579-86.
40. Mohamed JA, Murray BE. 2006. Influence of the fsr locus on biofilm formation by Enterococcus faecalis lacking gelE. J Med Microbiol 55:1747-1750.
41. Garsin DA. 2010. Ethanolamine utilization in bacterial pathogens: roles and regulation. Nat Rev Microbiol 8:290-5.
42. Paulsen IT, Banerjei L, Myers GS, Nelson KE, Seshadri R, Read TD, Fouts DE, Eisen JA, Gill SR, Heidelberg JF, Tettelin H, Dodson RJ, Umayam L, Brinkac L, Beanan M, Daugherty S, DeBoy RT, Durkin S, Kolonay J, Madupu R, Nelson W, Vamathevan J, Tran B, Upton J, Hansen T, Shetty J, Khouri H, Utterback T, Radune D, Ketchum KA, Dougherty BA, Fraser CM. 2003. Role of mobile DNA in the evolution of vancomycin-resistant Enterococcus faecalis. Science 299:2071-4.

43. Jain D. 2015. Allosteric control of transcription in GntR family of transcription regulators: A structural overview. IUBMB Life 67:556-63.
44. Liu GF, Wang XX, Su HZ, Lu GT. 2021. Progress on the GntR family transcription regulators in bacteria. Yi Chuan 43:66-73.
45. Fujita Y, Fujita T. 1986. Identification and nucleotide sequence of the promoter region of the Bacillus subtilis gluconate operon. Nucleic Acids Res 14:1237-52.
46. Blancato VS, Repizo GD, Suarez CA, Magni C. 2008. Transcriptional regulation of the citrate gene cluster of Enterococcus faecalis Involves the GntR family transcriptional activator CitO. J Bacteriol 190:7419-30.
47. Swint-Kruse L, Matthews KS. 2009. Allostery in the LacI/GalR family: variations on a theme. Curr Opin Microbiol 12:129-37.
48. Nguyen CC, Saier MH, Jr. 1995. Phylogenetic, structural and functional analyses of the LacI-GalR family of bacterial transcription factors. FEBS Lett 377:98-102.
49. Murakami KS, Masuda S, Campbell EA, Muzzin O, Darst SA. 2002. Structural basis of transcription initiation: an RNA polymerase holoenzyme-DNA complex. Science 296:1285-90.
50. Lee DJ, Minchin SD, Busby SJ. 2012. Activating transcription in bacteria. Annu Rev Microbiol 66:125-52.
51. Murakami KS, Darst SA. 2003. Bacterial RNA polymerases: the wholo story. Curr Opin Struct Biol 13:31-9.
52. Gruber TM, Gross CA. 2003. Multiple sigma subunits and the partitioning of bacterial transcription space. Annu Rev Microbiol 57:441-66.
53. Campbell EA, Muzzin O, Chlenov M, Sun JL, Olson CA, Weinman O, Trester-Zedlitz ML, Darst SA. 2002. Structure of the bacterial RNA polymerase promoter specificity sigma subunit. Mol Cell 9:527-39.
54. Paget MS, Helmann JD. 2003. The sigma70 family of sigma factors. Genome Biol 4:203.
55. Souza BM, Castro TL, Carvalho RD, Seyffert N, Silva A, Miyoshi A, Azevedo V. 2014. sigma(ECF) factors of gram-positive bacteria: a focus on Bacillus subtilis and the CMNR group. Virulence 5:587-600.
56. Paget MS. 2015. Bacterial Sigma Factors and Anti-Sigma Factors: Structure, Function and Distribution. Biomolecules 5:1245-65.
57. Kristich CJ, Chandler JR, Dunny GM. 2007. Development of a host-genotype-independent counterselectable marker and a high-frequency conjugative delivery system and their use in genetic analysis of Enterococcus faecalis. Plasmid 57:131-44.
58. Hechard Y, Pelletier C, Cenatiempo Y, Frere J. 2001. Analysis of sigma(54)-dependent genes in Enterococcus faecalis: a mannose PTS permease (EII(Man)) is involved in sensitivity to a bacteriocin, mesentericin Y105. Microbiology (Reading) 147:1575-1580.
59. Iyer VS, Hancock LE. 2012. Deletion of sigma(54) (rpoN) alters the rate of autolysis and biofilm formation in Enterococcus faecalis. J Bacteriol 194:368-75.
60. Keffeler EC, Iyer VS, Parthasarathy S, Ramsey MM, Gorman MJ, Barke TL, Varahan S, Olson S, Gilmore MS, Abdullahi ZH, Hancock EN, Hancock LE. 2021. Influence of the Alternative Sigma Factor RpoN on Global Gene Expression and Carbon Catabolism in Enterococcus faecalis V583. mBio 12.
61. Benachour A, Muller C, Dabrowski-Coton M, Le Breton Y, Giard JC, Rince A, Auffray Y, Hartke A. 2005. The Enterococcus faecalis sigV protein is an extracytoplasmic function sigma factor contributing to survival following heat, acid, and ethanol treatments. J Bacteriol 187:1022-35.
62. Le Jeune A, Torelli R, Sanguinetti M, Giard JC, Hartke A, Auffray Y, Benachour A. 2010. The extracytoplasmic function sigma factor SigV plays a key role in the original model of lysozyme resistance and virulence of Enterococcus faecalis. PLoS One 5:e9658.
63. Parthasarathy S, Wang X, Carr K, Varahan S, Hancock EB, Hancock LE. 2021. SigV mediates lysozyme resistance in Enterococcus faecalis via RsiV and PgdA. Journal of Bacteriology *accepted*.

64. Varahan S, Iyer VS, Moore WT, Hancock LE. 2013. Eep confers lysozyme resistance to enterococcus faecalis via the activation of the extracytoplasmic function sigma factor SigV. J Bacteriol 195:3125-34.
65. Lonetto M, Gribskov M, Gross CA. 1992. The sigma 70 family: sequence conservation and evolutionary relationships. J Bacteriol 174:3843-9.
66. Merrick MJ. 1993. In a class of its own--the RNA polymerase sigma factor sigma 54 (sigma N). Mol Microbiol 10:903-9.
67. Débarbouillé M, Martin-Verstraete I, Klier A, Rapoport G. 1991. The transcriptional regulator LevR of Bacillus subtilis has domains homologous to both sigma 54- and phosphotransferase system-dependent regulators. Proc Natl Acad Sci U S A 88:2212-6.
68. Feklistov A, Sharon BD, Darst SA, Gross CA. 2014. Bacterial sigma factors: a historical, structural, and genomic perspective. Annu Rev Microbiol 68:357-76.
69. Buck M, Cannon W. 1992. Specific binding of the transcription factor sigma-54 to promoter DNA. Nature 358:422-4.
70. Studholme DJ, Buck M, Nixon T. 2000. Identification of potential sigma(N)-dependent promoters in bacterial genomes. Microbiology (Reading) 146 Pt 12:3021-3023.
71. Buck M, Gallegos MT, Studholme DJ, Guo Y, Gralla JD. 2000. The bacterial enhancer-dependent sigma(54) (sigma(N)) transcription factor. J Bacteriol 182:4129-36.
72. Danson AE, Jovanovic M, Buck M, Zhang X. 2019. Mechanisms of sigma(54)-Dependent Transcription Initiation and Regulation. J Mol Biol 431:3960-3974.
73. Bush M, Dixon R. 2012. The role of bacterial enhancer binding proteins as specialized activators of sigma54-dependent transcription. Microbiol Mol Biol Rev 76:497-529.
74. Buck M, Woodcock J, Cannon W, Mitchenall L, Drummond M. 1987. Positional requirements for the function of nif-specific upstream activator sequences. Mol Gen Genet 210:140-4.
75. Ghosh T, Bose D, Zhang X. 2010. Mechanisms for activating bacterial RNA polymerase. FEMS Microbiol Rev 34:611-27.
76. Hartman CE, Samuels DJ, Karls AC. 2016. Modulating Salmonella Typhimurium's Response to a Changing Environment through Bacterial Enhancer-Binding Proteins and the RpoN Regulon. Front Mol Biosci 3:41.
77. Taylor M, Butler R, Chambers S, Casimiro M, Badii F, Merrick M. 1996. The RpoN-box motif of the RNA polymerase sigma factor sigma N plays a role in promoter recognition. Mol Microbiol 22:1045-54.
78. Bordes P, Wigneshweraraj SR, Schumacher J, Zhang X, Chaney M, Buck M. 2003. The ATP hydrolyzing transcription activator phage shock protein F of Escherichia coli: identifying a surface that binds sigma 54. Proc Natl Acad Sci U S A 100:2278-83.
79. Wong C, Tintut Y, Gralla JD. 1994. The domain structure of sigma 54 as determined by analysis of a set of deletion mutants. J Mol Biol 236:81-90.
80. Cannon WV, Chaney MK, Wang X, Buck M. 1997. Two domains within sigmaN (sigma54) cooperate for DNA binding. Proc Natl Acad Sci U S A 94:5006-11.
81. Kill K, Binnewies TT, Sicheritz-Ponten T, Willenbrock H, Hallin PF, Wassenaar TM, Ussery DW. 2005. Genome update: sigma factors in 240 bacterial genomes. Microbiology (Reading) 151:3147-3150.
82. Hirschman J, Wong PK, Sei K, Keener J, Kustu S. 1985. Products of nitrogen regulatory genes ntrA and ntrC of enteric bacteria activate glnA transcription in vitro: evidence that the ntrA product is a sigma factor. Proc Natl Acad Sci U S A 82:7525-9.
83. Pfluger-Grau K, Gorke B. 2010. Regulatory roles of the bacterial nitrogen-related phosphotransferase system. Trends Microbiol 18:205-14.
84. Garcia E, Bancroft S, Rhee SG, Kustu S. 1977. The product of a newly identified gene, gInF, is required for synthesis of glutamine synthetase in Salmonella. Proc Natl Acad Sci U S A 74:1662-6.

85. Wiegeshoff F, Beckering CL, Debarbouille M, Marahiel MA. 2006. Sigma L is important for cold shock adaptation of Bacillus subtilis. J Bacteriol 188:3130-3.
86. Okada Y, Makino S, Okada N, Asakura H, Yamamoto S, Igimi S. 2008. Identification and analysis of the osmotolerance associated genes in Listeria monocytogenes. Food Addit Contam Part A Chem Anal Control Expo Risk Assess 25:1089-94.
87. Zhao K, Liu M, Burgess RR. 2010. Promoter and regulon analysis of nitrogen assimilation factor, sigma54, reveal alternative strategy for E. coli MG1655 flagellar biosynthesis. Nucleic Acids Res 38:1273-83.
88. Fisher MA, Grimm D, Henion AK, Elias AF, Stewart PE, Rosa PA, Gherardini FC. 2005. Borrelia burgdorferi sigma54 is required for mammalian infection and vector transmission but not for tick colonization. Proc Natl Acad Sci U S A 102:5162-7.
89. Saldias MS, Lamothe J, Wu R, Valvano MA. 2008. Burkholderia cenocepacia requires the RpoN sigma factor for biofilm formation and intracellular trafficking within macrophages. Infect Immun 76:1059-67.
90. Riordan JT, Tietjen JA, Walsh CW, Gustafson JE, Whittam TS. 2010. Inactivation of alternative sigma factor 54 (RpoN) leads to increased acid resistance, and alters locus of enterocyte effacement (LEE) expression in Escherichia coli O157 : H7. Microbiology (Reading) 156:719-730.
91. Visick KL. 2009. An intricate network of regulators controls biofilm formation and colonization by Vibrio fischeri. Mol Microbiol 74:782-9.
92. Wolfe AJ, Millikan DS, Campbell JM, Visick KL. 2004. Vibrio fischeri sigma54 controls motility, biofilm formation, luminescence, and colonization. Appl Environ Microbiol 70:2520-4.
93. Arous S, Buchrieser C, Folio P, Glaser P, Namane A, Hebraud M, Hechard Y. 2004. Global analysis of gene expression in an rpoN mutant of Listeria monocytogenes. Microbiology (Reading) 150:1581-1590.
94. Deutscher J, Francke C, Postma PW. 2006. How phosphotransferase system-related protein phosphorylation regulates carbohydrate metabolism in bacteria. Microbiol Mol Biol Rev 70:939-1031.
95. Stevens MJA, Molenaar D, de Jong A, De Vos WM, Kleerebezem M. 2010. sigma54-Mediated control of the mannose phosphotransferase sytem in Lactobacillus plantarum impacts on carbohydrate metabolism. Microbiology (Reading) 156:695-707.
96. Morett E, Segovia L. 1993. The sigma 54 bacterial enhancer-binding protein family: mechanism of action and phylogenetic relationship of their functional domains. J Bacteriol 175:6067-74.
97. Studholme DJ, Buck M. 2000. The biology of enhancer-dependent transcriptional regulation in bacteria: insights from genome sequences. FEMS Microbiol Lett 186:1-9.
98. Francke C, Groot Kormelink T, Hagemeijer Y, Overmars L, Sluijter V, Moezelaar R, Siezen RJ. 2011. Comparative analyses imply that the enigmatic Sigma factor 54 is a central controller of the bacterial exterior. BMC Genomics 12:385.
99. Dalet K, Briand C, Cenatiempo Y, Hechard Y. 2000. The rpoN gene of Enterococcus faecalis directs sensitivity to subclass IIa bacteriocins. Curr Microbiol 41:441-3.
100. Cotter PD, Ross RP, Hill C. 2013. Bacteriocins - a viable alternative to antibiotics? Nat Rev Microbiol 11:95-105.
101. Morisset D, Berjeaud JM, Marion D, Lacombe C, Frere J. 2004. Mutational analysis of mesentericin y105, an anti-Listeria bacteriocin, for determination of impact on bactericidal activity, in vitro secondary structure, and membrane interaction. Appl Environ Microbiol 70:4672-80.
102. Chikindas ML, Garcia-Garcera MJ, Driessen AJ, Ledeboer AM, Nissen-Meyer J, Nes IF, Abee T, Konings WN, Venema G. 1993. Pediocin PA-1, a bacteriocin from Pediococcus acidilactici PAC1.0, forms hydrophilic pores in the cytoplasmic membrane of target cells. Appl Environ Microbiol 59:3577-84.
103. Aymerich T, Holo H, Havarstein LS, Hugas M, Garriga M, Nes IF. 1996. Biochemical and genetic characterization of enterocin A from Enterococcus faecium, a new antilisterial bacteriocin in the pediocin family of bacteriocins. Appl Environ Microbiol 62:1676-82.

104. Cintas LM, Casaus P, Havarstein LS, Hernandez PE, Nes IF. 1997. Biochemical and genetic characterization of enterocin P, a novel sec-dependent bacteriocin from Enterococcus faecium P13 with a broad antimicrobial spectrum. Appl Environ Microbiol 63:4321-30.
105. Franz CM, Grube A, Herrmann A, Abriouel H, Starke J, Lombardi A, Tauscher B, Holzapfel WH. 2002. Biochemical and genetic characterization of the two-peptide bacteriocin enterocin 1071 produced by Enterococcus faecalis FAIR-E 309. Appl Environ Microbiol 68:2550-4.
106. Saier MH, Jr., Reizer J. 1994. The bacterial phosphotransferase system: new frontiers 30 years later. Mol Microbiol 13:755-64.
107. Thomas VC, Hiromasa Y, Harms N, Thurlow L, Tomich J, Hancock LE. 2009. A fratricidal mechanism is responsible for eDNA release and contributes to biofilm development of Enterococcus faecalis. Mol Microbiol 72:1022-36.
108. Thomas VC, Thurlow LR, Boyle D, Hancock LE. 2008. Regulation of autolysis-dependent extracellular DNA release by Enterococcus faecalis extracellular proteases influences biofilm development. J Bacteriol 190:5690-8.
109. Lebreton F, Willems RJL, Gilmore MS. 2014. Enterococcus Diversity, Origins in Nature, and Gut Colonization. *In* Gilmore MS, Clewell DB, Ike Y, Shankar N (ed), Enterococci: From Commensals to Leading Causes of Drug Resistant Infection, Boston.
110. Ramsey M, Hartke A, Huycke M. 2014. The Physiology and Metabolism of Enterococci. *In* Gilmore MS, Clewell DB, Ike Y, Shankar N (ed), Enterococci: From Commensals to Leading Causes of Drug Resistant Infection, Boston.
111. Postma PW, Lengeler JW, Jacobson GR. 1993. Phosphoenolpyruvate:carbohydrate phosphotransferase systems of bacteria. Microbiol Rev 57:543-94.
112. Saier MH, Jr. 2001. The bacterial phosphotransferase system: structure, function, regulation and evolution. J Mol Microbiol Biotechnol 3:325-7.
113. Saier MH, Hvorup RN, Barabote RD. 2005. Evolution of the bacterial phosphotransferase system: from carriers and enzymes to group translocators. Biochem Soc Trans 33:220-4.
114. Shankar N, Baghdayan AS, Gilmore MS. 2002. Modulation of virulence within a pathogenicity island in vancomycin-resistant Enterococcus faecalis. Nature 417:746-50.
115. Grand M, Aubourg M, Pikis A, Thompson J, Deutscher J, Hartke A, Sauvageot N. 2019. Characterization of the gen locus involved in beta-1,6-oligosaccharide utilization by Enterococcus faecalis. Mol Microbiol 112:1744-1756.
116. Le Breton Y, Pichereau V, Sauvageot N, Auffray Y, Rince A. 2005. Maltose utilization in Enterococcus faecalis. J Appl Microbiol 98:806-13.
117. Bruckner R, Titgemeyer F. 2002. Carbon catabolite repression in bacteria: choice of the carbon source and autoregulatory limitation of sugar utilization. FEMS Microbiol Lett 209:141-8.
118. Stulke J, Hillen W. 1999. Carbon catabolite repression in bacteria. Curr Opin Microbiol 2:195-201.
119. Warner JB, Lolkema JS. 2003. CcpA-dependent carbon catabolite repression in bacteria. Microbiol Mol Biol Rev 67:475-90.
120. Gorke B, Stulke J. 2008. Carbon catabolite repression in bacteria: many ways to make the most out of nutrients. Nat Rev Microbiol 6:613-24.
121. Deutscher J. 2008. The mechanisms of carbon catabolite repression in bacteria. Curr Opin Microbiol 11:87-93.
122. Fujita Y. 2009. Carbon catabolite control of the metabolic network in Bacillus subtilis. Biosci Biotechnol Biochem 73:245-59.
123. Galinier A. 2018. [Carbon catabolite repression or how bacteria choose their favorite sugars]. Med Sci (Paris) 34:531-539.
124. Singh KD, Schmalisch MH, Stulke J, Gorke B. 2008. Carbon catabolite repression in Bacillus subtilis: quantitative analysis of repression exerted by different carbon sources. J Bacteriol 190:7275-84.

125. Schumacher MA, Allen GS, Diel M, Seidel G, Hillen W, Brennan RG. 2004. Structural basis for allosteric control of the transcription regulator CcpA by the phosphoprotein HPr-Ser46-P. Cell 118:731-741.
126. Deutscher J, Kuster E, Bergstedt U, Charrier V, Hillen W. 1995. Protein kinase-dependent HPr/CcpA interaction links glycolytic activity to carbon catabolite repression in gram-positive bacteria. Mol Microbiol 15:1049-53.
127. Mijakovic I, Poncet S, Galinier A, Monedero V, Fieulaine S, Janin J, Nessler S, Marquez JA, Scheffzek K, Hasenbein S, Hengstenberg W, Deutscher J. 2002. Pyrophosphate-producing protein dephosphorylation by HPr kinase/phosphorylase: a relic of early life? Proc Natl Acad Sci U S A 99:13442-7.
128. Weickert MJ, Adhya S. 1992. A family of bacterial regulators homologous to Gal and Lac repressors. J Biol Chem 267:15869-74.
129. Zalieckas JM, Wray LV, Jr., Fisher SH. 1999. trans-acting factors affecting carbon catabolite repression of the hut operon in Bacillus subtilis. J Bacteriol 181:2883-8.
130. Henkin TM, Grundy FJ, Nicholson WL, Chambliss GH. 1991. Catabolite repression of alpha-amylase gene expression in Bacillus subtilis involves a trans-acting gene product homologous to the Escherichia coli lacl and galR repressors. Mol Microbiol 5:575-84.
131. Miwa Y, Saikawa M, Fujita Y. 1994. Possible function and some properties of the CcpA protein of Bacillus subtilis. Microbiology (Reading) 140 (Pt 10):2567-75.
132. Miwa Y, Fujita Y. 2001. Involvement of two distinct catabolite-responsive elements in catabolite repression of the Bacillus subtilis myo-inositol (iol) operon. J Bacteriol 183:5877-84.
133. Miwa Y, Nakata A, Ogiwara A, Yamamoto M, Fujita Y. 2000. Evaluation and characterization of catabolite-responsive elements (cre) of Bacillus subtilis. Nucleic Acids Res 28:1206-10.
134. Schumacher MA, Sprehe M, Bartholomae M, Hillen W, Brennan RG. 2011. Structures of carbon catabolite protein A-(HPr-Ser46-P) bound to diverse catabolite response element sites reveal the basis for high-affinity binding to degenerate DNA operators. Nucleic Acids Res 39:2931-42.
135. Gosseringer R, Kuster E, Galinier A, Deutscher J, Hillen W. 1997. Cooperative and non-cooperative DNA binding modes of catabolite control protein CcpA from Bacillus megaterium result from sensing two different signals. J Mol Biol 266:665-76.
136. Turinsky AJ, Grundy FJ, Kim JH, Chambliss GH, Henkin TM. 1998. Transcriptional activation of the Bacillus subtilis ackA gene requires sequences upstream of the promoter. J Bacteriol 180:5961-7.
137. Moreno MS, Schneider BL, Maile RR, Weyler W, Saier MH, Jr. 2001. Catabolite repression mediated by the CcpA protein in Bacillus subtilis: novel modes of regulation revealed by whole-genome analyses. Mol Microbiol 39:1366-81.
138. Marciniak BC, Pabijaniak M, de Jong A, Duhring R, Seidel G, Hillen W, Kuipers OP. 2012. High- and low-affinity cre boxes for CcpA binding in Bacillus subtilis revealed by genome-wide analysis. BMC Genomics 13:401.
139. Henrissat B. 1991. A classification of glycosyl hydrolases based on amino acid sequence similarities. Biochem J 280 (Pt 2):309-16.
140. Henrissat B, Bairoch A. 1993. New families in the classification of glycosyl hydrolases based on amino acid sequence similarities. Biochem J 293 (Pt 3):781-8.
141. Davies G, Henrissat B. 1995. Structures and mechanisms of glycosyl hydrolases. Structure 3:853-9.
142. Sjogren J, Collin M. 2014. Bacterial glycosidases in pathogenesis and glycoengineering. Future Microbiol 9:1039-51.
143. Vermassen A, Leroy S, Talon R, Provot C, Popowska M, Desvaux M. 2019. Cell Wall Hydrolases in Bacteria: Insight on the Diversity of Cell Wall Amidases, Glycosidases and Peptidases Toward Peptidoglycan. Front Microbiol 10:331.

144. Juers DH, Heightman TD, Vasella A, McCarter JD, Mackenzie L, Withers SG, Matthews BW. 2001. A structural view of the action of Escherichia coli (lacZ) beta-galactosidase. Biochemistry 40:14781-94.
145. Juers DH, Matthews BW, Huber RE. 2012. LacZ beta-galactosidase: structure and function of an enzyme of historical and molecular biological importance. Protein Sci 21:1792-807.
146. Wheatley RW, Lo S, Jancewicz LJ, Dugdale ML, Huber RE. 2013. Structural explanation for allolactose (lac operon inducer) synthesis by lacZ beta-galactosidase and the evolutionary relationship between allolactose synthesis and the lac repressor. J Biol Chem 288:12993-3005.
147. Bieberich E. 2014. Synthesis, Processing, and Function of N-glycans in N-glycoproteins. Adv Neurobiol 9:47-70.
148. Garbe J, Collin M. 2012. Bacterial hydrolysis of host glycoproteins - powerful protein modification and efficient nutrient acquisition. J Innate Immun 4:121-31.
149. Du JJ, Klontz EH, Guerin ME, Trastoy B, Sundberg EJ. 2020. Structural insights into the mechanisms and specificities of IgG-active endoglycosidases. Glycobiology 30:268-279.
150. Bhattacharya D, Nagpure A, Gupta RK. 2007. Bacterial chitinases: properties and potential. Crit Rev Biotechnol 27:21-8.
151. Frederiksen RF, Paspaliari DK, Larsen T, Storgaard BG, Larsen MH, Ingmer H, Palcic MM, Leisner JJ. 2013. Bacterial chitinases and chitin-binding proteins as virulence factors. Microbiology (Reading) 159:833-847.
152. Gerlach JQ, Kilcoyne M, Farrell MP, Kane M, Joshi L. 2012. Differential release of high mannose structural isoforms by fungal and bacterial endo-beta-N-acetylglucosaminidases. Mol Biosyst 8:1472-81.
153. Karamanos Y, Bourgerie S, Barreaud JP, Julien R. 1995. Are there biological functions for bacterial endo-N-acetyl-beta-D-glucosaminidases? Res Microbiol 146:437-43.
154. Bohle LA, Mathiesen G, Vaaje-Kolstad G, Eijsink VG. 2011. An endo-beta-N-acetylglucosaminidase from Enterococcus faecalis V583 responsible for the hydrolysis of high-mannose and hybrid-type N-linked glycans. FEMS Microbiol Lett 325:123-9.
155. Collin M, Fischetti VA. 2004. A novel secreted endoglycosidase from Enterococcus faecalis with activity on human immunoglobulin G and ribonuclease B. J Biol Chem 279:22558-70.
156. Leisner JJ, Larsen MH, Ingmer H, Petersen BO, Duus JO, Palcic MM. 2009. Cloning and comparison of phylogenetically related chitinases from Listeria monocytogenes EGD and Enterococcus faecalis V583. J Appl Microbiol 107:2080-7.
157. Vaaje-Kolstad G, Bohle LA, Gaseidnes S, Dalhus B, Bjoras M, Mathiesen G, Eijsink VG. 2012. Characterization of the chitinolytic machinery of Enterococcus faecalis V583 and high-resolution structure of its oxidative CBM33 enzyme. J Mol Biol 416:239-54.
158. Hamid R, Khan MA, Ahmad M, Ahmad MM, Abdin MZ, Musarrat J, Javed S. 2013. Chitinases: An update. J Pharm Bioallied Sci 5:21-9.
159. Chen W, Jiang X, Yang Q. 2020. Glycoside hydrolase family 18 chitinases: The known and the unknown. Biotechnol Adv 43:107553.
160. Chen JK, Shen CR, Liu CL. 2010. N-acetylglucosamine: production and applications. Mar Drugs 8:2493-516.
161. Funkhouser JD, Aronson NN, Jr. 2007. Chitinase family GH18: evolutionary insights from the genomic history of a diverse protein family. BMC Evol Biol 7:96.
162. Chaudhuri S, Bruno JC, Alonzo F, 3rd, Xayarath B, Cianciotto NP, Freitag NE. 2010. Contribution of chitinases to Listeria monocytogenes pathogenesis. Appl Environ Microbiol 76:7302-5.
163. DebRoy S, Dao J, Soderberg M, Rossier O, Cianciotto NP. 2006. Legionella pneumophila type II secretome reveals unique exoproteins and a chitinase that promotes bacterial persistence in the lung. Proc Natl Acad Sci U S A 103:19146-51.
164. Larsen MH, Leisner JJ, Ingmer H. 2010. The chitinolytic activity of Listeria monocytogenes EGD is regulated by carbohydrates but also by the virulence regulator PrfA. Appl Environ Microbiol 76:6470-6.

165. Frederiksen RF, Yoshimura Y, Storgaard BG, Paspaliari DK, Petersen BO, Chen K, Larsen T, Duus J, Ingmer H, Bovin NV, Westerlind U, Blixt O, Palcic MM, Leisner JJ. 2015. A diverse range of bacterial and eukaryotic chitinases hydrolyzes the LacNAc (Galβ1-4GlcNAc) and LacdiNAc (GalNAcβ1-4GlcNAc) motifs found on vertebrate and insect cells. J Biol Chem 290:5354-66.
166. Fairbanks AJ. 2017. The ENGases: versatile biocatalysts for the production of homogeneous N-linked glycopeptides and glycoproteins. Chem Soc Rev 46:5128-5146.
167. Garbe J, Sjogren J, Cosgrave EF, Struwe WB, Bober M, Olin AI, Rudd PM, Collin M. 2014. EndoE from Enterococcus faecalis hydrolyzes the glycans of the biofilm inhibiting protein lactoferrin and mediates growth. PLoS One 9:e91035.
168. Naegeli A, Bratanis E, Karlsson C, Shannon O, Kalluru R, Linder A, Malmstrom J, Collin M. 2019. Streptococcus pyogenes evades adaptive immunity through specific IgG glycan hydrolysis. J Exp Med 216:1615-1629.
169. Zhang A, Mo X, Zhou N, Wang Y, Wei G, Chen J, Chen K, Ouyang P. 2020. A novel bacterial beta-N-acetyl glucosaminidase from Chitinolyticbacter meiyuanensis possessing transglycosylation and reverse hydrolysis activities. Biotechnol Biofuels 13:115.
170. Roberts G, Tarelli E, Homer KA, Philpott-Howard J, Beighton D. 2000. Production of an endo-beta-N-acetylglucosaminidase activity mediates growth of Enterococcus faecalis on a high-mannose-type glycoprotein. J Bacteriol 182:882-90.
171. Val-Cid C, Biarnes X, Faijes M, Planas A. 2015. Structural-Functional Analysis Reveals a Specific Domain Organization in Family GH20 Hexosaminidases. PLoS One 10:e0128075.
172. Itoh Y, Wang X, Hinnebusch BJ, Preston JF, 3rd, Romeo T. 2005. Depolymerization of beta-1,6-N-acetyl-D-glucosamine disrupts the integrity of diverse bacterial biofilms. J Bacteriol 187:382-7.
173. Kaplan JB, Ragunath C, Ramasubbu N, Fine DH. 2003. Detachment of Actinobacillus actinomycetemcomitans biofilm cells by an endogenous beta-hexosaminidase activity. J Bacteriol 185:4693-8.
174. Kaplan JB, Ragunath C, Velliyagounder K, Fine DH, Ramasubbu N. 2004. Enzymatic detachment of Staphylococcus epidermidis biofilms. Antimicrob Agents Chemother 48:2633-6.

Author Contributions

The work present in this dissertation was conducted by myself except for the following. Preliminary observations associated with Chapter 2, Figure 1A-D was done by Vijayalakshmi Iyer. The DNA microarray associated with Chapter 2 was conducted by Matthew Ramsey with assistance by Michael Gilmore. The subsequent transcriptomic analysis of the *rpoN* mutant DNA microarray was contributed by Vijayalakshmi S Iyer. Assessment of the *rpoN* and *ccpA* mutants, as well as their respective complements, under drip-flow biofilm conditions with MM9YEGC as the media composition (Chapter 2, Figure 7A and C) was conducted by Srivatsan Parthasarathy. Examination of the *rpoN* and *ccpA* mutants in the catheter-associated urinary tract infection (CAUTI) model was performed by Lynn Hancock, Vijayalakshmi Iyer, Sriram Varahan, and Theresa L Barke. Examination of the *rpoN* mutant in the rabbit endocarditis model was performed by Sally Olson with accompaniment by Lynn Hancock, Vijayalakshmi Iyer, Sriram Varahan, and Theresa L Barke. The assessment of the triple GH18 glycosidase mutant (Δ*ef0114*Δ*ef0362-61*Δ*ef2863*) (Chapter 3, Figure 11) in the CAUTI model was performed by Nancy Schwarting with accompaniment by myself, Srivatsan Parthasarathy, and Lynn Hancock. The following individuals contributed to the construction of in-frame markerless deletion mutants or in-frame markerless complements throughout this work, Vijayalakshmi Iyer, Matthew Gorman, Zakria Abdullahi, Emmaleigh Hancock, Andrew Henderson, Ian Huck, Analaura Cortez, and Srivatsan Parthasarathy.

Chapter 2: Influence of the alternative sigma factor RpoN on global gene expression and carbon catabolism in *Enterococcus faecalis* V583

Abstract

The alternative sigma factor σ^{54} has been shown to regulate the expression of a wide array of virulence-associated genes in bacterial pathogens as well as central metabolism. In Gram-positive organisms the σ^{54} is commonly associated with carbon metabolism. In this study, we show that the *Enterococcus faecalis* alternative sigma factor σ^{54} (RpoN) and its cognate enhancer binding protein MptR, are essential for mannose utilization and are primary contributors to glucose uptake through the Mpt phosphotransferase system. To gain further insight into how RpoN contributes to global transcriptional changes, we performed microarray transcriptional analysis of strain V583 and an isogenic *rpoN* mutant grown in a chemically defined medium with glucose as the sole carbon source. Transcript abundance from 340 genes was differentially affected in the *rpoN* mutant, and whose predicted functions mainly related to nutrient acquisition. Among these differentially expressed genes included those with predicted *cre* sites, consistent with loss of repression by the major carbon catabolite repressor, CcpA. To determine if the inability to efficiently metabolize glucose/mannose affected infection outcome, we utilized two distinct infection models. We found that the *rpoN* mutant is significantly attenuated in both rabbit endocarditis and murine catheter associated urinary tract infection (CAUTI). We examined a *ccpA* mutant in the CAUTI model and show that the absence of carbon catabolite control also significantly attenuates bacterial tissue burden in this model. Our data highlight the contribution of central carbon metabolism to growth of *E. faecalis* at various sites of infection.

Importance

Hospital acquired infections account for 2 billion dollars in increased healthcare expense annually, causing more than 100,000 deaths in the U.S. alone. Enterococci are the 2nd leading cause of hospital acquired infections. They form biofilms at surgical sites and are often associated with infections of the urinary tract following catheterization. Nutrient uptake and growth are key factors that influence their ability to cause disease. Our research identified a large set of genes that illuminate nutrient uptake pathways in enterococci. Perturbation of the metabolic circuit reduces virulence in a rabbit endocarditis model as well as in catheter associated urinary tract infection in mice. Targeting metabolic pathways important in infection may lead to new treatments against multidrug resistant enterococcal infections.

Introduction

Enterococci have emerged as leading causes of hospital associated infections often associated with biofilms, including endocarditis and catheter associated urinary tract infections (CAUTI) (1). Both disease manifestations for endocarditis and CAUTI are thought to be biofilm-mediated and enterococci now rank as the second leading cause of CAUTI in U.S. hospitals (1). The ability of enterococci to cause such infections is, in part, due to their ability to adapt and survive in a variety of host environments, which are often nutrient poor (2). Critical nutrient substrates that permit microbial proliferation and induce pathology at the site of infection remain to be defined for many types of infection. While several studies have examined transcriptional profiles of enterococci grown in urine, serum and abscesses (3-5), little is known of preferred nutrients and how *E. faecalis* acquires them in the host.

We previously showed that the alternative sigma factor σ^{54} (RpoN) contributes to *in vitro* biofilm formation in *E. faecalis* as an *rpoN* deletion mutant was shown to have an altered biofilm matrix composition when grown in rich medium (6). The *rpoN* mutant was less efficient at autolysis (less eDNA in the matrix) and the biofilm became more labile to protease K treatment compared with the parental strain. In addition, σ^{54} (RpoN) is also known to regulate several phosphotransferase systems (PTS) in *E. faecalis,* including a mannose/glucose permease Mpt (7) making it a good candidate to explore its contribution to *in vivo* fitness.

In contrast to other sigma factors, σ^{54} is unable to initiate open complex formation upon association with target DNA and the core RNA polymerase and requires the assistance of a bacterial enhancer binding protein (bEBP) (8). In *E. faecalis,* four bEBPs are encoded on the V583 genome (MptR, MpoR, MphR, LpoR) with a 5th (XpoR) disrupted by an insertion element (7). The genes encoding each of these bEBPs are positioned immediately upstream of their respective sugar PTS genes (7). The best characterized PTS in *E. faecalis* is the aforementioned Mpt mannose/glucose permease

(7, 9, 10), owing to the fact that components of this PTS complex are known cellular receptors for class IIa and IIc bacteriocins (11).

Work by Opsata et al. (10) characterized the transcriptional profile of a mutant of *mptD*, a component of the Mpt PTS complex, that conferred resistance to pediocin PA-1, a known class IIa bacteriocin. These authors identified a number of differentially expressed genes in the *mptD* mutant that contained putative catabolite responsive elements (*cre*) sites based on similarity to consensus *cre* sites from *Bacillus subtilis* (12). *Cre* sites are pseudo-palindromes and are considered a low-conserved consensus sequence of WTGNNARCGNWWWCAW, where strongly conserved residues are underlined (13). In low G-C Gram-positive bacteria, c*re* sites on DNA are bound by a protein complex consisting of the carbon catabolite repressor CcpA and the phosphorylated Ser-46 form of Hpr (Hpr-46-P) (14). CcpA is a global regulatory protein that plays a critical role in regulating the expression of genes involved in secondary catabolite uptake and utilization in Gram-positive bacteria (15).

Because σ^{54} has been shown to regulate the expression of various genes involved in metabolism and virulence in other bacteria (16-20), we performed a microarray transcriptional analysis to identify genes whose expression was differentially expressed in the *E. faecalis* V583 strain and an isogenic Δ*rpoN* mutant. Furthermore, we also tested the role of RpoN and CcpA in biofilm formation under drip-flow conditions, as well as colonization *in vivo* using a rabbit endocarditis infection model and a murine model of catheter associated urinary tract infection to determine whether RpoN-dependent metabolic pathways contribute to biofilm-associated infections. To our knowledge, this report represents the first examination of the contribution of either σ^{54} (RpoN) or CcpA to *in vivo* fitness in *E. faecalis*. Overall, this study provides important evidence linking basic

metabolism with *in vivo* growth and provides the rationale for several distinct pathways that could be targeted as a potential therapeutic for treating enterococcal infections.

Materials and Methods

Bacterial strains and growth conditions:

Bacterial strains used in this study are listed in Table S1. For propagation of plasmids, *Escherichia coli* ElectroTen-Blue from Stratagene was cultivated in Luria-Bertani (LB) broth supplemented with appropriate antibiotics whenever necessary. Unless otherwise mentioned, *E. faecalis* was cultured in Todd-Hewitt broth (THB; BD Biosciences) containing appropriate antibiotics. For antibiotic selection, chloramphenicol (Cm) at a concentration of 10µg/ml and 15µg/ml was used for *E. coli* and *E. faecalis* respectively.

Construction of in-frame markerless deletion:

Using the temperature sensitive cloning vector, pLT06 (21), isogenic in-frame deletion mutants of the genes encoding the four bEBPs were generated in *E. faecalis* V583. Upstream and downstream flaking regions of the targeted activators were amplified using primers listed in Table S2. The primer pairs MptRP1/MptRP2 and MptRP3/MptRP4 were used to amplify flanking regions upstream and downstream of *mptR* respectively. To facilitate cloning, primers MptRP1/ MptRP2 were designed with EcoRI/BamHI restriction sites respectively whereas MptRP3/MptRP4 were designed with BamHI/PstI sites respectively. For the construction of the insert, the amplified regions were digested with BamHI, ligated and re-amplified with MptRP1 and MptRP4. To generate pMG07 (*mptR* deletion vector), the amplified insert fragment was digested and ligated with EcoRI/PstI cut pLT06 cloning vector. The ligated vector and insert was electroporated into *E. coli* ElectroTen - Blue and correct constructs were identified by colony PCR. The construct was screened by restriction digest analysis and then electroporated into competent *E. faecalis* V583 cells. MG07 [V583Δ*mptR*] was subsequently generated as previously described (21) and confirmed by PCR using the primers MptR-Up and MptR-Down and the paired genetic revertant

from this screen was designated MG07R (V583Ω*mptR*). A similar approach was used to create all the remaining mutants and/or revertants used in this study (Table S1).

Construction of in-frame markerless complement:

Using the temperature sensitive cloning vector, pLT06 (21), isogeneic in-frame *ccpA* complement strain was generated in *E. faecalis* V583. The entirety of the *ccpA* gene, including its upstream and downstream flanking DNA regions was amplified using the primer pair CcpAP1/CcpAP4 (Table S*2*). For cloning purposes, CcpAP1 and CcpAP4 were designed with EcoRI and PstI restriction sites, respectively. The amplified region was digested with EcoRI and PstI and ligated into the EcoRI/PstI digested pLT06 cloning vector and then electroporated into *E. coli* ElectroTen-Blue cells. The presence of the correct clone containing the recombinant plasmid was identified by colony PCR. The plasmid construct was confirmed by restriction digest analysis and sequenced. This plasmid was designated pEK26 and was subsequently electroporated into *E. faecalis* V583Δ*ccpA* cells. The insertion and excision of pEK26 to generate V583Δ*ccpA*::*ccpA* [EK26] was performed as previously described (21) and confirmed by colony PCR using the primers CcpAUp and CcpADown.

Growth assessment in nutrient limiting conditions:

Using a single colony of each strain, liquid cultures were started in THB and grown at 37°C overnight. For growth analysis, overnight cultures were diluted 1:100 in complete defined medium (CDM) (22, 23) supplemented with a range of either glucose, mannose, fructose, or N-acetylglucosamine concentrations (10mM and 100mM). Growth was monitored for 12 hours in an Infinite M200 Pro plate reader (Tecan Trading AG, Switzerland) at 37°C with orbital shaking at 250 rpm. The experiment was biologically repeated three times, which included three technical

replicates each time. A similar approach was used to assess the growth of *rpoN* and *ccpA* mutant strains in the drip-flow biofilm growth medium, MM9YEGC or MM9YEFC, relative to V583.

Microarray analysis:

Colony biofilms (24) were grown similar to those reported previously (25). Briefly, *E. faecalis* strains were grown overnight in 2mL of CDM cultures with 100 mM glucose and 20μM hematin added, shaking at 150 rpm at 37°C. Overnight cultures were sub-cultured 1:1000 in the same growth conditions and allowed to grow to an OD of approximately 0.2 then diluted in fresh medium to an A600 of 0.1 (approximately 10^8 cells/mL). 10μL of this solution was added in three discrete spots to a 25 mm, 0.2 μm pore polycarbonate membrane affixed to the surface of CDM+1% agarose solid medium in a 100mm Petri dish. Plates were incubated ~16 hours at 37°C and polycarbonate membranes were moved to unoccupied areas of the dish and further incubated at 37°C for an additional 4 hours. Membranes were then transferred to 1.5mL microcentrifuge tubes containing 1mL of RNALater (Ambion) and vortexed until no visible cells remained attached to the membrane surface. Cells were pelleted by centrifugation (2 mins at 10,000xg), supernatants and cell pellets stored for RNA purification. RNA purification and Affymetrix microarray preparations were performed as described elsewhere (25, 26).

Array analyses were performed using RMA analysis through the University of Oklahoma Bioinformatics Core Facility (http://www.ou.edu/microarray/). 2Sigma analysis was used to determine the significant difference of fold change with a 95% confidence interval. Significant fold changes were considered for values greater than 3.4 fold for the *rpoN* mutant vs. wild-type and greater than 1.8 fold for the complement vs. wild-type comparisons. The raw array data has been deposited in the NCBI Gene Expression Omnibus (http//:www.ncbi.nlm.nih.gov/projects/geo/) under accession number GSE40237.

***In silico* analysis of identified proteins:**

Signal peptide sequences were predicted using SignalP 5.0 and SignalP-HMM algorithms (http://www.cbs.dtu.dk/services/SignalP-5.0/) (27). Transmembrane domains were predicted using TMHMM (hidden Markov model) (http://www.cbs.dtu.dk/services/TMHMM/) (28) and TMpred (transmembrane helix propensity scale) (https://embnet.vital-it.ch/software/TMPRED_form.html) (29). LPXTG-motifs were identified using PHI-Blast and the pattern query for the sortase cell wall sorting signal (L-P-[SKTAQEHLDN]-[TA]-[GN]-[EDASTV]) (30) with the *E. faecalis* collagen adhesion protein, Ace, as template query (31). Lipoprotein predictions were conducted using the Pred-Lipo software (http://www.compgen.org/tools/PRED-LIPO) (32). Default settings for Gram-positive bacteria were used in all cases.

Quantitative real time (q-RT) PCR:

Synthesis of cDNA was performed using Superscript III Reverse Transcriptase (Life Technologies) from 1 µg of DNase treated (Ambion Turbo DNase) RNA templates following the manufacturer's instructions (Zymo Research). Random hexamer primers (Invitrogen) were used in the initial synthesis reaction. The primers used in q-RT PCR analysis are listed in Table S2. The q-RT PCR reaction was performed with 1 µg of prepared cDNA and 300 nM of each primer using PowerUp SYBR Green Master Mix (ThermoFisher Scientific) on a Quant Studio 3 Real Time PCR system (ThermoFisher Scientific). Following denaturation at 95°C for three minutes, the q-RT PCR reaction was set for 50 cycles with 95°C for 10 seconds, 60°C for 20 seconds and 72°C for 10 seconds. Differential gene expression was calculated using the ΔΔCt method using the threshold cycle values for the gene of interest (*ef0019, ef2223, ef0891, ef1017, ef3210,* and *ef0255*)

and the endogenous control [*ef0005* (*gyrB*)]. Each qRT-PCR experiment was repeated with three biological replicates.

Biofilm formation assessment using a drip-flow biofilm reactor (DFBR):

The Drip-flow biofilm reactor (DFBR) was utilized as previously described (33, 34) to assess V583, Δ*rpoN*, Δ*rpoN::rpoN*, Δ*ccpA*, and Δ*ccpA::ccpA* strains on their ability to form biofilms. Briefly, the channels of the growth chamber of the DFBR were seeded with diluted overnight cultures grown in THB (1:100) in either MM9YEGC (G=15 mM glucose) or MM9YEFC (F=15 mM fructose) media and incubated at 37°C for 8 hours to allow initial adherence. Subsequently, 0.1X MM9YEGC or MM9YEFC media was fed into the 10° tilted growth chamber of the DFBR by inlet valves and tubing at 125 µL/min for 72 hours. Biofilm enumeration was conducted, aseptically, by removing the glass slides and scraping the biofilm into a 50 ml conical test tube containing 5mL 1X Phosphate Buffered Saline (PBS). Homogenization of the biofilm was conducted using a tissue tearor homogenizer (Bio-Spec Products) with a 15 second pulse, followed by serial dilution and plating on THB plates. The experiment was performed with three biological replicates.

Animal models:

All the procedures in the rabbit model to study experimental endocarditis and murine model for catheter associated urinary tract infection were performed in compliance with Animal Welfare Act and other federal statutes and regulations relating to animals and experiments involving animals. All animal protocols were approved by the Institutional Animal Care and Use Committee for Kansas State University (IACUC 3043, rabbit endocarditis) and (IACUC 3267, murine CAUTI).

Experimental endocarditis and determination of bacterial burden:

Left sided endocarditis was induced in New Zealand white rabbits (Charles River Laboratories International, Inc.) by introducing a polyethylene catheter with an internal diameter of 0.86 mm (Becton Dickinson, MD) followed by injection of bacterial cultures (10^7 CFU ; *E. faecalis* V583(35) and Δ*rpoN* (6)) via marginal ear vein after 24 hours of catheterization as previously described (36). In preparation for injections, bacterial cultures grown to stationary phase were washed twice and diluted to achieve a concentration of 10^7 CFU/ml in sterile saline. Group of eight rabbits were injected with each bacterial strain (V583 and Δ*rpoN*) and two negative controls were injected with sterile saline. The rabbits were monitored for 48 hrs after bacterial inoculation and euthanized by intraperitoneal administration of sodium pentobarbital. Immediately after euthanasia, a cardiac stick was performed to determine bacterial CFU in blood at the time of sacrifice. Bacterial burden in the heart, liver, spleen and kidney was assessed by plate count following previously described protocol (36) and expressed as log10 CFU/gm of tissue.

Murine model for catheter associated urinary tract infection (CAUTI):

Catheter associated urinary tract infections using six-seven week old female wild-type C57BL/6 mice. The mice were anesthetized by isoflurane inhalation and a 5-6 mm platinum cured silicone implant tubing (Renasil Sil025; Braintree Inc) was transurethrally placed in the urinary bladder of the mice as previously described (37). Post implantation, the mice were injected with 50 µl inocula of either sterile PBS or bacterial suspension (~ $2x10^7$ CFU) by transurethral catheterization. The mice were monitored for 48 hours post implantation and infection. They were euthanized by cervical dislocation after inhalation of isoflurane. To determine the degree of infection, kidneys and bladder were harvested aseptically and their bacterial burden was determined. Also, the

silicone implant tubing was retrieved from the bladder and the bacterial burden enumerated using THB media.

Bioinformatics and statistical analysis:

Cre (Catabolite responsive elements) sites were identified upstream of the differentially expressed genes using the pattern analysis option in Regulatory Sequence Analysis Tools (http://rsat.ulb.ac.be/rsat/) using the *cre* consensus from Schumacher et al. (13) [WTGNNARCGNWWWCAW], as well as Miwa et al. [WTGWAARCGYWWWCW] (12) and allowing for a 1-bp mismatch. The statistical analysis of the various growth curves performed were measured using a one-way ANOVA test. The statistical analysis of the bacterial burden determined in the various organs in the endocarditis study and CAUTI was performed using GraphPad Prism 5 software (San Diego, CA). Statistical significance was measured using a non-parametric T-test (Mann-Whitney Test).

Results

RpoN and MptR regulate glucose uptake and are essential for mannose utilization

We previously demonstrated that deletion of *rpoN* has no growth defect in rich media, including tryptic soy broth and Todd-Hewitt broth (6). Several sugar uptake systems in *E. faecalis* are known to be regulated by RpoN (7). Therefore, it was of interest to determine whether RpoN contributed to fitness in a chemically defined medium (CDM) (22, 23) supplemented with varying sugars as the sole carbon source. As RpoN also requires a bEBP for open complex formation in order for transcription to proceed, we also evaluated the contribution of the four bEBPs in *E. faecalis* V583 by constructing deletion mutants for *lpoR*, *mphR*, *mpoR* and *mptR*. The fifth bEBP (XpoR) identified in *E. faecalis* possesses a natural insertion of an IS256 element in the *xpoR* gene in the *E. faecalis* V583 genome. Because of the location of the IS256 insertion within *xpoR*, it was unclear whether XpoR function was disrupted by the IS256 element, we therefore constructed a deletion mutant that removed the corresponding *xpoABCD* PTS system and assessed its contribution directly. The deletion of *mphR*, *mpoR*, *lpoR*, or *xpoABCD* did not impact growth when glucose or mannose was present as the sole carbon source (Figure S1). In contrast, the *rpoN* and *mptR* deletion mutants displayed poor growth. Figure 1A shows that both the *rpoN* and *mptR* mutants grew very poorly in CDM supplemented with 10mM glucose, and that this phenotype is complementable as the *rpoN* complement and the *mptR* genetic revertant grew equivalent to the parental strain.

A

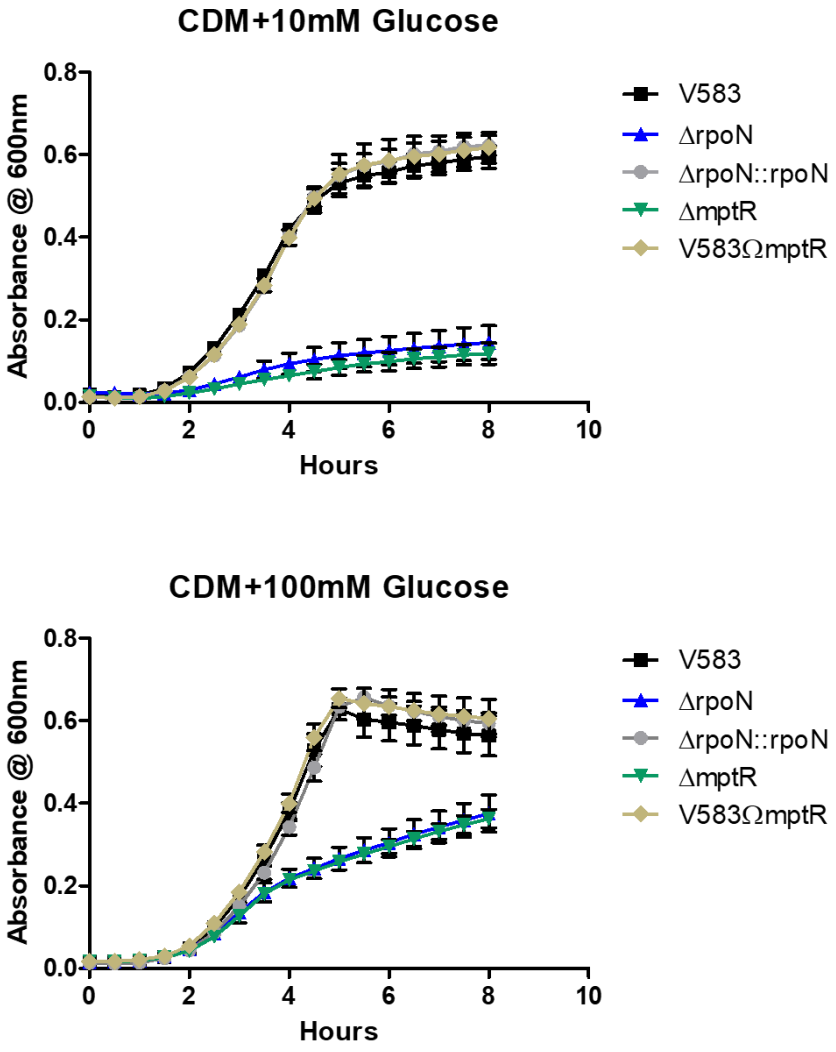

Figure 1A: Growth of *E. faecalis* in chemically defined medium with glucose indicated as the principal carbon sources. The respective sugar concentrations are indicated above each graph. Each graph is the average of three biological replicates, with three technical replicates each time (n=9) with standard error of the mean shown. The growth curves are shown in black (V583), blue (Δ*rpoN*), green (Δ*mptR*), grey (Δ*rpoN*::*rpoN*), and gold (V583Ω*mptR* revertant).

Because deletion of *rpoN* and *mptR* had such a drastic impact on glucose-dependent growth, it was of interest to determine whether a homolog of the primary glucose transporter (PtsG) in *Bacillus subtilis* contributed to glucose uptake in *E. faecalis*, we therefore constructed a deletion mutant of

ef1516 and assessed its growth in CDM supplemented with either 10mM or 100mM glucose (Figure S2). EF1516 shares approximately 39% amino acid sequence identity and 56% sequence similarity with PtsG in *B. subtilis*. We did not detect a role for EF1516 in growth with glucose as the sole carbon source in *E. faecalis,* as there was no significant difference between the *ef1516* mutant and the parental V583 strain (Figure S2).

To confirm that the poor growth of *mptR* related to the direct regulation of the Mpt PTS system, we also constructed and evaluated an *mptBACD* mutant. The *mptBACD* mutant phenocopied the growth of *mptR*, suggesting that the inability of *rpoN* and *mptR* mutants to activate expression of the Mpt PTS system is responsible for the poor growth in glucose-dependent conditions (Figure S1). At 100 mM glucose, the *rpoN* and *mptR* mutants showed improved growth but never achieved the maximal growth observed with the parental strain (OD600 ~ 0.4 vs. ~ 0.6), suggesting alternative routes of glucose uptake at increasing concentrations of glucose. In contrast, the growth defect of the mutants in CDM that included mannose as the principal carbon source was not rescued by supplementation with increasing the concentration of mannose (Figure 1B), suggesting that the Mpt PTS controlled by σ^{54} and MptR represents the sole mannose transporter in the cell.

B

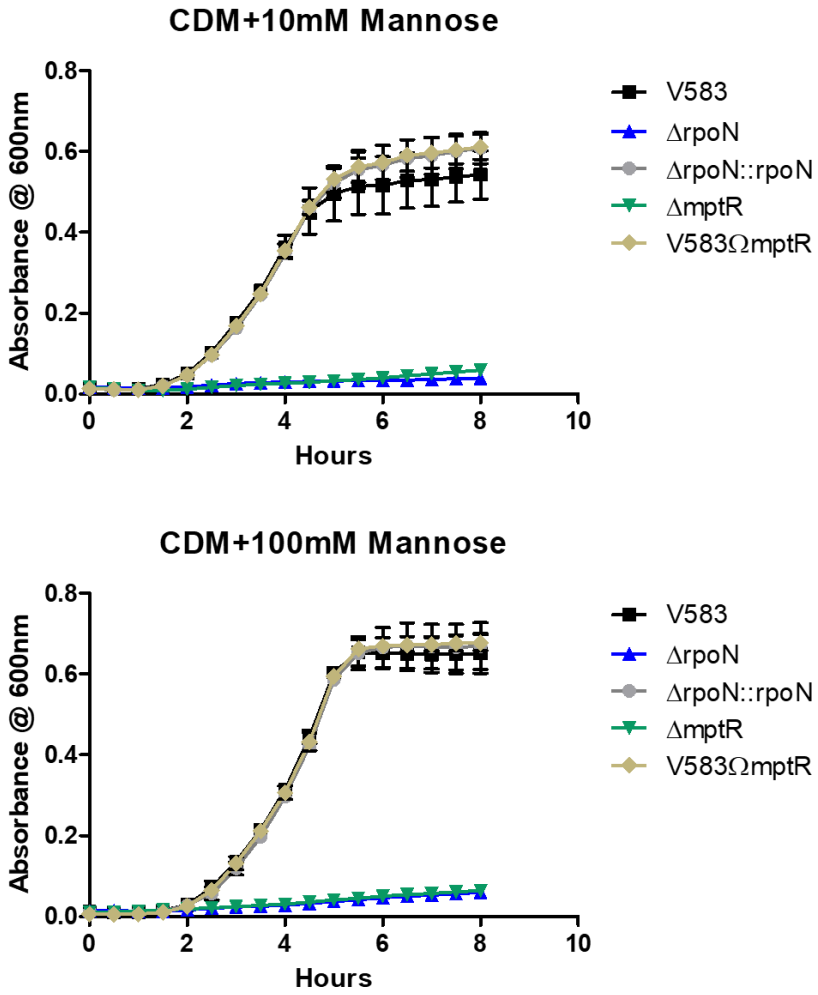

Figure 1B: Growth of *E. faecalis* in chemically defined medium with mannose indicated as the principal carbon sources. The respective sugar concentrations are indicated above each graph. Each graph is the average of three biological replicates, with three technical replicates each time (n=9) with standard error of the mean shown. The growth curves are shown in black (V583), blue (Δ*rpoN*), green (Δ*mptR*), grey (Δ*rpoN*::*rpoN*), and gold (V583Ω*mptR* revertant).

To ascertain the sugar specificity of the PTS controlled by MptR and σ^{54}, we also grew cells in CDM with N-acetylglucosamine (GlcNAc) and fructose as a carbon source. As shown in Figure 1C and 1D, the absence of either σ^{54} or MptR does not alter growth when N-acetylglucosamine or fructose is the main carbon source.

C

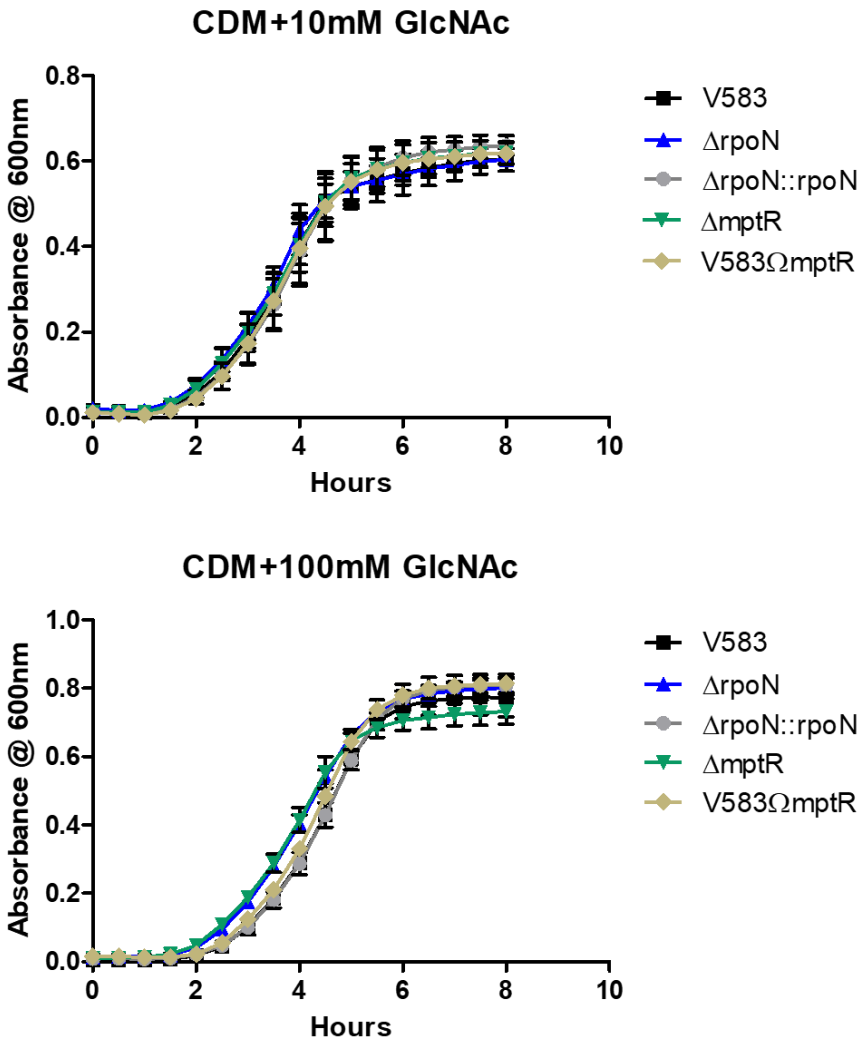

Figure 1C: Growth of *E. faecalis* in chemically defined medium with N-acetylglucosamine indicated as the principal carbon sources. The respective sugar concentrations are indicated above each graph. Each graph is the average of three biological replicates, with three technical replicates each time (n=9) with standard error of the mean shown. The growth curves are shown in black (V583), blue (Δ*rpoN*), green (Δ*mptR*), grey (Δ*rpoN*::*rpoN*), and gold (V583Ω*mptR* revertant).

D

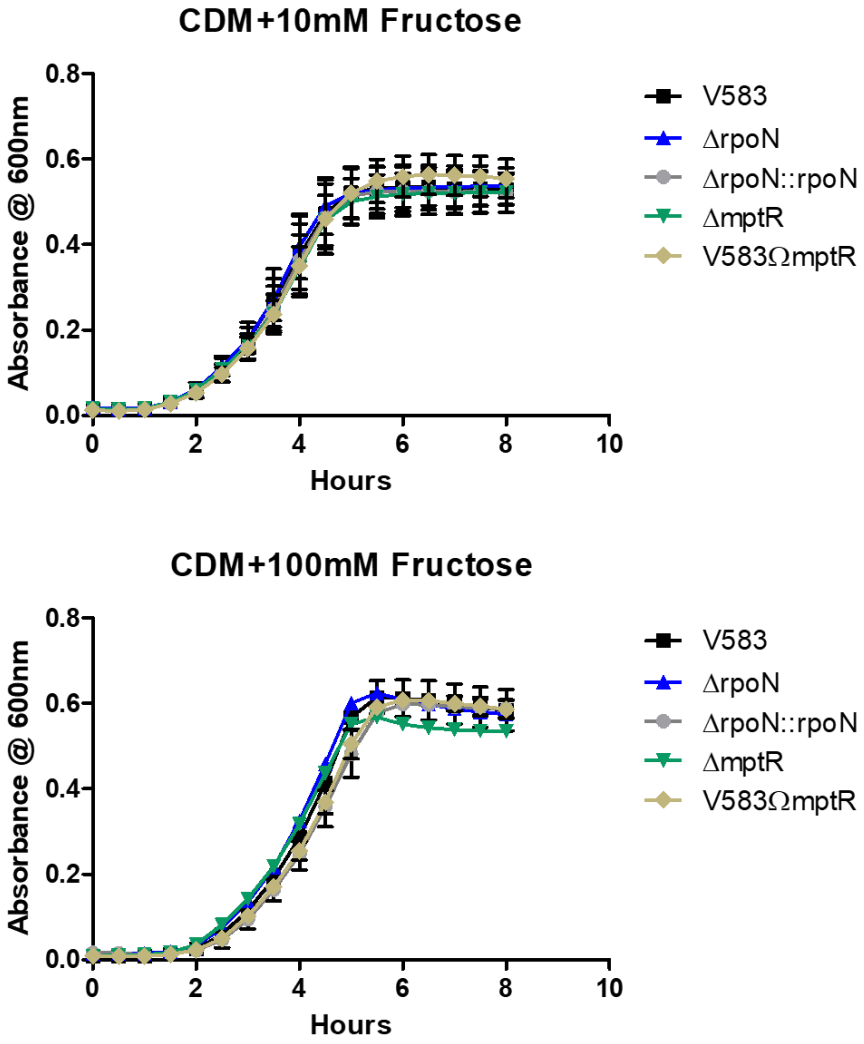

Figure 1D: Growth of *E. faecalis* in chemically defined medium with fructose indicated as the principal carbon sources. The respective sugar concentrations are indicated above each graph. Each graph is the average of three biological replicates, with three technical replicates each time (n=9) with standard error of the mean shown. The growth curves are shown in black (V583), blue (Δ*rpoN*), green (Δ*mptR*), grey (Δ*rpoN*::*rpoN*), and gold (V583Ω*mptR* revertant).

Transcriptional Analysis of *E. faecalis* V583Δ*rpoN*

RpoN orthologs impact global gene expression in a variety of bacteria, but the genes that they regulate are functionally divergent (19, 38, 39). In *E. faecalis*, the only genes predicted to be

directly regulated by RpoN are putative PTS operons, each of which contains the distinct -24/-12 promoter element (TTGGCACNNNNNTTGCT) thought to be responsive to RpoN (7). Because of its role in glucose uptake, we hypothesized that RpoN likely affects a larger regulatory gene network at the transcriptional level. Therefore, using DNA microarrays of *E. faecalis* strain V583, the transcriptional profile of V583Δ*rpoN* was compared to that of the parental strain V583 and an *rpoN* complemented strain. Compared to the parental strain and the *rpoN* complemented strain, mRNA abundance in the *rpoN* mutant differed for transcripts corresponding to 340 genes (Figure 2, Table S4). Of the 340 differentially expressed genes in the V583Δ*rpoN* strain, transcripts for 255 genes were increased and 85 genes were decreased (≥ 3-fold), compared to the parental and complemented strain. Of the differentially regulated genes, 23% are predicted to encode hypothetical proteins with no known function, 18% encode transport and binding proteins, 17% are energy metabolism related, and 13% encode PTS proteins. Of the six PTS systems known to contain the -24/-12 RpoN binding site in their promoter element (Mpt, Mpo, Mph, Lpo, Lpt, and Xpo), three were significantly downregulated (*mpt* (*ef0019-22*), *xpo* (*ef3210-13*) and *lpt* (*ef1017-19*)*;* 152-fold, 6-fold and 4-fold respectively) and no significant difference in expression was observed in the *lpo*, *mpo* and *mph* PTS systems.

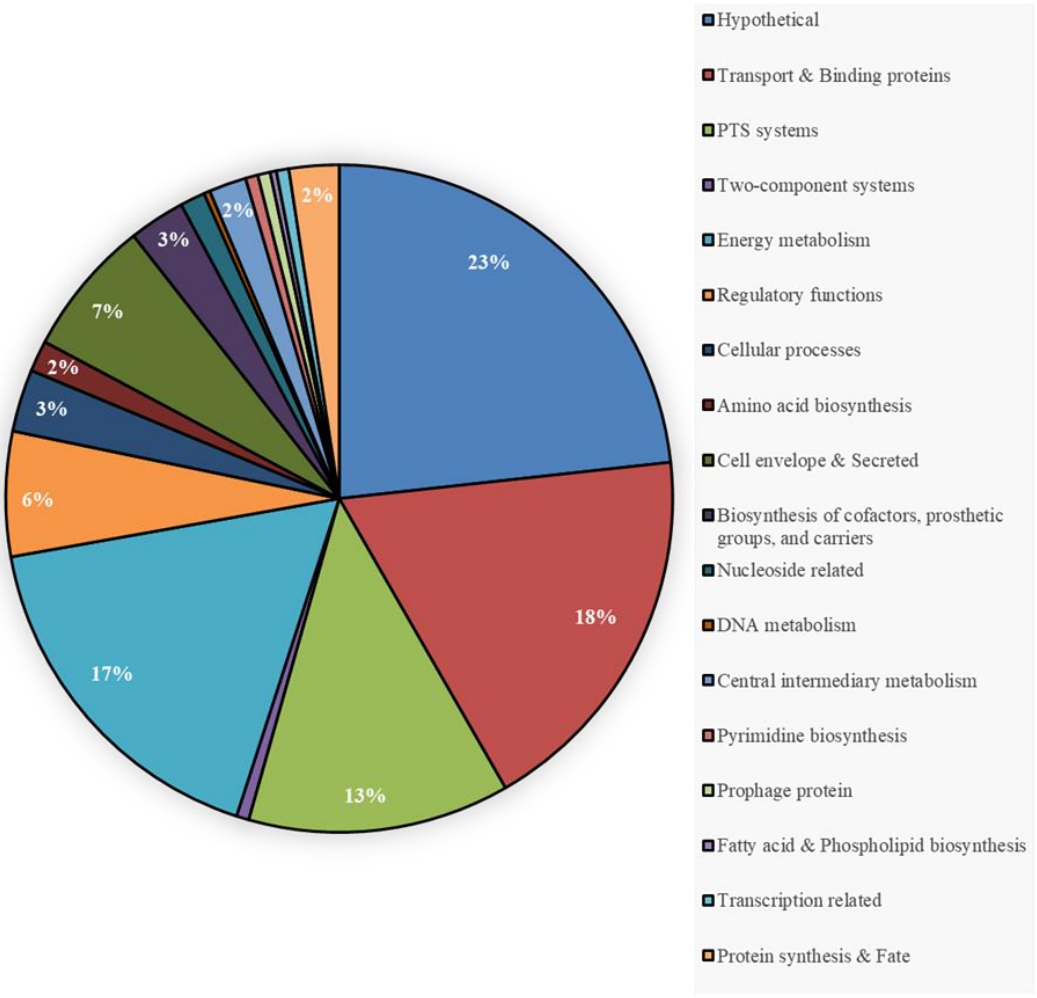

Figure 2: Pie chart depicting the functional distribution of the 340 differentially regulated genes in Δ*rpoN*. The number in each functional category is the percentage of the total differentially regulated genes.

Catabolite repression elements (*cre*) in differentially expressed genes in V583Δ*rpoN*

The increased expression levels of genes encoding several sugar uptake systems as well as ABC transporters in the transcription profile of the *rpoN* mutant suggested a loss of catabolite control. In order to determine the basis of such regulation, we searched the regions upstream of the differentially expressed genes in the *rpoN* mutant to identify *cre* sites. We used the *cre* consensus

sequences suggested for low G-C Gram-positive bacteria 5`-WTGNNARCGNWWWCAW-3` (13) as well as 5'-WTGWAARCGYWWWCW-3' (12) as our pattern queries and used the Regulatory Sequence Analysis Tool (http://rsat.ulb.ac.be/) allowing for a 1-bp mismatch to identify *cre* sites upstream of the genes that were upregulated in the *rpoN* mutant. Of the 255 genes that were upregulated in the *rpoN* mutant, *cre* sites were present in the promoter regions of 46 genes, and due to some loci comprising operons this accounts for 109 genes, which represents 42.74% of the upregulated genes in the *rpoN* mutant (Table S5). Of note, we identified a three gene operon (*ef1017-19*), which encodes the Lpt PTS complex that was downregulated in the *rpoN* mutant that also contained a *cre* site, indicating this operon may also be regulated by CcpA for expression.

Identification of cell-envelope associated or secreted gene products among the differentially expressed genes in the *rpoN* mutant that contain *cre* sites

To identify cell-envelope associated or secreted gene products from the pool of differentially expressed genes in the *rpoN* mutant that also contained *cre* sites, we analyzed the 112 differentially regulated gene products (109 upregulated, 3 downregulated in an *rpoN* mutant) identified in Table S5 for the presence of a signal peptide sequence and Signal Peptidase cleavage site (SignalP 5.0) followed by analysis for the presence of transmembrane domains (TMHMM/TMpred) or LPXTG-cell wall anchoring motifs using PHI-Blast and the pattern query for the sortase cell wall sorting signal (L-P-[SKTAQEHLDN]-[TA]-[GN]-[EDASTV]) (30) with the *E. faecalis* collagen adhesion protein, Ace, as template query (31). Identification of predicted lipoproteins was performed using Pred-Lipo. As summarized in Table 1, 36 of the 112 gene products analyzed contained a signal peptide sequence and/or predicted transmembrane helices, suggesting that these differentially expressed and *cre* site containing genes encode proteins that are cell-envelope

associated or secreted. Among these 36 genes, there are 27 predicted transport proteins, five of which are predicted lipoproteins (*ef1234*, *ef1397*, *ef2221*, *ef2234* and *ef2237*) involved in substrate binding associated with ABC transporters. One notable PTS system potentially regulated by the presence of a predicted *cre* site near the translation start site was EF0551-55. This PTS system resides within the known pathogenicity island present in V583 (40). In addition to transport functions, a putative family 8 polysaccharide lyase (EF3023) and a family 31 glycosyl hydrolase (EF1824) were the only gene products from this cohort that contain a predicted LPXTG-cell wall anchoring motif, suggesting that these proteins are anchored on the bacterial cell surface and interact with the external environment. Lastly, three of the 31 genes listed in Table 1 encode glycosyl hydrolases (*ef0114*, *ef0361* and *ef2863*) thought to be secreted into the external environment as they contain predicted signal peptides and signal peptidase cleavage sites. Encoded in the same operon as *ef0361*, *ef0362* encodes a chitin-binding protein that is also predicted to be secreted into the surrounding environment. Overall, this set of *in silico* analyses indicates that a relatively small cohort of differentially expressed genes in the *rpoN* mutant that also contain predicted *cre* sites are likely to be involved in the interaction of the bacterial cell with its environment.

Table 1: Putative cell-enveloped associated or secreted gene products that are differentially regulated in the *rpoN* mutant that also possess *cre* sites

Operon	Gene	Function	Fold Change	Start	End	*cre* Sequence of operon or gene	Signal Peptide Prob.	No. of TMHs
EF0104-08	EF0108	C4-dicarboxylate transporter, putative	13.04	-146	-132	ATGAAAGCGCATTCT	0.997	13
	EF0114	Glycosyl hydrolase, family 20	48.20	-35	-21	GTGTATGCGCTTTCT	0.980	1
EF0292-91	EF0292	PTS system, IIC component	6.62	-51	-37	ATGTAAACGGATACA	N/A	10
EF0362-61	EF0361	chitinase, family 2	69.31	-41	-27	CTGTAAGCGCATACA	1.000	0
	EF0362	Chitin binding protein, putative	83.75	-41	-27	CTGTAAGCGCATACA	1.000	1
	EF0439	immunity protein PlnM, putative	13.54	-49	-35	ATGAAAACGTTATCA	N/A	2
EF0551-55	EF0552	PTS system, IIC component	6.21	-85	-70	ATACAAACGCTTTCAT	N/A	6
	EF0553	PTS system, IID component	11.35	-85	-70	ATACAAACGCTTTCAT	N/A	5
	EF0569	potassium-transporting ATPase, subunit C	-3.16	-169	-154	ATGCTAGTGGAATCAA	0.979	1
	EF0635	amino acid permease family protein	-5.11	-270	-255	TTAGGAGCGTAAACAT	0.920	12
EF1017-19	EF1019	PTS system, IIB component	-4.49	-173	-158	TTGGAAACGCACACAA	N/A	8
	EF1207	citrate carrier protein, CCS family	8.54	-53	-39	ATGTAAACGTTTTCT	N/A	12
EF1232-34	EF1232	ABC transporter, permease protein	8.63	-81	-67	ATGTAAGGGTTTACA	N/A	6
	EF1233	ABC transporter, permease protein	13.83	-81	-67	ATGTAAGGGTTTACA	0.999	6
	EF1234	ABC transporter, substrate-binding protein, putative	12.52	-81	-67	ATGTAAGGGTTTACA	1.000	6
EF1392-1400	EF1397	molybdenum ABC transporter, molybdenum-binding protein	23.85	-38	-24	GTGTAAACGTTAACA	0.999	1
	EF1398	molybdenum ABC transporter, permease protein	26.30	-38	-24	GTGTAAACGTTAACA	N/A	5
	EF1400	cadmium-translocating P-type ATPase	6.43	-38	-24	GTGTAAACGTTAACA	N/A	6
EF1663-1557	EF1657	PTS IIC membrane protein, putative	5.80	-61	-47	ATGTAAACGCATACA	0.765	8
	EF1800	Hypothetical protein	4.01	-61	-47	ATGAAAGCGTGTTCA	1.000	2
EF1805-01	EF1802	PTS system, IID component	7.35	-30	-16	TTGAAAGCGTTTACT	N/A	5
	EF1803	PTS system, IIC component	8.28	-30	-16	TTGAAAGCGTTTACT	N/A	7
	EF1824	Glycosyl hydrolase, family 31	6.82	-255	-241	ATGAAAACGCATTCA	0.827	1
*EF1929-27	EF1927	glycerol uptake facilitator protein	36.40	-146 -36	-132 -22	TTGAAAGCGTTGTCT TTGAAATCGTTTTCT	0.724	6

EF2223-21	EF2221	ABC transporter, substrate-binding protein	128.09	-38	-24	ATGAAAACGCTATTA	1.000	1
	EF2222	ABC transporter, permease protein	114.80	-38	-24	ATGAAAACGCTATTA	0.996	6
	EF2223	ABC transporter, permease protein	257.25	-38	-24	ATGAAAACGCTATTA	0.986	6
EF2237-32	EF2232	ABC transporter, permease protein	4.20	-35	-21	ATTAAAGCGCTTTCT	0.997	6
	EF2233	ABC transporter, permease protein	8.46	-35	-21	ATTAAAGCGCTTTCT	0.972	5
	EF2234	sugar ABC transporter, sugar-binding protein, putative	17.24	-35	-21	ATTAAAGCGCTTTCT	1.000	1
	EF2237	Lipoprotein	7.17	-35	-21	ATTAAAGCGCTTTCT	1.000	1
	EF2863	Endo-beta-N-acetylglucosaminidase	62.34	-45	-31	TTGTAAGCGCTAACA	1.000	1
	EF3023	Polysaccharide lyase, family 8	8.85	-209	-195	GTGAAAGCGTAAACA	1.000	2
*EF3142-34	EF3138	PTS system, IID component	17.41	-374 -68	-360 -34	ATGAAAAGGCATTCA ATGTAAACGATTACA	N/A	5
	EF3139	PTS system, IIC component	7.55	-374 -68	-360 -34	ATGAAAAGGCATTCA ATGTAAACGATTACA	N/A	7
	EF3327	citrate transporter	7.22	-45	-31	TTGTAAGCGTTAACA	N/A	12

Strongly conserved residues of the *cre* consensus sequence are underlined. (*) indicate genes/operons with more than one predicted *cre* site.

Quantitative real time PCR of differentially expressed genes in the *rpoN* mutant that are CcpA-dependent and -independent

To validate the microarray data, we performed qRT-PCR on a set of genes that represented both up- (*ef0891* and *ef2223*) and down-regulated (*ef0019* (*mptB*); *ef1017* (*lptB*); *ef3210* (*xpoA*)) genes in the *rpoN* mutant. This list of validated genes included those whose expression profiles were found to be in common with the previous *mptR/mptD* transcriptome (*ef0019* and *ef2223*) (10) as well as those genes that were found to be unique to the *rpoN* mutant (*ef1017, ef3210* and *ef0891*). We examined the expression of *ef0891* and *ef2223* in the *rpoN* mutant by comparing transcript abundance by qRT-PCR to the parental and *rpoN* complement strains. The results shown in Figure 3A and 3B validate the array data as relative expression for *ef0891* and *ef2223* was significantly increased in the *rpoN* mutant. The expression of *ef2223-21,* an operon encoding an ABC

transporter was the most abundantly upregulated transcript in the *rpoN* mutant that also contained a *cre* site within the promoter region (Table S4 and S5). To confirm whether the expression of *ef2223* is also CcpA-dependent, qRT-PCR was performed on RNA isolated from wildtype, *ccpA* mutant, and the *ccpA* complement. Figure 3B shows that the expression of *ef2223* is highly upregulated in the *ccpA* mutant background relative to the parental V583 strain and *ccpA* complement. In contrast, *ef0891* expression appears to be independent of CcpA as there was no significant difference in *ef0891* expression in the *ccpA* mutant background relative to the parental V583 and complement strains (Figure 3A). This result indicates that the expression of *ef2223* is likely indirectly upregulated as a consequence of *rpoN* deletion and directly regulated by CcpA due to the presence of a predicted *cre* site near its promoter region. In contrast, the differential expression of *ef0891* is unique to the *rpoN* mutant, as no change was observed in a *ccpA* mutant.

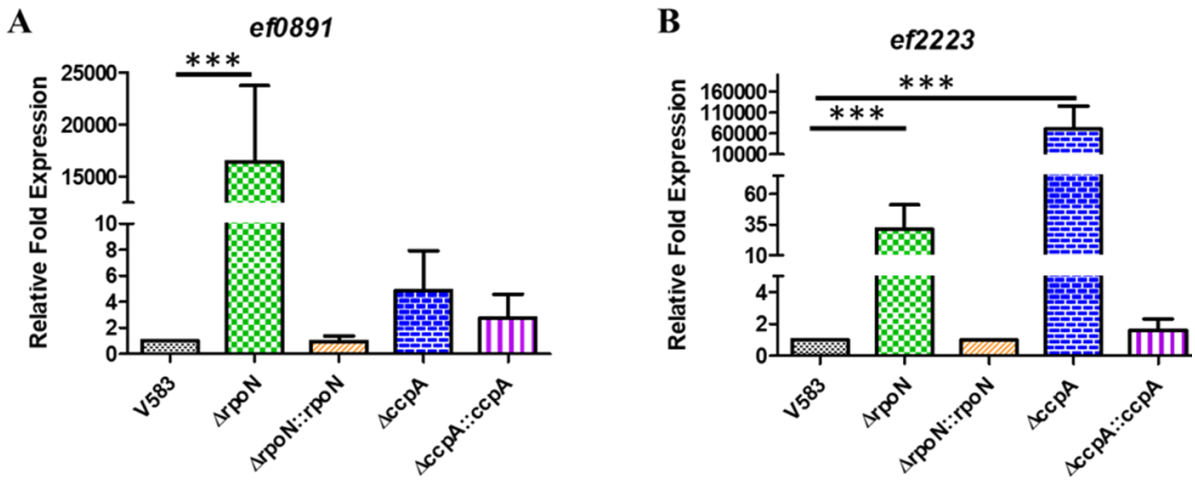

Figure 3: qRT-PCR analysis of selected CcpA-dependent and -independent regulated genes that were highly upregulated in Δ*rpoN*. RNA was isolated from midlog cultures of V583, Δ*rpoN*, Δ*rpoN*::*rpoN*, Δ*ccpA*, and Δ*ccpA*::*ccpA* strains grown in CDM supplemented with 100mM glucose and subsequently converted to cDNA. The cDNA was subjected to qPCR analysis and quantified using the ΔΔCt method using the threshold cycle values for the gene of interest ((**A**) *ef0891,* **(B)** *ef2223*) normalized to the endogenous control [*ef0005*(*gyrB*)]. Results represent the averages of three independent biological experiments. Error bars indicate the standard deviation of the mean. Statistical analysis was done by one-way ANOVA, with significance values set to $P < 0.0001$ (***).

To confirm expression of genes that were down-regulated in the *rpoN* mutant, we focused on three PTS operons predicted to contain the consensus -24/-12 RpoN-dependent promoter (*ef0019*, *ef1017*, and *ef3210).* The results shown in Figure 4A-4C confirmed that these three genes were significantly down-regulated in the *rpoN* mutant relative to the parental V583 and *rpoN* complement strains.

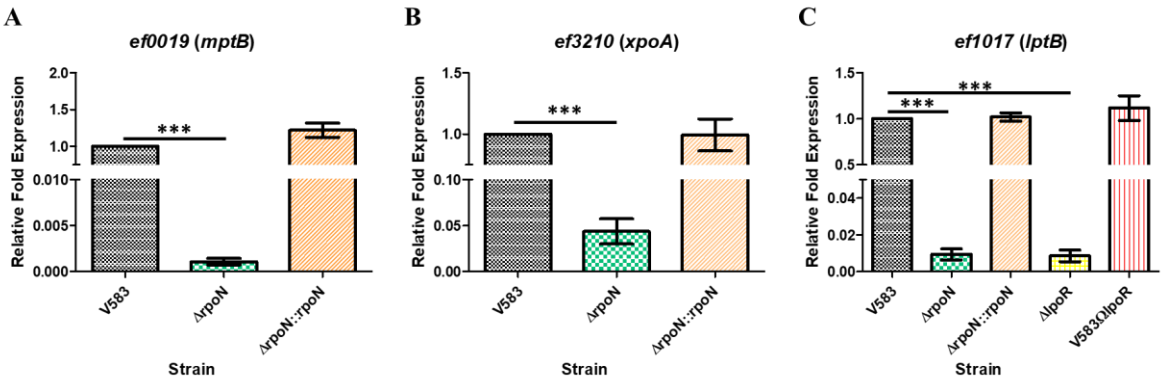

Figure 4: qRT-PCR analysis of RpoN-dependent expression of (A) *ef0019* (*mptB*) and (B) *ef3210* (*xpoA*). RNA was isolated from cultures of V583, Δ*rpoN*, and Δ*rpoN*::*rpoN* grown in CDM supplemented with 100mM glucose and subsequently converted to cDNA. (C) qRT-PCR analysis of RpoN- and LpoR-dependent expression of *ef1017* (*lptB*). RNA was isolated from cultures of V583, Δ*rpoN*, Δ*rpoN*::*rpoN*, Δ*lpoR*, and V583Ω*lpoR* revertant grown in CDM supplemented with 100mM glucose and subsequently converted to cDNA. The cDNA was subjected to qPCR analysis and quantified using the ΔΔCt method using the threshold cycle values for *ef0019, ef1017,* and *ef3210* normalized to the endogenous control [*ef0005* (*gyrB*)]. Results represent averages of three independent biological experiments. Error bars indicate the standard deviation of the mean. Statistical analysis was done by one-way ANOVA, with significant values set to $P < 0.0001$ (***).

The most down-regulated genes in the *rpoN* mutant array were the *mptBACD* operon encoding the Mpt PTS system and this was confirmed in the qRT-PCR data using *mptB* (*ef0019*), which was reduced ~ 930-fold in the *rpoN* mutant compared to the parental strain. In addition to *mpt* genes, we also confirmed reduced expression of the *lptBAC* operon using *lptB* (*ef1017*), which was reduced ~ 100-fold in the *rpoN* mutant as well as reduced expression of the *xpoABCD* operon using *xpoA* (*ef3210*), which was reduced ~ 20-fold (Figure 4). These observations are consistent with RpoN playing a direct role in the regulation of these PTS systems as the promoters for each

of these PTS systems contains a predicted -24/-12 consensus RpoN-dependent promoter. As the *lptBAC* operon is unique among RpoN-dependent genes in that it is not immediately proceeded by a gene encoding a bEBP, we hypothesized that LpoR (*ef1010*) is likely involved in regulating the expression of the *lptBAC* (*ef1017-19*) PTS operon as it is encoded in close proximity. We observed by qRT-PCR that the deletion of *lpoR* resulted in a ~ 100-fold decrease in expression of *lptB* (*ef1017*) in CDM supplemented with 100mM glucose relative to the parental and *lpoR* genetic revertant strains (Figure 4C). This suggests that the LpoR bEBP is involved in activating the expression of the *lpt* PTS operon.

Of the differentially expressed genes that were downregulated in the *rpoN* mutant, only the *lptBAC* promoter region possessed a putative *cre* site (Table S5). To confirm whether the regulation of the *lpt* PTS operon is also dependent on CcpA, qRT-PCR was performed on RNA isolated from wild-type, the *ccpA* mutant, and the *ccpA* complement grown to mid-exponential phase in CDM supplemented with 100mM glucose. Figure 5A shows that the expression of *lptB* (*ef1017*) is upregulated 10-fold in the *ccpA* mutant background relative to the parental V583 and *ccpA* complement strains. In contrast, *mptB* (*ef0019*) and *xpoA* (*ef3210*) expression appears to be independent of CcpA as there was no significant difference in expression in the *ccpA* mutant background relative to the parental V583 and complement strains (Figure 5B and 5C).

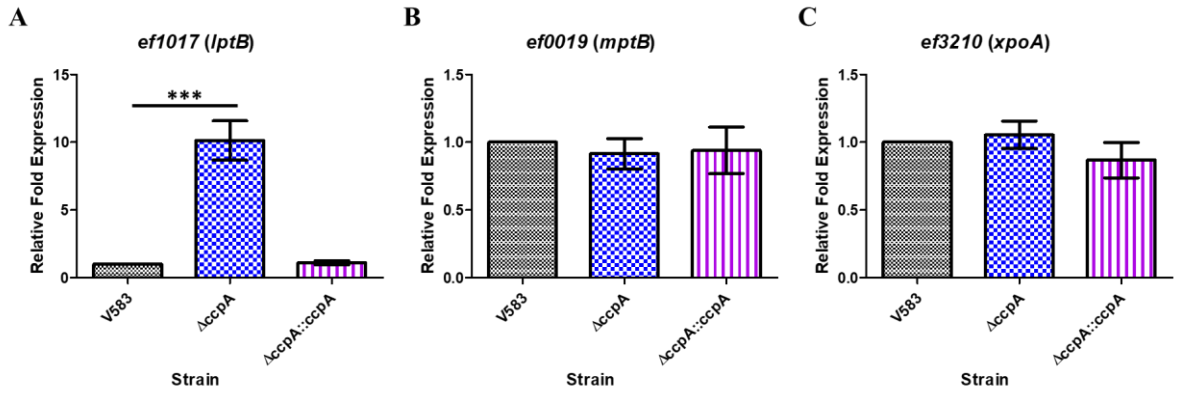

Figure 5: qRT-PCR analysis of selected CcpA-dependent and -independent regulated genes that are RpoN-dependent. RNA was isolated from midlog cultures of V583, Δ*ccpA*, and Δ*ccpA*::*ccpA* strains grown in CDM supplemented with 100mM glucose and subsequently converted to cDNA. The cDNA was subjected to qPCR analysis and quantified using the ΔΔCt method using the threshold cycle values for the gene of interest ((**A**) *ef1017*, **(B)** *ef0019*, and **(C)** *ef3210*) normalized to the endogenous control [*ef0005*(*gyrB*)]. Results represent the averages of three independent biological experiments. Error bars indicate the standard deviation of the mean. Statistical analysis was done by one-way ANOVA, with significance values set to $P < 0.0001$ (***).

The EF2223-21 ABC transporter contributes to glucose importation

In the presence of high glucose concentrations (100mM), the growth defect in both the *mptR* and *rpoN* mutants appeared to be partially rescued suggesting that at higher concentrations, glucose is being transported via other uptake system(s). The upregulation of several PTS systems and transport proteins in the *rpoN* mutant gives credence to this hypothesis. Of note is gene *ef2223* which encodes an ABC transporter permease protein, a member of the *ef2223-21* ABC transporter operon that was found to be 257.25-fold upregulated in the *rpoN* mutant, possesses a *cre* site, and was also confirmed to be highly upregulated in the *ccpA* mutant (Table S4, Figure 3). We hypothesized that when the Mpt PTS system is incapable of importing glucose efficiently into the cell as a consequence of the *rpoN* deletion, CcpA will derepress to allow expression of *ef2223-21* in order to bring glucose into the cell as a non-PTS glucose importer. To test this hypothesis, *ef2223-21* deletion mutants, singly and in combination with Δ*rpoN*, were grown in CDM

supplemented with 10mM or 100mM glucose. Figure 6 illustrates that deletion of *ef2223-21* singly does not impede the overall growth relative to wild-type in CDM supplemented with either concentration of glucose. However, a double deletion mutant of *rpoN* and *ef2223-21* results in a significant attenuation in growth relative to V583Δ*rpoN* alone and this reduction in growth is most pronounced in CDM supplemented with 10mM glucose. At the higher concentration of glucose (100mM), the difference in growth of the double mutant [Δ*rpoN*Δ*ef2223-21*] relative to the *rpoN* mutant is less pronounced, suggesting that additional low-affinity glucose transporters likely contribute to glucose importation.

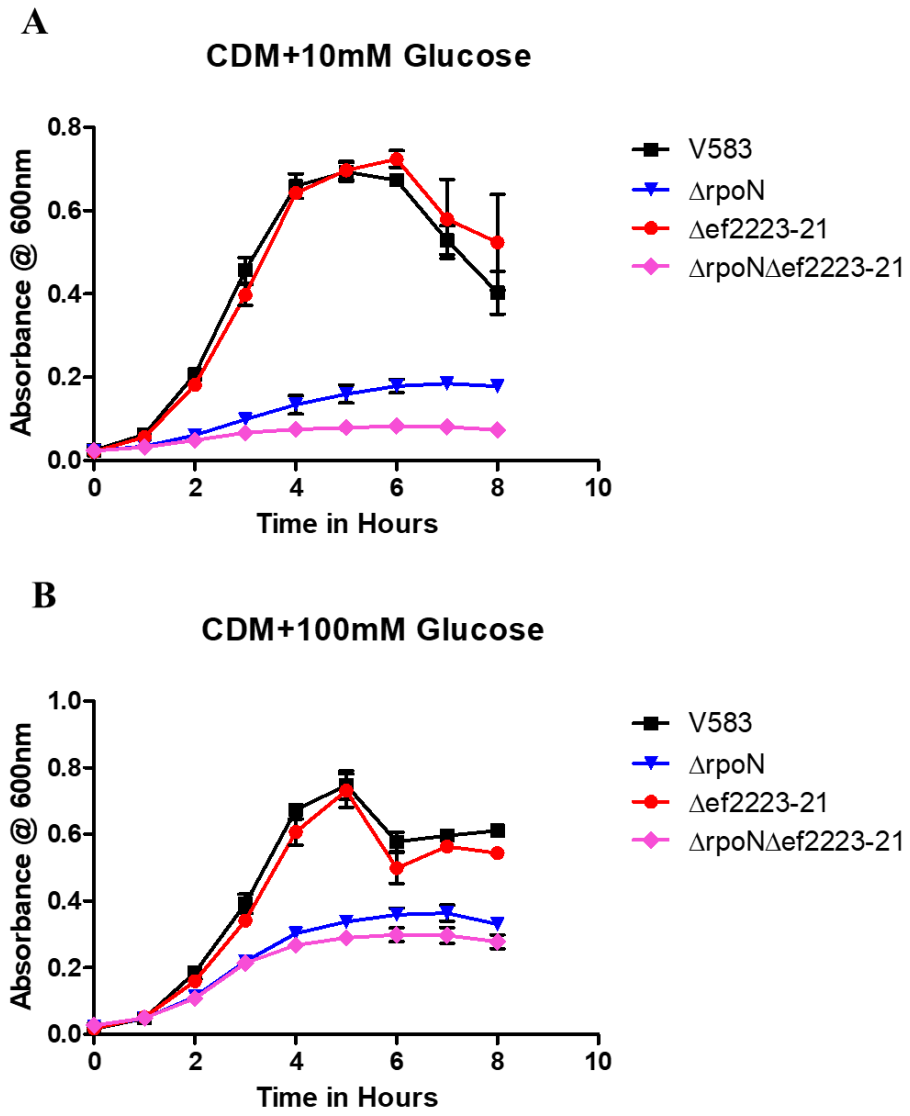

Figure 6: Growth of *E. faecalis* in chemically defined medium with glucose as the sole carbon source. The respective glucose concentrations are indicated below each panel. Each graph is the average of three biological replicates, with three technical replicates each time (n=9) with standard error of the mean shown. The growth curves are shown in black (V583), blue (Δ*rpoN*), red (Δ*ef2223-21*), and pink (Δ*rpoN*Δ*ef2223-21*).

Role of RpoN and CcpA in enterococcal biofilm formation

We have previously shown that *E. faecalis* V583Δ*rpoN* exhibited resistance to autolysis and formed altered biofilm structures in which the matrix was more protease K labile (6). The biofilm conditions in the prior study were based on a static biofilm under nutrient rich conditions, and we

were interested in knowing how RpoN and CcpA might contribute to biofilm formation under flow conditions in nutrient poor conditions to more closely mimic the environment that is likely encountered at sites of infection. To assess the role of RpoN and CcpA in regulating biofilm formation, we quantified the level of biofilm formation under flow conditions of *rpoN* and *ccpA* mutant strains using a drip-flow bioreactor (DFBR) (33, 34) in .1 X MM9YEGC. In the absence of *rpoN,* there is a significant 6-fold decrease in biofilm formation relative to the parental V583 strain and *rpoN* complement, whereas, in the absence of *ccpA,* there is a more drastic decrease in biofilm formation represented by an approximate 170-fold decrease in biofilm formation compared to parental V583 or the *ccpA* complement (Figure 7A and 7C). This suggests that factors regulated by RpoN and CcpA play a role in enterococcal biofilm formation.

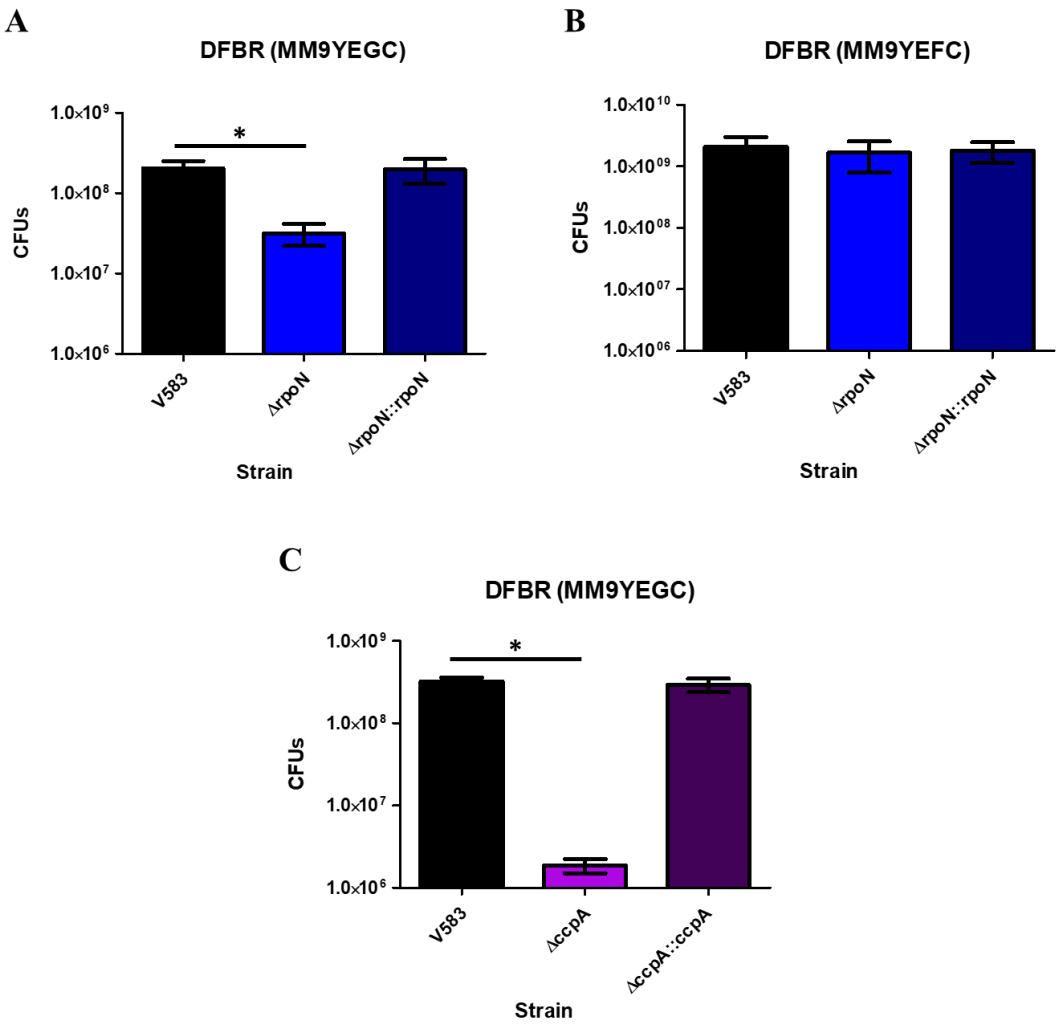

Figure 7A-C: Quantification of biofilm formation of V583, Δ*rpoN*, and Δ*rpoN*::*rpoN* strains using a drip-flow biofilm reactor (DFBR) in (A) MM9YEC + 15mM glucose and (B) MM9YEC + 15mM fructose media. (C) Quantification of biofilm formation of V583, Δ*ccpA*, and Δ*ccpA*::*ccpA* strains using a drip-flow biofilm reactor (DFBR) in MM9YEGC media. Results represent the averages of three independent biological experiments with error bars indicating the standard deviation of the mean. Statistical analysis was done by one-way ANOVA, with significance values set to $p < 0.05$ (*).

The *rpoN* mutant did exhibit a slight planktonic growth defect in the biofilm growth medium (MM9YEGC) (Figure 7D), whereas there was not a significant difference in growth relative to V583 in rich laboratory media (Todd-Hewitt broth) (Figure 7F). In contrast to the *rpoN* mutant, the *ccpA* mutant did not exhibit significant differences in planktonic growth relative to the parental V583 strain in biofilm growth medium (MM9YEGC) or rich laboratory medium (Todd-Hewitt

broth) (Figure 7D and 7F), indicating that the biofilm growth defect observed in the *ccpA* mutant is unique to the biofilm microenvironment. To ascertain whether the biofilm phenotype associated with the *rpoN* mutant was linked to the inability to import the available carbon source in the biofilm medium, the *rpoN* mutant was assessed under drip-flow biofilm conditions with the biofilm growth media containing fructose instead of glucose. Under these biofilm growth conditions, there is no significant difference between the *rpoN* mutant relative to wild-type and the *rpoN* complement strains (Figure 7B).

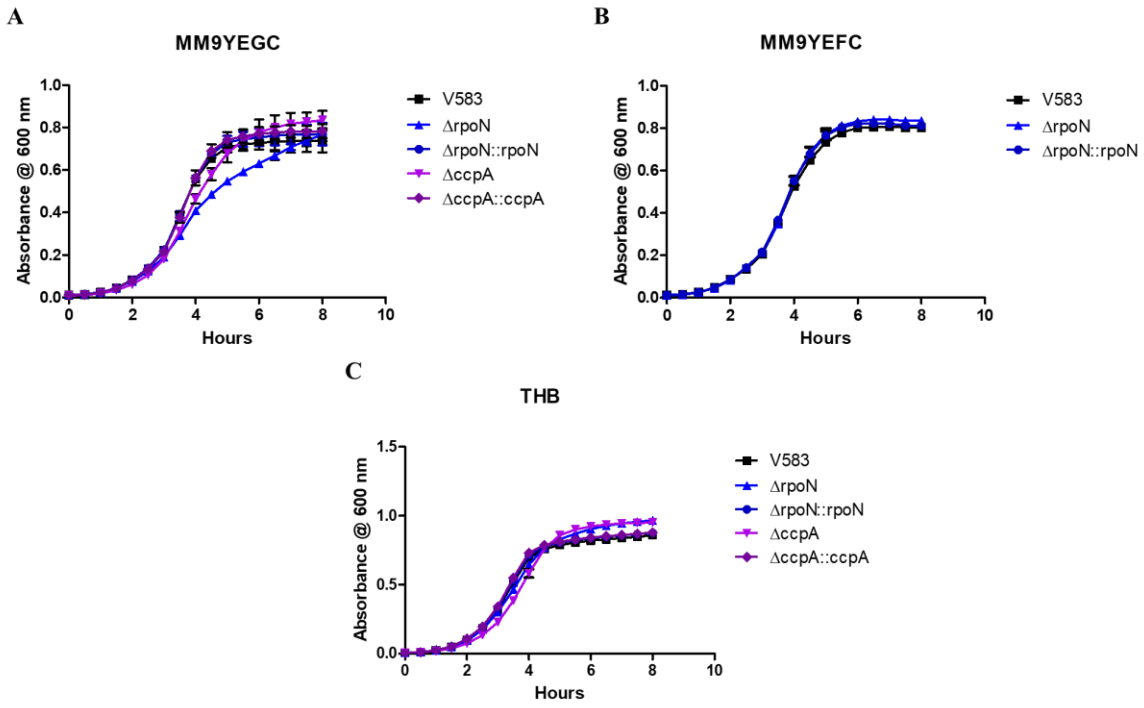

Figure 7D-F: Growth of *E. faecalis* in (D) MM9YEC + 15mM glucose, (E) MM9YEC + 15mM fructose, and (F) THB. Each graph is the average of three biological replicates, with three technical replicates each time (n=9) with standard error of the mean shown. The growth curves are shown in black (V583), blue (Δ*rpoN*), dark blue (Δ*rpoN*::*rpoN*), purple (Δ*ccpA*), and dark purple (Δ*ccpA*::*ccpA*).

Role of RpoN and CcpA in enterococcal virulence

On the basis of the biofilm results and the observation that RpoN plays a key role in regulating the uptake of mannose and glucose, we hypothesized an important contribution of RpoN to the *in vivo* fitness of *E. faecalis*. To determine the role of enterococcal RpoN in virulence we used two models of infection: rabbit endocarditis (36) and a murine model of catheter associated urinary tract infection (37). In the rabbit endocarditis model, the parental strain (V583) was compared to its isogenic *rpoN* mutant for the ability to establish infective endocarditis, and mean bacterial burden on the heart valve vegetation, heart, liver, spleen and kidneys as well as in the blood were assessed. As observed in figure 8, a significant reduction ($p < 0.05$) of approximately 10-fold in the mean bacterial burden was noted in the blood and all examined organs of the rabbits infected with Δ*rpoN* in comparison to the parental strain suggesting that *rpoN* contributes to infective endocarditis in rabbits.

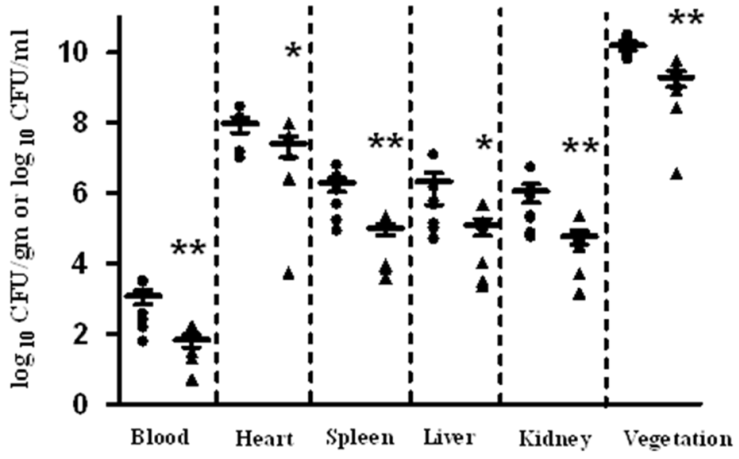

Figure 8: Enterococcal burden in rabbits infected with *E. faecalis* strains. Rabbits were euthanized post-infection and organs were harvested to enumerate bacterial burden. Bacterial burden for wild-type V583 (●) and Δ*rpoN* (▲) are expressed as log10 CFU/gram of harvested tissue. The horizontal line represents the median value for each group. Mann-Whitney test was used to determine significance and is indicated as follows: **, significant p-value less than 0.05 relative to V583; *, significant p value less than 0.1 relative to V583.

We also assessed the contribution of both RpoN as well as CcpA in the murine model of CAUTI. Similar to the observation in the endocarditis model, the *rpoN* mutant was significantly attenuated in CAUTI as observed by the reduced number of bacteria ($p<0.05$) recovered from the bladder (6.7-fold) and catheter (32.6-fold) of the Δ*rpoN* infected mice compared to the wild-type strain V583 (Figure 9). By comparison to the wild-type, the *ccpA* mutant was more highly attenuated for *in vivo* fitness as the mean bacterial numbers for the *ccpA* mutant isolated from the catheter and bladder were respectively 500-fold and 90-fold lower than the wild-type ($p<0.005$).

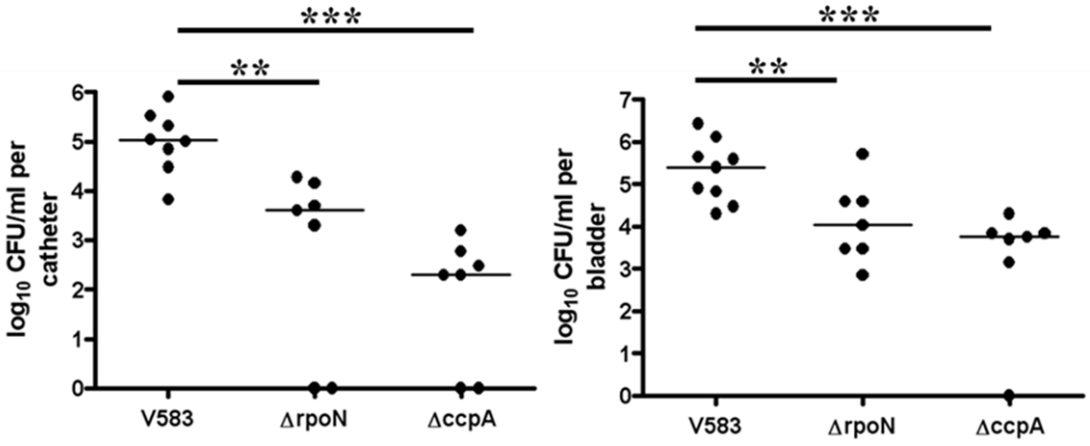

Figure 9: RpoN and CcpA contribute to enterococcal virulence in the murine model of CAUTI. Female C57BL/6 mice were euthanized after 48 hours post infection. Bacterial burden is expressed in logarithmic scale for wild type V583, Δ*rpoN* and Δ*ccpA* in (A) implanted catheters retrieved from the mice and (B) homogenized bladders. The horizontal bar represents the median of each group of mice. Statistical significance as determined by Mann-Whitney test is represented as follows: **, significant p value less than 0.05 relative to V583; ***, significant p value less than 0.005 relative to V583.

Discussion

Sigma-54 (RpoN) has historically been linked to the regulation of nitrogen metabolism even before the protein was recognized as a sigma factor (41). However, it is now well established that RpoN regulates a plethora of cellular processes, including flagellar biosynthesis in *E. coli* (38), cold shock adaptation in *B. subtilis* (42), sporulation and toxin production in *B. cereus* (43), biofilm formation in *E. faecalis* (6), and PTS-mediated regulation in Gram-negative and Gram-positive organisms (39, 44, 45). Others have conducted several comparative studies for understanding Sigma-54 and bEBP-mediated regulation with the intent of identifying a unifying biological theme for the wide range of RpoN-dependent processes (46-48). Francke et al. performed an extensive comparative genomic analyses and proposed that Sigma-54 is a central player in the control of cellular processes that involve the physical interaction of an organism with its environment (host colonization, biofilm, etc.) by directly regulating the expression of genes involved in the transport and biosynthesis of the main precursors of the bacterial exterior (49).

Sigma 54 binding sites (TTGGCACNNNNNTTGCT) have previously been identified upstream of genes predicted to encode sugar PTS systems (Mpt, Mpo, Lpo, Lpt, Mph and Xpo) in *E. faecalis*, and each PTS system is thought to be regulated by a bEBP that is predicted to interact with RpoN to allow open complex formation (7). Of the six predicted RpoN-dependent PTS systems, three (*mpt*, *lpt* and *xpo*) were found to be differentially expressed in CDM plus glucose growth conditions, but only the Mpt system plays a significant role in glucose- and mannose-dependent growth, as the *mptR* mutant and the *mptBACD* mutant phenocopies the *rpoN* mutant for growth in CDM supplemented with glucose or mannose. We have also previously shown that an Δ*rpoN* mutant is resistant to 2-deoxyglucose (a toxic homologue of glucose; 2DG) (6) and mutants resistant to 2DG have been shown to localize mutations within *mptR* or the *mptBACD* operon (7, 50) thus strengthening the notion that Mpt is the major glucose uptake system in *E. faecalis*.

In contrast, none of the other known bEBP (MphR, MpoR and LpoR) nor the XpoABCD PTS system contribute to glucose-dependent growth. We also show for the first time that the *lptBAC* PTS operon expression is dependent on the LpoR bEBP. Why the Lpt and Xpo PTS systems are induced with glucose as principal carbon source is unclear, as neither appears to contribute to glucose-dependent growth in a chemically defined medium. Previously, it was hypothesized that the Xpo PTS complex was inactive in *E. faecalis* V583 due to a truncated XpoR which lacks its C-terminal regulatory domain due to an IS256 insertion in the *xpoR* gene (7). However, our results indicate that the expression of the *xpo* PTS system is dependent on RpoN, suggesting that the truncated XpoR may still be functional. Others have shown that a bEBP that only possesses its AAA+ ATPase domain is capable of stimulating transcription of RpoN-dependent promoters in *Salmonella* Typhimurium LT2 (51), suggesting that, in some instances, bEBPs may activate transcription of its RpoN-dependent genes without possessing regulatory and/or DNA-binding domains. Another possibility is that one of the other five bEBPs encoded in the *E. faecalis* V583 genome may be used to activate the RpoN-dependent *xpo* operon. Deciphering the sugar specificity of the Xpo system remains an active area of investigation.

One of the common themes observed with the transcriptional profile of the *rpoN* mutant was the significant upregulation of genes with predicted *cre* sites, suggestive of an involvement with the major catabolite control protein CcpA. Amongst the cohort of *cre*-regulated genes, the only *cre* containing genes that were significantly downregulated in the *rpoN* microarray was the *lpt* PTS operon. Our observations confirm a role for CcpA in the regulation of the *lpt* PTS. In general *cre* sites present in the promoter regions of genes repressed by CcpA overlap the -10 promoter element or can be found immediately downstream of the -10 box (52). Based on our *cre* site query, we identified a *cre* site located 158 bp upstream of the start codon of *ef1017* (*lptB*) and positioned 92

bp upstream of the predicted -24/-12 promoter. RpoN-mediated transcriptional activation requires the binding of bEBP to an upstream activation sequence (UAS) to facilitate open complex formation. The UAS is generally positioned 80-150 bp upstream of the -24/-12 promoter and bEBP binding to the UAS requires DNA looping to bring the bEBP into close contact with the RNA polymerase (53). The location of the *cre* site positioned 92 bp upstream of the *lpt* operon -24/-12 promoter suggests that CcpA may actively compete with LpoR for binding to an as yet identified UAS. To our knowledge, this would be the first instance in which CcpA exhibits repressor activity by competing with a bEBP rather than RNA polymerase to prevent transcription of target genes. Understanding the specifics of this observation, as well as the sugar specificity of the Lpt PTS complex remains a component of ongoing studies.

Based on the *in silico* analysis conducted in this study, among the cohort of *cre*-regulated genes, nearly a third (32.1%) are predicted to be cell-envelope associated or secreted gene products. The majority of the genes listed in Table 1, encode transport and transport binding proteins, including a novel PTS system (EF0551-55) that resides within a known pathogenicity island in strain V583 (40), potentially linking sugar metabolism with pathogenesis or increased competitive fitness in a complex intestinal ecology. The remaining *cre* site regulated genes encode either cell wall-anchored proteins or secreted glycosyl hydrolases (exo- or endo-glycosidases). Endoglycosidases are enzymes that function to release oligosaccharides from glycoproteins or glycolipids, and do not require the presence of a terminal sugar residue to affect cleavage, thus distinguishing them from known exoglycosidases. The endoglycosidases also serve to release available nutrients from the host and can therefore be thought of as nutrient acquisition systems. The genes for each of the endoglycosidases (*ef0114* [*EndoE*]; *ef0362-61* [*chiBA*] and *ef2863*) were approximately ≥ 50-fold upregulated in the *rpoN* deletion mutant compared to V583 (Table S4 and S5). These genes have

also been shown to be upregulated in various transcriptomic studies conducted in human urine, serum, and an *in vivo* subdermal abscess model (3-5), indicating biological host colonization relevance in an environment that is glucose-limited. The contribution of these glycosyl hydrolases in *E. faecalis* virulence are a component of ongoing studies. With respect to the cohort of genes described in Table 1, we propose that the differentially expressed genes in the *rpoN* mutant that are putatively regulated by CcpA are involved in the physical interaction with its glucose-limited host environment, further supporting the findings in Francke et al. (49) that RpoN is involved in the central control of the bacterial exterior.

Leboeuf et al. showed that a *ccpA* insertion mutant in strain JH2-2 had a significantly altered growth rate in semi-synthetic medium (Bacto Folic AOAC Medium) plus 0.15% glucose. A *ccpA* deletion mutant displayed a slightly altered growth in CDM with 10mM glucose (Figure S3), but in contrast, growth was not significantly altered in either THB or MM9YEGC. These combined observations suggest that growth alterations caused by *ccpA* gene disruption are likely to be growth medium as well as strain dependent. As previously stated, CcpA is known to play a critical role in secondary carbon metabolism by repressing secondary catabolite genes when preferred carbon sources are readily available, but CcpA also participates in the positive regulation of gene products known to be involved in central glycolytic pathways and overflow metabolism (54). Although secondary nutrient acquisition systems would be predicted to be overexpressed in a *ccpA* mutant, in our study this mutant performs poorly *in vivo*, as well as when grown under biofilm conditions *in vitro*. The dysregulation of normal central metabolism that would occur in a *ccpA* mutant likely explains its attenuated biofilm and *in vivo* phenotypes and is consistent with a growing body of evidence for the role of CcpA in Gram-positive bacterial pathogenesis (55-57). Of note, one of the *E. faecalis* lactate dehydrogenase genes, *ef0255* (*ldh-1*) contains a putative *cre* site. The

location of the putative *cre* site within the promoter region of *ldh-1* predicts that CcpA acts as an activator of *ldh-1* expression. Leboeuf et al. (58) demonstrated by Northern blot that *ldh-1* expression was marginally reduced (2-fold) in a *ccpA* insertion mutant, suggesting that CcpA partially contributes to the positive regulation of *ldh-1* expression. While we did not observe differential regulation of *ldh-1* expression in the *rpoN* mutant, Opsata et al. (10) observed a slight drop (2.4-fold) in expression of *ldh-1* in an *mptD* insertion mutant. Experimental differences in terms of strain background, media composition and growth phase between our study in comparison to other studies (10, 58) likely explains why we were unable to observe a decrease in *ldh-1* expression in our *rpoN* transcriptomic data.

Ldh-1 has been linked to promoting extracellular electron transfer (EET) for biofilm matrix-associated iron-augmented energy production, thus leading to enhanced biofilm growth in *E. faecalis* (59). With this link between lactate dehydrogenase and biofilm formation, we hypothesize that when glucose is available, CcpA positively regulates the expression of *ldh-1,* thus leading to enhanced biofilm growth. In support of this hypothesis, increased glucose concentrations in biofilm culture medium has been shown to enhance biofilm formation in *E. faecalis* (60, 61), suggesting that replete glucose conditions during biofilm formation maintains CcpA-regulated *ldh* expression, thus leading to enhanced biofilm growth. We observed by qRT-PCR that a *ccpA* deletion mutant showed reduced *ldh-1* expression in CDM supplemented with 15 mM glucose (Figure S4). The inability to fully activate *ldh-1* expression in the *ccpA* mutant could partially explain the attenuated biofilm formation phenotypes we observed. Additionally, recent work by Kaval et al. (62) showed that CcpA regulates bacterial microcompartment (BMC) formation required for the utilization of ethanolamine in *E. faecalis* by binding to a *cre* site in the *eutS* promoter. The absence of CcpA predictably increases the expression of *eut* genes and BMC

formation. The dysregulation of *eut* gene expression observed in a *ccpA* mutant likely results in increased BMC formation and a predictable decrease in cell growth, likely due to the metabolic demand placed on a cell to produce additional BMCs or the potential toxicity associated with ethanolamine utilization (63). This defect would be expected to be most pronounced in environments where ethanolamine utilization would occur, particularly in the GI tract or possibly in other host anatomic sites, likely contributing to the *in vivo* defect of a *ccpA* mutant. Our *in vitro* growth conditions lacked supplemental ethanolamine and we therefore did not observe a significant change in gene expression for *eut* genes. Collectively, the observations with the *rpoN* and *ccpA* mutants both *in vitro* and *in vivo* suggest that regulated metabolism is key to successful colonization and infection. Too little nutrient acquisition of essential host sugars (glucose and/or mannose) in the case of the *rpoN* mutant and dysregulated metabolism observed in the *ccpA* mutant results in poor fitness compared to the parental strain.

In vivo the organism will face more hostile growth conditions, as preferable nutrient sources are kept at growth limiting conditions (i.e. glucose is present in normal human serum at 4-8 mM (64) and similar blood glucose levels are also observed in rabbits (65). Importantly, secondary carbon sources in a host environment could be host glycoproteins and high-mannose containing host glycoproteins have been shown to serve as a potential nutrient source for *E. faecalis in vitro* (66). Thus, beyond glucose, an *rpoN* mutant's failure to grow on mannose likely also contributes to its attenuated phenotype *in vivo*.

It was noteworthy that the most abundantly upregulated transcript in the *rpoN* mutant was a predicted sugar ABC transporter (EF2223-21). Deletion of this operon in V583 did not display a significant change in growth, however deletion of *ef2223-21* in the *rpoN* mutant background resulted in further attenuation of growth in CDM with 10 mM glucose compared to the *rpoN*

mutant alone. Increasing the glucose concentration to 100 mM rescued this growth defect, suggesting that additional glucose transporters are present in *E. faecalis*. In both *S. aureus* (67) and *S. pyogenes* (68) GlcU has been shown to contribute to glucose uptake under low affinity conditions, and a GlcU homolog is also present in the V583 genome (*ef0928*). Recent work by Kumar et al. (69) showed that GlcU expression compensates for PTS-dependent glucose transport when *E. faecalis* is exposed to the lantibiotic nisin. Their findings indicated that glucose was shuttled through the pentose phosphate shunt pathway under GlcU-dependent conditions as opposed to the conventional glycolytic pathway. GlcU was first characterized in *Bacillus subtilis* by Paulsen et al. as a glucose: H^+ symporter, which is dependent on the proton motive force for activity (70). It will be of interest to examine whether GlcU in *E. faecalis* is responsible for the improved growth of the *rpoN* and *ef2223-21* mutant under elevated glucose conditions. Although the nearest PtsG homolog in *E. faecalis* (EF1516) is not the primary glucose transporter when the RpoN-dependent Mpt PTS system is functional, we cannot rule out a glucose uptake contribution in the absence of the Mpt system. Intriguingly, the deletion of *rpoN* resulted in a 14-fold increase in *ef1516* expression, suggesting that it may play a role in glucose uptake, but this will require additional investigation. The gene encoding EF1516 does not appear to possess a *cre* site, so understanding how the absence of *rpoN* influences the expression of *ef1516* remains to be elucidated in subsequent studies.

We present a model for how RpoN and CcpA interface in the cell to regulate central carbon metabolism (Figure 10). In the absence of RpoN there would be an alteration in the relative abundance of the glycolytic intermediates glucose-6-phosphate and fructose-1,6,-bisphosphate within the cell indicating insufficient carbon flow which would trigger the phosphatase activity of the bifunctional enzyme HprK/P that dephosphorylates the PTS intermediate Hpr(Ser-P) (Figure

10). A dephosphorylated Hpr no longer binds to the catabolite control protein A (CcpA), and the dissociation of the Hpr(Ser-P) – CcpA complex would alleviate the repression of transcription of *cre*-dependent genes (20). In the Δ*rpoN* mutant, the inability to efficiently import glucose or mannose into the cell via the Mpt PTS complex influences the rate of carbon catabolite derepression. The expression seen in the array data with respect to *cre* site containing genes is consistent with this interpretation.

MptR belongs to the LevR-like family of regulators, whose bEBP activation is triggered by signal sensing through phosphotransferase regulation domains (PRDs)

(8, 71). The activity of LevR-like regulators is controlled via phosphorylation of the bEBP regulatory domain by the PTS enzymes, which the bEBP in-turn regulates. The regulatory domains of LevR-like bEBPs contain two unique PRDs, one domain undergoes HPr-mediated phosphorylation that leads to the activation of the bEBPs (PRD1), while PRD2 undergoes EII-mediated phosphorylation that is inhibitory (8, 71). Of note, it has been described that when the substrate is present, EIIB preferentially phosphorylates the sugar, not the bEBP, to complete the PTS cascade (8, 71, 72). In the model depicted in figure 10A, we also propose that when glucose is readily available, HPr becomes phosphorylated by EI via the phosphotransfer from the phosphoenolpyruvate (PEP) donor. HPr will transfer its phosphoryl group to the EII complex of the PTS system in addition to MptR PRD1. Phosphorylated-MptR (MptR-PRD1) then can elicit open complex formation of RpoN, to turn on expression of the *mpt* PTS complex. In contrast, when glucose is not readily available, MptR is phosphorylated by EIIB (MptR-PRD2), which inhibits MptR activation, thus inhibiting the expression of the *mpt* PTS genes (Figure 10B).

In *E. faecalis*, the transcription profile of the *rpoN* mutant clearly shows that this sigma factor contributes to the activation of several PTS systems, as well as its impact on controlling the activity

state of the Hpr (Ser-46) CcpA repressor. Approximately 10% of the genome is differentially expressed by disruption of RpoN function and understanding these complex metabolic circuits that also likely feed into the virulence potential of *E. faecalis* will be the focus of ongoing studies.

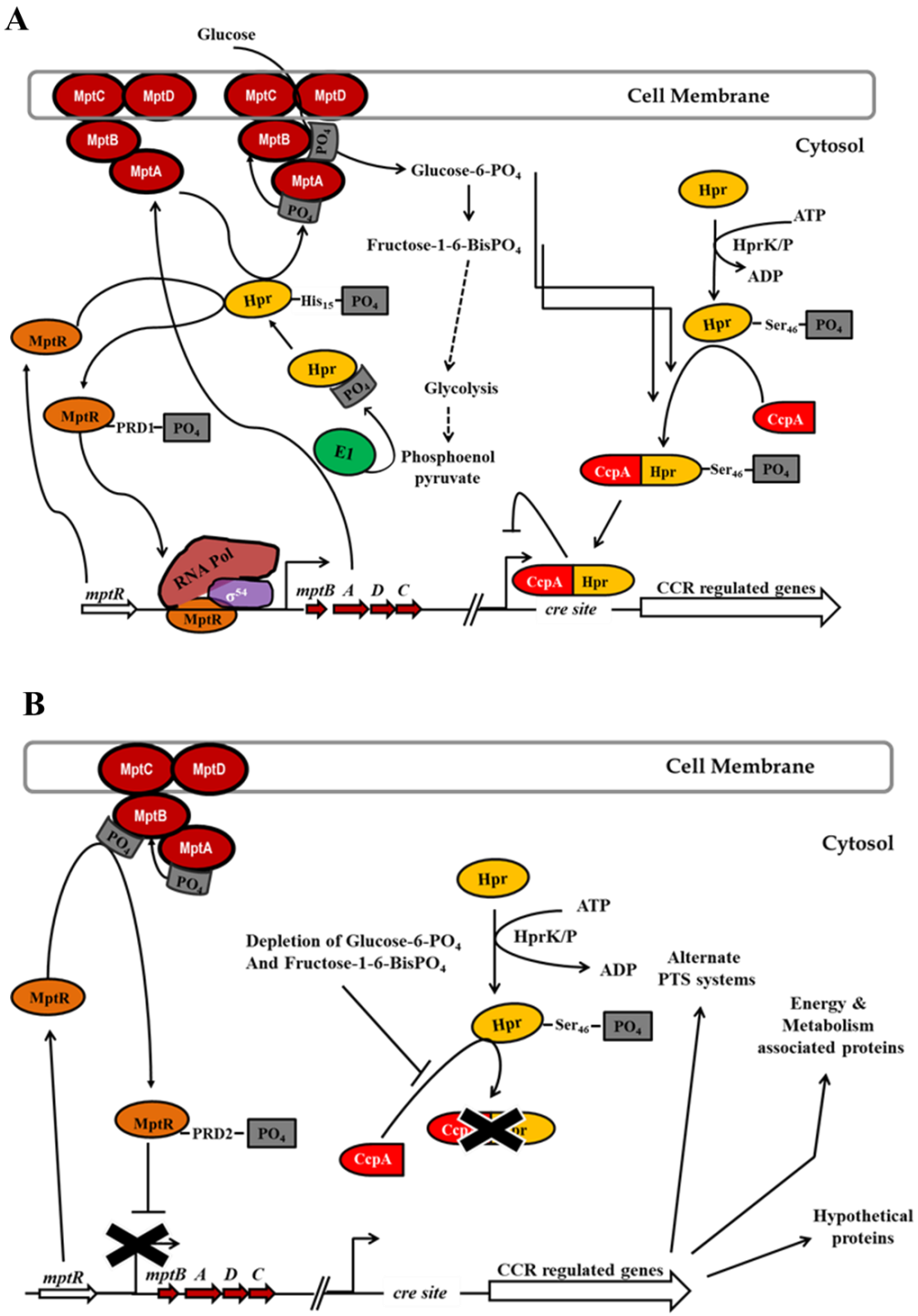

Figure 10: Model for Sigma 54 mediated carbon catabolite repression (CCR). Panel A: Regulation of CCR dependent genes in wild type *E. faecalis* V583; Panel B Alleviation of CCR in the *rpoN* or *mptR* mutant. CcpA, Catabolite Control Protein A; Mpt, Mannose PTS; *cre*, catabolite responsive elements; Hpr, Histidine containing phosphocarrier protein; EI, Enzyme I; HprK/P, Bifunctional ATP-dependent Hpr kinase/phosphatase; ATP, Adenosine triphosphate; ADP, Adenosine diphosphate; PRD, phosphotransferase regulation domain.

Supplemental Figures

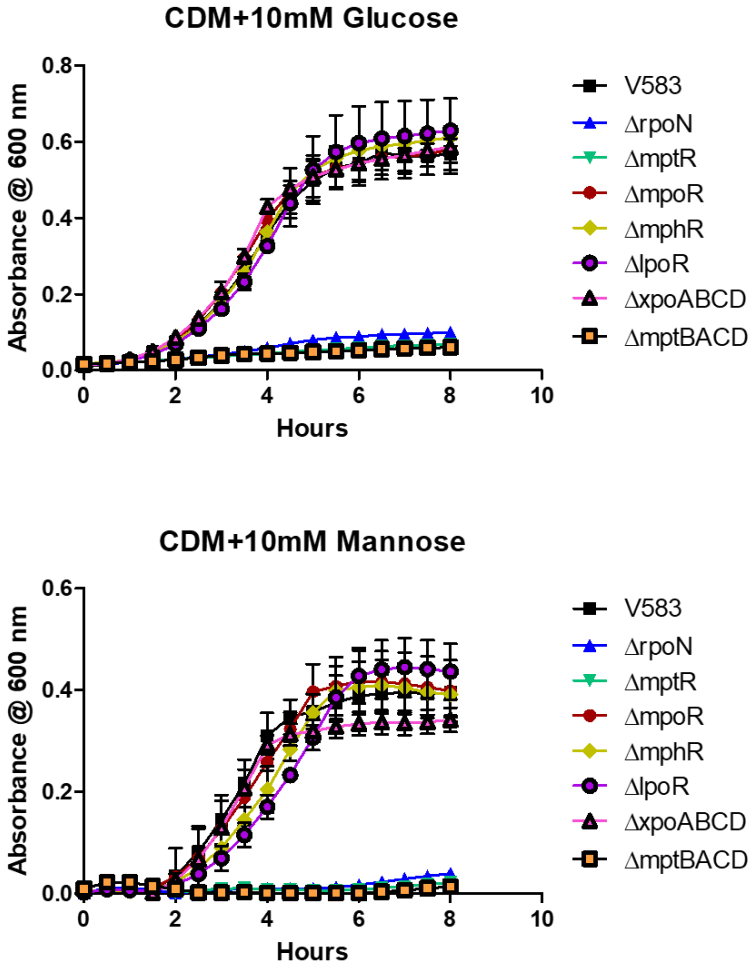

Figure S1: Growth of *E. faecalis* in CDM supplemented with 10mM glucose or mannose. Each graph is the average of three biological replicates, with three internal replicates each time (n=9) with standard error of the mean shown. The growth curves are represented as black (V583), blue (Δ*rpoN*), green (Δ*mptR*), red (Δ*mpoR*), yellow (Δ*mphR*), purple (Δ*lpoR*), pink (Δ*xpoABDC*), and orange (*ΔmptBACD*).

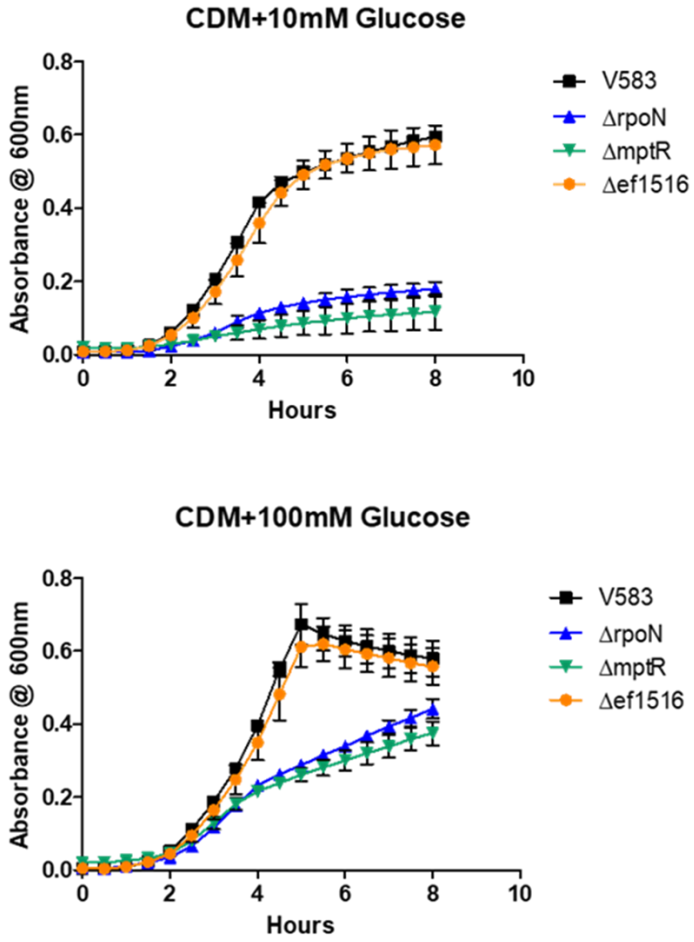

Figure S2: Growth of *E. faecalis* activator mutants in CDM containing 10mM or 100mM glucose. Each graph is the average of three internal replicates, repeated thrice with standard error of the mean shown. The growth curves are represented as black (V583), blue (Δ*rpoN*), green (Δ*mptR*), and orange (Δ*ef1516*).

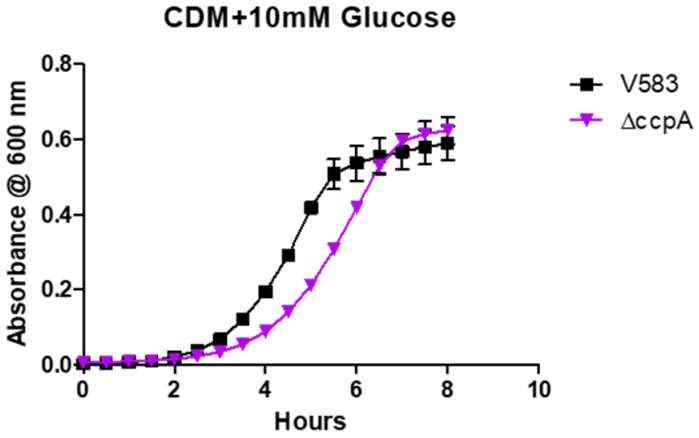

Figure S3: Growth of *E. faecalis* in chemically defined medium supplemented with 10mM glucose. Each graph is the average of three biological replicates, with three internal replicates each time (n=9) with standard error of the mean shown. The growth curves are shown in black (V583) and purple (Δ*ccpA*).

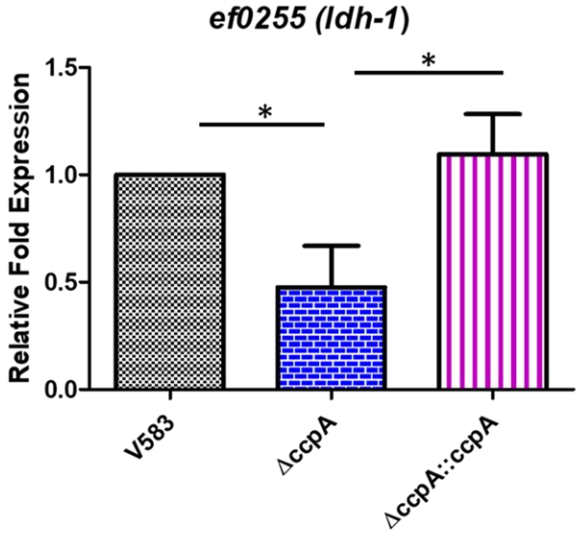

Figure S4: qRT-PCR analysis of CcpA-dependent expression of *ef0255* (*ldh-1*). RNA was isolated from cultures of V583, Δ*ccpA*, and Δ*ccpA*::*ccpA* grown in CDM supplemented with 15mM glucose and subsequently converted to cDNA. The cDNA was subjected to qPCR analysis and quantified using the ΔΔCt method using the threshold cycle values for *ef0255* normalized to the endogenous control [*ef0005* (*gyrB*)]. Results represent averages of three independent biological experiments. Error bars indicate the standard deviation of the mean. Statistical analysis was done by one-way ANOVA, with significant values set to $P < 0.05$ (*).

Supplemental Tables

Table S1. *E. faecalis* strains used in this study

Strain	Genotype or Description	Reference
V583	Parental strain	Clinical isolate (35)
VI01	V583Δ*rpoN*	(6)
VI40	V583Δ*rpoN*::*rpoN*	(6)
MG07	V583Δ*mptR*	This study
MG07R	V583Ω*mptR*	This study
MG08	V583Δ*lpoR*	This study
MG08R	V583Ω*lpoR*	This study
MG09	V583Δ*mpoR*	This study
MG10	V583Δ*mphR*	This study
IH10	V583Δ*mptBACD*	This study
KC01	V583Δ*xpoABCD*	This study
EH01	V583Δ*ccpA*	This study
EK26	V583Δ*ccpA*::*ccpA*	This study
ZA06	V583Δ*ef2223-21*	This study
ZA10	V583Δ*rpoN*Δ*ef2223-21*	This study
EK02	V583Δ*ef1516*	This study

Table S2. Oligonucleotides used in this study

Primer	Sequence (5'-3')
LpoRP1	GAGAGAATTCGATTGACAAGTTAAAAAAACG
LpoRP2	CTCTGGATCCCTTCCGAGATTTCATGGAATC
LpoRP3	GAGAGGATCCGAAGCGGAAGTTGCGCAT
LpoRP4	CTCTCTGCAGGATAGCCAATGTACCATTCC
LpoR-Up	ATGCAAATTGCTGAAGTTGCT
LpoR-Down	GCTAGCTCATTCACATTGTAT
MphRP1	GAGAGGATCCGCTTCAATATCATCAATCGTTTA

MphRP2	CTCTTCTAGATAACATAAAATCACCTCTCGC
MphRP3	GAGATCTAGAACGGAGTTTAACAACGCAGA
MphRP4	CTCTCCATGGATGCAACCTAAAAGAATCGCT
MphRUp	GTGATGAAGTGAAATGCTTTC
MphRDown	CTTGAAAGCAACGAGGTTCC
MpoRP1	GAGAGGATCCGAGCACATTCGTCAACGAATG
MpoRP2	CTCTCTGCAGGTGAAACTGTTTTAACGCTTGATG
MpoRP3	GAGACTGCAGAAGGCTTAATTCAAACGGAAATG
MpoRP4	GCTGAGACAGCATGCCTGAA
MpoRUp	GCAGCAGTAACGATGGAAGA
MpoRDown	GTGGAGGTGACTCCGAGATA
MptRP1	GAGAGAATTCATTTTGTCGCTAGTTGGCTTG
MptRP2	CTCTGGATCCAATCCGCTCATTTTTGATGG
MptRP3	GAGAGGATCCACCGAAATTGATACACTAGAT
MptRP4	CTCTCTGCAGAAAGATCATTGCACCAGATTG
MptRUp	CGAGAGGAAGGCTTGAATGTC
MptRDown	CGATGCAATGGCTTCTTGCA
XpoABCDP1	CAAGTGCTTCATGCTGGTGT
XpoABCDP2	CTAAGTTTCCGTGACTAGC
XpoABCDP3	CTAGGATTACTAGGCATCTGT
XpoABCDP4	CTTCGTCCACGTTGATGTC
XpoABCDUp	CAAGTGATTGACTCCTTGGTT
XpoABCDDown	TTATCGACTTCCGTGACTAG
MptBACDP1	GAAGACTATGAAATTATTGCG
MptBACDP2	TAATCGATCATCAATTCGAGCTA
MptBACDP3	GGCTTATTATAAGAATGACGAGG
MptBACDP4	CAGTCCATTCCATGATGTTGT
MptBACDUp	TAGACTGGCATTTAGAAGTGA
MptBACDDown	GCAATTCTTTCATACGATTACG
CcpAP1	GAGAGAATTCCAGAAGGTTCCAAGTAGCTG

CcpAP2	CTCTGGATCCATTTGCCTCTCTAGCAACATC
CcpAP3	GAGAGGATCCACAGTTGTTTTACCTTATGGAATTG
CcpAP4	CTCTCTGCAGGACTTATGCTGATGGTCGTG
CcpA-Up	GCTGTAACACCAGGTTTCAC
CcpA-Down	GATCGTCAAGTTGGTTCTACG
EF0019f	ATTGGCGGAATGAGTTTCAG
EF0019r	GCTGGCGTTATTTTCTTTGC
EF2223f	AACATCGGCGGTATCTTCAG
EF2223r	TGGTTCAATTCGACGAACAA
EF0891f	TGTCACAGCAAGCAGGAATC
EF0891r	TTCCACAAAAGGAACGGAAG
EF0013f	TTGGATGATGCAGAACGAAG
EF0013r	CTTGCAAGCCAGCAGTCAT
EF0005f	GGTGTTGGTTCCTCTGTTGT
EF0005r	CGCACCACGACGATATTCTT
EF2223-21P1	GAGAGGATCCTAACAAGTGTCGGTGATGAAC
EF2223-21P2	CTCTTCTAGACTTCTTCATTCGTTTCGCTCCTTTC
EF2223-21P3	GAGATCTAGAGAAATGCAAACACAATTAGACG
EF2223-21P4	CTCTGCATGCCTTCTAAGTCAGGAAAGGTGC
EF2223-21Up	CGAAAATGGTGTCCTAAACAAAG
EF2223-21Down	CTTCTAAGTCAGGAAAGGTGC
EF0255f	CGGAGATACAGAATTCCCAGTTT
EF0255r	GCTTTAGTGATACGCGCTAGT
EF3210f	CTGAGGACTACACGCCAATTAT
EF3210r	TGACACTACCACCATATAAATCTGT
EF1017f	CGTGGTATGGAAGCAGACAT
EF1017r	ACGAACTTGTGGGCCTAATAA
EF1516P1	GAGAGAATTCCAATGTGGTGTACAATGGTTAC
EF1516P2	CTCTTCTAGACGCTTTCATTATACGTAACTCCT
EF1516P3	GAGATCTAGAGATGTAATCGGAAATGTTACC

EF1516P4	CTCTGCATGCATCAGTTACATCCCTTCTAGT
EF1516Up	CGAGCACATATAAGTATGCCT
EF1516Down	GAAGGCCTAACTCTTTCTGCTT

Underlined sequences depict restriction sites used for cloning purposes

Table S3. Plasmids used in this study.

Plasmid	**Description**	**Reference**
pLT06	Markerless exchange vector; chloramphenicol resistance	(21)
pKS200	pLT06 + engineered *ccpA* deletion	This study
pMG07	pLT06 + engineered *mptR* deletion	This study
pMG08	pLT06 + engineered *lpoR* deletion	This study
pMG09	pLT06 + engineered *mpoR* deletion	This study
pMG10	pLT06 + engineered *mphR* deletion	This study
pKC02	pLT06 + engineered *xpoABDC* deletion	This study
pIH03	pLT06 + engineered *mptBACD* deletion	This study
pEK26	pLT06 + engineered *ccpA* complement	This study
pZA13	pLT06 + engineered *ef2223-21* deletion	This study
pEK04	pLT06 + engineered *ef1516* deletion	This study

Table S4: Differentially expressed genes in V583Δ*rpoN* compared to V583

Gene		Function	Fold Change
Former Locus Tag	**Current Locus Tag**		
HYPOTHETICAL PROTEINS AND PROTEINS WITH UNKNOWN FUNCTIONS			
EF0054	EF_RS00250	hypothetical protein	58.53
EF0384	EF_RS01920	hypothetical protein	34.97
EF0711	EF_RS03420	conserved hypothetical protein	32.33
EF1394	EF_RS06735	MOSC domain-containing protein	29.49
EF0383	EF_RS01915	protein FdrA conserved hypothetical protein	29.34
EF0664	EF_RS03195	C-GCAxxG-C-C family protein	27.97
EF1227	EF_RS05930	NADPH-dependent oxidoreductase	21.74
EF2570	EF_RS12210	selenium-dependent xanthine dehydrogenase	21.17
EF1226	EF_RS05925	NAD(P)H-dependent oxidoreductase	21.02
EF2566	EF_RS12190	sulfurtransferase-like selenium metabolism protein YedF	19.48
EF2220	EF_RS10620	conserved hypothetical protein	18.53
EF2236	EF_RS10700	conserved hypothetical protein	18.24
EF0678	EF_RS03260	acetyltransferase, GNAT family	16.96
EF0743	EF_RS03555	hypothetical protein	16.44
EF0392	EF_RS01955	hypothetical protein	15.39
EF2564	EF_RS12180	putative selenium-dependent hydroxylase accessory protein YqeC	14.57
EF2565	EF_RS12185	conserved hypothetical protein	12.22
EF2563	EF_RS12175	selenium-dependent molybdenum hydroxylase system protein	11.38
EF3142	EF_RS14885	6-phosphogluconate dehydrogenase family protein	8.83
EF1237	EF_RS05975	endonuclease/exonuclease/phosphatase family protein	8.26
EF3105	EF_RS14705	hypothetical protein	7.74
EF1912	EF_RS09170	ROK family protein	7.19
EF0405	EF_RS02010	Cof-type HAD-IIB family hydrolase	7.16
EF1229	EF_RS05940	AP2 domain-containing protein	6.71
EF1035	EF_RS04930	DUF4767 domain-containing protein	6.62
EF1066	EF_RS05155	sugar O-acetyltransferase	6.47

EF3087	EF_RS14625	hypothetical protein	6.39
EF1228	EF_RS05935	hypothetical protein	6.29
EF0389	EF_RS01945	membrane protein, putative	6.19
EF1919	EF_RS09195	acetyltransferase, GNAT family	5.87
EF0377	EF_RS01885	ankyrin repeat family protein	5.56
EF2441	EF_RS11600	conserved hypothetical protein	5.50
EF0052	EF_RS00240	hypothetical protein	5.41
EF3088	EF_RS14630	hypothetical protein	5.34
EF1075	EF_RS05195	acetyltransferase, GNAT family	5.25
EF1077	EF_RS05205	acetyltransferase, GNAT family	5.09
EF3103	EF_RS14695	hypothetical protein	5.04
EF3326	EF_RS15745	conserved hypothetical protein	4.85
EF3102	EF_RS14690	hypothetical protein	4.82
EF1535	EF_RS07400	conserved hypothetical protein	4.69
EF1061	EF_RS05135	amidohydrolase family protein	4.53
EF2577	EF_RS12240	aspartateornithine carbamoyltransferase family protein	4.30
EF3092	EF_RS14650	glyoxalase family protein	4.16
EF1407	EF_RS06795	hypothetical protein	4.07
EF1800	EF_RS08635	conserved hypothetical protein	4.01
EF3032	EF_RS14375	photosystem I biogenesis protein BtpA	3.77
EF1062	EF_RS05140	amidohydrolase family protein	3.68
EF0244	EF_RS01110	acetyltransferase, GNAT family	3.54
EF0460	EF_RS02265	serine hydrolase	3.48
EF1362	EF_RS06575	conserved domain protein	3.41
EF1933	EF_RS09255	hypothetical protein	3.39
EF1512	EF_RS07310	transglutaminase domain-containing protein	3.37
EF0113	EF_RS00505	ParB N-terminal domain-containing protein	3.35
EF1322	EF_RS06370	conserved hypothetical protein	3.31
EF3009	EF_RS14270	conserved hypothetical protein	3.20
EF3007	EF_RS14260	chloride ion channel protein	3.15
EF1239	EF_RS05985	conserved hypothetical protein	3.08
EF3010	EF_RS14275	acyl-CoA synthetase FdrA	3.05
EF1528	EF_RS07375	hypothetical protein	3.01
EF3245	EF_RS15340	phosphatase PAP2/LCP family protein	-3.10
EF2944	EF_RS13960	hypothetical protein	-3.10
EF0708	EF_RS03405	conserved hypothetical protein	-3.16
EF0672	EF_RS03230	hypothetical protein	-3.31
EF0341	EF_RS01710	hypothetical protein	-3.33
EF1841	EF_RS08835	HD domain-containing protein	-3.79
EF1199	EF_RS05795	conserved hypothetical protein	-4.04
EF0747	EF_RS03575	conserved hypothetical protein	-4.26

EF2899	EF_RS13745	NAD(P)/FAD-dependent oxidoreductase	-4.35
EF0419	EF_RS02075	conserved hypothetical protein	-4.54
EF1258	EF_RS06065	hypothetical protein	-5.02
EF2216	EF_RS10600	FUSC family protein	-5.66
EF2214	EF_RS10590	VOC family protein	-6.21
EF2215	EF_RS10595	SRPBCC family protein	-7.27
EF2896	EF_RS13735	hypothetical protein	-7.39
EF0083	EF_RS00370	hypothetical protein	-7.77
EF1231	EF_RS05945	metallophosphoesterase	-10.70
EF0802	EF_RS03825	hypothetical protein	-29.61
TRANSPORT AND BINDING PROTEINS			
EF2223	EF_RS10635	ABC transporter, permease protein	257.25
EF2221	EF_RS10625	ABC transporter, substrate-binding protein	128.09
EF2222	EF_RS10630	ABC transporter, permease protein	114.80
EF0892	EF_RS04240	amino acid ABC transporter, ATP-binding protein	40.84
EF0893	EF_RS04245	amino acid ABC transporter, amino acid-bindingpermease protein	39.81
EF1927	EF_RS09230	glycerol uptake facilitator protein	36.40
EF0385	EF_RS01925	major facilitator family transporter	27.11
EF1398	EF_RS06755	molybdenum ABC transporter, permease protein	26.30
EF1397	EF_RS09100	molybdenum ABC transporter, molybdenum-binding protein	23.85
EF2234	EF_RS10690	sugar ABC transporter, sugar-binding protein, putative	17.24
EF0387	EF_RS01935	sodiumdicarboxylate symporter family protein	16.14
EF1233	EF_RS05955	ABC transporter, permease protein	13.83
EF1920	EF_RS09200	C4-dicarboxylate anaerobic carrier	13.23
EF1399	EF_RS06760	molybdenum ABC transporter, ATP-binding protein, putative	13.1
EF0938	EF_RS04460	ABC transporter, ATP-bindingTOBE domain protein	12.53
EF1234	EF_RS05960	ABC transporter, substrate-binding protein, putative	12.52
EF1345	EF_RS06500	sugar ABC transporter, sugar-binding protein	11.76
EF1344	EF_RS06495	sugar ABC transporter, permease protein	10.11
EF1232	EF_RS05950	ABC transporter, permease protein	8.63
EF1207	EF_RS05835	citrate carrier protein, CCS family	8.54
EF2233	EF_RS10685	ABC transporter, permease protein	8.46
EF2992	EF_RS14195	major facilitator family transporter	7.38
EF3327	EF_RS15750	citrate transporter	7.22
EF0556	EF_RS02720	xylose isomerase	7.01
EF1343	EF_RS06490	sugar ABC transporter, permease protein	6.65
EF1400	EF_RS06765	cadmium-translocating P-type ATPase	6.43
EF3104	EF_RS14700	ABC transporter, ATP-binding protein	5.46
EF2442	EF_RS11605	phosphate transporter family protein	5.45

EF3000	EF_RS14225	cytosinepurines, uracil, thiamine, allantoin permease family protein	4.56
EF1513	EF_RS07315	pheromone binding protein	4.23
EF2232	EF_RS10680	ABC transporter, permease protein	4.20
EF3109	EF_RS14725	peptide ABC transporter, ATP-binding protein	4.07
EF3108	EF_RS14720	peptide ABC transporter, permease protein	3.84
EF3110	EF_RS14730	peptide ABC transporter, ATP-binding protein	3.53
EF1060	EF_RS05130	pheromone binding protein	3.49
EF0063	EF_RS00285	pheromone binding protein, putative	3.42
EF3107	EF_RS14715	peptide ABC transporter, permease protein	3.40
EF3106	EF_RS14710	peptide ABC transporter, peptide-binding protein	3.35
EF0243	EF_RS01105	branched-chain amino acid transport system II carrier protein	3.22
EF0429	EF_RS02120	TRAP dicarboxylate transporter, DctP subunit	3.16
EF0807	EF_RS03850	pheromone binding protein, putative	3.15
EF2593	EF_RS03850	ABC transporter, ATP-bindingpermease protein	-3.05
EF0569	EF_RS02755	potassium-transporting ATPase, subunit C	-3.16
EF3069	EF_RS14545	formatenitrite transporter family protein	-3.16
EF0804	EF_RS03835	amino acid ABC transporter, amino acid-binding protein	-3.19
EF1198	EF_RS05790	permease	-3.26
EF0568	EF_RS02750	potassium-transporting ATPase, subunit B	-3.37
EF0805	EF_RS03840	amino acid ABC transporter, ATP-binding protein	-3.56
EF3004	EF_RS14245	sulfate transporter familySTAS domain protein	-3.57
EF1968	EF_RS09390	ECF transporter S component	-3.66
EF0806	EF_RS03845	amino acid ABC transporter, permease protein	-3.72
EF0420	EF_RS02080	drug resistance transporter, EmrBQacA family protein	-3.84
EF0567	EF_RS02745	potassium-transporting ATPase, subunit A	-3.95
EF1304	EF_RS06285	magnesium-translocating P-type ATPase	-4.12
EF0635	EF_RS03060	amino acid permease family protein	-5.11
EF1053	EF_RS05100	ABC transporter, ATP-binding protein	-5.23
EF0636	EF_RS03065	Na+H+ antiporter	-6.49
EF0082	EF_RS00365	major facilitator family transporter	-6.82
EF1814	EF_RS08700	drug resistance transporter, EmrBQacA family protein	-8.11
EF1192	EF_RS05760	aquaporin Z	-11.87
EF1054	EF_RS05105	ABC transporter, permease protein	-17.50
CELL ENVELOPE/SECRETED			
EF0362	EF_RS01815	chitin binding protein, putative	83.75
EF0361	EF_RS01810	chitinase, family 2	69.31
EF2863	EF_RS13555	endo-beta-N-acetylglucosaminidase	62.34
EF0713	EF_RS03425	WxL domain-containing protein	58.00
EF0114	EF_RS00510	glycosyl hydrolase, family 20	48.20
EF0714	EF_RS03430	WxL domain-containing protein	29.26

EF0108	EF_RS00480	YfcC family protein	13.04
EF2237	EF_RS10705	lipoprotein, putative	7.17
EF1657	EF_RS07965	membrane protein, putative	5.80
EF0062	EF_RS00280	LPXTG cell wall anchor domain-containing protein	4.40
EF0673	EF_RS03235	membrane protein, putative	4.05
EF2662	EF_RS12620	choline binding protein	3.50
EF2627	EF_RS12460	teichoic acid glycosylation protein, putative	-3.11
EF1340	EF_RS06475	pheromone cAM373 precursor lipoprotein	-3.16
EF2746	EF_RS13000	dltD protein	-3.45
EF0468	EF_RS02305	LemA family protein	-3.71
EF2749	EF_RS13015	D-alanine-activating enzyme, putative	-3.83
EF2748	EF_RS13010	basic membrane protein DtlB	-4.01
EF2747	EF_RS13005	D-alanyl carrier protein	-4.07
EF0443	EF_RS02180	LysM peptidoglycan-binding domain-containing protein	-4.25
EF2750	EF_RS13020	teichoic acid D-Ala incorporation-associated protein DltX	-4.95
EF0746	EF_RS03570	penicillin-binding protein, putative	-11.48
ENERGY METABOLISM			
EF1929	EF_RS09240	glycerol kinase	53.22
EF1928	EF_RS09235	alpha-glycerophosphate oxidase	43.44
EF0253	EF_RS01155	aldehyde dehydrogenase	35.88
EF2562	EF_RS12170	flavodoxin	19.95
EF0106	EF_RS00470	carbamate kinase	19.07
EF1068	EF_RS05160	aldose 1-epimerase	18.97
EF0677	EF_RS03255	phosphoglucomutasephosphomannomutase family protein	18.13
EF0386	EF_RS01930	carbamate kinase	16.9
EF0104	EF_RS00460	arginine deiminase	15.83
EF1661	EF_RS07985	branched-chain alpha-keto acid dehydrogenase, E3 component, dihydrolipoamide dehydrogenase	14.95
EF1658	EF_RS07970	branched-chain alpha-keto acid, E2 component, dihydrolipoamide acetyltransferase	14.28
EF3135	EF_RS14850	mannonate dehydratase, putative	13.37
EF3134	EF_RS14845	2-dehydro-3-deoxyphosphogluconate aldolase4-hydroxy-2-oxoglutarate aldolase	10.43
EF2559	EF_RS12155	pyruvate flavodoxinferredoxin oxidoreductase family protein	9.99
EF0388	EF_RS01940	ureidoglycolate dehydrogenase	9.27
EF1659	EF_RS07975	branched-chain alpha-keto acid dehydrogenase, E1 component, beta subunit	8.46
EF1349	EF_RS06515	glycosyl hydrolase, family 13	7.96
EF2235	EF_RS10695	glucuronyl hydrolase, putative	7.81
EF0390	EF_RS01950	amidohydrolase family protein	7.61

EF1824	EF_RS08745	glycosyl hydrolase, family 31fibronectin type III domain protein	6.82
EF0900	EF_RS04270	aldehyde-alcohol dehydrogenase	6.69
EF1206	EF_RS05830	malate dehydrogenase, decarboxylating	6.26
EF2579	EF_RS12250	diaminopropionate ammonia-lyase, putative	6.21
EF1236	EF_RS05970	acetyl xylan esterase, putative	5.82
EF3325	EF_RS15740	sodium ion-translocating decarboxylase, biotin carboxyl carrier protein	5.29
EF1347	EF_RS06505	glycosyl hydrolase, family 13	5.18
EF1660	EF_RS07980	branched-chain alpha-keto acid dehydrogenase, E1 component, alpha subunit	5.14
EF1662	EF_RS07990	butyrate kinase	5.13
EF1503	EF_RS07270	fructose-1,6-bisphosphatase	4.95
EF1805	EF_RS08660	glycosyl hydrolase, family 35	4.81
EF2268	EF_RS10830	alginate lyase family protein	4.73
EF2440	EF_RS11595	ChbG/HpnK family deacetylase	4.71
EF1360	EF_RS06565	dihydroxyacetone kinase subunit DhaK	4.70
EF2575	EF_RS12235	carbamate kinase	4.52
EF2581	EF_RS12260	putative selenate reductase subunit YgfK	4.41
EF0271	EF_RS01375	glycosyl hydrolase, family 1	4.33
EF2996	EF_RS14210	(S)-ureidoglycine aminohydrolase	4.13
EF0291	EF_RS01465	glycosyl hydrolase, family 1	4.06
EF0551	EF_RS02695	glycosyl hydrolase, family 31	3.89
EF2265	EF_RS10815	carbohydrate kinase, pfkB family	3.88
EF2264	EF_RS10810	4-deoxy-l-threo-5-hexosulose-uronate ketol-isomerase	3.87
EF1361	EF_RS06570	dihydroxyacetone kinase subunit L	3.84
EF1238	EF_RS05980	glycosyl hydrolase, family 3	3.79
EF3157	EF_RS14945	glycosyl hydrolase, family 65	3.78
EF0459	EF_RS02260	N-acetylmuramic acid 6-phosphate etherase	3.77
EF2272	EF_RS10850	glucuronyl hydrolase, putative	3.74
EF3158	EF_RS14950	beta-phosphoglucomutase	3.69
EF1348	EF_RS06510	glucan 1,6-alpha-glucosidase, putative	3.61
EF2709	EF_RS12840	glycosyl hydrolase, family 2	3.56
EF1158	EF_RS05600	N4-(beta-N-acetylglucosaminyl)-L-asparaginase, putative	3.52
EF1071	EF_RS05175	galactose-1-phosphate uridylyltransferase	3.33
EF2646	EF_RS12545	glycerate kinase, putative	3.32
EF1069	EF_RS05165	galactokinase	3.17
EF1707	EF_RS08205	alpha-mannosidase	3.07
EF2722	EF_RS12890	L-serine dehydratase, iron-sulfur-dependent, alpha subunit	-3.19
EF2500	EF_RS11875	glycine cleavage system protein H	-3.69
EF2721	EF_RS12885	L-serine dehydratase, iron-sulfur-dependent, beta subunit	-3.77
PTS SYSTEMS			

EF2213	EF_RS10585	PTS system, IIBC components	23.3
EF3138	EF_RS14865	PTS system, IID component	17.41
EF3137	EF_RS14860	PTS system, IIB component	16.00
EF1516	EF_RS07325	PTS system, IIABC components	14.22
EF3136	EF_RS14855	PTS system, IIA component	12.08
EF0553	EF_RS02705	PTS system, IID component	11.35
EF0554	EF_RS02710	PTS system, IIB component	9.6
EF1529	EF_RS07380	PTS system, IIC component, putative	8.56
EF1803	EF_RS08650	PTS system, IIC component	8.28
EF3139	EF_RS14870	PTS system, IIC component	7.55
EF1802	EF_RS08645	PTS system, IID component	7.35
EF3031	EF_RS14370	PTS system, IIB component	7.03
EF0270	EF_RS01370	PTS system, beta-glucoside-specific IIABC component	6.91
EF0292	EF_RS01470	PTS system, IIC component	6.62
EF1804	EF_RS08655	PTS system, IIB component	6.36
EF0552	EF_RS02700	PTS system, IIC component	6.21
EF1836	EF_RS08810	PTS system, IIA component, putative	5.84
EF1837	EF_RS08815	PTS system, IIB component, putative	5.74
EF0816	EF_RS03890	PTS system, IIC component	5.32
EF1359	EF_RS06560	PTS-dependent dihydroxyacetone kinase phosphotransferase subunit DhaM	4.70
EF3030	EF_RS14365	PTS system, IIC component	4.58
EF1801	EF_RS08640	PTS system, IIA component	4.42
EF3029	EF_RS14360	PTS system, IID component	4.32
EF2269	EF_RS10835	PTS system, IID component	4.14
EF0958	EF_RS04555	PTS system, IIABC components	3.91
EF0815	EF_RS03885	PTS system, IIAB components	3.81
EF0817	EF_RS03895	PTS system, IID component	3.77
EF0555	EF_RS02715	PTS system, IIA component	3.75
EF0456	EF_RS02245	PTS system, IID component	3.75
EF2270	EF_RS10840	PTS system, IIC component	3.59
EF2267	EF_RS10825	PTS system, IIA component	3.42
EF1018	EF_RS04845	PTS system, IIA component	-3.05
EF1019	EF_RS04850	PTS system, IIC component	-4.12
EF3213	EF_RS15200	PTS system, IID component	-4.3
EF1017	EF_RS04840	PTS system, IIB component	-4.49
EF3212	EF_RS15195	PTS system, IIC component	-5.34
EF3210	EF_RS15185	PTS system, IIA component, putative	-6.27
EF3211	EF_RS15190	PTS system, IIB component	-6.57
EF0020	EF_RS00090	PTS system, mannose-specific IIAB components	-90.38
EF0021	EF_RS00095	PTS system, mannose-specific IIC component	-100.36
EF0022	EF_RS00100	PTS system, mannose-specific IID component	-107.49
EF0019	EF_RS00085	PTS system, IIB component	-152.11

REGULATORY FUNCTIONS			
EF0107	EF_RS00475	transcriptional regulator, CrpFnr family	18.06
EF1515	EF_RS07320	transcription antiterminator, bglG family	14.09
EF0432	EF_RS02135	transcriptional regulator, AraC family	12.37
EF1656	EF_RS07960	transcriptional regulator, LysR family	8.75
EF1591	EF_RS07670	transcriptional regulator, AraC family	8.39
EF3144	EF_RS14890	phosphosugar-binding transcriptional regulator, RpiR family	8.25
EF2711	EF_RS12850	transcriptional regulator, AraC family	7.88
EF0103	EF_RS00455	transcriptional regulator, ArgR family	5.68
EF3008	EF_RS14265	PucR family transcriptional regulator	3.56
EF0102	EF_RS00450	transcriptional regulator, ArgR family	3.33
EF0382	EF_RS01910	PucR family transcriptional regulator	3.32
EF3328	EF_RS15755	transcriptional regulator, GntR family	3.07
EF0676	EF_RS03250	arginine repressor	3.05
EF2933	EF_RS13905	redox-sensing transcriptional repressor Rex	3.03
EF2594	EF_RS12320	transcriptional regulator, TetR family	-3.45
EF2703	EF_RS12815	transcriptional regulator	-4.07
EF1302	EF_RS06275	transcriptional regulator, putative	-4.41
EF1224	EF_RS05915	transcriptional regulator, CroCI family	-4.56
EF1303	EF_RS06280	transcriptional regulator, LysR family	-4.92
EF0782	EF_RS03735	RNA polymerase sigma-54 factor	-132.88
CELLULAR PROCESSES			
EF2569	EF_RS12205	molybdenum cofactor cytidylyltransferase	21.29
EF0439	EF_RS02170	immunity protein PlnM, putative	11.35
EF3023	EF_RS14340	polysaccharide lyase, family 8	8.85
EF1076	EF_RS05200	streptomycin 3-adenylyltransferase, putative	5.84
EF0818	EF_RS03900	polysaccharide lyase, family 8	3.61
EF1502	EF_RS07265	beta-lactamase, putative	3.25
EF1959	EF_RS09350	toll/interleukin-1 receptor domain-containing protein	3.23
EF2739	EF_RS12970	alkyl hydroperoxide reductase, C subunit	-3.04
EF1300	EF_RS06265	cell division protein, FtsWRodASpovE family	-3.69
EF1301	EF_RS06270	cell division protein, FtsWRodASpovE family	-3.89
AMINO ACID BIOSYNTHESIS			
EF0891	EF_RS04235	aspartate aminotransferase, putative	47.93
EF0105	EF_RS00465	ornithine carbamoyltransferase	19.35
EF2568	EF_RS12200	aminotransferase, class V	18.70
EF2560	EF_RS12160	glutamate synthase (NADPH), homotetrameric	10.5
EF2994	EF_RS14200	alanine--glyoxylate aminotransferase family protein	3.41

TWO COMPONENT SYSTEMS			
EF2218	EF_RS10610	DNA-binding response regulator, AraC family	12.18
EF2219	EF_RS10615	sensor histidine kinase	11.03
BIOSYNTHESIS OF COFACTORS,PROSTHETIC GROUPS AND CARRIERS			
EF1395	EF_RS06740	molybdenum cofactor biosynthesis family protein	38.35
EF1396	EF_RS06745	molybdenum cofactor biosynthesis family protein, putative	35.07
EF1393	EF_RS06730	molybdopterin cofactor biosynthesis protein A, putative	30.09
EF1225	EF_RS05920	thiamin biosynthesis ApbE, putative	23.88
EF1392	EF_RS06725	molybdenum cofactor biosynthesis protein MoaC	4.44
EF1655	EF_RS07955	2-dehydropantoate 2-reductase, putative	4.3
EF1391	EF_RS06720	molybdenum cofactor biosynthesis family protein	3.06
EF1969	EF_RS09395	phosphomethylpyrimidine kinase, putative	-3.38
EF2445	EF_RS11620	2-dehydropantoate 2-reductase, putative	-4.14
DNA METABOLISM			
EF0053	EF_RS00245	DNA polymerase III, epsilon subunit	7.74
TRANSCRIPTION			
EF0115	EF_RS00515	endoribonuclease L-PSP, putative	30.17
EF3214	EF_RS15205	ATP-dependent helicase, DEAH-box family, putative	-3.63
PRYRIMIDINE RIBONUCLEOTIDE BIOSYNTHESIS			
EF2561	EF_RS12165	dihydroorotate dehydrogenase electron transfer subunit, putative	13.65
EF2999	EF_RS14220	allantoinase, putative	5.82
NUCLEOTIDE RELATED			
EF1921	EF_RS09205	inosine-uridine preferring nucleoside hydrolase	15.75
EF1036	EF_RS04935	nucleoside diphosphate kinase	11.54
EF2580	EF_RS12255	D-hydantoinase	6.39
EF1958	EF_RS09345	deoxyguanosinetriphosphate triphosphohydrolase, putative	3.61
CENTRAL INTERMEDIARY METABOLISM			
EF3141	EF_RS14880	D-isomer specific 2-hydroxyacid dehydrogenase family protein	16.2
EF0895	EF_RS04250	glycerol dehydrogenase, putative	15.54
EF3140	EF_RS14875	alcohol dehydrogenase, iron-containing	9.99
EF1358	EF_RS06555	glycerol dehydrogenase, putative	4.88
EF1364	EF_RS06585	acetyl-CoA acetyltransferasehydroxymethylglutaryl-CoA reductase, degradative	-3.41
EF1813	EF_RS08695	sulfatase domain protein	-11.88

PHAGE PROTEINS			
EF0354	EF_RS01775	holin, putative	-3.02
EF0339	EF_RS01705	major capsid protein, putative	-3.15
FATTY ACID AND PHOSPHOLIPID METABOLISM			
EF1663	EF_RS07995	branched-chain phosphotransacylase	10.28
PROTEIN SYNTHESIS AND FATE			
EF2567	EF_RS12195	selenide, water dikinase	16.82
EF2471	EF_RS11740	arginyl-tRNA synthetase	7.8
EF2997	EF_RS14215	peptidase, M20M25M40 family	3.64
EF2578	EF_RS12245	peptidase, M20M25M40 family	3.02
EF2858	EF_RS13530	threonyl-tRNA synthetase	-3.14
EF3207	EF_RS15170	tRNA-dihydrouridine synthase	-3.64
EF0633	EF_RS03050	tyrosyl-tRNA synthetase	-4.39
EF0634	EF_RS03055	tyrosine decarboxylase	-4.90

Table S5: Putative *cre* sites in differentially expressed genes in V583Δ*rpoN* compared to V583

Gene		Function	Fold change	Start	End	*cre* Sequence (WTGNNARCGNWWWCAW)
Former Locus Tag	Current Locus Tag					
Upregulated						
EF0052	EF_RS00240	hypothetical protein	5.41			
EF0053	EF_RS00245	DNA polymerase III, epsilon subunit	7.74			
EF0054	EF_RS00250	hypothetical protein	58.53	-92	-78	TCGAAAGCGCTTTCT
EF0104	EF_RS00460	arginine deiminase	15.83	-146	-132	ATGAAAGCGCATTCT
EF0105	EF_RS00465	ornithine carbamoyltransferase	19.35			
EF0106	EF_RS00470	carbamate kinase	19.07			
EF0107	EF_RS00475	transcriptional regulator, CrpFnr family	18.06			
EF0108	EF_RS00480	C4-dicarboxylate transporter, putative	13.04			
EF0114	EF_RS00510	glycosyl hydrolase, family 20	48.20	-35	-21	GTGTATGCGCTTTCT
EF0115	EF_RS00515	endoribonuclease L-PSP, putative	30.17	-49	-35	ATGTAAGCGGAATCA
EF0253	EF_RS01155	aldehyde dehydrogenase	35.88	-38	-24	TTGTAAGCGGATACA
EF0291	EF_RS01465	glycosyl hydrolase, family 1	4.06			
EF0292	EF_RS01470	PTS system, IIC component	6.62	-51	-37	ATGTAAACGGATACA
EF0361	EF_RS01810	chitinase, family 2	69.31			
EF0362	EF_RS01815	chitin binding protein, putative	83.75	-41	-27	CTGTAAGCGCATACA
EF0382	EF_RS01910	PucR family transcriptional regulator	3.32	-76	-62	ATGAAAACACTTTCT
EF0383	EF_RS01915	protein FdrA conserved hypothetical protein	29.34	-61	-47	ATGAAAACACTTTCT
EF0405	EF_RS02010	hydrolase, haloacid dehalogenase-like family	7.16	-71	-57	ATGTAAACGGATTCT
EF0439	EF_RS02170	immunity protein PlnM, putative	13.54	-49	-35	ATGAAAACGTTATCA
EF0551	EF_RS02695	glycosyl hydrolase, family 31	3.89	-85	-70	ATACAAACGCTTTCAT
EF0552	EF_RS02700	PTS system, IIC component	6.21			
EF0553	EF_RS02705	PTS system, IID component	11.35			
EF0554	EF_RS02710	PTS system, IIB component	9.6			
EF0555	EF_RS02715	PTS system, IIA component	3.75			
EF0664	EF_RS03195	hypothetical protein	27.97	-17	-3	ATGAAAGCGGATACA
EF0938	EF_RS04460	ABC transporter, ATP-bindingTOBE domain protein	12.53	-60	-46	ATGAAAACGCTATCT
EF1036	EF_RS04935	nucleoside diphosphate kinase	11.54	-75	-61	ATGAAAGCGGATACT
EF1066	EF_RS05155	hexapeptide-repeat containing-acetyltransferase	6.47			
EF1068	EF_RS05160	aldose 1-epimerase	18.97	-126	-112	TTGAAAACGTGTACA
EF1069	EF_RS05165	galactokinase	3.17	-109	-95	TTGTACACGTTTTCA
EF1158	EF_RS05600	N4-(beta-N-acetylglucosaminyl)-L-asparaginase, putative	3.52	-61	-46	TCGTTAACGCTTACAT
EF1206	EF_RS05830	malate dehydrogenase, decarboxylating	6.26			

EF1207	EF_RS05835	citrate carrier protein, CCS family	8.54	-53	-39	ATGTAAACGTTTTCT
EF1232	EF_RS05950	ABC transporter, permease protein	8.63	-81	-67	ATGTAAGGGTTTACA
EF1233	EF_RS05955	ABC transporter, permease protein	13.83			
EF1234	EF_RS05960	ABC transporter, substrate-binding protein, putative	12.52			
EF1358	EF_RS06555	glycerol dehydrogenase, putative	4.88	-51	-37	ATGAAAGCGTTTTAT
EF1359	EF_RS06560	PTS-dependent dihydroxyacetone kinase phosphotransferase subunit DhaM	4.70			
EF1360	EF_RS06565	dihydroxyacetone kinase subunit DhaK	4.70			
EF1361	EF_RS06570	dihydroxyacetone kinase subunit L	3.84			
EF1392	EF_RS06725	molybdenum cofactor biosynthesis protein MoaC	4.44	-38	-24	GTGTAAACGTTAACA
EF1393	EF_RS06730	molybdopterin cofactor biosynthesis protein A, putative	30.09			
EF1394	EF_RS06735	conserved hypothetical protein	29.49			
EF1395	EF_RS06740	molybdenum cofactor biosynthesis family protein	38.35			
EF1396	EF_RS06745	molybdenum cofactor biosynthesis family protein, putative	35.07			
EF1397	EF_RS09100	molybdenum ABC transporter, molybdenum-binding protein	23.85			
EF1398	EF_RS06755	molybdenum ABC transporter, permease protein	26.3			
EF1399	EF_RS06760	molybdenum ABC transporter, ATP-binding protein, putative	13.1			
EF1400	EF_RS06765	cadmium-translocating P-type ATPase	6.43			
EF1407	EF_RS06795	hypothetical protein	4.07	-59	-44	ATGATAACGATTTCTT
EF1591	EF_RS07670	transcriptional regulator, AraC family	8.39	-32	-17	TAGAAAGCGGATACAA
EF1656	EF_RS07960	transcriptional regulator, LysR family	8.75	-33	-19	TTAAAAGCGCTTACA
EF1657	EF_RS07965	membrane protein, putative	5.8			
EF1658	EF_RS07970	branched-chain alpha-keto acid, E2 component, dihydrolipoamide acetyltransferase	14.28			
EF1659	EF_RS07975	branched-chain alpha-keto acid dehydrogenase, E1 component, beta subunit	8.46			
EF1660	EF_RS07980	branched-chain alpha-keto acid dehydrogenase, E1 component, alpha subunit	5.14			
EF1661	EF_RS07985	branched-chain alpha-keto acid dehydrogenase, E3 component, dihydrolipoamide dehydrogenase	14.95			
EF1662	EF_RS07990	butyrate kinase	5.13			
EF1663	EF_RS07995	branched-chain phosphotransacylase	10.28	-61	-47	ATGTAAACGCATACA
EF1800	EF_RS08635	conserved hypothetical protein	4.01	-41	-27	ATGAAAGCGTGTTCA
EF1801	EF_RS08640	PTS system, IIA component	4.42			
EF1802	EF_RS08645	PTS system, IID component	7.35			
EF1803	EF_RS08650	PTS system, IIC component	8.28			
EF1804	EF_RS08655	PTS system, IIB component	6.36			
EF1805	EF_RS08660	glycosyl hydrolase, family 35	4.81	-30	-16	TTGAAAGCGTTTACT

EF1824	EF_RS08745	glycosyl hydrolase, family 31fibronectin type III domain protein	6.82	-255	-241	ATGAAAACGCATTCA
EF1836	EF_RS08810	PTS system, IIA component, putative	5.84	-63	-49	TTGAAAGCGTTTTAT
EF1837	EF_RS08815	PTS system, IIB component, putative	5.74			
EF1919	EF_RS09195	acetyltransferase, GNAT family	5.87			
EF1920	EF_RS09200	C4-dicarboxylate anaerobic carrier	13.23			
EF1921	EF_RS09205	inosine-uridine preferring nucleoside hydrolase	15.75	-76	-61	TTAACAGCGCTTTCAT
EF1927	EF_RS09230	glycerol uptake facilitator protein	36.4			
EF1928	EF_RS09235	alpha-glycerophosphate oxidase	43.44			
EF1929	EF_RS09240	glycerol kinase	53.22	-146 -36	-132 -22	TTGAAAGCGTTGTCT TTGAAATCGTTTTCT
EF2221	EF_RS10625	ABC transporter, substrate-binding protein	128.09			
EF2222	EF_RS10630	ABC transporter, permease protein	114.8			
EF2223	EF_RS10635	ABC transporter, permease protein	257.25	-38	-24	ATGAAAACGCTATTA
EF2232	EF_RS10680	ABC transporter, permease protein	4.2			
EF2233	EF_RS10685	ABC transporter, permease protein	8.46			
EF2234	EF_RS10690	sugar ABC transporter, sugar-binding protein, putative	17.24			
EF2235	EF_RS10695	glucuronyl hydrolase, putative	7.81			
EF2236	EF_RS10700	conserved hypothetical protein	18.24			
EF2237	EF_RS10705	lipoprotein, putative	7.17	-35	-21	ATTAAAGCGCTTTCT
EF2559	EF_RS12155	pyruvate flavodoxinferredoxin oxidoreductase family protein	9.99			
EF2560	EF_RS12160	glutamate synthase (NADPH), homotetrameric	10.5			
EF2561	EF_RS12165	dihydroorotate dehydrogenase electron transfer subunit, putative	13.65			
EF2562	EF_RS12170	flavodoxin	19.95	-68	-53	ATGTAAGGGGTTACAA
EF2709	EF_RS12840	glycosyl hydrolase, family 2	3.56	-56	-41	TTGGAAACGATATGAA
EF2711	EF_RS12850	transcriptional regulator, AraC family	7.88	-37	-23	ATGTAAAGGCTTTCT
EF2863	EF_RS13555	endo-beta-N-acetylglucosaminidase	62.34	-45	-31	TTGTAAGCGCTAACA
EF2996	EF_RS14210	conserved hypothetical protein	4.13			
EF2997	EF_RS14215	peptidase, M20M25M40 family	3.64			
EF2999	EF_RS14220	allantoinase, putative	5.82			
EF3000	EF_RS14225	cytosinepurines, uracil, thiamine, allantoin permease family protein	4.56	-118	-104	TTGTAAGCGCTTTTT
EF3023	EF_RS14340	polysaccharide lyase, family 8	8.85	-209	-195	GTGAAAGCGTAAACA
EF3088	EF_RS14630	hypothetical protein	5.34	-58	-44	ATAAAAACGTTTTCT
EF3134	EF_RS14845	2-dehydro-3-deoxyphosphogluconate aldolase4-hydroxy-2-oxoglutarate aldolase	10.43			
EF3135	EF_RS14850	mannonate dehydratase, putative	13.37			
EF3136	EF_RS14855	PTS system, IIA component	12.08			
EF3137	EF_RS14860	PTS system, IIB component	16			
EF3138	EF_RS14865	PTS system, IID component	17.41			
EF3139	EF_RS14870	PTS system, IIC component	7.55			

EF3140	EF_RS14875	alcohol dehydrogenase, iron-containing	9.99			
EF3141	EF_RS14880	D-isomer specific 2-hydroxyacid dehydrogenase family protein	16.2			
EF3142	EF_RS14885	6-phosphogluconate dehydrogenase family protein	8.83	-68	-34	ATGTAAACGATTACA
EF3144	EF_RS14890	phosphosugar-binding transcriptional regulator, RpiR family	8.25	-53	-39	ATGAAAAGGCATTCA
EF3325	EF_RS15740	sodium ion-translocating decarboxylase, biotin carboxyl carrier protein	5.29			
EF3326	EF_RS15745	conserved hypothetical protein	4.85	-373	-359	TTGTAAGCGTTAACA
EF3327	EF_RS15750	citrate transporter	7.22	-45	-31	TTGTAAGCGTTAACA
Downregulated						
EF1017	EF_RS04840	PTS system, IIB component	-4.49	-173	-158	TTGGAAACGCACACAA
EF1018	EF_RS04845	PTS system, IIA component	-3.05			
EF1019	EF_RS04850	PTS system, IIC component	-4.12			

Strongly conserved residues of the *cre* consensus sequence are underlined.

References

1. Weiner LM, Webb AK, Limbago B, Dudeck MA, Patel J, Kallen AJ, Edwards JR, Sievert DM. 2016. Antimicrobial-Resistant Pathogens Associated With Healthcare-Associated Infections: Summary of Data Reported to the National Healthcare Safety Network at the Centers for Disease Control and Prevention, 2011-2014. Infect Control Hosp Epidemiol 37:1288-1301.
2. Fiore E, Van Tyne D, Gilmore MS. 2019. Pathogenicity of Enterococci. Microbiol Spectr 7.
3. Vebo HC, Snipen L, Nes IF, Brede DA. 2009. The transcriptome of the nosocomial pathogen Enterococcus faecalis V583 reveals adaptive responses to growth in blood. PLoS One 4:e7660.
4. Vebo HC, Solheim M, Snipen L, Nes IF, Brede DA. 2010. Comparative genomic analysis of pathogenic and probiotic Enterococcus faecalis isolates, and their transcriptional responses to growth in human urine. PLoS One 5:e12489.
5. Frank KL, Colomer-Winter C, Grindle SM, Lemos JA, Schlievert PM, Dunny GM. 2014. Transcriptome analysis of Enterococcus faecalis during mammalian infection shows cells undergo adaptation and exist in a stringent response state. PLoS One 9:e115839.
6. Iyer VS, Hancock LE. 2012. Deletion of sigma(54) (rpoN) alters the rate of autolysis and biofilm formation in Enterococcus faecalis. J Bacteriol 194:368-75.
7. Hechard Y, Pelletier C, Cenatiempo Y, Frere J. 2001. Analysis of sigma(54)-dependent genes in Enterococcus faecalis: a mannose PTS permease (EIIMan) is involved in sensitivity to a bacteriocin, mesentericin Y105. Microbiology-Sgm 147:1575-1580.
8. Deutscher J, Ake FM, Derkaoui M, Zebre AC, Cao TN, Bouraoui H, Kentache T, Mokhtari A, Milohanic E, Joyet P. 2014. The bacterial phosphoenolpyruvate:carbohydrate phosphotransferase system: regulation by protein phosphorylation and phosphorylation-dependent protein-protein interactions. Microbiol Mol Biol Rev 78:231-56.
9. Dalet K, Briand C, Cenatiempo Y, Hechard Y. 2000. The rpoN gene of Enterococcus faecalis directs sensitivity to subclass IIa bacteriocins. Current Microbiology 41:441-443.
10. Opsata M, Nes IF, Holo H. 2010. Class IIa bacteriocin resistance in Enterococcus faecalis V583: the mannose PTS operon mediates global transcriptional responses. BMC Microbiol 10:224.
11. Diep DB, Skaugen M, Salehian Z, Holo H, Nes IF. 2007. Common mechanisms of target cell recognition and immunity for class II bacteriocins. Proc Natl Acad Sci U S A 104:2384-9.
12. Miwa Y, Nakata A, Ogiwara A, Yamamoto M, Fujita Y. 2000. Evaluation and characterization of catabolite-responsive elements (cre) of Bacillus subtilis. Nucleic Acids Res 28:1206-10.
13. Schumacher MA, Sprehe M, Bartholomae M, Hillen W, Brennan RG. 2011. Structures of carbon catabolite protein A-(HPr-Ser46-P) bound to diverse catabolite response element sites reveal the basis for high-affinity binding to degenerate DNA operators. Nucleic Acids Res 39:2931-42.
14. Saier MH, Jr., Chauvaux S, Cook GM, Deutscher J, Paulsen IT, Reizer J, Ye JJ. 1996. Catabolite repression and inducer control in Gram-positive bacteria. Microbiology 142 (Pt 2):217-30.
15. Gorke B, Stulke J. 2008. Carbon catabolite repression in bacteria: many ways to make the most out of nutrients. Nat Rev Microbiol 6:613-24.
16. da Silva Neto JF, Koide T, Gomes SL, Marques MV. 2010. Global gene expression under nitrogen starvation in Xylella fastidiosa: contribution of the σ54 regulon. BMC Microbiol 10:231.
17. da Silva Neto JF, Koide T, Abe CM, Gomes SL, Marques MV. 2008. Role of sigma54 in the regulation of genes involved in type I and type IV pili biogenesis in Xylella fastidiosa. Arch Microbiol 189:249-61.
18. Leang C, Krushkal J, Ueki T, Puljic M, Sun J, Juárez K, Núñez C, Reguera G, DiDonato R, Postier B, Adkins RM, Lovley DR. 2009. Genome-wide analysis of the RpoN regulon in Geobacter sulfurreducens. BMC Genomics 10:331.
19. Damron FH, Owings JP, Okkotsu Y, Varga JJ, Schurr JR, Goldberg JB, Schurr MJ, Yu HD. 2012. Analysis of the Pseudomonas aeruginosa regulon controlled by the sensor kinase KinB and sigma factor RpoN. J Bacteriol 194:1317-30.

20. Reitzer L, Schneider BL. 2001. Metabolic context and possible physiological themes of sigma(54)-dependent genes in Escherichia coli. Microbiol Mol Biol Rev 65:422-44.
21. Thurlow LR, Thomas VC, Hancock LE. 2009. Capsular Polysaccharide Production in Enterococcus faecalis and Contribution of CpsF to Capsule Serospecificity. Journal of Bacteriology 191:6203-6210.
22. Socransky SS, Dzink JL, Smith CM. 1985. Chemically defined medium for oral microorganisms. J Clin Microbiol 22:303-5.
23. Brown SA, Whiteley M. 2007. A novel exclusion mechanism for carbon resource partitioning in Aggregatibacter actinomycetemcomitans. J Bacteriol 189:6407-14.
24. Walters MC, 3rd, Roe F, Bugnicourt A, Franklin MJ, Stewart PS. 2003. Contributions of antibiotic penetration, oxygen limitation, and low metabolic activity to tolerance of Pseudomonas aeruginosa biofilms to ciprofloxacin and tobramycin. Antimicrob Agents Chemother 47:317-23.
25. Ramsey MM, Whiteley M. 2009. Polymicrobial interactions stimulate resistance to host innate immunity through metabolite perception. Proc Natl Acad Sci U S A 106:1578-83.
26. Ramsey MM, Whiteley M. 2004. Pseudomonas aeruginosa attachment and biofilm development in dynamic environments. Mol Microbiol 53:1075-87.
27. Bendtsen JD, Nielsen H, von Heijne G, Brunak S. 2004. Improved prediction of signal peptides: SignalP 3.0. J Mol Biol 340:783-95.
28. Krogh A, Larsson B, von Heijne G, Sonnhammer EL. 2001. Predicting transmembrane protein topology with a hidden Markov model: application to complete genomes. J Mol Biol 305:567-80.
29. Hofmann KS, W. 1993. A Database of Membrane Spanning Protein Segments.
30. Janulczyk R, Rasmussen M. 2001. Improved pattern for genome-based screening identifies novel cell wall-attached proteins in gram-positive bacteria. Infect Immun 69:4019-26.
31. Sillanpää J, Xu Y, Nallapareddy SR, Murray BE, Höök M. 2004. A family of putative MSCRAMMs from Enterococcus faecalis. Microbiology (Reading) 150:2069-2078.
32. Bagos PG, Tsirigos KD, Liakopoulos TD, Hamodrakas SJ. 2008. Prediction of lipoprotein signal peptides in Gram-positive bacteria with a Hidden Markov Model. J Proteome Res 7:5082-93.
33. Parthasarathy S, Jordan LD, Schwarting N, Woods MA, Abdullahi Z, Varahan S, Passos PMS, Miller B, Hancock LE. 2020. Involvement of Chromosomally Encoded Homologs of the RRNPP Protein Family in Enterococcus faecalis Biofilm Formation and Urinary Tract Infection Pathogenesis. J Bacteriol 202.
34. Schwartz K, Stephenson R, Hernandez M, Jambang N, Boles BR. 2010. The use of drip flow and rotating disk reactors for Staphylococcus aureus biofilm analysis. J Vis Exp doi:10.3791/2470.
35. Sahm DF, Kissinger J, Gilmore MS, Murray PR, Mulder R, Solliday J, Clarke B. 1989. In vitro susceptibility studies of vancomycin-resistant Enterococcus faecalis. Antimicrob Agents Chemother 33:1588-91.
36. Thurlow LR, Thomas VC, Narayanan S, Olson S, Fleming SD, Hancock LE. 2010. Gelatinase contributes to the pathogenesis of endocarditis caused by Enterococcus faecalis. Infect Immun 78:4936-43.
37. Guiton PS, Hung CS, Hancock LE, Caparon MG, Hultgren SJ. 2010. Enterococcal biofilm formation and virulence in an optimized murine model of foreign body-associated urinary tract infections. Infect Immun 78:4166-75.
38. Zhao K, Liu MZ, Burgess RR. 2010. Promoter and regulon analysis of nitrogen assimilation factor, Sigma(54), reveal alternative strategy for E-coli MG1655 flagellar biosynthesis. Nucleic Acids Research 38:1273-1283.
39. Arous S, Buchrieser C, Folio P, Glaser P, Namane A, Hebraud M, Hechard Y. 2004. Global analysis of gene expression in an rpoN mutant of Listeria monocytogenes. Microbiology 150:1581-90.
40. Shankar N, Baghdayan AS, Gilmore MS. 2002. Modulation of virulence within a pathogenicity island in vancomycin-resistant Enterococcus faecalis. Nature 417:746-50.

41. Hirschman J, Wong PK, Sei K, Keener J, Kustu S. 1985. Products of nitrogen regulatory genes ntrA and ntrC of enteric bacteria activate glnA transcription in vitro: evidence that the ntrA product is a sigma factor. Proc Natl Acad Sci U S A 82:7525-9.
42. Wiegeshoff F, Beckering CL, Debarbouille M, Marahiel MA. 2006. Sigma L is important for cold shock adaptation of Bacillus subtilis. J Bacteriol 188:3130-3.
43. Hayrapetyan H, Tempelaars M, Nierop Groot M, Abee T. 2015. Bacillus cereus ATCC 14579 RpoN (Sigma 54) Is a Pleiotropic Regulator of Growth, Carbohydrate Metabolism, Motility, Biofilm Formation and Toxin Production. PLoS One 10:e0134872.
44. Deutscher J, Francke C, Postma PW. 2006. How phosphotransferase system-related protein phosphorylation regulates carbohydrate metabolism in bacteria. Microbiol Mol Biol Rev 70:939-1031.
45. Pfluger-Grau K, Gorke B. 2010. Regulatory roles of the bacterial nitrogen-related phosphotransferase system. Trends Microbiol 18:205-14.
46. Morett E, Segovia L. 1993. The sigma 54 bacterial enhancer-binding protein family: mechanism of action and phylogenetic relationship of their functional domains. J Bacteriol 175:6067-74.
47. Buck M, Gallegos MT, Studholme DJ, Guo Y, Gralla JD. 2000. The bacterial enhancer-dependent sigma(54) (sigma(N)) transcription factor. J Bacteriol 182:4129-36.
48. Studholme DJ, Buck M. 2000. The biology of enhancer-dependent transcriptional regulation in bacteria: insights from genome sequences. Fems Microbiology Letters 186:1-9.
49. Francke C, Groot Kormelink T, Hagemeijer Y, Overmars L, Sluijter V, Moezelaar R, Siezen RJ. 2011. Comparative analyses imply that the enigmatic Sigma factor 54 is a central controller of the bacterial exterior. BMC Genomics 12:385.
50. Muraoka A, Ito K, Nagasaki H, Tanaka S. 1991. [Phosphoenolpyruvate:carbohydrate phosphotransferase systems in Enterococcus faecalis]. Nihon Saikingaku Zasshi 46:515-22.
51. Samuels DJ, Frye JG, Porwollik S, McClelland M, Mrazek J, Hoover TR, Karls AC. 2013. Use of a promiscuous, constitutively-active bacterial enhancer-binding protein to define the sigma(5)(4) (RpoN) regulon of Salmonella Typhimurium LT2. BMC Genomics 14:602.
52. Henkin TM. 1996. The role of CcpA transcriptional regulator in carbon metabolism in Bacillus subtilis. FEMS Microbiol Lett 135:9-15.
53. Bush M, Dixon R. 2012. The Role of Bacterial Enhancer Binding Proteins as Specialized Activators of σ54-Dependent Transcription. Microbiol Mol Biol Rev 76:497-529.
54. Tobisch S, Zuhlke D, Bernhardt J, Stulke J, Hecker M. 1999. Role of CcpA in regulation of the central pathways of carbon catabolism in Bacillus subtilis. J Bacteriol 181:6996-7004.
55. Iyer R, Baliga NS, Camilli A. 2005. Catabolite control protein A (CcpA) contributes to virulence and regulation of sugar metabolism in Streptococcus pneumoniae. J Bacteriol 187:8340-9.
56. Li C, Sun F, Cho H, Yelavarthi V, Sohn C, He C, Schneewind O, Bae T. 2010. CcpA mediates proline auxotrophy and is required for Staphylococcus aureus pathogenesis. J Bacteriol 192:3883-92.
57. Watson ME, Jr., Nielsen HV, Hultgren SJ, Caparon MG. 2013. Murine vaginal colonization model for investigating asymptomatic mucosal carriage of Streptococcus pyogenes. Infect Immun 81:1606-17.
58. Leboeuf C, Leblanc L, Auffray Y, Hartke A. 2000. Characterization of the ccpA gene of Enterococcus faecalis: identification of starvation-inducible proteins regulated by ccpA. J Bacteriol 182:5799-806.
59. Keogh D, Lam LN, Doyle LE, Matysik A, Pavagadhi S, Umashankar S, Low PM, Dale JL, Song Y, Ng SP, Boothroyd CB, Dunny GM, Swarup S, Williams RBH, Marsili E, Kline KA. 2018. Extracellular Electron Transfer Powers Enterococcus faecalis Biofilm Metabolism. mBio 9.
60. Pillai SK, Sakoulas G, Eliopoulos GM, Moellering RC, Jr., Murray BE, Inouye RT. 2004. Effects of glucose on fsr-mediated biofilm formation in Enterococcus faecalis. J Infect Dis 190:967-70.
61. Tendolkar PM, Baghdayan AS, Gilmore MS, Shankar N. 2004. Enterococcal surface protein, Esp, enhances biofilm formation by Enterococcus faecalis. Infect Immun 72:6032-9.

62. Kaval KG, Gebbie M, Goodson JR, Cruz MR, Winkler WC, Garsin DA. 2019. Ethanolamine Utilization and Bacterial Microcompartment Formation Are Subject to Carbon Catabolite Repression. J Bacteriol 201.
63. Garsin DA. 2010. Ethanolamine utilization in bacterial pathogens: roles and regulation. Nat Rev Microbiol 8:290-5.
64. Wright EM, Hirayama BA, Loo DF. 2007. Active sugar transport in health and disease. J Intern Med 261:32-43.
65. Hewitt CD, Innes DJ, Savory J, Wills MR. 1989. Normal biochemical and hematological values in New Zealand white rabbits. Clin Chem 35:1777-9.
66. Roberts G, Tarelli E, Homer KA, Philpott-Howard J, Beighton D. 2000. Production of an endo-beta-N-acetylglucosaminidase activity mediates growth of Enterococcus faecalis on a high-mannose-type glycoprotein. J Bacteriol 2000 Feb;182(4):882-90 182:882-90.
67. Vitko NP, Grosser MR, Khatri D, Lance TR, Richardson AR. 2016. Expanded Glucose Import Capability Affords Staphylococcus aureus Optimized Glycolytic Flux during Infection. mBio 7.
68. Sundar GS, Islam E, Braza RD, Silver AB, Le Breton Y, McIver KS. 2018. Route of Glucose Uptake in the Group a Streptococcus Impacts SLS-Mediated Hemolysis and Survival in Human Blood. Front Cell Infect Microbiol 8:71.
69. Kumar S, Narayan KS, Shandilya S, Sood SK, Kapila S. 2019. Role of non-PTS dependent glucose permease (GlcU) in maintaining the fitness cost during acquisition of nisin resistance by Enterococcus faecalis. FEMS Microbiol Lett 366.
70. Paulsen IT, Chauvaux S, Choi P, Saier MH, Jr. 1998. Characterization of glucose-specific catabolite repression-resistant mutants of Bacillus subtilis: identification of a novel hexose:H+ symporter. J Bacteriol 180:498-504.
71. Hartman CE, Samuels DJ, Karls AC. 2016. Modulating Salmonella Typhimurium's Response to a Changing Environment through Bacterial Enhancer-Binding Proteins and the RpoN Regulon. Front Mol Biosci 3:41.
72. Miller KA, Phillips RS, Mrazek J, Hoover TR. 2013. Salmonella utilizes D-glucosaminate via a mannose family phosphotransferase system permease and associated enzymes. J Bacteriol 195:4057-66.

Chapter 3: Activity of CcpA-regulated GH18 family glycosyl hydrolases that contribute to nutrient acquisition and fitness in *Enterococcus faecalis*

Abstract

The ability of *Enterococcus faecalis* to colonize host anatomic sites is dependent on its adaptive response to host conditions. Three glycosyl hydrolase gene clusters, each belonging to the GH18 family (*ef0114, ef0361,* and *ef2863*) in *E. faecalis* were previously found to be upregulated under glucose-limiting conditions. The GH18 catalytic domain is predicted to contain β-1,4 endo-N-acetyl-beta-D-glucosaminidase (ENGase) activity, and such activity is commonly associated with cleaving N-linked glycoproteins, an abundant glycan structure on host epithelial surfaces. Here we show that all three hydrolases are negatively regulated by the transcriptional regulator Carbon Catabolite Protein A (CcpA). Additionally, we demonstrate that a constitutively active CcpA variant represses the expression of CcpA-regulated genes irrespective of glucose availability. Previous studies showed that the GH18 catalytic domain of EndoE (EF0114) and EfEndo18A (EF2863) were capable of deglycosylating RNase B, a model high-mannose type glycoprotein. However, it remained uncertain which glycosidase is primarily responsible for deglycosylation of high-mannose type glycoproteins. In this study, we show by mutation analysis as well as a dose-dependent analysis of recombinant protein expression that EfEndo18A is primarily responsible for deglycosylating high-mannose glycoproteins and the glycans removed by EfEndo18A support growth under nutrient-limiting conditions, *in vitro*. In contrast, IgG is representative of a complex type glycoprotein, and we demonstrate that the GH18 domain of EndoE is primarily responsible for removal of this glycan decoration. Lastly, our data highlight the combined contribution of glycosidases to virulence of *E. faecalis, in vivo.*

Importance

Enterococcus faecalis has emerged as a multidrug-resistant (MDR) nosocomial pathogen that causes life-threatening healthcare-associated infections. Nutrient acquisition systems and immune evasions strategies are key factors that contribute to enterococcal colonization and influence the overall pathogenic potential of this organism. The regulation of these factors is governed by metabolic cues, specifically the availability of glucose as a preferred carbon source. Our research identifies CcpA as a major regulator of secondary nutrient acquisition and expands on the importance of GH18 family glycosyl hydrolases in *E. faecalis*. These hydrolases contribute to the direct targeting of host glycoproteins both for nutrient acquisition, as well as potentially evading both the innate and adaptive immune response. Disrupting the function of these microbial enzymes may lead to new treatments against multidrug resistant enterococcal infections.

Introduction

Enterococcus faecalis is a well-known commensal bacterium that primarily inhabits the mucosal surfaces of the human gastrointestinal tract and oral cavity (1). However, enterococci have emerged as one of the leading causes of healthcare-associated infections, in part due to their intrinsic and acquired resistance to common antibiotics, and now rank second only behind the staphylococci as causative agents of disease in healthcare settings in the United States (2, 3). These hospital acquired infections are often associated with biofilms, including bloodstream infection associated with central-line catheters , surgical site infection and catheter associated urinary tract infections (CAUTI) (3). Some important strategies to adapt to varying host environments include immune evasion and the utilization of secondary nutrients in the absence of preferred carbon sources, which are often host limited (2, 4).

The presence of preferred carbon sources (i.e. glucose) often prevents the use of secondary carbon sources due to the regulatory phenomenon referred to as carbon catabolite repression (CCR) (5, 6). As a CCR mechanism in low G-C Gram-positive bacteria, catabolite responsive element (*cre*) sites in DNA are bound by a protein complex consisting of the catabolite repression protein A (CcpA) and Hpr [Ser-46-P] to inhibit transcription of target genes (6, 7). Under nutrient-limiting conditions, the CcpA and Hpr [Ser-46-P] complex disassociates leading to derepression of CcpA -regulated genes to allow the bacterium to survive in an unfavorable environment (8).

Previously, our lab has shown that the enterococcal alternative sigma factor σ^{54} (RpoN) and its cognate enhancer binding protein, MptR, contribute to nutrient acquisition via the Mpt glucose/mannose phosphotransferase system (PTS) (9). The transcriptomes of *E. faecalis* strain V583 and an isogeneic *rpoN* mutant were previously compared by microarray transcriptional analysis to identify differentially expressed genes in the *rpoN* mutant (9). Among the differentially expressed genes, *cre* sites were present in the promoter regions of a subset of the upregulated genes

present in an *rpoN* mutant, suggesting that they are under CcpA secondary catabolite control (9). Three gene clusters (*ef0114, ef0362-61,* and *ef2863*) that encode the respective endoglycosyl hydrolases (EndoE (10), EfChi18A (11) and EfEndo18A (12)) and a chitin-binding protein/lytic polysaccharide monooxygenase (EfCBM33A (11)) were highly upregulated in the *rpoN* mutant with identified putative *cre* sites within their promoter regions. These enzymes possess putative signal peptide sequences and signal peptide cleavage sites, suggesting that they are actively secreted into the surrounding environment and may contribute to the survival of this bacterium in nutrient limited environments (9).

The glycosyl hydrolases (EndoE (EF0114), EfChi18A (EF0361) and EfEndo18A (EF2863)) in this study are all members of the glycosyl hydrolase family 18 (GH18), based on the conserved catalytic motif defined by DXXDXDXE (12, 13). This family is further subdivided into two main groups, β-1,4 endo-β-N-acetylglucosaminidases (ENGases) and chitinases, based primarily on substrate specificity. EndoE and EfEndo18A are classified as ENGases (10, 12, 14, 15), whereas EfChi18A has been characterized as a chitinase (11, 16, 17). Additionally, EfChi18A is encoded in the same operon as its cognate chitin-binding protein/lytic polysaccharide monooxygenase, EfCBM33A, encoded by *ef0362*. Unlike EfEndo18A and EfChi18A, EndoE is a dual domain protein that also possesses a glycosyl hydrolase family 20 (GH20) domain. These glycosyl hydrolases are of interest due to their potential role in alternative carbon metabolism and immune evasion based on their catalytic activity against substrates containing N-acetylglucosamine, such as chitin, various high-mannose type glycoproteins present on host epithelial cells, as well as complex-type glycoproteins IgG and lactoferrin (10-12, 16, 18-20). In this study, we show that CcpA negatively regulates the expression of *ef0114, ef0362-61,* and *ef2863* in a CCR-dependent manner and that a CcpA variant locked into its high-affinity DNA binding conformation represses the expression of CcpA negatively regulated genes, irrespective of glucose availability.

Additionally, we show using genetic mutants that EfEndo18A is responsible for sustaining growth in nutrient limited conditions by deglycosylating a high-mannose type glycoprotein as a carbon source. We also demonstrate that recombinant EfEndo18A is more efficient than EndoE at deglycosylating the glycans from high-mannose type glycoproteins. In contrast, the GH18 catalytic domain of EndoE is primarily responsible for deglycosylation of the complex-type glycoprotein IgG. Lastly, to our knowledge, this report represents the first examination of the contribution of glycosyl hydrolases to *in vivo* fitness in *E. faecalis.* Overall, this study provides evidence that links metabolism of high-mannose type glycoproteins and deglycosylation of IgG with *in vivo* fitness.

Materials and Methods

Bacterial strains and growth conditions:

Bacterial strains used in this study are listed in Supplemental Table 1. For propagation of plasmids, *Escherichia coli* ElectroTen-Blue from Stratagene were cultivated in Luria-Bertani (LB) broth, supplemented with appropriate antibiotics, when necessary. Unless mentioned otherwise, *E. faecalis* was cultured in Todd-Hewitt broth (THB) (BD Biosciences), supplemented with appropriate antibiotics, when necessary. For antibiotic selection, chloramphenicol (Cm) at a concentration of 10ug/mL and 15ug/mL; spectinomycin (Spec) at a concentration of 150ug/mL and 500ug/mL were used for *E. coli* and *E. faecalis*, respectively; ampicillin (Amp) at a concentration of 100ug/mL was used for *E. coli;* and gentamicin (Gent) at a concentration of 250ug/mL was used for *E. faecalis.*

Construction of in-frame markerless deletion strains:

Using the temperature sensitive cloning vector, pLT06 (21), isogenic in-frame deletion mutants of the three glycosyl hydrolase genes were generated in *E. faecalis* V583. Upstream and downstream flanking DNA regions of the respective glycosyl hydrolases were amplified using primers listed in Supplemental Table 2. For example, the primer pairs EF0114P1/EF0114P2 and EF0114P3/EF0114P4 were used to amplify flanking regions upstream and downstream of *ef0114*, respectively. To facilitate cloning, primers EF0114P1/EF0114P2 were designed with EcoRI/BamHI (New England Biolabs (NEB)) restriction sites, respectively, whereas, EF0114P3/EF0114P4 were designed with BamHI/PstI (NEB) restriction sites, respectively. For the construction of the insert, the amplified regions were digested with BamHI, ligated and subsequently re-amplified using primers EF0114P1 and EF0114P4. To generate pIH04 (*ef0114* deletion construct), the amplified insert fragment was digested with EcoRI/PstI and ligated into

the digested pLT06 cloning vector. pIH04 was electroporated into *E. coli* ElectroTen-Blue cells and the plasmid was identified by colony PCR. The confirmed construct was screened by restriction digest analysis and subsequently electroporated into *E. faecalis* V583 cells. V583Δ*ef0114* [IH06] was subsequently generated as previously described (21) and confirmed by colony PCR using the primers EF0114Up and EF0114Down. A similar approach was used to create all the mutants used in this study (Table S1).

Construction of in-frame markerless complement strains:

Using the temperature sensitive cloning vector, pLT06 (21), isogeneic in-frame *ef2863* complement strain was generated in *E. faecalis* V583. The entirety of the *ef2863* gene, including its upstream and downstream flanking DNA regions was amplified using the primer pair EF2863P1/EF2863P4 (Table S2). For cloning purposes, EF2863P1 and EF2863P4 were designed with EcoRI and PstI restriction sites, respectively. The amplified region was digested with EcoRI and PstI and ligated into the digested pLT06 cloning vector, resulting in the creation of pEK11 (*ef2863* complement construct). pEK11 was electroporated into *E. coli* ElectroTen-Blue cells and the plasmid was identified by colony PCR. The confirmed construct was screened by restriction digest analysis and subsequently electroporated into *E. faecalis* V583Δ*ef2863* [AH01], V583Δ*ef0114*Δ*ef0362-61*Δ*ef2863* [AH09], and V583Δ*ccpA*Δ*ef2863* [AH10] cells. V583Δ*ef2863*::*ef2863* [AC04], V583Δ*ef0114*Δ*ef0362-61*Δ*ef2863*::*ef2863* [EK44], and V583Δ*ccpA*Δ*ef2863*::*ef2863* [EK41] was subsequently generated as previously described (21) and confirmed by colony PCR using the primers EF2863Up and EF2863Down.

Construction of the CcpA Phase-Lock mutant strain:

The creation of the CcpA PLM mutant was constructed similarly to the *ef2863* complement strains. However, due to complications with site-directed mutagenesis of the codon encoding the threonine

at amino acid position 307, a sub-region of *ccpA* encompassing this target codon was synthetically generated (IDT) with the desired codon altered from ACA to TAT. This synthetic insert was cloned into an ampicillin-resistant pUC-IDT vector and named pEK32 (Table S3). To create the *ccpA* T307Y insert that would be ligated into the temperature sensitive cloning vector, pLT06 (21), the synthetically generated *ccpA* T307Y fragment was amplified from pEK32 using the primer pair CcpA_PLM5'(EcoRV)/CcpA_PLM3'(AflII) and subsequently digested with EcoRV (NEB). Two-thirds of *ccpA,* as well as the upstream flanking DNA region was amplified using the primer pair CcpAP1/CcpA(EcoRV)Rev, followed by digestion with EcoRV. These two amplified and EcoRV digested fragments were ligated together and subsequently re-amplified using primers CcpAP1 and CcpA_PLM3'(AflII), creating a DNA fragment referred to as CcpA T307Y P1-AflII. This DNA fragment encompasses the entirety *ccpA* with the desired altered codon (TAT), upstream flanking DNA, and a sub-portion of downstream flanking DNA. For the remainder of downstream flanking DNA required for in-frame markerless exchange, the CcpA T307Y P1-AflII DNA fragment was digested with AflII (NEB) and ligated to an AflII digested fragment of DNA amplified using the primer pair CcpA(AflII)For/CcpAP4. Following ligation, the entirety of *ccpA* T307Y, including its upstream and downstream flanking DNA regions was re-amplified with primers CcpAP1/CcpAP4. As previously mentioned, CcpAP1 and CcpAP4 were designed with EcoRI and PstI restriction sites, respectively (9) (22). For cloning into the pLT06 temperature sensitive vector, the amplified *ccpA* T307Y insert was digested with EcoRI and PstI and ligated into pLT06, resulting in the creation of pEK39 (*ccpA* PLM construct). pEK39 was electroporated into *E. coli* ElectroTen-Blue cells and the plasmid was identified by colony PCR. The confirmed construct was screened by restriction digest analysis and subsequently electroporated into *E. faecalis* Δ*ccpA* [EH01] cells. V583Δ*ccpA*::*ccpA* T307Y [EK31], also referred to as CcpA PLM,

was generated as previously described (21) and confirmed by colony PCR using the primers CcpAUp and CcpADown, followed by DNA sequencing analysis.

5' rapid amplification of cDNA ends (RACE) analysis:

5' RACE was performed on isolated RNA (Zymo Direct-zol RNA kit) using a 2nd generation 5' RACE kit (Invitrogen) according to the manufacturer's instructions. RNA was isolated from the Δ*ccpA* mutant grown in THB to mid-exponential phase (OD_{600} ~ 0.5). The primers used for cDNA synthesis and subsequent PCR reactions are listed in Table S2.

Quantitative reverse transcriptase (q-RT) PCR:

E. faecalis strains were grown to mid-exponential or stationary phase in THB or in chemically defined medium (CDM) (23, 24) supplemented with glucose (15mM or 42mM), when indicated, followed by RNA isolation (Zymo Research). Synthesis of cDNA was performed using Superscript III Reverse Transcriptase (Invitrogen) from 1 μg of DNase treated (Invitrogen Turbo DNase). Random hexamer primers (Invitrogen) were used in the initial synthesis reaction. The primers used in q-RT PCR analysis are listed in Table S2. The q-RT PCR reaction was performed with 1 μg of prepared cDNA and 300 nM of each primer using PowerUp SYBR Green Master Mix (ThermoFisher Scientific) on a Quant Studio 3 Real Time PCR system (ThermoFisher Scientific). Following denaturation at 95°C for three minutes, the q-RT PCR reaction was set for 50 cycles with 95°C for 10 seconds, 60°C for 20 seconds and 72°C for 10 seconds. Differential gene expression was calculated using the ΔΔCt method using the threshold cycle values for the gene of interest (*ef0114*, *ef0362*, and *ef2863*) and the endogenous control [*ef0005* (*gyrB*)]. Each qRT-PCR experiment was repeated with three biological replicates.

Cloning, expression, and purification of EndoE (EF0114) and EfEndo18A (EF2863):

The plasmids bearing the protein overexpression constructs, listed in Table S3, are all derivatives of the pET21b vector (Novagen), and the primers used in their construction are also indicated in Table S2. The mutants *ef0114* E186Q, *ef0114* E662Q, and *ef2863* E170Q were created using seamless site-directed mutagenesis (25). Briefly, the *ef0114* E186Q mutagenesis was performed using PCR to make oligonucleotide-directed mutations at the desired position with primer EF0114_E186Q_Forward ,which contained the recognition site for the BsaI restriction endonuclease. This mutagenesis primer was paired with EF0114_3'(XhoI) to make the mutant DNA fragment. Second, a nonmutagenized PCR fragment was made, also using the BsaI restriction enzyme, with primers EF0114_E186Q_Reverse and EF0114_5'(NheI). Lastly, ligation of the mutant and wildtype DNA fragments allowed seamless reconstruction of the full-length *ef0114* E186Q gene to make pEK47. For overexpression and purification, *E.coli* BL21(DE3)-RIPL cells (Agilent Technologies) harboring protein overexpression constructs were grown to an OD_{600} 0.6-0.7 at 37°C, shaking, then induced using 1mM IPTG and further incubated for 16 hours at 16°C, after which the cells were harvested by centrifugation and resuspended in Buffer A (100mM TrisHCl, 0.5M NaCl, 10% glycerol, 15mM imidazole, pH 8.0). The bacteria were lysed using a French press and the soluble fractions were loaded onto a cobalt-affinity column (GE Healthcare TALON Superflow) equilibrated with Buffer A. Recombinant proteins were washed with Buffer A and eluted with an imidazole gradient using Buffers A and B (100mM TrisHCl, 0.5M NaCl,10% glycerol, 500mM imidazole, pH 8.0). Protein purity was analyzed by SDS-PAGE and the protein concentration was determined using the Bradford micro-assay (Bio-Rad Laboratories), according to the supplier's procedure.

RNase B assays:

The initial glycosyl hydrolase activity against high-mannose type glycoproteins was determined using the high mannose containing glycoprotein RNase B (17kDa) (Sigma) as the substrate. For culture supernatant assessment, the bacterial strains were grown overnight at 37°C, shaking in a chemically defined medium (CDM) (50, 51) containing 15mM or 42mM glucose, when indicated, and 20μM hematin. RNase B (5 mg/mL) was incubated with 16μL of filtered supernatants in 1X G7 Reaction Buffer for 16hr at 37°C, in a total reaction volume of 25μl. As controls, RNase B was incubated with buffer alone (negative control) and in the presence of EndoH (NEB) (positive control). Subsequently, the reactions were diluted 1:5 in dH_2O and analyzed by 15% SDS-PAGE under Tris/Tricine running conditions (100V for 1hr). Briefly, a 1X Tris/Tricine rich cathode buffer was prepared from a 10X buffer containing 121.1g of Tris base, 179.2g of Tricine, and 100mL of 10% SDS, pH 8.3 in 1L final volume with dH_2O. Additionally, a 1X Tris-based anode buffer was prepared from a 10X buffer containing 2M Tris, pH 8.8. Gels were stained with InstantBlue Reagent (Expedeon). For recombinant glycosyl hydrolase assessment, EfEndo18A (34.5kDa) and EndoE (88kDa) were overexpressed in *E. coli* BL21(DE3)-RIPL and purified using cobalt-affinity chromatography. For the dose-dependent RNase B experiments, RNase B (5 mg/mL) was incubated with dilutions (1μM, 100nM, 10nM, 1nM, 100pM, and 10pM) of EfEndo18A or EndoE in 1X G7 Reaction Buffer (NEB) for 16hr at 37°C, in a total reaction volume of 25μl. For the analysis of the EfEndo18A site-directed variant, RNase B (5 mg/mL) was incubated with 1μM of EfEndo18A or EfEndo18A E170Q in 1X G7 Reaction Buffer (NEB) for 16hr at 37°C, in a total reaction volume of 25μl. As a control in each assay, RNase B was incubated with buffer alone (negative control). The reactions were diluted 1:5 in dH_2O and analyzed by 15% SDS-PAGE under Tris/Tricine running conditions (100V for 1hr), described above.

Growth assessment in nutrient-limiting conditions supplemented with RNase B or IgG:

Using a single colony of each strain, liquid cultures were started in THB and incubated at 37°C, overnight. For growth analysis, overnight cultures were diluted 1:100 in CDM (23, 24), supplemented with 5 mg/mL of RNase B (294μM) or 44.1 mg/mL of human IgG (294 μM) (Lee Biosolutions). Growth was monitored for 12 hrs in an Infinite M200 Pro plate reader (Tecan Trading AG, Switzerland) at 37°C with orbital shaking at 250 rpm.

IgG lectin blot analysis:

For analysis of purified glycosyl hydrolase variants with IgG as the substrate, 10 μg of human IgG (150kDa ; heavy chain ~50kDa) (Lee Biosolutions) was incubated with 10μM, 1μM, 100nM, or 10nM of purified EfEndo18A or EndoE domain variants in a total reaction volume of 25 μl of PBS at 37°C for 16 hrs. Samples were separated on 12% SDS-PAGE followed by lectin blot analysis (26). Briefly, samples were blotted to Immobilon-P PVDF membranes (Millipore) and subsequently blocked with Tris-buffered saline with 0.1% Tween 20 (Fisher) (TBST) with the addition of 3% skim milk. The blocked membrane was incubated with 0.5 μg biotinylated GNL lectin (Vector Laboratories) for 1 hour, rocking at room temperature, followed by three washes with TBST. Washed membranes were incubated with 1 μg/ml peroxidase-labelled streptavidin (Vector Laboratories). After washing, membranes were developed using the SuperSignal West Pico Chemiluminescent kit (Sigma), wrapped in saran wrap and imaged using a ProteinSimple Gel Imaging & Doc System.

Biofilm assays on polystyrene microtiter plates:

Biofilm formation on 96-well polystyrene microtiter plates were quantified using the crystal violet staining method as previously described with the addition of treating *S. epidermidis* biofilms with 10μM EndoE or EfEndo18A (27). Briefly, *S. epidermidis* strains were grown overnight in TSB

with 0.25% glucose at 37°C. The overnight cultures were diluted 1:100 in 200µL of TSB (0.25% glucose) dispensed in a sterile round-bottom 96-well polystyrene microtiter plate. After 16hr growth at 37°C, wells were gently washed three times with 200µL of phosphate-buffered saline (PBS), followed by treatment with 10µM EndoE or EfEndo18A in 200µL PBS, or PBS alone for mock treated *S. epidermidis* parental and Δ*ica* biofilms. After 24hrs at 37°C, wells were gently washed three times with 200µL PBS, dried at 65°C for 2hrs, and stained with 1% crystal violet (200µL) for 20 min. The wells were rinsed, and the crystal violet was solubilized in 200µL of (80:20 vol/vol) ethanol-acetone. The optical density at 550 nm was measured using an Infinite M200 Pro plate reader (Tecan Trading AG, Switzerland). Each assay was performed with eight internal technical replicates and repeated twice (n=16).

High-mannose IgG Fc (HM-Fc) assays:

The experiments to assess dose-dependence of EndoE and EfEndo18A against high-mannose IgG Fc (HM-Fc) (~30kDa), was performed by incubating HM-Fc (28) (100 µg/mL) with dilutions (1µM, 100nM, 10nM, 1nM, 100pM, and 10pM) of EfEndo18A or EndoE in dH_20 for 16hr at 37°C, in a total reaction volume of 25µl. As a control in each assay, HM-Fc was incubated with dH_20 alone (negative control). The reactions were analyzed by 15% SDS-PAGE (200V for 1.25hrs). For culture supernatant assessment, the bacterial strains were grown overnight at 37°C, shaking in a chemically defined medium (CDM) (50, 51) containing 42mM glucose and 20µM hematin. Subsequently, HM-Fc (100 µg/mL) was incubated with 10µL of filtered supernatants in dH_20 for 16hr at 37°C, in a total reaction volume of 25µl. As controls, HM-Fc (100 µg/mL) was incubated with dH_20 alone (negative control). The reactions were analyzed by 15% SDS-PAGE (200V for 1.25hrs). Gels were stained with InstantBlue Reagent (Expedeon).

Animal models:

All the procedures in the murine model to study experimental catheter associate urinary tract infection were performed in compliance with Animal Welfare Act and other federal statutes and regulations relating to animals and experiments involving animals. All animal protocols were approved by the Institutional Animal Care and Use Committee for the University of Kansas (IACUC 219-02, murine CAUTI).

Murine model for catheter associated urinary tract infection (CAUTI)

The murine catheter-associated urinary tract infection (CAUTI) was performed using ten seven-week-old female wildtype C57BL/6 mice. The mice were anesthetized by isoflurane inhalation, followed by transurethral implantation of a platinum cured silicone implant tubing (~5-6mm in length) (Renasil Sil025; Braintree Inc.) into the urinary bladders of the mice as previously described (29). Post-implantation, the mice were injected with 50µL of bacterial suspension (~2 x 10^7 cfu) by transurethral catheterization. The mice were monitored for 48 hours post-implantation and infection. After 48 hours, the mice were euthanized via cervical dislocation after inhalation of isoflurane. To assess the degree of infection, the bladder was harvested aseptically. Once the catheters were removed from the bladder, the tissue was homogenized using a tissue tearor homogenizer (Bio-Spec Products) with a 15 second pulse, followed by serial dilution and plating on THB media to determine bacterial burden.

Bioinformatics and statistical analyses

Signal peptide cleavage sites were predicted using SignalP 5.0 (http://www.cbs.dtu.dk/services/SignalP/) (30). The statistical analyses of the various experiments were conducted using the GraphPad Prism 5 software (San Diego, CA).

Results

Genetic organization and transcriptional start site of *ef0114, ef0362-61,* and *ef2863* in *E. faecalis* V583

The genetic organization of the regions of *ef0114, ef0362-61,* and *ef2863* in the clinical isolate *E. faecalis* V583 is depicted in figure 1. EndoE is a two-domain protein that is predicted to possess both a glycosyl hydrolase family 18 (GH18) catalytic domain and a glycosyl hydrolase family 20 (GH20) catalytic domain (10), with an uncharacterized linker domain between the two known catalytic domains. GH18 catalytic domains are predicted to cleave β-1,4 glycosidic bonds that link two adjoining N-acetylglucosamine moieties (10, 12, 31). In contrast, GH20 catalytic domains are predicted to cleave non-reducing β-1,4- and/or β-1,6- glycosidic bonds between two adjacent N-acetylglucosamine moieties (32-34). EfCBM33A and EfChi18A are two gene products encoded in the same operon (*ef0362-61*), where EfCBM33A is a chitin-binding protein/lytic polysaccharide monooxygenase (11, 35) and its partner, EfChi18A, is a chitinase with a GH18 catalytic domain (11). Lastly, EfEndo18A also possesses a GH18 catalytic domain (12).

All three glycosyl hydrolases, as well as the cognate chitin-binding protein/lytic polysaccharide monooxygenase of EfChi18A, are predicted to be secreted proteins (9). The signal peptide cleavage site of EndoE is predicted between amino acids residues A55 and N56 (SignalP 5.0). As for EfCBM33A, the putative signal peptide cleavage site is between A28 and H29, and the predicted signal peptide cleavage site for EfChi18A is located between A29 and D30 (SignalP 5.0). Lastly, the putative signal peptide cleavage site for EfEndo18A is located between amino acid residues alanine 41 and alanine 42 (SignalP 5.0).

To characterize the promoter region of each of these glycosyl hydrolases in this study, the transcriptional start site (+1) of each of these genes in the *E. faecalis* strain V583 was determined by 5'-RACE analysis. The transcriptional start sites were identified either within or shortly

upstream of a putative *cre* site in each of the hydrolase promoter regions (Figure 1). Putative -10 and -35 motifs were found upstream of the transcriptional start site for each glycosyl hydrolase. Additionally, putative ribosomal binding sites were identified downstream of each transcriptional start site. It is well understood that the location of a binding site for a transcription factor often governs the type of transcriptional regulation of the target gene(s) (36, 37). The location of the *cre* sites that either overlap or reside adjacent to the transcriptional start site of each of these glycosyl hydrolases indicates that CcpA is acting as a transcriptional repressor.

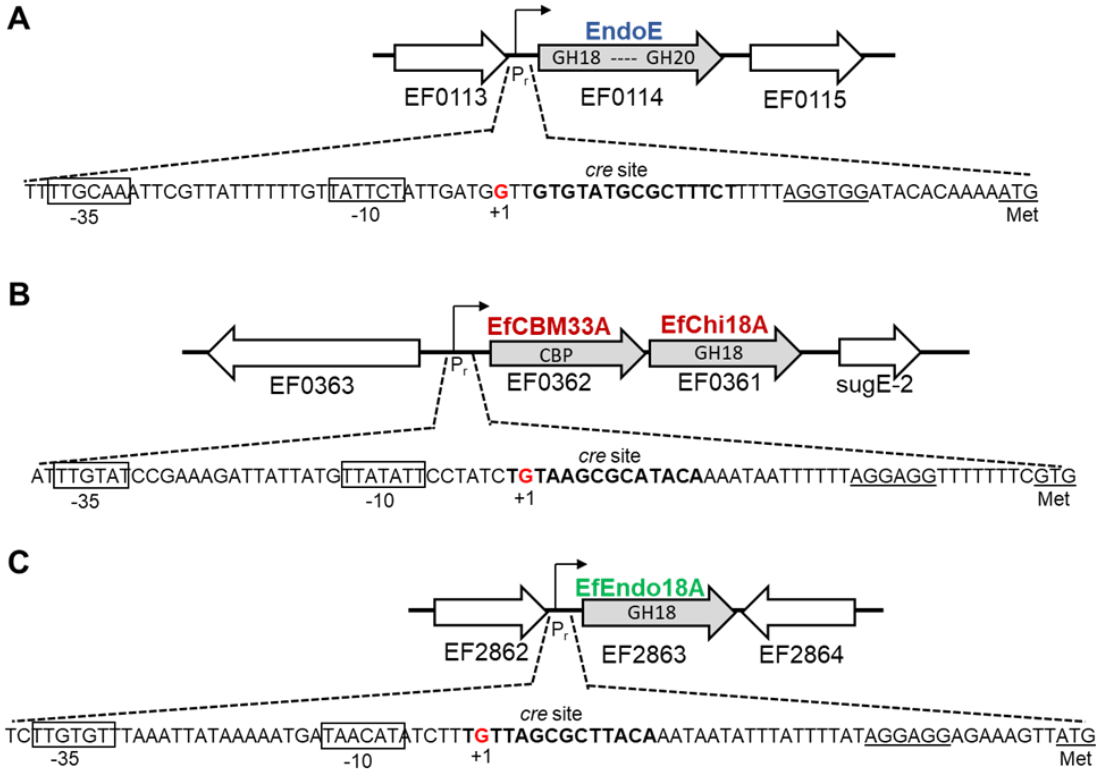

Figure 1: The genetic organization of the promoter region for (A) *ef0114*, (B) *ef0362-61*, and (C) *ef2863* in *E. faecalis* strain V583, respectively. Arrows represent the open reading frames and their orientation shown is the direction of transcription. Text within arrows represents the catalytic domain family for each hydrolase. Analysis of the promoter region upstream of (A) *ef0114*, (B) *ef0362-61*, and (C) *ef2863* in V583 is shown. The transcriptional start site (+1) for each glycosyl hydrolase determined by 5'-RACE is shown in bolded in red. The putative -35 and -10 motifs are boxed. The proposed ribosomal binding sequences (RBS) and the ATG start codons are underlined. The putative *cre* sites within each promoter region is bolded in black.

CcpA negatively regulates *ef0114, ef0362-61,* and *ef2863* expression

To confirm whether *ef0114*, *ef0362-61*, and *ef2863* are negatively regulated by CcpA, we performed qRT-PCR on RNA isolated from parental V583, the *ccpA* mutant, and *ccpA* complement strains grown to mid-exponential phase in Todd-Hewitt broth (THB) and examined transcript abundance of *ef0114*, *ef0362*, and *ef2863*. Figure 2 shows that the relative expression of these three enterococcal glycosyl hydrolases were all significantly increased in the *ccpA* mutant relative to the parental V583 and complement strains. This confirms that these three enterococcal glycosyl hydrolases are negatively regulated by CcpA.

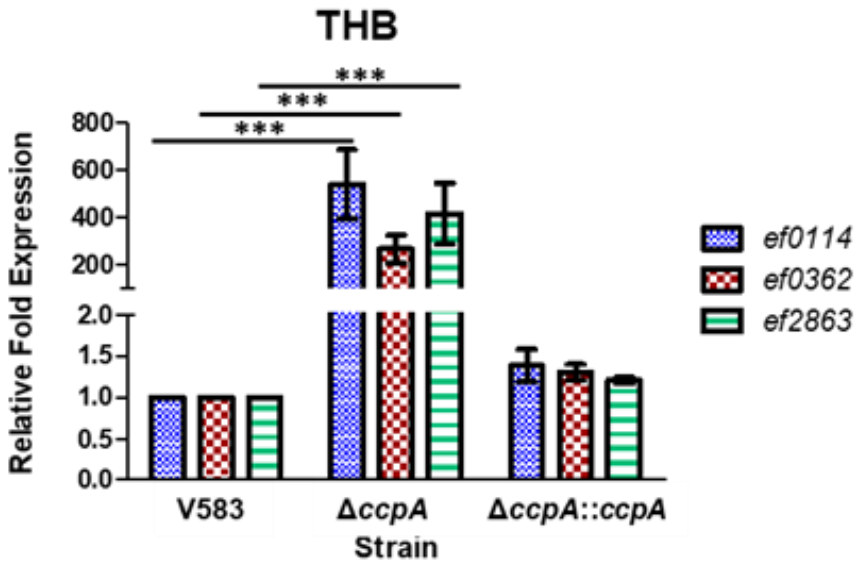

Figure 2: (A) qRT-PCR analysis of CcpA-regulated expression of *ef0114*, *ef0362*, and *ef2863*. RNA was isolated from cultures of V583, Δ*ccpA*, and Δ*ccpA*::*ccpA* grown to mid-exponential phase in THB and subsequently converted to cDNA. The cDNA was subjected to qPCR analysis and quantified using the ΔΔCt method using the threshold cycle values for *ef0114*, *ef0362*, and *ef2863* normalized to the endogenous control [*ef0005* (*gyrB*)]. Results represent averages of three independent biological experiments. Error bars indicate the standard deviation of the mean. Statistical analysis was done by one-way ANOVA, with significant values set to $P < 0.0001$ (***).

CcpA phase-lock mutant (PLM) represses the expression of *ef0114, ef0362-61,* and *ef2863* irrespective of glucose concentrations

As modeled in Gram-positive bacteria, when a rapidly fermentable carbon source, such as glucose, is readily available, the kinase activity of HprK is stimulated by the presence of glycolytic intermediates fructose-6-phosphate and fructose-1,6-bisphosphate and subsequently phosphorylates Hpr at amino acid residue serine 46 (5, 6, 22). Hpr [Ser-46-P] acts as a co-factor that binds to CcpA, triggering a reorientation of CcpA's DNA-binding domain (38). This reorientation event repositions the DNA-binding domain into a more favorable conformation for binding to *cre* sequences in DNA (38). In the Gram-positive bacterium *Bacillus subtilis*, Schumacher et al. (38) found that a key component in controlling the reorientation event for CcpA's DNA-binding conformation was the displacement of threonine 306. This displacement can be mimicked by substituting a tryptophan residue at position 306. In *E. faecalis* strain V583, this key residue is Thr307, similarly observed in *Streptococcus pyogenes* (39). Therefore, in *E. faecalis,* the creation of the mutant CcpAT307Y is predicted to phase-lock CcpA into its DNA-binding conformation irrespective of glucose availability. We refer to this constitutively active "phase-locked" CcpA mutant as CcpA PLM.

To examine whether a CcpA phase-lock mutant represses the expression of CcpA-regulated genes, irrespective of glucose concentrations, we performed qRT-PCR on RNA isolated from wild type, *ccpA* mutant, *ccpA* complement and the *ccpA* phase-lock mutant (CcpA PLM) that were grown overnight in a chemically defined medium (CDM) (23, 24) supplemented with either 15mM or 42mM glucose as the sole carbon source. A glucose concentration of 15mM is presumably low enough that after overnight growth, glucose is depleted from the medium resulting in carbon catabolite derepression. On the other hand, the excess of glucose in media containing 42mM glucose is presumably high enough that during overnight growth, glucose levels remain replete;

therefore, enforcing carbon catabolite repression (CCR). As shown in figure 3A, after overnight growth in media containing 15mM glucose, there is no significant difference in the expression of *ef0114*, *ef0362,* or *ef2863* in the *ccpA* mutant relative to wild-type and the *ccpA* complement. In contrast when grown overnight with excess glucose, the expression of these hydrolases is significantly increased in the absence of CcpA relative to wild-type and the *ccpA* complement (Figure 3B). This suggests that by adjusting the amount of glucose in the medium, we can manipulate the expression of these CcpA-regulated glycosyl hydrolases during overnight growth. With respect to the CcpA PLM strain, irrespective of the amount of glucose in the medium, the expression of *ef0114*, *ef0362,* and *ef2863* are all significantly decreased relative to wild-type, the *ccpA* mutant, and *ccpA* complement strains (Figure 3A and 3B), reinforcing the idea that the CcpA phase-lock mutant is capable of repressing the expression of CcpA-regulated genes, irrespective of glucose concentration.

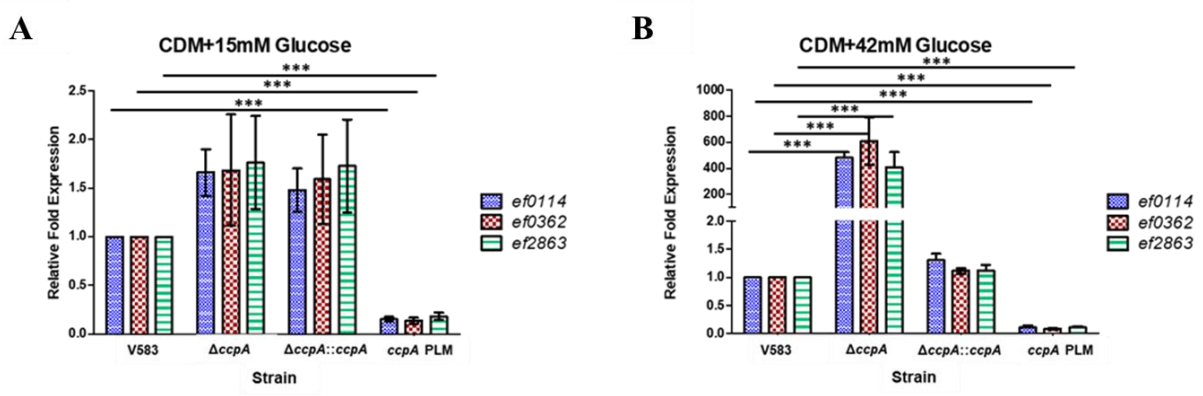

Figure 3: qRT-PCR analysis of *ef0114, ef0362,* and *ef2863* expression in the CcpA variants. RNA was isolated from cultures of V583, Δ*ccpA*, Δ*ccpA*::*ccpA*, and *ccpA* PLM grown overnight in (A) CDM + 15mM glucose or (B) CDM + 42mM glucose and subsequently converted to cDNA. The cDNA was subjected to qPCR analysis and quantified using the ΔΔCt method using the threshold cycle values for *ef0114, ef0362,* and *ef2863* normalized to the endogenous control [*ef0005* (*gyrB*)]. Results represent averages of three independent biological experiments. Error bars indicate the standard deviation of the mean. Statistical analysis was done by one-way ANOVA, with significant values set to $P < 0.0001$ (***).

Culture supernatant from the *ccpA* mutant results in the removal of glycans from RNase B, a model high-mannose type glycoprotein

Previous observations have shown that both the GH18 domain of EndoE and EfEndo18A are capable of deglycosylating RNase B (10, 12); however, these assessments were conducted independently with recombinant purified protein and not in the context of other glycosidases produced by *E. faecalis*. RNase B is often used as a model high-mannose type glycoprotein for studying glycosyl hydrolase activity due to its single N-glycosylation site that can range from five to nine mannose moieties attached to chitobiose (β-1,4-linked GlcNAc dimer) (Asn-$GlcNAc_2$-Man_{5-9}) (40) (Figure 4A). We hypothesized that culture supernatant from the *ccpA* mutant will be able to deglycosylate RNase B due to the presence of secreted endoglycosyl hydrolase(s). To assess this hypothesis, supernatants were collected from the *E. faecalis* V583 wild-type strain, the *ccpA* mutant, and the *ccpA* complement strain grown overnight in a chemically defined medium (CDM) with supplemented glucose (42mM) to ensure glucose replete conditions during growth. The filtered culture supernatants were subsequently incubated with RNase B, followed by analysis by SDS-PAGE. Deglycosylation of RNase B reduces the molecular weight of RNase B; therefore, increasing the mobility through an SDS-PAGE and resulting in a size shift. As controls, RNase B was incubated with buffer alone (negative control) and in the presence of EndoH (a known ENGase produced by *Streptomyces plicatus* as a positive control). As shown in figure 4B, *E. faecalis* strain V583 grown in media containing an increased glucose concentration results in minimal hydrolase activity, apparent by RNase B remaining mostly in its glycosylated form. On the other hand, full deglycosylation of RNase B was observed after treating this substrate with supernatant collected from the *ccpA* deletion mutant strain.

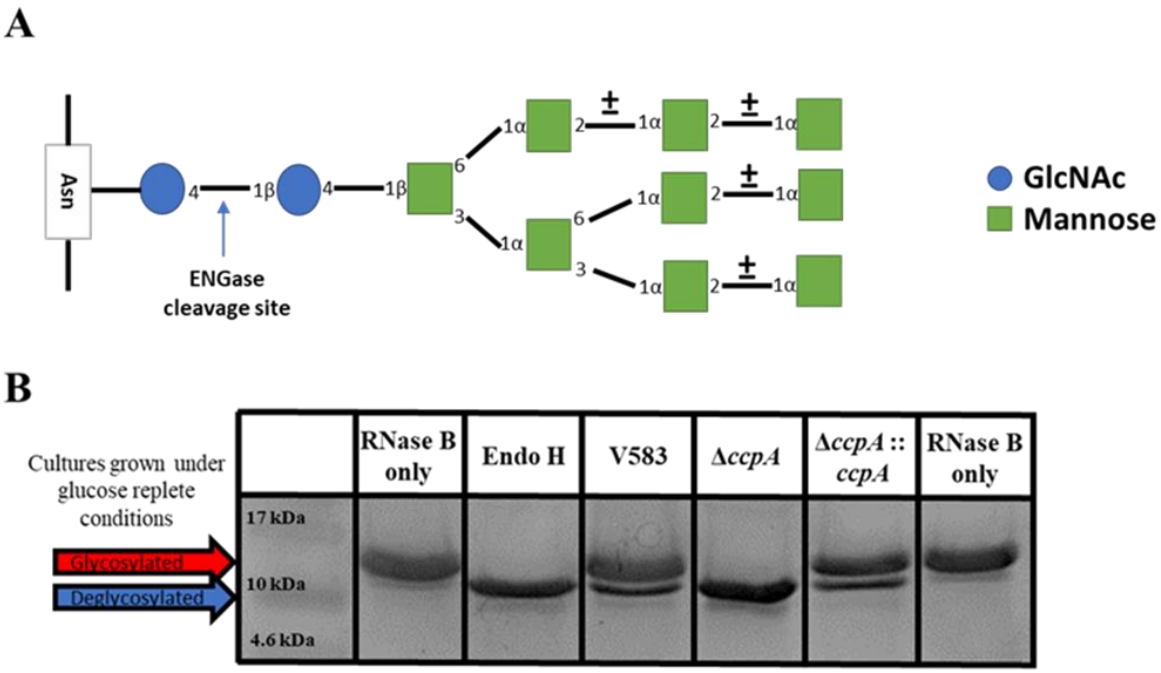

Figure 4: (A) Representation of RNase B glycan structure. The glycoforms of RNase B range from five to nine mannose moieties attached to chitobiose (β-1,4-linked GlcNAc dimer). (B) Endoglycosidase activity from filtered culture supernatants of *E. faecalis* V583, Δ*ccpA*, and Δ*ccpA*::*ccpA* against RNase B and separated on 15% SDS-PAGE as indicated. RNase B with reaction buffer was used as a negative control. RNase B incubated with Endo H was a positive control. Lane (1): MW Ladder; (2 and 7) RNase B only control; (3) RNase B treated with Endo H ; (4-6) RNase B treated with supernatants grown overnight in 42mM glucose (glucose replete conditions) of (4) V583; (5) Δ*ccpA*; (6) Δ*ccpA*::*ccpA*. The red arrow depicts the fully glycosylated form of RNase B and the blue arrow depicts deglycosylated RNase B.

Culture supernatant from the constitutively active CcpA PLM variant attenuates glycosidase activity towards RNase B

We next wanted to determine the effect of the CcpA phase-locked mutant on RNase B deglycosylation. Supernatants were collected from *E. faecalis* V583, the *ccpA* mutant, the *ccpA* complement, and the CcpA PLM strains that were grown overnight in CDM supplemented with glucose (15mM), which is low enough to allow glucose depletion during growth. Filtered supernatants were then incubated with RNase B, followed by analysis by SDS-PAGE. As shown in figure 5, *E. faecalis* V583, the *ccpA* mutant, and the *ccpA* complement grown in the presence

of 15mM glucose all result in full deglycosylation of RNase B. However, when CcpA is in its phase-locked-on state, there is a significant reduction in RNase deglycosylation relative to the wild type, the *ccpA* mutant, and *ccpA* complement strains. This further supports that when CcpA is constitutively locked into its high-affinity DNA-binding conformation, CcpA will bind to the *cre* sites within the promoter regions of the hydrolases, irrespective of available glucose in the medium.

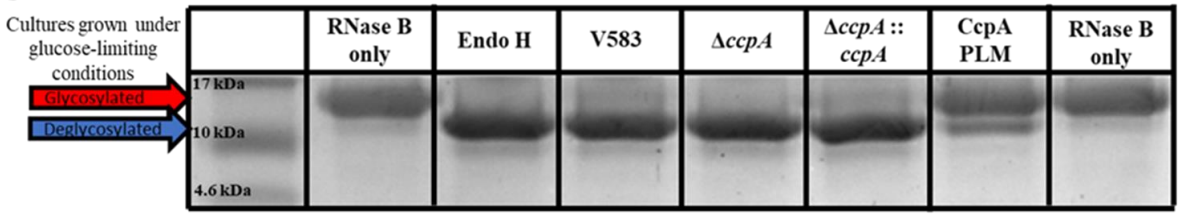

Figure 5: Endoglycosidase activity from filtered culture supernatants of V583, Δ*ccpA*, Δ*ccpA*::*ccpA* complement, and *ccpA* PLM against RNase B and separated on 15% SDS-PAGE as indicated. RNase B with reaction buffer was used as a negative control. RNase B incubated with Endo H was a positive control. Lane (1): MW Ladder; (2 and 8) RNase B only control; (3) RNase B treated with Endo H ; (4-7) RNase B treated with supernatants grown overnight in 15mM glucose (glucose-limiting conditions) of (4) V583; (5) Δ*ccpA*; (6) Δ*ccpA*::*ccpA;* (7) CcpA PLM. The red arrow depicts the fully glycosylated form of RNase B and the blue arrow depicts deglycosylated RNase B.

The deletion of *ef2863* results in a loss of glycosidase activity towards the high-mannose type glycoprotein, RNase B

To determine which of these glycosyl hydrolases under study contributes to the deglycosylation of RNase B by the *ccpA* mutant supernatant, supernatants were collected from the *E. faecalis* V583 strain, the *ccpA* deletion mutant strain, and various glycosyl hydrolase deletion mutants in the *ccpA* mutant background that were grown in CDM with supplemented glucose (42mM). Collected supernatants were subsequently incubated with RNase B, followed by analysis by SDS-PAGE. As shown in figure 6, only the deletion of *ef2863* results in the elimination of the deglycosylated form of RNase B. The phenotype associated with these *ef2863* mutants was corroborated by assessing

the Δ*ccpA*Δ*ef2863*::*ef2863* complement strain under the same RNase B assay condition (Figure S1). As shown in figure S1, RNase B incubated with the Δ*ccpA*Δ*ef2863*::*ef2863* complement supernatant resulted in near complete deglycosylation of RNase B. The data suggest that EfEndo18A (EF2863) is the primary contributor of glycosidase activity towards high-mannose type glycoproteins.

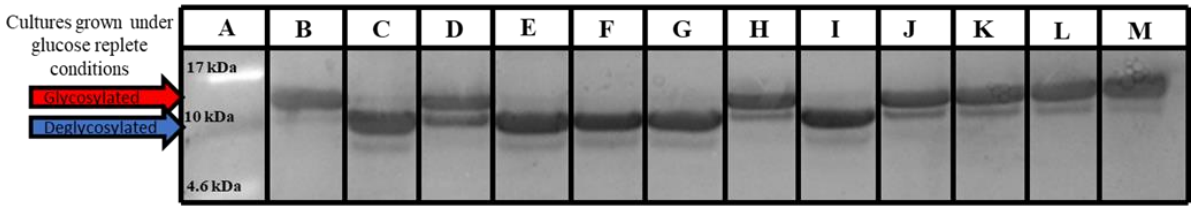

Figure 6: Endoglycosidase activity from filtered culture supernatants of *E. faecalis* V583, Δ*ccpA*, and the glycosyl hydrolase mutants in the *ccpA* mutant background against RNase B and separated on 15% SDS-PAGE as indicated. RNase B with reaction buffer was used as a negative control. RNase B incubated with Endo H was a positive control. (A) MW Ladder; (B and M) RNase B control; (C) RNase B treated with EndoH; (D-L) RNase B treated with supernatants grown overnight in 42mM glucose (glucose replete conditions) of (D) V583; (E) Δ*ccpA*; (F) Δ*ccpA*Δ*ef0114*; (G) Δ*ccpA*Δ*ef0362-61*; (H) Δ*ccpA*Δ*ef2863*; (I) Δ*ccpA*Δ*ef0114*Δ*ef0362-61*; (J) Δ*ccpA*Δ*ef0362-61*Δ*ef2863*; (K) Δ*ccpA*Δ*ef0114*Δ*ef2863*; (L) Δ*ccpA*Δ*ef0114*Δ*ef0362-61*Δ*ef2863*. The red arrow depicts the fully glycosylated form of RNase B and the blue arrow depicts the fully deglycosylated form of RNase B.

The ability to utilize the glycans from high-mannose type glycoproteins as a carbon source is dependent on the activity of EfEndo18A and the Mpt PTS complex

Based on the observations from Roberts et al. (20) where RNase B can support growth of *E. faecalis* strain BC002, as well as our observations from figures 4 and 6, we hypothesized that EfEndo18A would be responsible for sustaining growth in nutrient limited conditions by deglycosylating a high-mannose type glycoprotein as the sole carbon source, *in vitro*. To address this, various hydrolase deletion mutants were assessed for their ability to utilize RNase B as the sole carbon source in CDM. The deletion of *ef0114* or *ef0362-61* did not impact growth when RNase B was present as the sole carbon source (Figure 7A). However, the deletion of *ef2863* significantly reduces growth on this substrate relative to the parental strain and phenocopied the

growth of the triple GH18 glycosyl hydrolase mutant (Δ*ef0114*Δ*ef0362-61*Δ*ef2863*) (Figure 7A). The phenotype associated with the Δ*ef2863* mutant and Δ*ef0114*Δ*ef0362-61*Δ*ef2863* mutant were corroborated by assessing the Δ*ef2863*::*ef2863* complement strain and the Δ*ef0114*Δ*ef0362-61*Δ*ef2863*::*ef2863* complement strain under the same growth conditions (Figure 7A). This suggests that the ability of *E. faecalis* to sustain growth on high-mannose type glycoproteins is dependent on the activity of EfEndo18A.

The observation that RNase B can support growth of *E. faecalis* and that such growth is dependent on EfEndo18A activity led us to hypothesize that the mannose moieties liberated following EfEndo18A cleavage of RNase B would be imported into the cell via the *E. faecalis* Mpt PTS complex. The Mpt PTS complex has been shown to be the sole mannose transporter for *E. faecalis* and its expression is dependent on the alternative sigma factor 54 (RpoN) and its corresponding bacterial enhancer binding protein (bEBP), MptR (9) (22). As shown in figure 7B, the absence of either RpoN, MptR, or the Mpt PTS system (MptBACD) resulted in a significant growth defect when grown in CDM supplemented with RNase B as the sole carbon source. These results are corroborated by assessing the Δ*rpoN*::*rpoN* complement strain, in addition to the genetic revertants of *mptR* and the *mptBACD* deletion strains (Figure 7B).

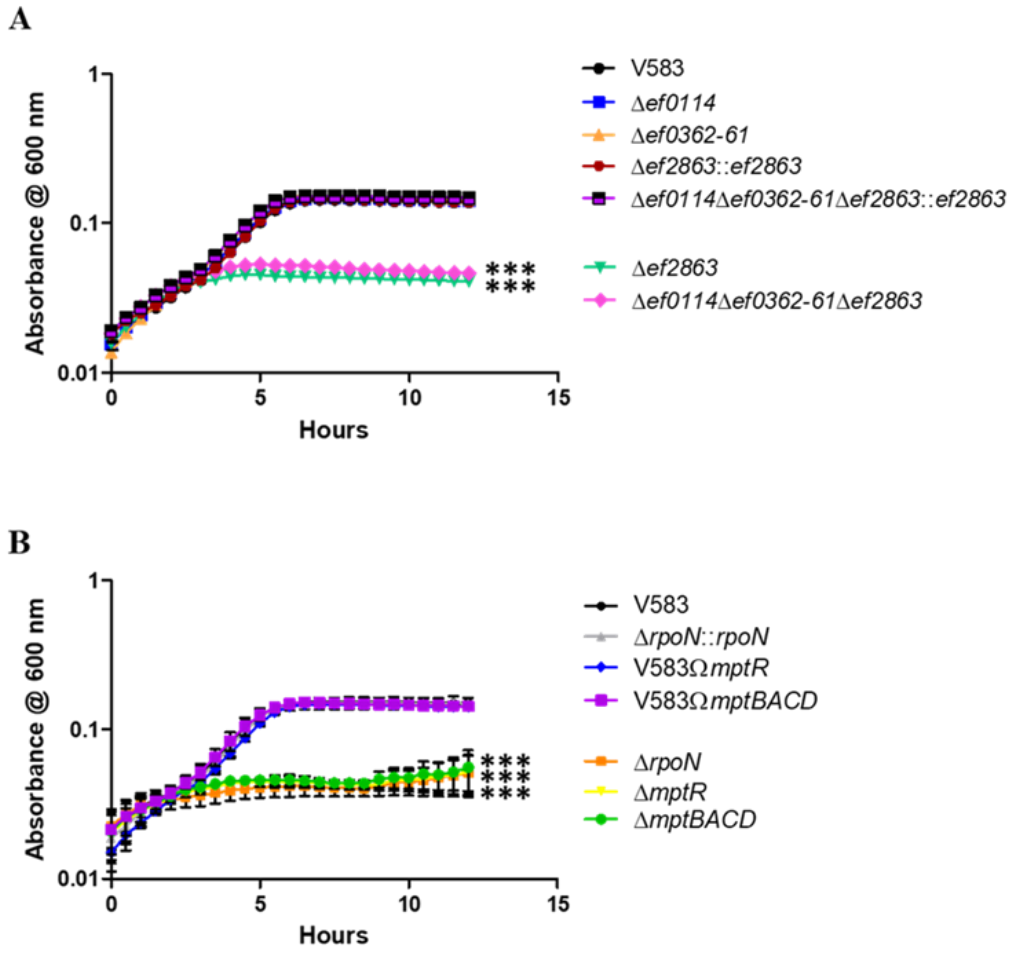

Figure 7: Growth of *E. faecalis* in CDM supplemented with 5 mg/mL RNase B. Each graph is the average of three biological replicates, with six technical replicates each time (n=18).The statistical significance was calculated using a two-way ANOVA test, p value of <0.0001 is indicated as (***). (A) The growth curves in CDM+5mg/mL RNase B are shown in black (V583), blue (Δ*ef0114*), orange (*Δef0362-61*), green (Δ*ef2863*), magenta (Δ*ef0114*Δ*ef0362-61*Δ*ef2863*), red (Δ*ef2863*::*ef2863*), and purple (Δ*ef0114*Δ*ef0362-61*Δ*ef2863*::*ef2863*). (B) The growth curves in CDM+5mg/mL RNase B are shown in black (V583), orange (Δ*rpoN*), grey (Δ*rpoN*::*rpoN*), yellow (Δ*mptR*), blue (V583Ω*mptR* revertant), green (Δ*mptBACD*), and purple (V583Ω*mptBACD* revertant).

Dose-dependent analysis of EfEndo18A and EndoE hydrolase activity against the high-mannose type glycoprotein, RNase B

EndoE and EfEndo18A have previously been characterized for their ability to cleave β-1,4 N-acetylglucosamine glycosidic bonds within RNase B, based on recombinant expression of

individual proteins (10, 12). Since our mutant analysis identified EfEndo18A as being responsible for the glycosidase activity towards RNase B, we wanted to assess the efficacy of EndoE and EfEndo18A by incubating RNase B with a series of dilutions ranging from 1μM to 10pM of purified recombinant EfEndo18A or EndoE (Figure 8). Based on our dose-dependent analysis of EfEndo18A and EndoE hydrolase activity against RNase B, EfEndo18A is capable of fully deglycosylating RNase B at protein concentrations ranging as low as 1nM, whereas EndoE only partially deglycosylates RNase B at the protein concentration of 1μM (Figure 8A and B). This suggests that although EndoE is capable of removing the glycans from RNase B, the glycosidase activity of this glycosyl hydrolase is much less efficient than EfEndo18A. Additionally, it has been hypothesized that a key glutamate residue in the GH18 catalytic domain of EfEndo18A serves as the proton donor during hydrolysis (12). We mutated residue 170 from a glutamate to an uncharged glutamine in EfEndo18A (E170Q) and found that this change resulted in a loss of glycosidase activity against RNase B (Figure 8C).

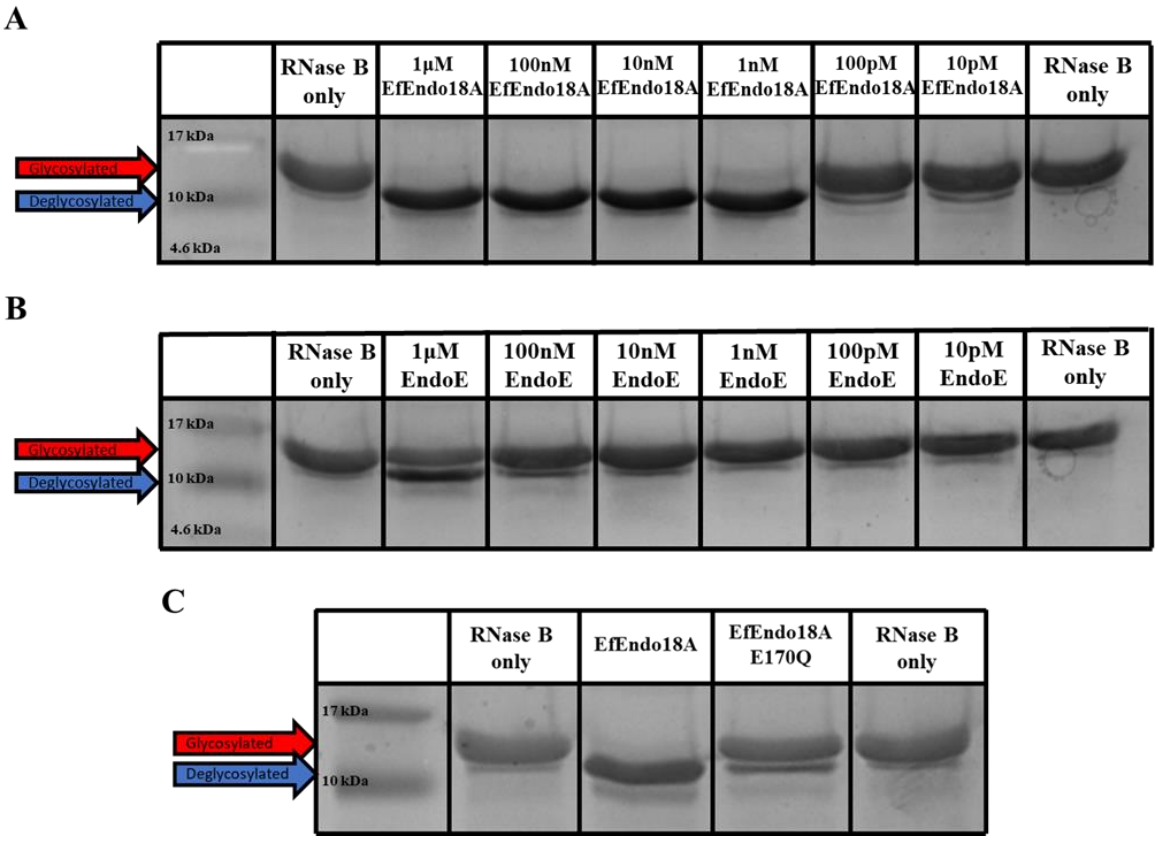

Figure 8: Endoglycosidase activity of purified recombinant glycosyl hydrolases on RNase B. (A) RNase B was incubated with dilutions of purified EfEndo18A and separated on 15% SDS-PAGE as indicated. RNase B with reaction buffer was used as a negative control. Lane (1) MW Ladder; (2 and 9) RNase B only control; (3) 1µM EfEndo18A; (4) 100nM EfEndo18A; (5) 10nM EfEndo18A; (6) 1nM EfEndo18A; (7) 100pM EfEndo18A; (8) 10pM EfEndo18A. (B) RNase B was incubated with purified EndoE and separated on 15% SDS-PAGE as indicated. Lane (1) MW Ladder; (2 and 9) RNase B only control; (3) 1µM EndoE; (4) 100nM EndoE; (5) 10nM EndoE; (6) 1nM EndoE; (7) 100pM EndoE; (8) 10pM EndoE. (C) RNase B was incubated with 1µM of purified EfEndo18A and EfEndo18A E170Q, followed by separation on 15% SDS-PAGE as indicated. Lane (1): MW Ladder; (2 and 5) RNase B only control; (3) 1µM EfEndo18A; (4) 1µM EfEndo18A E170Q. The red arrow depicts the fully glycosylated form of RNase B and the blue arrow depicts deglycosylated RNase B.

Analysis of EndoE and EfEndo18A hydrolase activity on the complex glycoprotein, IgG

The β1,4-linked GlcNAc glycosidic bond of N-linked high-mannose type and complex type glycoproteins is a target of GH18 containing glycosyl hydrolases, as recombinant EfEndo18A and EndoE possess activity against RNase B (10, 12). EndoE is also responsible for deglycosylating the complex glycoproteins IgG and lactoferrin (10, 19). The N-linked glycans of IgG are generally

biantennary complex structures consisting of a conserved core structure of an Asn297-attached chitobiose (β1,4-$GlcNAc_2$) followed by three mannose and two more GlcNAc moieties (Asn^{297}-$GlcNAc_2Man_3GlcNAc_2$), as depicted in figure 9A (41, 42). Depending on the host glycosylation machinery, additional sugars such as galactose or sialic acid may be added to the terminal GlcNAc residues and the first GlcNAc residue of the chitobiose attached to the conserved Asn297 residue of IgG is also fucosylated (41, 42) (Figure 9A). Because multiple enterococcal hydrolases possess GH18 domains, it was of interest to utilize lectin blotting to determine which glycosyl hydrolase produced by *E. faecalis* V583 is primarily responsible for deglycosylating IgG. The lectin blot analysis allows for better detection of IgG hydrolysis since separation on SDS-PAGE often results in limited resolution of molecular weight difference between glycosylated and deglycosylated IgG forms. Human IgG was incubated with 10μM of recombinant EndoE or EfEndo18A followed by analysis of SDS-PAGE and lectin blot analysis using the *Galanthus nivalis* (GNL) lectin, which specifically binds to mannose residues of N-linked glycans (10, 26). As shown in figure 9B, EfEndo18A and full-length EndoE, at a concentration of 10μM, possessed glycosidase activity against IgG, represented by the loss of lectin blot signal.

Because EndoE is a dual catalytic domain protein, we created individual recombinant domain constructs as well as two site-directed mutants and assessed their ability to deglycosylate human IgG. We refer to the GH18 domain of EndoE as EndoE α, whereas the GH20 domain of EndoE is referred to as EndoE γ. The role of a central linker region, which we term the β domain, due to its predicted secondary structure was also evaluated to determine if it contributed to overall enzymatic function. Therefore, additional EndoE domain constructs were created that included the linker region (EndoE α+β and EndoE β+γ, respectively). IgG lectin blot analysis of EndoE domains shows that the constructs containing the GH18 catalytic domain (EndoE α) or in the presence of the central linker region (EndoE α+β) possess glycosidase activity against IgG (Figure 9B). In

contrast, EndoE domain variants possessing the GH20 catalytic domain alone (EndoE γ) or in the presence of the linker region (EndoE β+γ) did not hydrolyze IgG (Figure 9B). Additionally, the replacement of a key glutamate residue involved in proton transfer during hydrolysis within the GH18 catalytic domain of EndoE to glutamine (EndoE E186Q) results in a restored lectin blot signal, highlighting the important role of the GH18 domain in the enzymatic activity of EndoE. In contrast, the replacement of a key enzymatic residue in the GH20 domain (EndoE E662Q) retained glycosidase activity towards IgG. Collectively, this suggests that the GH18 catalytic domain of EndoE is responsible for hydrolyzing IgG by cleaving the β-1,4 glycosidic bond between two adjacent N-acetylglucosamines within the heavy chain of IgG. With respect to EfEndo18A, the EfEndo18A E170Q variant is unable to hydrolyze IgG (Figure 9B).

Because EndoE and EfEndo18A both possess glycosyl hydrolase activity against human IgG, we wanted to assess the efficacy of EndoE and EfEndo18A by incubating human IgG with a series of protein dilutions ranging from 10μM to 10nM of purified recombinant EfEndo18A or EndoE (Figure 9C). This dose-dependent analysis shows that EndoE deglycosylates IgG at protein concentrations ranging from 10μM-100nM, whereas EfEndo18A only deglycosylates IgG at the protein concentration of 10μM (Figure 9C), indicating that EndoE is more efficient at removing the glycans from IgG.

To assess the physiological levels of secreted glycosyl hydrolases active against IgG, we examined culture supernatants from glycosyl hydrolase deletion mutants in the *ccpA* mutant background grown overnight in CDM + glucose for activity against human IgG. As shown in figure 9D, the deletion of *ef0114*, singly or in combination with other hydrolase deletion mutants, results in the loss of glycosidase activity against IgG, highlighting the important role of EndoE in targeting human IgG.

It was of interest to determine whether *E. faecalis* is capable of sustaining growth on IgG as the sole carbon source; therefore *E. faecalis* V583 and a glycosyl hydrolase deletions were assessed for growth in CDM supplemented with human IgG. As shown in figure S2, single deletions of *ef0114*, *ef0362-61*, and *ef2863*, as well as the triple mutant (Δ*ef0114*Δ*ef0362-61*Δ*ef2863*) did not result in a significant growth defect relative to the parental strain.

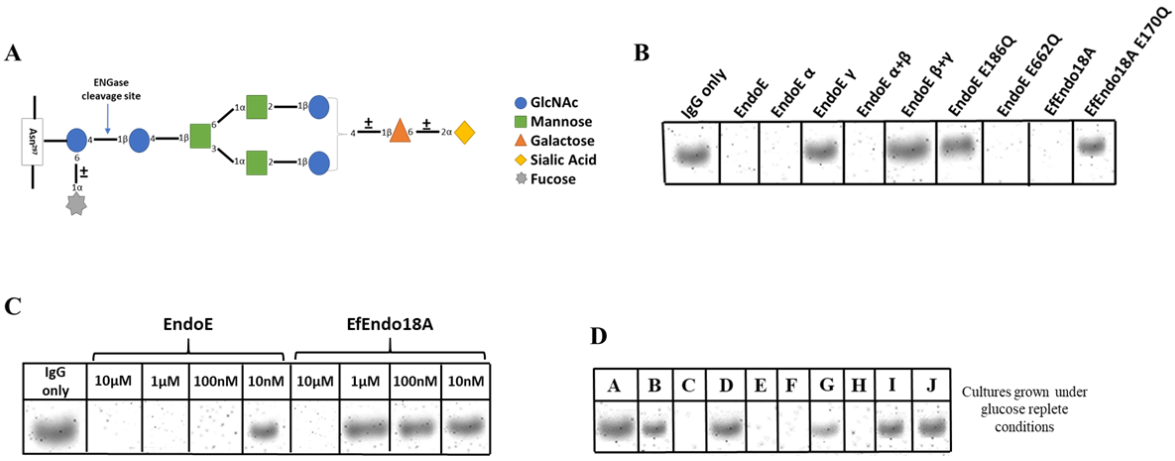

Figure 9: (A) Representation of IgG glycan structure. Galactose or sialic acid may be added to the terminal GlcNAc residues. The first GlcNAc residue of the chitobiose attached to the conserved Asn297 residue IgG is predominately fucosylated. (B) Human IgG was incubated with 10 μM purified EfEndo18A and EndoE variants and separated on 12% SDS-PAGE, electroblotted onto PVDF membranes for GNL lectin analysis. (C) Human IgG was incubated with a series of dilutions ranging from 10 μM to 10 nM of purified EndoE and EfEndo18A. IgG reactions in PBS alone were used as a negative control. (D) Human IgG was incubated with filtered culture supernatant from *E. faecalis* V583, Δ*ccpA*, and the glycosyl hydrolase mutants in the *ccpA* mutant background. (A) IgG only control; IgG treated with supernatants grown overnight in 42mM glucose (glucose replete conditions) of (B) V583; (C) Δ*ccpA*; (D) Δ*ccpA*Δ*ef0114*; (E) Δ*ccpA*Δ*ef0362-61*; (F) Δ*ccpA*Δ*ef2863*; (G) Δ*ccpA*Δ*ef0114*Δ*ef0362-61*; (H) Δ*ccpA*Δ*ef0362-61*Δ*ef2863*; (I) Δ*ccpA*Δ*ef0114*Δ*ef2863*; (J) Δ*ccpA*Δ*ef0114*Δ*ef0362-61*Δ*ef2863*. A signal in the lectin blot represents the glycosylated form of IgG.

EndoE does not contribute to the dispersal of bacterial biofilms

As EndoE possessed an additional GH20 family glycosyl hydrolase domain, it was of interest to explore the function of this domain. GH20 glycosyl hydrolases are reported to possess the ability to hydrolyze the β1,4 linked terminal non-reducing *N*-acetyl-D-hexosamine residues and/or the β-1,6-glycosidic linkage between two adjoining N-acetylglucosamine moieties (32-34, 43). Based

on the NCBI Conserved Domain Database, the GH20 domain of *E. faecalis* V583 EndoE possesses Dispersin B-like GH20 catalytic domain sharing homology with the well-studied Dispersin B (DspB) produced by the oral pathogen, *Aggregatibacter actinomycetemcomitans* (33, 44-47). A number of studies have shown that Dispersin B disaggregates self-produced biofilms, as well as biofilms produced by several bacterial species including *Staphylococcus epidermidis*, *Escherichia coli*, *Yersinia pestis*, and *Pseudomonas fluorescens* (33, 44, 46, 48). The mode of action of DspB is to disaggregate the aforementioned biofilms by cleaving the β-1,6-linkage between N-acetylglucosamine residues, a major component of the extracellular polysaccharide matrix produced by many bacterial species (33, 44-46, 48). Based on the sequence conservation between EndoE GH20 domain and Dispersin B, we hypothesized that EndoE would possesses substrate specificity towards polymers containing β-1,6-linked N-acetylglucosamine. One such substrate is the staphylococcal intercellular adhesion, Ica, and this repeat polymer of β-1,6-linked N-acetylglucosamine is responsible for polysaccharide-dependent biofilm formation in *S. epidermidis* (49). Based on our results (Figure S3), EndoE does not appear to function as a biofilm dispersing enzyme, as EndoE had no significant effect on *S. epidermidis* biofilms (Figure S3).

Analysis of glycosidase activity against a synthetic high-mannose IgG Fc glycoform (HM-Fc)

Our evidence indicates that EfEndo18A is the primary hydrolase responsible for liberating high-mannose type glycans. However, this assessment was based upon activity against only one high-mannose type glycoprotein, RNase B. It was therefore of interest to assess whether EfEndo18A is capable of deglycosylating additional high-mannose glycoproteins beyond RNase B. Due to limited commercial availability of high-mannose type glycoproteins, as an alternative for RNase B, we assessed the activity of EfEndo18A and EndoE against a synthetic high-mannose IgG Fc

glycoform (28). This particular glycoform is referred to as HM-Fc as it contains only the Fc region of IgG and possesses a high-mannose glycan instead of the typical complex glycan (28). We wanted to assess the efficacy of EfEndo18A relative to EndoE by incubating HM-Fc with a series of dilutions ranging from 1μM to 10pM of purified recombinant EfEndo18A or EndoE (Figure 10). Based on this dose-dependent analysis against HM-Fc, EfEndo18A is capable of fully deglycosylating HM-Fc at protein concentrations ranging as low as 10nM and partially deglycosylates this substrate at a protein concentration of 1nM (Figure 10A). On the other hand, EndoE only partially deglycosylates HM-Fc at the protein concentration of 1μM (Figure 10B). This suggests that swapping the glycan structure of IgG from complex to high-mannose reduces the activity of EndoE and increases the glycosidase activity of EfEndo18A. This combined analysis highlights important differences in the specificity of both EfEndo18A and EndoE as targeting high-mannose and complex-type glycoproteins, respectively.

To assess the physiological levels of secreted glycosyl hydrolases active against HM-Fc, we examined culture supernatants from glycosyl hydrolase deletion mutants in the *ccpA* mutant background grown overnight in CDM + glucose for activity against HM-Fc. As shown in figure 10C, the single deletion of *ef2863* results in the loss of glycosidase activity against HM-Fc, highlighting the important role of EfEndo18A in targeting high-mannose type glycoproteins.

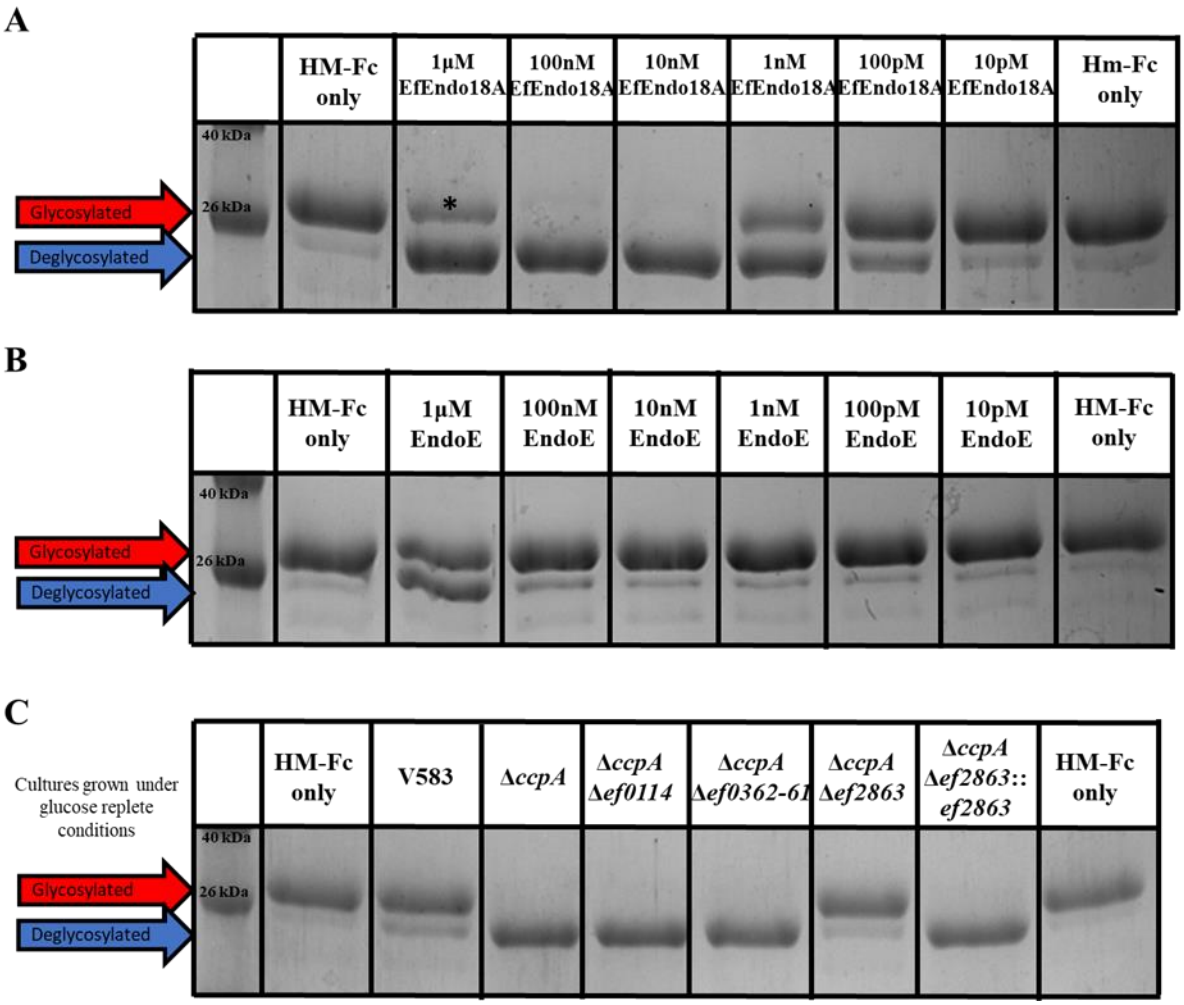

Figure 10: Endoglycosidase activity against the high-mannose IgG Fc glycoform (HM-Fc) (~30kDa). (A) HM-Fc was incubated with dilutions of purified recombinant EfEndo18A and separated on 15% SDS-PAGE as indicated. HM-Fc with reaction buffer was used as a negative control. The asterisk (*) indicates purified EfEndo18A (34.5kDa). Lane (1) MW Ladder; (2 and 9) HM-Fc only control; (3) 1µM EfEndo18A; (4) 100nM EfEndo18A; (5) 10nM EfEndo18A; (6) 1nM EfEndo18A; (7) 100pM EfEndo18A; (8) 10pM EfEndo18A. (B) HM-Fc was incubated with dilutions of purified recombinant EndoE and separated on 15% SDS-PAGE as indicated. Lane (1) MW Ladder; (2 and 9) HM-Fc only control; (3) 1µM EndoE; (4) 100nM EndoE; (5) 10nM EndoE; (6) 1nM EndoE; (7) 100pM EndoE; (8) 10pM EndoE. (C) HM-Fc was incubated with filtered culture supernatant from *E. faecalis* V583, Δ*ccpA*, and the glycosyl hydrolase mutants in the *ccpA* mutant background. Lane (1) MW Ladder; (2 and 9) HM-Fc only control; HM-Fc treated with supernatants grown overnight in 42mM glucose (glucose replete conditions) of (3) V583; (4) Δ*ccpA*; (5) Δ*ccpA*Δ*ef0114*; (6) Δ*ccpA*Δ*ef0362-61*; (7) Δ*ccpA*Δ*ef2863*; (8) Δ*ccpA*Δ*ef2863*::*ef2863*. The red arrow depicts the fully glycosylated form of RNase B and the blue arrow depicts deglycosylated RNase B.

Glycosyl hydrolase activity contributes to enterococcal virulence

Because of the potential functional redundancy of the GH18 domain containing proteins in V583, we assessed the triple glycosyl hydrolase mutant (Δ*ef0114*Δ*ef0362*-61Δ*ef2863*) in a catheter-associated UTI (CAUTI) model relative to the parental strain (29). As shown in figure 11, the triple glycosyl hydrolase mutant was significantly attenuated as observed by the reduced number of bacteria ($p<0.05$) recovered from the bladder (24.7-fold) of the Δ*ef0114*Δ*ef0362-61*Δ*ef2863* infected mice compared to the wild-type V583 strain.

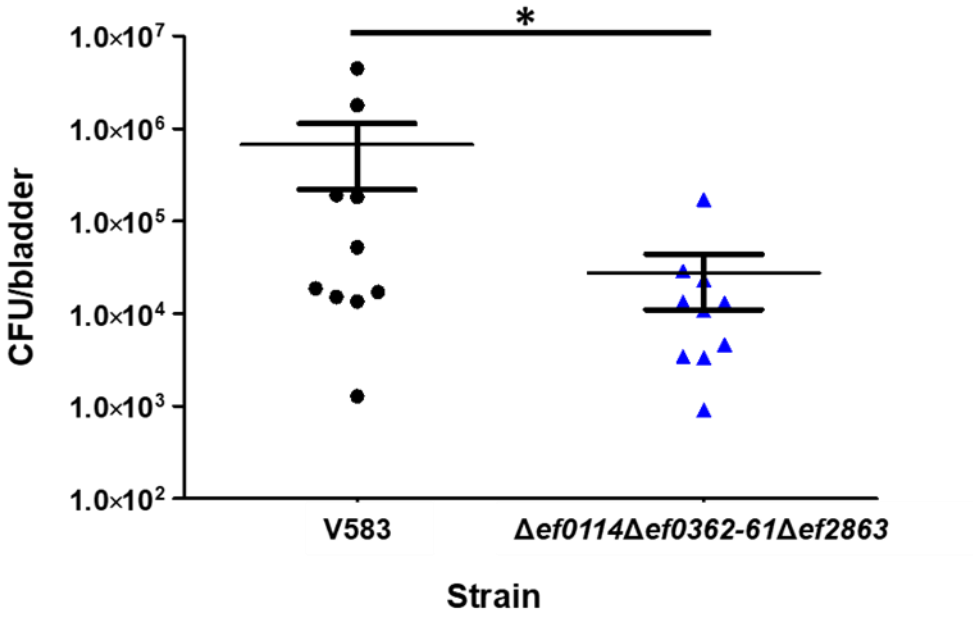

Figure 11: Glycosyl hydrolases contribute to enterococcal virulence in the murine model of CAUTI. Female C57BL/6 mice were euthanized after 48 hours post infection. Bacterial burden is expressed in logarithmic scale for wild type V583 (black) and Δ*ef0114*Δ*ef0362-61*Δ*ef2863* (blue) in homogenized bladders. The horizontal bar represents the median of each group of mice. Statistical significance as determined by Mann-Whitney test is represented as: (*), significant p value less than 0.05 relative to V583.

Discussion

In this work, we show that three glycosyl hydrolase gene clusters (*ef0114*, *ef0362-61*, and *ef2863*) are negatively regulated by CcpA and further characterize the utilization of EfEndo18A and EndoE with respect to enterococcal physiology by assessing isogenic glycosyl hydrolase deletion mutants and recombinantly purified protein variants. We successfully mapped the transcription start sites (TSS) for the genes encoding these glycosyl hydrolases, and our findings for *ef2863* and *ef0362-61* transcript start sites are consistent with recent reports examining the global transcriptome of *E. faecalis* reported by Michaux et al. (50) and Innocenti et al. (51). However, the TSS of *ef0114* did not match the identified TSS from Michaux et al. (50), as their identified TSS was located in the middle of the *ef0114* coding region, and the analysis conducted by Innocenti et al. was unable to determine a TSS for *ef0114* (51). Overall, the locations of the TSS for each glycosyl hydrolase gene reported in this study are also consistent with these genes being directly regulated by CcpA, given the identification of predicted *cre* sites that overlapped or were immediately adjacent to the TSS. This was further confirmed by qRT-PCR analysis comparing transcript abundance between the parental and the Δ*ccpA* strain.

These enterococcal glycosyl hydrolases became of interest based on these genes being upregulated in a transcriptomic study involving the alternative sigma factor 54 (RpoN) (9) and among other transcriptomic studies conducted in human urine, blood, and in an *in vivo* subdermal abscess model (52-54), indicating biological host colonization relevance. Glucose in a normal host is strictly regulated and is often present at concentrations (55) that are growth limiting to most microorganisms including enterococci (56). Shepard et al. showed that growth of *E. faecalis* is restricted in both serum and urine and reaches a cell density that is 10-20 fold less than rich laboratory media (56). Microarray analysis of *E. faecalis* grown in blood (53) and urine (54), respectively revealed that alternative carbon sources are utilized *in vivo*, and this includes

expression of the GH18 glycosyl hydrolases to take advantage of these host resources. As we have shown in the present manuscript, this is likely a consequence of CcpA derepression attributed to a limited glucose supply in the host. The effect of CcpA derepression results in the expression of a number of secondary carbon utilization pathways including the GH18 family glycosyl hydrolases. Although their catalytic mechanisms are conserved (14), the substrates for chitinases and ENGases of the GH18 family are known to differ. It has been well studied that chitinases, such as EfChi18A (EF0361) encoded in the *E. faecalis* V583 genome, break down chitin, a linear polymer of β-1,4-linked-N-acetylglucosamine (11, 14, 16). Chitin-binding proteins/lytic polysaccharide monooxygenases, such as EfCBM33A (EF0362), assist chitinases in the breakdown of chitin by creating breaks in the chitin chains, thus facilitating the accessibility of chitinases to chitinous substrates (57, 58). On the other hand, ENGases are capable of hydrolyzing the Asn-attached chitobiose (β-1,4-$GlcNAc_2$) of N-linked glycans, such as those present on high-mannose and complex type glycoproteins (10, 14, 16, 20).

Complex and high-mannose oligosaccharides are often associated with the glycoproteins of animals, including humans (59-61). Importantly, glycoproteins are abundantly expressed on epithelial surfaces as well as being secreted and present an attractive target for nutrient acquisition at potential sites of enterococcal colonization, including the urinary tract (62, 63). It has previously been shown that the GH18 domain of EndoE and EfEndo18A are capable of deglycosylating RNase B via enzymatic assessments with recombinant EndoE and EfEndo18A (10, 12). However, the relative contribution of their activity against RNase B was assessed individually with recombinant protein and not in the context of other glycosidases produced by *E. faecalis*. The enterococcal chitinase has not previously been examined for activity against high-mannose type glycoproteins as Vaaje-Kolstad et al. reported specificity of EfChi18A for chitin (11). Gerlach et al. (64) have also noted that despite the similar structure between the chitobiose core of N-linked

glycans and chitin, there have been no reports describing chitinase cleavage of N-linked glycoproteins. We excluded EfChi18A (EF0361) in our enzymatic assessment based on these reports as well as the fact that our culture supernatant plus RNase B experiment did not indicate any physiologically relevant contribution of EF0362-61 against high-mannose type glycoproteins. Based on our results, EfEndo18A is principally responsible for deglycosylating RNase B, a known high mannose containing glycoprotein. The high mannose specificity was confirmed using a synthetic construct HM-Fc that swaps the complex N-linked structure for a high mannose type. We would anticipate that EfEndo18A is likely capable of cleaving any high mannose type N-linked glycoprotein.

With the observation of EfEndo18A being the primary glycosidase of high-mannose type glycoproteins, we hypothesize that once EfEndo18A removes the glycan core from these glycoproteins, additional α-mannosidases would be responsible for further liberation of the mannose residues that could be imported into the cell via the *E. faecalis* Mpt PTS complex (9). This is consistent with observations reported by both Roberts (20) and Li (65), who demonstrated α-mannosidase activity in *E. faecalis* culture filtrates only after pre-treatment of RNase B with either commercially-sourced EndoH from *S. plicatus* (20) or PNGase F from *Flavobacterium meningosepticum* (65). As shown in this study, the Mpt PTS system is required for importation of mannose residues from the released glycans of high-mannose type glycoproteins, as the *mptBACD* mutant had a significant growth defect when grown on RNase B as a carbon source. Three α-mannosidases are annotated in the *E. faecalis* V583 genome, *ef1708-07* and *ef2217*. EF1708 is a putative family 125 glycosyl hydrolase that putatively targets the α-1,6-linked non-reducing terminal mannose residues of N-glycans (66), EF1707 is a putative family 38 glycosyl hydrolase that is thought to target α-1,3-mannosidic linkages (67), whereas EF2217 belongs to the family 92 glycosyl hydrolase family and has been shown to cleave α-1,2-linked mannose residues of

liberated N-linked glycans of RNase B (RNase B treated with PNGase F) (65). This suggests that EfEndo18A, the Mpt PTS complex, EF1708-07 and EF2217 likely act in a coordinated fashion to metabolize the sugar moieties of N-linked high-mannose host glycoproteins. The contribution of α-mannosidase activity by EF1708-07 and/or EF2217 is a component of ongoing studies to determine how these abundant host nutrient sources are utilized by *E. faecalis*.

The deglycosylation of IgG by EndoE was first assessed by Collin et al. (10) and they concluded that the GH20 catalytic domain was responsible for the deglycosylating activity against IgG. This observation is perplexing as it has been established that ENGases, including EndoE and EfEndo18A, target the Asn-attached chitobiose of high-mannose and complex type glycoproteins (14). Based on our IgG deglycosylation analysis using recombinant EndoE domains, as well as site-directed mutants, we observed that the GH18 catalytic domain of EndoE is responsible for removing the glycans from IgG, which is in contrast to the results reported by Collin et al. (10). Collin et al. (11) also observed that the GH18 catalytic domain of EndoE is responsible for cleaving the chitobiose structure of the high-mannose type glycoprotein RNase B, as well as the complex type glycoprotein human lactoferrin (19). In further support of our observations that the GH18 domain of EndoE is responsible for deglycosylating IgG, we also note that EndoE shares 46% sequence similarity with EndoS, an endoglycosidase secreted by *Streptococcus pyogenes* responsible for IgG glycan hydrolysis (68, 69) and the sequence similarity is restricted to the GH18 domain, as EndoS does not possess a GH20 family domain.

N-glycosylation at the conserved asparagine residue at position 297 within the heavy chain of the Fc region of IgG has been discovered as an essential player in Fc effector functions such as antibody-dependent cellular cytotoxicity and optimal activation of the classical complement pathway (70, 71). Alterations of glycan composition or removal of the glycan can severely impact the effector functions due to conformational changes of the Fc domain, ultimately affecting the

binding affinity to Fcγ receptors (41, 71, 72) and complement C1q binding to activate the classical complement pathway (73). The loss of deglycosylation activity of IgG in the absence of the streptococcal EndoS glycosidase resulted in a decrease of *S. pyogenes* resistance to phagocytic killing *in vitro* and decreased virulence, *in vivo* (68, 69), and EndoS has been proposed as an immunomodulatory therapy in the treatment of autoimmune anemias (73). These observations link bacterial glycosidase-dependent IgG glycan hydrolysis to immune evasion. This also suggests that EndoE likely plays a similar role in enterococcal immune evasion, as our study identified EndoE as the primary glycosidase against IgG. While EfEndo18A is also capable of deglycosylating IgG, it is far less efficient and only active at non-physiologic levels and is consistent with previous observations (12) as well as our results from culture filtrate experiments against IgG, where only the deletion of *ef0114* resulted in a loss of deglycosylating activity against IgG.

In a biological host, bacteria will encounter a more hostile environment as preferable nutrient sources are often host limited and the organism is subject to attack from the host immune system. Although the mice used in this study were not immunized with enterococci prior to infection, the presence of natural IgGs have been found to provide innate protection against commensal bacteria (68, 74) and these natural IgGs would be subject to deglycosylation by EndoE. Additionally, potential alternative host nutrient sources are both high-mannose and complex type glycoproteins present on mammalian epithelial cells (59-61). Uroplakin is an abundant cell-surface associated protein complex in the urinary tract epithelium, and is comprised of four major proteins, termed uroplakin Ia, Ib, II and IIIa. Proteins Ia, Ib and IIIa are modified with N-linked glycans, specifically Ia possesses high-mannose glycans, whereas Ib is exclusively comprised of complex type glycosylation (75). Uromodulin or Tamm-Horsfall glycoprotein is the most abundant protein in urine and possesses high-mannose glycosylation (62). Thus, the inability to utilize high-mannose or complex type glycoproteins as a nutrient source as a consequence of the loss of *ef2863*

and/or *ef0114* would be predicted to alter host colonization efficiency. In addition, the loss of *ef0114* would result in an increased susceptibility to IgG effector functions including complement activation and phagocytic clearance, based on the inability to remove this complex-type glycan decoration. Recent observations have also shown that bacterial chitinases secreted by bacterial pathogens, such as *Listeria monocytogenes* (76, 77) and *Legionella pneumophila* (78), serve as virulence factors during infection (58, 79); suggesting a functional role for the enterococcal chitinase, EfChi18A, during infection. Although chitin is not produced by mammalian hosts, it has been postulated that mammalian sugar polymers containing LacdiNAc (GalNAcβ1-4GlcNAc) are potential targets of bacterial chitinases (58, 80), but to date, no reports have identified a specific mammalian target of chitinases. The combined loss of all three GH18 glycosyl hydrolases (Δ*ef0114*Δ*ef0362-61*Δ*ef2863*) likely explains the attenuated *in vivo* phenotype. It will be of interest to assess single and double deletions of *ef0114*, *ef0362-61*, and *ef2863* for their individual or combined contribution to *in vivo* fitness and will be a component of ongoing studies.

Overall, our study highlights that *E. faecalis* has evolved to produce two CcpA-regulated glycosyl hydrolases that have a specific effectiveness towards certain glycoprotein types, as EfEndo18A is required for the utilization of high-mannose type glycoproteins as a carbon source, whereas the activity of EndoE is required to deglycosylate complex type glycoproteins (IgG) and could therefore be considered an innate and adaptive immune evasion strategy by compromising IgG-dependent functions. Subtle differences exist in the carbohydrate composition of these major N-linked glycoproteins, but one major difference is the presence of a fucosylated chitobiose linkage in complex-type glycans that is absent in the high-mannose forms and may explain why the two enzymes evolved their substrate specificities. Exploring the specificity of this decoration and how it impacts enzymatic activity will be an area of future research interest.

Supplemental Figures

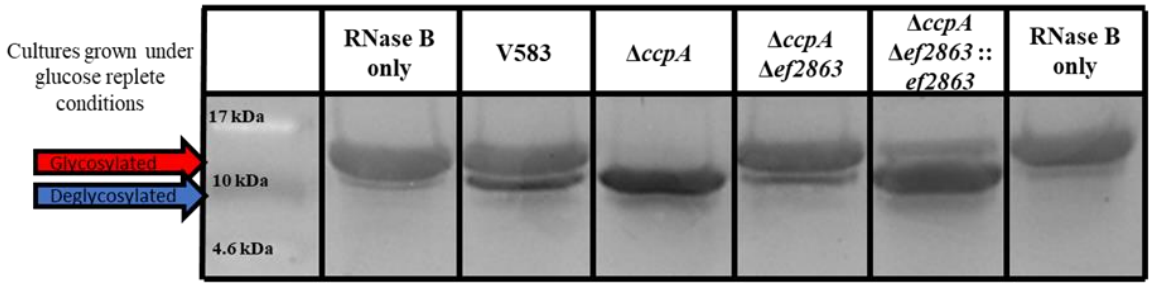

Figure S1: Endoglycosidase activity from filtered cultured supernatants of *E. faecalis* V583, Δ*ccpA*, Δ*ccpA*Δ*ef2863*, and Δ*ccpA*Δ*ef2863*::*ef2863* against RNase B and separated on 15% SDS-PAGE as indicated. RNase B with reaction buffer was used as a negative control. Lane (1): MW Ladder; (2 and 7) RNase B only control; (3-6) RNase B treated with supernatants grown overnight in 42mM glucose (glucose replete conditions) of (3) V583; (4) Δ*ccpA*; (5) Δ*ccpA*Δ*ef2863;* (6) Δ*ccpA*Δ*ef2863*::*ef2863*. The red arrow depicts the fully glycosylated form of RNase B and the blue arrow depicts deglycosylated RNase B.

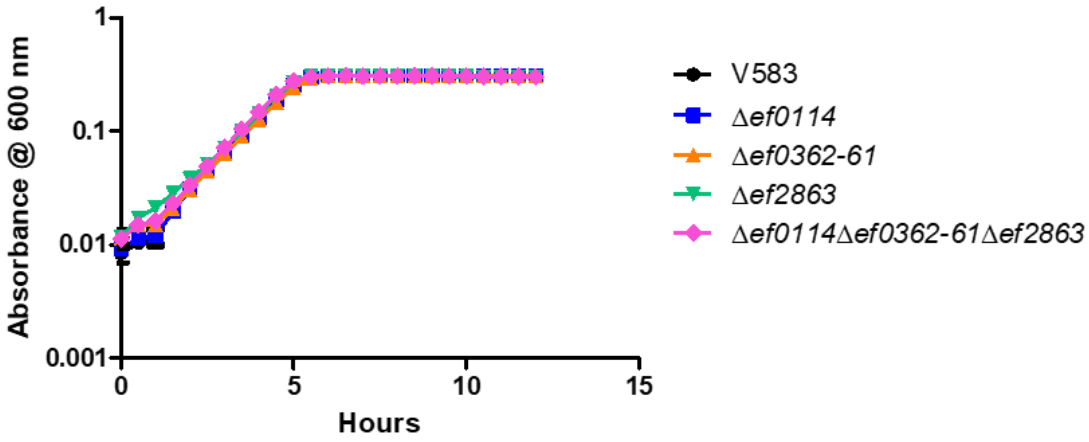

Figure S2: Growth of *E. faecalis* in CDM supplemented with 44.1 mg/mL human IgG. The growth curves are shown in black (V583), blue (Δ*ef0114*), orange (Δ*ef0362-61*), green (Δ*ef2863*), and magenta (Δ*ef0114*Δ*ef0362-61*Δ*ef2863*). The graph is the average of two biological replicates, with three technical replicates each time (n=6).

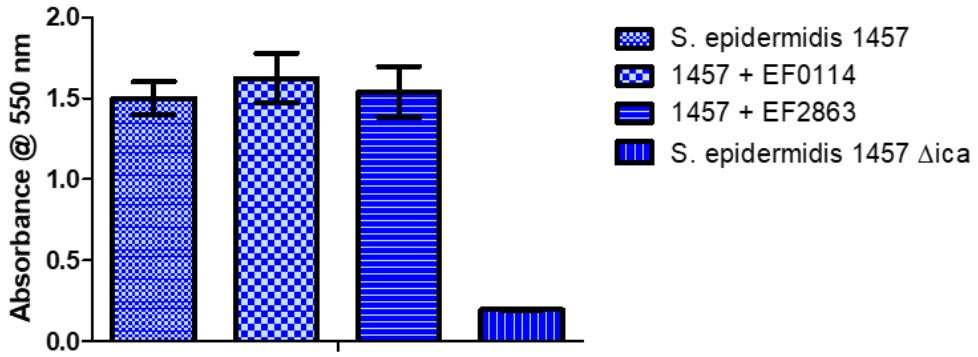

Figure S3: Biofilm formation by parental and mutant *S. epidermidis* strains in 96-well polystyrene plates. *S. epidermidis* biofilms were treated with 10μM EF0114 or EF2863 in PBS for 24 hours, followed by staining with crystal violet. *S. epidermidis* parental and Δ*ica* mutant strains were mock treated with PBS (controls). The graph is an average of two biological replicates, with eight technical replicates each time (n=16).

Supplemental Tables

Supplemental Table 1: Bacterial strains used in this study

***Enterococcus faecalis* bacterial strains**		
Strain	**Genotype or Description**	**Reference**
V583	Parental strain	Clinical isolate (81)
EH01	V583Δ*ccpA*	(9)
EK26	V583Δ*ccpA*::c*cpA*	(9)
EK31	V583Δ*ccpA*::cc*pA* T307Y (Phase-Lock Mutant)	This study
IH06	V583Δ*ef0114*	This study
AH03	V583Δ*ef0362-61*	This study
AH01	V583Δ*ef2863*	This study
AH08	V583Δ*ef0114*Δ*ef0362-61*	This study
AH07	V583Δ*ef0114*Δ*ef2863*	This study
AH06	V583Δ*ef0362-61*Δ*ef2863*	This study
AH09	V583Δ*ef0114*Δ*ef0362-61*Δ*ef2863*	This study
VI70	V583Δ*ccpA*Δ*ef0114*	This study
AH05	V583Δ*ccpA*Δ*ef0362-61*	This study
AH10	V583Δ*ccpA*Δ*ef2863*	This study
IH09	V583Δ*ccpA*Δ*ef0114*Δ*ef0362-61*	This study

IH12	V583Δ*ccpA*Δ*ef0362-61*Δ*ef2863*	This study
IH08	V583Δ*ccpA*Δ*ef0114*Δ*ef2863*	This study
IH13	V583Δ*ccpA*Δ*ef0114*Δ*ef0362-61*Δ*ef2863*	This study
AC04	V583Δ*ef2863*::*ef2863*	This study
EK41	V583*ΔccpA*Δ*ef2863*::*ef2863*	This study
EK44	V583Δ*ef0114*Δ*ef0362-61*Δ*ef2863*::*ef2863*	This study
VI01	V583Δ*rpoN*	(9)
VI40	V583Δ*rpoN*::*rpoN*	(9)
MG07	V583Δ*mptR*	(9)
MG07R	V583Ω*mptR*	(9)
IH10	V583Δ*mptBACD*	(9)
IH10R	V583Ω*mptBACD*	(9)
***Staphylococcus epidermidis* bacterial strains**		
1457	1457 PIA-positive, Aap-positive	Clinical isolate (82)
1457 Δ*ica*	icaADBC allelic replacement mutant, PIA-negative, Aap-positive, Tmp^r	(49)

Supplemental Table 2: Oligonucleotides used in this study

Primer	**Sequence (5'-3')**
EF0114P1	GAGAGAATTCCGTGAAGTTACACTGAACAAG
EF0114P2	GAGAGGATCCTCCTTTCTGCACTCCGTTCAT
EF0114P3	GAGAGGATCCCGCTAATGGATACGTTCTCG
EF0114P4	GAGACTGCAGCTTGATTGACAGCTTCCAGC
EF0114Up	GATGGGAAGCCAGTAATAAGAG
EF0114Down	CGTGCTGGCATATAATTGACC
EF0362-61P1	GAGAGAATTCGATGGATAGTATCTTTCATGCC
EF0362-61P2	GAGAGGATCCAACAAAACTAAAAGCCAGGACG
EF0362-61P3	GAGAGGATCCGCGACACGTTATAGTAACCTTG
EF0362-61P4	GAGACTGCAGCGACTAAAGTGTTAATGAACAG
EF0362-61Up	GCGATATTACGAGATACATG
EF0362-61Down	TGAAGTCATGGCAGTGACGT

EF2863P1	GAGAGAATTCTCGATACGTTGGCCATCTTC
EF2863P2	GAGAGGATCCAGTGCTCAATTGATGCCCCAT
EF2863P3	GAGAGGATCCCGAACTATTCACCAACTGTTC
EF2863P4	GAGACTGCAGATCCTCTAAAGTTGAAGAGACG
EF2863Up	CTGATCCGGAACTGTTACTG
EF2863Down	TATCATTAACTGCTTGTCGG
CcpAP1	GAGAGAATTCCAGAAGGTTCCAAGTAGCTG
CcpAP4	GAGACTGCAGGACTTATGCTGATGGTCGTG
CcpAUp	GCTGTAACACCAGGTTTCAC
CcpADown	GATCGTCAAGTTGGTTCTACG
CcpA_PLM5’	ATATGATATCGGTGCCGTGTCAATGCG
CcpA_PLM3’	GAGACTTAAGTAAAATGAACTATCCAGCTTCAGATGC
CcpA(EcoRV)Rev	GGCACCGATATCATATAAAGGTTGTGTAATAC
CcpA(AflII)For	TACTTAAGTAGTGATTGTAAGAGAAATTATCATCACCC
EF0114_GSP1	CATAAGGAATATCGTGC
EF0114_GSP2	GGCAATGTTGTATTAACTCCTTGC
EF0114_GSP3	CCATAAAATGTTTCTCTTGGGTCGG
EF0362_GSP1	GGGACCTGTTGTAATG
EF0362_GSP2	GTAGCTGTTTGTTCATCCAAAGG
EF0362_GSP3	CCAGTAATAAACGTATTTTTGGGCG
EF2863_GSP1	TGGCTGCAAAAATAATC
EF2863_GSP2	GGTTCCAGCTAAAGTATATTTTCCCA
EF2863_GSP3	CATACATGACTGTTTTAGGTGTAACA
EF0114_qPCR_for	AACCACAACCGGGTTTCA
EF0114_qPCR_rev	GCCAACAACCGATCCATTTC
EF0362_qPCR_for	GGTAGTTCTGCTGGTGGTAAC
EF0362_qPCR_rev	GACACCTGCACTGGCTAAT
EF2863_qPCR_for	CTAAATGAACGGGTCCAACAAAC
EF2863_qPCR_rev	TTAGGCAACCATGAAGGC
EF0005_qPCR_for	GGTGTTGGTTCCTCTGTTGT
EF0005_qPCR_rev	CGCACCACGACGATATTCTT
EF0114_5’(NheI)	GAGAGCTAGCCCAATGAGCCGACCCAAG
EF0114_3’(XhoI)	GAGACTCGAGTTTAACCACCATATAC

EF0114_α3'(XhoI)	GAGACTCGAGATTATAGGTGCGACCATCG
EF0114_β5'(NheI)	GAGAGCTAGCAAACCTTCTAATTTACTTTGGAC
EF0114_γ5'(NheI)	GAGAGCTAGCAAAAGTGTCTTTTCCATTGATGC
EF0114_E186Q_For(BsaI)	GAGAGGTCTCGTTAGATATTGACATGCAAACTCGTCC
EF0114_E186Q_Rev(BsaI)	GAGAGGTCTCTCTAACCCATCAATTCCTAAATCATCGAC
EF0114_E662Q_For(BsaI)	GAGAGGTCTCCAATTTTGGCGGCGATCAGTATGC
EF0114_E662Q_Rev(BsaI)	GAGAGGTCTCAAATTGAAAATTTCACTATGCGCGG
EF2863_5'(NdeI)	GAGACATATGGCATCAACTGTTACACCTAAAAC
EF2863_3'(XhoI)	GAGACTCGAGAGGTGTTGGAACAGTTGGTG
EF2863_E170Q_For(BsaI)	GAGAGGTCTCGATTTTGATGATCAGTATGCTGAATACGG
EF2863_E170Q_Rev(BsaI)	GAGAGGTCTCAAAATCAATACCATCTAAATGATACGTAT

Underlined sequences depict restriction sites used for cloning purposes

Supplemental Table 3: Plasmids used in this study

Plasmid	**Description**	**Reference**
pLT06	Markerless exchange vector; chloramphenicol resistance	(21)
pKS12A	LacZ-reporter fusion vector; spectinomycin resistance	(83)
pET21b	Protein overexpression vector; ampicillin resistance	(Novagen)
pIH04	pLT06 + engineered *ef0114* deletion	This study
pAH02	pLT06 + engineered *ef0362-61* deletion	This study
pAH01	pLT06 + engineered *ef2863* deletion	This study
pEK32	pUC-IDT + synthetic *ccpA* T307Y region	This study
pEK39	pLT06 + engineered *ccpA* PLM deletion	This study
pEK05	pKS12A + *ef0114* promoter	This study
pEK06	pKS12A + *ef0362-61* promoter	This study
pSP10	pKS12A + *ef2863* promoter	This study
pEK28	pET21b + EF2863 + His6 overexpression	This study
pEK33	pET21b + EF0114 (full length) + His6 overexpression	This study
pEK34	pET21b + EF0114 (α) + His6 overexpression	This study
pEK36	pET21b + EF0114 (γ) + His6 overexpression	This study
pEK37	pET21b + EF0114 (α+β) + His 6 overexpression	This study
pEK38	pET21b + EF0114 (β+γ) + His6 overexpression	This study

pEK47	pET21b + EF0114 E186Q + His6 overexpression	This study
pEK48	pET21b + EF0114 E662Q + His6 overexpression	This study
pEK58	pET21b + EF2863 E170Q + His6 overexpression	This study
pEK11	pLT06 + engineered *ef2863* complement	This study

References

1. Lebreton F, Willems RJL, Gilmore MS. 2014. Enterococcus Diversity, Origins in Nature, and Gut Colonization. *In* Gilmore MS, Clewell DB, Ike Y, Shankar N (ed), Enterococci: From Commensals to Leading Causes of Drug Resistant Infection, Boston.
2. Garcia-Solache M, Rice LB. 2019. The Enterococcus: a Model of Adaptability to Its Environment. Clin Microbiol Rev 32.
3. Weiner-Lastinger LM, Abner S, Edwards JR, Kallen AJ, Karlsson M, Magill SS, Pollock D, See I, Soe MM, Walters MS, Dudeck MA. 2019. Antimicrobial-resistant pathogens associated with adult healthcare-associated infections: Summary of data reported to the National Healthcare Safety Network, 2015-2017. Infect Control Hosp Epidemiol doi:10.1017/ice.2019.296:1-18.
4. Fiore E, Van Tyne D, Gilmore MS. 2019. Pathogenicity of Enterococci. Microbiol Spectr 7.
5. Gorke B, Stulke J. 2008. Carbon catabolite repression in bacteria: many ways to make the most out of nutrients. Nat Rev Microbiol 6:613-24.
6. Warner JB, Lolkema JS. 2003. CcpA-dependent carbon catabolite repression in bacteria. Microbiol Mol Biol Rev 67:475-90.
7. Fujita Y. 2009. Carbon catabolite control of the metabolic network in Bacillus subtilis. Biosci Biotechnol Biochem 73:245-59.
8. Bruckner R, Titgemeyer F. 2002. Carbon catabolite repression in bacteria: choice of the carbon source and autoregulatory limitation of sugar utilization. FEMS Microbiol Lett 209:141-8.
9. Keffeler EC, Iyer VS, Parthasarathy S, Ramsey MM, Gorman MJ, Barke TL, Varahan S, Olson S, Gilmore MS, Abdullahi ZH, Hancock EN, Hancock LE. 2021. Influence of the Alternative Sigma Factor RpoN on Global Gene Expression and Carbon Catabolism in Enterococcus faecalis V583. mBio 12.
10. Collin M, Fischetti VA. 2004. A novel secreted endoglycosidase from Enterococcus faecalis with activity on human immunoglobulin G and ribonuclease B. J Biol Chem 279:22558-70.
11. Vaaje-Kolstad G, Bohle LA, Gaseidnes S, Dalhus B, Bjoras M, Mathiesen G, Eijsink VG. 2012. Characterization of the chitinolytic machinery of Enterococcus faecalis V583 and high-resolution structure of its oxidative CBM33 enzyme. J Mol Biol 416:239-54.
12. Bohle LA, Mathiesen G, Vaaje-Kolstad G, Eijsink VG. 2011. An endo-beta-N-acetylglucosaminidase from Enterococcus faecalis V583 responsible for the hydrolysis of high-mannose and hybrid-type N-linked glycans. FEMS Microbiol Lett 325:123-9.
13. Synstad B, Gåseidnes S, Van Aalten DM, Vriend G, Nielsen JE, Eijsink VG. 2004. Mutational and computational analysis of the role of conserved residues in the active site of a family 18 chitinase. Eur J Biochem 271:253-62.
14. Du JJ, Klontz EH, Guerin ME, Trastoy B, Sundberg EJ. 2020. Structural insights into the mechanisms and specificities of IgG-active endoglycosidases. Glycobiology 30:268-279.
15. Tzelepis GD, Melin P, Jensen DF, Stenlid J, Karlsson M. 2012. Functional analysis of glycoside hydrolase family 18 and 20 genes in Neurospora crassa. Fungal Genet Biol 49:717-30.
16. Leisner JJ, Larsen MH, Ingmer H, Petersen BO, Duus JO, Palcic MM. 2009. Cloning and comparison of phylogenetically related chitinases from Listeria monocytogenes EGD and Enterococcus faecalis V583. J Appl Microbiol 107:2080-7.
17. Svitil AL, Kirchman DL. 1998. A chitin-binding domain in a marine bacterial chitinase and other microbial chitinases: implications for the ecology and evolution of 1,4-beta-glycanases. Microbiology (Reading) 144 (Pt 5):1299-1308.
18. Garbe J, Collin M. 2012. Bacterial hydrolysis of host glycoproteins - powerful protein modification and efficient nutrient acquisition. J Innate Immun 4:121-31.
19. Garbe J, Sjogren J, Cosgrave EF, Struwe WB, Bober M, Olin AI, Rudd PM, Collin M. 2014. EndoE from Enterococcus faecalis hydrolyzes the glycans of the biofilm inhibiting protein lactoferrin and mediates growth. PLoS One 9:e91035.

20. Roberts G, Tarelli E, Homer KA, Philpott-Howard J, Beighton D. 2000. Production of an endo-beta-N-acetylglucosaminidase activity mediates growth of Enterococcus faecalis on a high-mannose-type glycoprotein. J Bacteriol 182:882-90.
21. Thurlow LR, Thomas VC, Fleming SD, Hancock LE. 2009. *Enterococcus faecalis* capsular polysaccharide serotypes C and D and their contributions to host innate immune evasion. Infection and Immunity 77.
22. Keffeler EC IV, Parthasarathy S, Ramsey MM; Gorman MJ, Barke TL, Varahan S, Olson S, Gilmore MS, Abdullahi Z, Hancock EN, Hancock LE 2021. Influence of the alternative sigma factor RpoN on global gene expression and carbon catabolism in *Enterococcus faecalis* V583. mBio.
23. Brown SA, Whiteley M. 2007. A novel exclusion mechanism for carbon resource partitioning in Aggregatibacter actinomycetemcomitans. J Bacteriol 189:6407-14.
24. Socransky SS, Dzink JL, Smith CM. 1985. Chemically defined medium for oral microorganisms. J Clin Microbiol 22:303-5.
25. LaPointe CF, Taylor RK. 2000. The type 4 prepilin peptidases comprise a novel family of aspartic acid proteases. J Biol Chem 275:1502-10.
26. Towbin H, Staehelin T, Gordon J. 1979. Electrophoretic transfer of proteins from polyacrylamide gels to nitrocellulose sheets: procedure and some applications. Proc Natl Acad Sci U S A 76:4350-4.
27. Toledo-Arana A, Valle J, Solano C, Arrizubieta MJ, Cucarella C, Lamata M, Amorena B, Leiva J, Penades JR, Lasa I. 2001. The enterococcal surface protein, Esp, is involved in Enterococcus faecalis biofilm formation. Appl Environ Microbiol 67:4538-45.
28. Okbazghi SZ, More AS, White DR, Duan S, Shah IS, Joshi SB, Middaugh CR, Volkin DB, Tolbert TJ. 2016. Production, Characterization, and Biological Evaluation of Well-Defined IgG1 Fc Glycoforms as a Model System for Biosimilarity Analysis. J Pharm Sci 105:559-574.
29. Guiton PS, Hung CS, Hancock LE, Caparon MG, Hultgren SJ. 2010. Enterococcal biofilm formation and virulence in an optimized murine model of foreign body-associated urinary tract infections. Infect Immun 78:4166-75.
30. Bendtsen JD, Nielsen H, von Heijne G, Brunak S. 2004. Improved prediction of signal peptides: SignalP 3.0. J Mol Biol 340:783-95.
31. Funkhouser JD, Aronson NN, Jr. 2007. Chitinase family GH18: evolutionary insights from the genomic history of a diverse protein family. BMC Evol Biol 7:96.
32. Jiang YL, Yu WL, Zhang JW, Frolet C, Di Guilmi AM, Zhou CZ, Vernet T, Chen Y. 2011. Structural basis for the substrate specificity of a novel beta-N-acetylhexosaminidase StrH protein from Streptococcus pneumoniae R6. J Biol Chem 286:43004-12.
33. Ramasubbu N, Thomas LM, Ragunath C, Kaplan JB. 2005. Structural analysis of dispersin B, a biofilm-releasing glycoside hydrolase from the periodontopathogen Actinobacillus actinomycetemcomitans. J Mol Biol 349:475-86.
34. Val-Cid C, Biarnes X, Faijes M, Planas A. 2015. Structural-Functional Analysis Reveals a Specific Domain Organization in Family GH20 Hexosaminidases. PLoS One 10:e0128075.
35. Forsberg Z, Sorlie M, Petrovic D, Courtade G, Aachmann FL, Vaaje-Kolstad G, Bissaro B, Rohr AK, Eijsink VG. 2019. Polysaccharide degradation by lytic polysaccharide monooxygenases. Curr Opin Struct Biol 59:54-64.
36. Henkin TM. 1996. The role of CcpA transcriptional regulator in carbon metabolism in Bacillus subtilis. FEMS Microbiol Lett 135:9-15.
37. Miwa Y, Nakata A, Ogiwara A, Yamamoto M, Fujita Y. 2000. Evaluation and characterization of catabolite-responsive elements (cre) of Bacillus subtilis. Nucleic Acids Res 28:1206-10.
38. Schumacher MA, Allen GS, Diel M, Seidel G, Hillen W, Brennan RG. 2004. Structural basis for allosteric control of the transcription regulator CcpA by the phosphoprotein HPr-Ser46-P. Cell 118:731-741.

39. Paluscio E, Watson ME, Jr., Caparon MG. 2018. CcpA Coordinates Growth/Damage Balance for Streptococcus pyogenes Pathogenesis. Sci Rep 8:14254.
40. Kawasaki N, Ohta M, Hyuga S, Hashimoto O, Hayakawa T. 1999. Analysis of carbohydrate heterogeneity in a glycoprotein using liquid chromatography/mass spectrometry and liquid chromatography with tandem mass spectrometry. Anal Biochem 269:297-303.
41. Liu L. 2015. Antibody glycosylation and its impact on the pharmacokinetics and pharmacodynamics of monoclonal antibodies and Fc-fusion proteins. J Pharm Sci 104:1866-1884.
42. Lu G, Holland LA. 2019. Profiling the N-Glycan Composition of IgG with Lectins and Capillary Nanogel Electrophoresis. Anal Chem 91:1375-1383.
43. Robb M, Robb CS, Higgins MA, Hobbs JK, Paton JC, Boraston AB. 2015. A Second beta-Hexosaminidase Encoded in the Streptococcus pneumoniae Genome Provides an Expanded Biochemical Ability to Degrade Host Glycans. J Biol Chem 290:30888-900.
44. Itoh Y, Wang X, Hinnebusch BJ, Preston JF, 3rd, Romeo T. 2005. Depolymerization of beta-1,6-N-acetyl-D-glucosamine disrupts the integrity of diverse bacterial biofilms. J Bacteriol 187:382-7.
45. Kaplan JB, Ragunath C, Ramasubbu N, Fine DH. 2003. Detachment of Actinobacillus actinomycetemcomitans biofilm cells by an endogenous beta-hexosaminidase activity. J Bacteriol 185:4693-8.
46. Kaplan JB, Ragunath C, Velliyagounder K, Fine DH, Ramasubbu N. 2004. Enzymatic detachment of Staphylococcus epidermidis biofilms. Antimicrob Agents Chemother 48:2633-6.
47. Stacy A, Abraham N, Jorth P, Whiteley M. 2016. Microbial Community Composition Impacts Pathogen Iron Availability during Polymicrobial Infection. PLoS Pathog 12:e1006084.
48. Kaplan JB, Velliyagounder K, Ragunath C, Rohde H, Mack D, Knobloch JK, Ramasubbu N. 2004. Genes involved in the synthesis and degradation of matrix polysaccharide in Actinobacillus actinomycetemcomitans and Actinobacillus pleuropneumoniae biofilms. J Bacteriol 186:8213-20.
49. Handke LD, Slater SR, Conlon KM, O'Donnell ST, Olson ME, Bryant KA, Rupp ME, O'Gara JP, Fey PD. 2007. SigmaB and SarA independently regulate polysaccharide intercellular adhesin production in Staphylococcus epidermidis. Can J Microbiol 53:82-91.
50. Michaux C, Hansen EE, Jenniches L, Gerovac M, Barquist L, Vogel J. 2020. Single-Nucleotide RNA Maps for the Two Major Nosocomial Pathogens Enterococcus faecalis and Enterococcus faecium. Front Cell Infect Microbiol 10:600325.
51. Innocenti N, Golumbeanu M, Fouquier d'Herouel A, Lacoux C, Bonnin RA, Kennedy SP, Wessner F, Serror P, Bouloc P, Repoila F, Aurell E. 2015. Whole-genome mapping of 5' RNA ends in bacteria by tagged sequencing: a comprehensive view in Enterococcus faecalis. RNA 21:1018-30.
52. Frank KL, Colomer-Winter C, Grindle SM, Lemos JA, Schlievert PM, Dunny GM. 2014. Transcriptome analysis of Enterococcus faecalis during mammalian infection shows cells undergo adaptation and exist in a stringent response state. PLoS One 9:e115839.
53. Vebo HC, Snipen L, Nes IF, Brede DA. 2009. The transcriptome of the nosocomial pathogen Enterococcus faecalis V583 reveals adaptive responses to growth in blood. PLoS One 4:e7660.
54. Vebo HC, Solheim M, Snipen L, Nes IF, Brede DA. 2010. Comparative genomic analysis of pathogenic and probiotic Enterococcus faecalis isolates, and their transcriptional responses to growth in human urine. PLoS One 5:e12489.
55. Wright EM, Hirayama BA, Loo DF. 2007. Active sugar transport in health and disease. J Intern Med 261:32-43.
56. Shepard BD, Gilmore MS. 2002. Differential expression of virulence-related genes in Enterococcus faecalis in response to biological cues in serum and urine. Infect Immun 70:4344-52.
57. Chen W, Jiang X, Yang Q. 2020. Glycoside hydrolase family 18 chitinases: The known and the unknown. Biotechnol Adv 43:107553.
58. Frederiksen RF, Paspaliari DK, Larsen T, Storgaard BG, Larsen MH, Ingmer H, Palcic MM, Leisner JJ. 2013. Bacterial chitinases and chitin-binding proteins as virulence factors. Microbiology (Reading) 159:833-847.

59. Fujiwara S, Shinkai H, Deutzmann R, Paulsson M, Timpl R. 1988. Structure and distribution of N-linked oligosaccharide chains on various domains of mouse tumour laminin. Biochem J 252:453-61.
60. Furukawa K, Roberts DD, Endo T, Kobata A. 1989. Structural study of the sugar chains of human platelet thrombospondin. Arch Biochem Biophys 270:302-12.
61. Sherblom AP, Smagula RM. 1993. High-mannose chains of mammalian glycoproteins. Methods Mol Biol 14:143-9.
62. Cavallone D, Malagolini N, Monti A, Wu XR, Serafini-Cessi F. 2004. Variation of high mannose chains of Tamm-Horsfall glycoprotein confers differential binding to type 1-fimbriated Escherichia coli. J Biol Chem 279:216-22.
63. Taganna J, de Boer AR, Wuhrer M, Bouckaert J. 2011. Glycosylation changes as important factors for the susceptibility to urinary tract infection. Biochem Soc Trans 39:349-54.
64. Gerlach JQ, Kilcoyne M, Farrell MP, Kane M, Joshi L. 2012. Differential release of high mannose structural isoforms by fungal and bacterial endo-β-N-acetylglucosaminidases. Mol Biosyst 8:1472-81.
65. Li Y, Li R, Yu H, Sheng X, Wang J, Fisher AJ, Chen X. 2020. Enterococcus faecalis alpha1-2-mannosidase (EfMan-I): an efficient catalyst for glycoprotein N-glycan modification. FEBS Lett 594:439-451.
66. Gregg KJ, Zandberg WF, Hehemann JH, Whitworth GE, Deng L, Vocadlo DJ, Boraston AB. 2011. Analysis of a new family of widely distributed metal-independent alpha-mannosidases provides unique insight into the processing of N-linked glycans. J Biol Chem 286:15586-96.
67. Suits MD, Zhu Y, Taylor EJ, Walton J, Zechel DL, Gilbert HJ, Davies GJ. 2010. Structure and kinetic investigation of Streptococcus pyogenes family GH38 alpha-mannosidase. PLoS One 5:e9006.
68. Naegeli A, Bratanis E, Karlsson C, Shannon O, Kalluru R, Linder A, Malmstrom J, Collin M. 2019. Streptococcus pyogenes evades adaptive immunity through specific IgG glycan hydrolysis. J Exp Med 216:1615-1629.
69. Sjogren J, Okumura CY, Collin M, Nizet V, Hollands A. 2011. Study of the IgG endoglycosidase EndoS in group A streptococcal phagocyte resistance and virulence. BMC Microbiol 11:120.
70. Boune S, Hu P, Epstein AL, Khawli LA. 2020. Principles of N-Linked Glycosylation Variations of IgG-Based Therapeutics: Pharmacokinetic and Functional Considerations. Antibodies (Basel) 9.
71. Li W, Zhu Z, Chen W, Feng Y, Dimitrov DS. 2017. Crystallizable Fragment Glycoengineering for Therapeutic Antibodies Development. Front Immunol 8:1554.
72. Mimura Y, Katoh T, Saldova R, O'Flaherty R, Izumi T, Mimura-Kimura Y, Utsunomiya T, Mizukami Y, Yamamoto K, Matsumoto T, Rudd PM. 2018. Glycosylation engineering of therapeutic IgG antibodies: challenges for the safety, functionality and efficacy. Protein Cell 9:47-62.
73. Allhorn M, Briceno JG, Baudino L, Lood C, Olsson ML, Izui S, Collin M. 2010. The IgG-specific endoglycosidase EndoS inhibits both cellular and complement-mediated autoimmune hemolysis. Blood 115:5080-8.
74. Panda S, Zhang J, Tan NS, Ho B, Ding JL. 2013. Natural IgG antibodies provide innate protection against ficolin-opsonized bacteria. EMBO J 32:2905-19.
75. Xie B, Zhou G, Chan SY, Shapiro E, Kong XP, Wu XR, Sun TT, Costello CE. 2006. Distinct glycan structures of uroplakins Ia and Ib: structural basis for the selective binding of FimH adhesin to uroplakin Ia. J Biol Chem 281:14644-53.
76. Chaudhuri S, Bruno JC, Alonzo F, 3rd, Xayarath B, Cianciotto NP, Freitag NE. 2010. Contribution of chitinases to Listeria monocytogenes pathogenesis. Appl Environ Microbiol 76:7302-5.
77. Larsen T, Petersen BO, Storgaard BG, Duus JO, Palcic MM, Leisner JJ. 2011. Characterization of a novel Salmonella Typhimurium chitinase which hydrolyzes chitin, chitooligosaccharides and an N-acetyllactosamine conjugate. Glycobiology 21:426-36.

78. DebRoy S, Dao J, Soderberg M, Rossier O, Cianciotto NP. 2006. Legionella pneumophila type II secretome reveals unique exoproteins and a chitinase that promotes bacterial persistence in the lung. Proc Natl Acad Sci U S A 103:19146-51.
79. Bhattacharya D, Nagpure A, Gupta RK. 2007. Bacterial chitinases: properties and potential. Crit Rev Biotechnol 27:21-8.
80. Frederiksen RF, Yoshimura Y, Storgaard BG, Paspaliari DK, Petersen BO, Chen K, Larsen T, Duus J, Ingmer H, Bovin NV, Westerlind U, Blixt O, Palcic MM, Leisner JJ. 2015. A diverse range of bacterial and eukaryotic chitinases hydrolyzes the LacNAc (Galβ1-4GlcNAc) and LacdiNAc (GalNAcβ1-4GlcNAc) motifs found on vertebrate and insect cells. J Biol Chem 290:5354-66.
81. Sahm DF, Kissinger J, Gilmore MS, Murray PR, Mulder R, Solliday J, Clarke B. 1989. In vitro susceptibility studies of vancomycin-resistant Enterococcus faecalis. Antimicrob Agents Chemother 33:1588-91.
82. Mack D, Siemssen N, Laufs R. 1992. Parallel induction by glucose of adherence and a polysaccharide antigen specific for plastic-adherent Staphylococcus epidermidis: evidence for functional relation to intercellular adhesion. Infect Immun 60:2048-57.
83. Varahan S, Iyer VS, Moore WT, Hancock LE. 2013. Eep confers lysozyme resistance to enterococcus faecalis via the activation of the extracytoplasmic function sigma factor SigV. J Bacteriol 195:3125-34.

Chapter 4: Metabolism of poly-β1,4-N-acetylglucosamine substrates and importation of N-acetylglucosamine and glucosamine by *Enterococcus faecalis*

Abstract

The ability of *Enterococcus faecalis* to use a variety of carbon sources enables colonization at various anatomic sites within a mammalian host. N-acetylglucosamine (GlcNAc) is one of the most abundant natural sugars and provides bacteria with a source of carbon and nitrogen when metabolized. N-acetylglucosamine is also a component of bacterial peptidoglycan, further highlighting the significance of N-acetylglucosamine utilization. In this study, we show that CcpA-regulated enzymes are required for growth on the poly-β1,4-linked GlcNAc substrate, chitopentaose (β1,4-linked $GlcNAc_5$). We also show that EF0114 (EndoE) is required for growth on chitobiose (β1,4-linked $GlcNAc_2$), and that the GH20 domain of EndoE is required for the conversion of $GlcNAc_2$ to N-acetylglucosamine. GlcNAc is transported into the cell via two separate PTS systems, either the PTS IICBA system encoded by *ef1516* (*nagE*) or the Mpt glucose/mannose permease complex (MptBACD). The Mpt PTS system is also the primary glucosamine transporter. In order for N-acetylglucosamine to be utilized as a carbon source, phosphorylated N-acetylglucosamine (GlcNAc-6-P) must be deacetylated and here we show that this activity is mediated by EF1317 (an N-acetylglucosamine-6-phosphate deacetylase; NagA homolog), as a deletion of *ef1317* is unable to grow on GlcNAc as the carbon source. Deamination of glucosamine to fructose-6-phosphate is required for entry into glycolysis and we show that growth on glucosamine is dependent on EF0466 (a glucosamine-6-phosphate deaminase; NagB homolog). Collectively, our data highlight the chitinolytic machinery required for breaking down exogenous chitinous substrates, as well as the uptake and cytosolic enzymes needed for metabolizing N-acetylglucosamine.

Importance

Enterococcus faecalis causes life-threatening healthcare-associated infections in part due to its intrinsic and acquired antibiotic resistance, its ability to form biofilms, as well as its nutrient versatility. Alternative nutrient acquisition systems are key factors that contribute to enterococcal colonization at biologically unique host anatomic sites. Although *E. faecalis* can metabolize an array of carbon sources, little is known of how this bacterium acquires these secondary nutrient sources in mammalian hosts. Our research identifies the glycosidase machinery required for degrading exogenous chitinous substrates into N-acetylglucosamine monomers for transport and metabolism of one of the most abundant naturally occurring sugars, N-acetylglucosamine. Disrupting the function of this N-acetylglucosamine acquisition pathway may lead to new treatments against multidrug resistant enterococcal infections.

Introduction

Enterococcus faecalis is a Gram-positive commensal that primarily inhabits the mucosa of human gastrointestinal tracts and the oral cavity (1). However, enterococci have emerged as a hospital-adapted, multidrug resistant (MDR) pathogen that now ranks second on the list of causative agents of disease in healthcare settings in the United States (2-4). This opportunistic, nosocomial pathogen causes a variety of infections, including endocarditis, bacteremia associated with central-line catheters, surgical site infections, and catheter associated urinary tract infections (CAUTI) (4). The ability of *E. faecalis* to colonize these host anatomic sites is, in part, governed by its ability to metabolize secondary carbon sources in nutrient poor host environments (1, 5). Although, *E. faecalis* can metabolize approximately 70 different carbon sources (6), little is known of the metabolic machinery required for the uptake and utilization of these substrates.

N-acetylglucosamine (GlcNAc) is a monosaccharide derivative of glucose that is an important carbon and nitrogen source for several bacteria (7-12). Additionally, this amino sugar is a structural component of bacterial peptidoglycan (13, 14), the cell walls of fungi (15), as well as the exoskeleton of arthropods (16). N-acetylglucosamine is the monomeric unit of the second most abundant natural polysaccharide, chitin, which is a linear polymer of β-1,4-linked GlcNAc (17, 18). Chitin also provides prebiotic and antioxidant properties when consumed as a source of insoluble fiber (19-21). Bacteria have evolved specific machinery to efficiently degrade chitin and GlcNAc-containing substrates, including chitinases as well as chitin-binding proteins (CBPs) with lytic polysaccharide monooxygenase activity (22). Recent evidence indicates that chitinases serve as virulence factors for bacterial pathogens during infection of mammalian hosts (23, 24). Although chitin is not naturally present in mammalian hosts, the biological role of bacterial chitinases during infection have been characterized from bacterial pathogens, such as *Listeria monocytogenes* (25, 26) and *Legionella pneumophila* (27), suggesting that additional substrates

for these chitinases likely exist in mammalian hosts. Recent observations indicate that chitinases produced by *Salmonella* and *Listeria* also have specificity towards LacNac (Galβ1–4GlcNAc) and LacdiNAc (GalNAcβ1–4GlcNAc) sugar linkages present in mammalian N and O-linked glycans, glycolipids and glycosaminoglycans (24, 28). Although chitinolytic machinery has been identified in *E. faecalis* (29, 30), little is known of how it contributes to enterococcal metabolism and overall pathogenesis.

Based on observations from Vaaje-Kolstad et al. (30), all currently available enterococcal genomes contain an enzymatic system for cleaving chitin, chitobiose, and extracellular GlcNAc. Vaaje-Kolstad et al. show by analogy with other known microbial chitinolytic systems that EF0362 and EF0361(EfCBM33A and EfChi18A, respectively) act synergistically to depolymerize poly-N-acetylglucosamine (poly-GlcNAc) substrates into $GlcNAc_2$ dimers (30). EfCBM33A is a copper-dependent enzyme that cleaves chitin via an oxidative mechanism and belongs to a growing number of lytic polysaccharide monooxygenases (22). EfChi18A is a glycosyl family 18 hydrolase and possesses chitinolytic activity and is homologous to the related

ChiA enzyme in *L. monocytogenes* (25).

It was of interest to determine enzyme(s) responsible for converting $GlcNAc_2$ to GlcNAc monomers as well as the transport system(s) required for GlcNAc and glucosamine (GlcN) importation. Entry of phosphorylated GlcNAc into glycolysis requires deacetylation and deamination into fructose-6-phosphate. We predicted the *E. faecalis* homologs responsible for these activities and provide further characterization of their function in the use of GlcNAc as a key carbon source.

Materials and Methods

Bacterial strains and growth conditions:

Bacterial strains used in this study are listed in Table S1. For propagation of plasmids, *Escherichia coli* ElectroTen-Blue from Stratagene were cultivated in Luria-Bertani (LB) broth, supplemented with appropriate antibiotics, when necessary. Unless mentioned otherwise, *E. faecalis* was cultured in Todd-Hewitt broth (THB) (BD Biosciences), supplemented with appropriate antibiotics, when necessary. For antibiotic selection, chloramphenicol (Cm) at a concentration of 10ug/mL and 15ug/mL were used for *E. coli* and *E. faecalis*, respectively; ampicillin (Amp) at a concentration of 100ug/mL was used for *E. coli;* and gentamicin (Gent) at a concentration of 250ug/mL was used for *E. faecalis.*

Construction of in-frame markerless deletion strains:

Using the temperature sensitive cloning vector, pLT06 (31), isogenic in-frame deletion mutants were generated in *E. faecalis* V583. Upstream and downstream flanking DNA regions of the respective gene target were amplified using primers listed in Table S2. For example, the primer pairs EF1317P1/EF1317P2 and EF1317P3/EF1317P4 were used to amplify flanking regions upstream and downstream of *ef1317*, respectively. To facilitate cloning, primers EF1317P1/EF1317P2 were designed with EcoRI/BamHI (New England Biolabs (NEB)) restriction sites, respectively, whereas, EF1317P3/EF1317P4 were designed with BamHI/PstI (NEB) restriction sites, respectively. For the construction of the insert, the amplified regions were digested with BamHI, ligated and subsequently re-amplified using primers EF1317P1 and EF1317P4. To generate pSP20 (*ef1317* deletion construct), the amplified insert fragment was digested with EcoRI/PstI and ligated into the digested pLT06 cloning vector. pSP20 was electroporated into *E. coli* ElectroTen-Blue cells and the plasmid was identified by colony PCR.

The confirmed construct was screened by restriction digest analysis and subsequently electroporated into *E. faecalis* V583 cells. V583Δ*ef1317* [SP27] was subsequently generated as previously described following plasmid integration and excision events (31) and confirmed by colony PCR using the primers EF1317Up and EF1317Down. In addition to the gene deletion mutants, paired genetic revertants (32, 33) from this PCR screen were also selected based on the restoration to the parental genotype following excision of the integrated plasmid and designated as V583Ω*ef1317*. A similar approach was used to create all the gene deletion mutants and paired genetic revertants used in this and prior studies (34, 35) referenced in Table S1.

Construction of in-frame markerless complement strains:

Using the temperature sensitive cloning vector, pLT06 (31), isogeneic in-frame EF1317 complement strain was generated in *E. faecalis* V583. The entirety of the *ef1317* gene, including its upstream and downstream flanking DNA regions was amplified using the primer pair EF1317P1/EF1317P4 (Table S2). For cloning purposes, EF1317P1 and EF1317P4 were designed with EcoRI and PstI restriction sites, respectively. The amplified region was digested with EcoRI and PstI and ligated into the digested pLT06 cloning vector, resulting in the creation of pEK60 (*ef1317* complement construct). pEK60 was electroporated into *E. coli* ElectroTen-Blue cells and the plasmid was identified by colony PCR. The confirmed construct was screened by restriction digest analysis and subsequently electroporated into *E. faecalis* V583Δ*ef1317* [SP27] cells. V583Δ*ef1317*::*ef1317* [EK47] was subsequently generated as previously described (31) and confirmed by colony PCR using the primers EF1317Up and EF1317Down.

Growth assessment in nutrient limiting conditions:

Using a single colony of each strain, liquid cultures were started in THB and incubated at 37°C, overnight. For growth analysis, overnight cultures were diluted 1:100 in a chemically defined medium (CDM) (36, 37), supplemented with either chitopentaose ($GlcNAc_5$) (Seikagaku Kogyo Co.), chitobiose ($GlcNAc_2$) (Seikagaku Kogyo Co.), N-acetylglucosamine (GlcNAc) (Acros Organics), glucosamine (GlcN) (Acros Organics), or fructose (Sigma Aldrich). Growth was monitored for 12 hrs in an Infinite M200 Pro plate reader (Tecan Trading AG, Switzerland) at 37°C with orbital shaking at 250 rpm.

Expression and purification of EF0114 variants

The plasmids bearing the protein overexpression constructs, listed in Table S3, are all derivatives of the pET21b vector (Novagen), and details of their construction are described in Keffeler et al. (34). For overexpression and purification, *E.coli* BL21(DE3)-RIPL cells (Agilent Technologies) harboring protein overexpression constructs were grown to an OD_{600} 0.6-0.7 at 37°C, shaking, then induced using 1mM IPTG and further incubated for 16 hours at 16°C, after which the cells were harvested by centrifugation and resuspended in Buffer A (100mM TrisHCl, 0.5M NaCl, 10% glycerol, 15mM imidazole, pH 8.0). The bacteria were lysed using a French press and the soluble fractions were loaded onto a cobalt-affinity column (GE Healthcare TALON Superflow) equilibrated with Buffer A. Recombinant proteins were washed with Buffer A and eluted with an imidazole gradient using Buffers A and B (100mM TrisHCl, 0.5M NaCl,10% glycerol, 500mM imidazole, pH 8.0). Protein purity was analyzed by SDS-PAGE and the protein concentration was determined using the Bradford micro-assay (Bio-Rad Laboratories), according to the supplier's procedure.

Chitinolytic assays:

Glycosidase activity against the fluorogenic substrate 4MU-methylumbelliferyl-β-D-N-acetylglucosamine ($GlcNAc_2$ analogue) (Sigma Aldrich) was used determined by incubating the fluorogenic substrate with filtered supernatants of bacterial cultures grown overnight (37°C, shaking) in a chemically defined medium (CDM) supplemented with 42mM glucose. Briefly, 4MU-GlcNAc (50μM) was incubated in prewarmed 25mM citrate buffer (pH 6.0) for 15min at 37°C, in a reaction volume of 150μL. Filtered supernatant (50μL) was subsequently added to the prewarmed chitinolytic reactions, briefly mixed, and incubated for 15min at 37°C, resulting in a total reaction volume of 200μL. The fluorescence intensity (excitation 390nm, emission 485nm) was measured using an Infinite M200 Pro plate reader (Tecan Trading AG, Switzerland). Chitinolytic activity is expressed as relative fluorescence calculated by dividing the fluorescence emitted at 485nm by the OD600nm of the culture. For analysis of purified recombinant EF0114 variants, 1μM of recombinant enzyme was incubated with prewarmed chitinolytic reactions, in a total reaction volume of 200μL. Chitinolytic activity is expressed as the fluorescence emitted at 485nm.

Statistical analyses

The statistical analyses of the various experiments were conducted using the GraphPad Prism 5 software (San Diego, CA).

Results

The deletion of the enterococcal chitinase and chitin-binding protein, *ef0362-61*, impacts growth on a poly-β1,4-N-acetylglucosamine substrate

Based on the observations that recombinant EF0362 (EfCBM33A) and EF0361 (EfChi18A) act synergistically to hydrolyze poly-β1,4-N-acetylglucosamine substrates into β1,4-$GlcNAc_2$ oligomeric dimers (30), it was of interest to assess whether the deletion of *ef0362-61* impacted growth with a poly-β1,4-GlcNAc substrate as the sole carbon source. Since the enterococcal chitinase and chitin binding protein are encoded in a single operon and both are involved in the degradation of chitinous substrates, we therefore constructed the *ef0362-61* deletion mutant where we removed the entire operon from the *E. faecalis* V583 genome. Since EF0361 is one of three glycosyl hydrolases encoded in the *E. faecalis* V583 genome that belongs to the glycosyl hydrolase family 18 (GH18) (29, 34, 38, 39), we also assessed single deletion mutants of *ef0114* and *ef2863*, as well as a triple glycosidase mutant (Δ*ef0114*Δ*ef0362-61*Δ*ef2863*) for their ability to utilize chitopentaose (β1,4-$GlcNAc_5$) as the sole carbon source in a chemically defined medium (CDM) (36, 37). The deletion of *ef2863* did not impact growth when chitopentaose was present as the sole carbon source. However, the deletion of *ef0362-61* or *ef0114* significantly impacted growth relative to the parental strain (Figure 1). Theses phenotypes are complementable as the *ef0362-61* genetic revertant and the *ef0114* complement grew equivalent to the parental strain. This indicates that the ability of *E. faecalis* to sustain growth on poly- β1,4-N-acetylglucosamine substrates is dependent on the activity of EF0362-61 and EF0114.

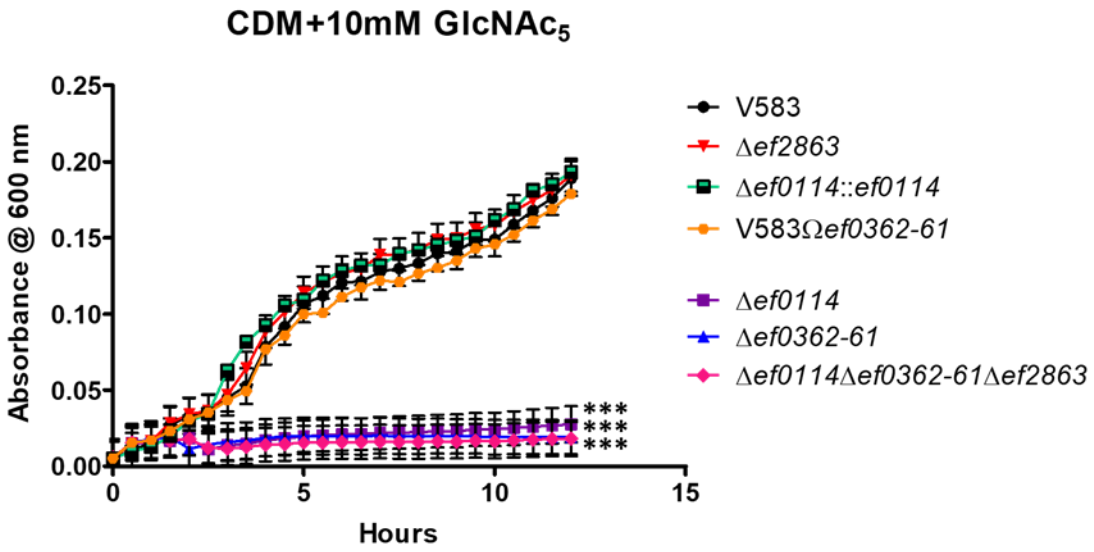

Figure 1: Growth of *E. faecalis* in CDM supplemented with 10mM chitopentaose ($GlcNAc_5$). Each graph is the average of three biological replicates, with three technical replicates each time (n=9). The statistical significance was calculated using a two-way ANOVA test, p value of <0.0001 is indicated as (***). The growth curves are shown in black (V583), purple (Δ*ef0114*), blue (Δ*ef0362-61*), red (Δ*ef2863*), pink (Δ*ef0114*Δ*ef0362*-61Δ*ef2863*), green (Δ*ef0114*::*ef0114*), and orange (V583Ω*ef0362-61* revertant).

EF0114 is responsible for degrading β1,4-$GlcNAc_2$ into GlcNAc prior to importation into the bacterial cell

Vaaje-Kolstad et al. (30) proposed that an essential component of the chitinolytic machinery to metabolize chitinous substrates is a secreted glycosyl hydrolase that would be responsible for cleaving β1,4-$GlcNAc_2$ into GlcNAc, prior to the transport of the amino sugar into the cell. Possible glycosyl hydrolase candidates for degrading β1,4-$GlcNAc_2$ into GlcNAc are EF0114 and EF2863, as both are capable of cleaving β1,4-linked GlcNAc glycosidic bonds (34, 38-40). Since the expression of *ef0114* and *ef2863* are negatively regulated by CcpA (34), we hypothesized that culture supernatant from a *ccpA* mutant would hydrolyze the fluorogenic β1,4-$GlcNAc_2$ analogue, 4MU-methylumbelliferyl-β-D-N-acetylglucosamine (4-MU-GlcNAc), resulting in an increase in fluorescence due to the release of the fluorogenic product after enzymatic cleavage. To assess this

hypothesis, supernatants were collected from the *E. faecalis* V583 wild-type strain and the *ccpA* mutant strain grown overnight in CDM supplemented with 42mM glucose to ensure glucose replete conditions during growth (34). The filtered supernatants were subsequently incubated with 4-MU-GlcNAc to assess glycosidase activity. As shown in figure 2A, the *ccpA* mutant supernatant possesses significant chitinolytic activity against the fluorogenic β1,4-$GlcNAc_2$ analogue relative to filtered supernatant collected from the parental strain.

To determine which of the CcpA-regulated glycosyl hydrolases is responsible for degrading β1,4-$GlcNAc_2$ to GlcNAc, supernatants were also collected from various glycosyl hydrolase deletion mutants in the *ccpA* mutant background grown overnight in CDM supplemented with glucose (42mM). Figure 2A illustrates that only the deletion of *ef0114* results in the elimination of chitinolytic activity against the fluorogenic β1,4-$GlcNAc_2$ analogue relative to the *ccpA* mutant supernatant. The phenotype associated with the various *ef0114* mutants were corroborated by assessing the Δ*ccpA*Δ*ef0114*::*ef0114* complement strain under the same 4MU-GlcNAc assay conditions (Figure 2A). Incubating the fluorogenic 4MU-GlcNAc substrate with the Δ*ccpA*Δ*ef0114*::*ef0114* complement supernatant resulted in the restoration of glycosidase activity against this substrate. The data indicates that EF0114 is responsible for degrading extracellular β1,4-$GlcNAc_2$ into GlcNAc.

Because EF0114 displays activity against the fluorogenic β1,4-$GlcNAc_2$ analogue, it was of interest to assess the ability of the *ef0114* genetic mutant to sustain growth with $GlcNAc_2$ as the sole carbon source. We assessed the growth of single deletions of *ef0114*, *ef0362-61* and *ef2863* and the parental V583 strain in CDM supplemented with 10 mM $GlcNAc_2$. The deletion of *ef0114* significantly impacts growth on this substrate relative to the parental strain (Figure 2B), whereas growth of ef*0362-61* and ef*2863* were unchanged relative to V583 (Figure 2B), further

highlighting that EF0114 is principally responsible for hydrolyzing dimers of GlcNAc into its monomeric form.

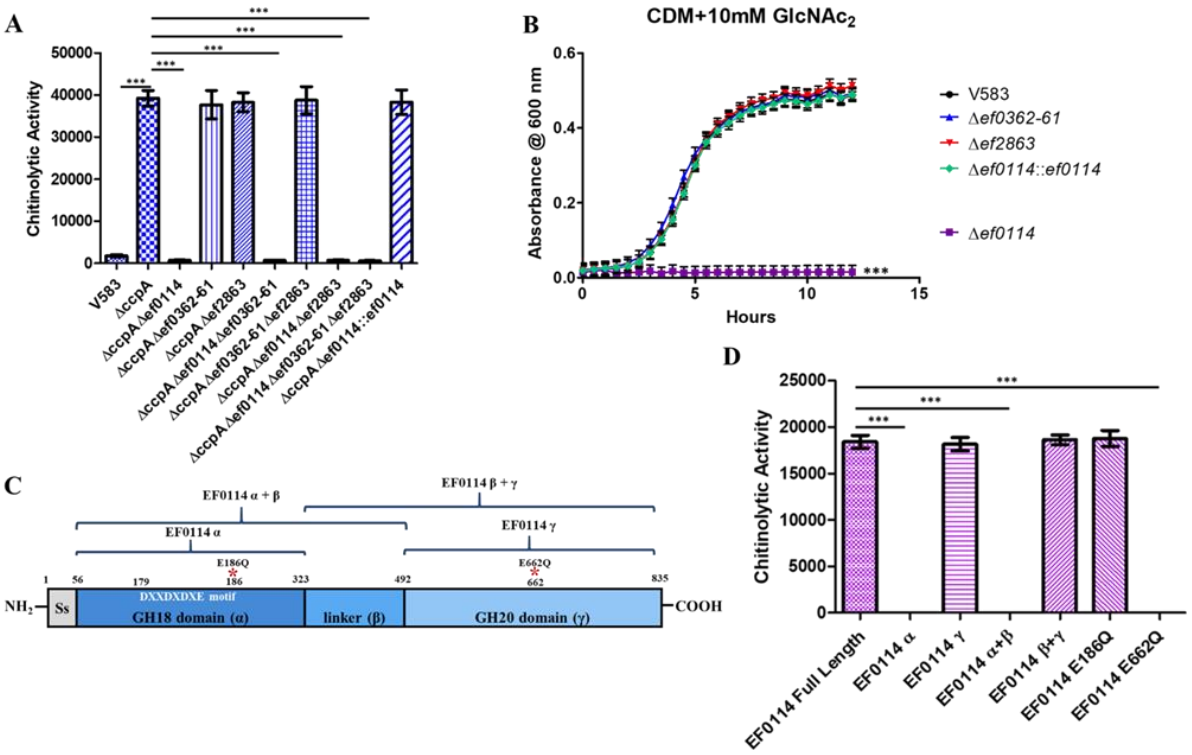

Figure 2: (A) Chitinolytic activity from culture supernatants were measured by determining the ability to hydrolyze the fluorogenic substrate 4MU-methylumbelliferyl-β-D-N-acetylglucosamine ($GlcNAc_2$ analogue). Chitinolytic activity is expressed as relative fluorescence emitted at 485 nm by the absorbance of the culture at OD_{600nm}. Each graph is the average of three biological replicates, with three technical replicates each time (n=9). The statistical significance was calculated using an unpaired t test, p value of <0.0001 is indicated as (***). (B) Growth of *E. faecalis* in CDM supplemented with 10mM chitobiose ($GlcNAc_2$). Each graph is the average of three biological replicates, with three technical replicates each time (n=9). The statistical significance was calculated using a two-way ANOVA test, p value of <0.0001 is indicated as (***). The growth curves are shown in black (V583), purple (Δ*ef0114*), blue (Δ*ef0362-61*), red (Δ*ef2863*), and green (Δ*ef0114*::*ef0114*). (C) Representation of EF0114 domain structure. The putative signal peptide sequence is located between amino acid residues 1 and 56. The GH18 catalytic domain, described as α, is located between amino acid residues 56-323, with the GH18 DXXDXDXE catalytic motif located between amino acid residues 179-186. The uncharacterized linker region is described as the β domain (amino acid residues 323-492). The GH20 domain (γ) is located between amino acid residues 492-835. Listed above the EF0114 domain schematic are representations of the various EF0114 recombinant domain variants used in figure 2D. (D) Chitinolytic activity of purified recombinant EF0114 variants against the fluorogenic substrate 4MU-methylumbelliferyl-β-D-N-acetylglucosamine ($GlcNAc_2$ analogue). Chitinolytic activity is expressed as the fluorescence emitted at 485nm. Each graph is the average of three biological replicates, with three technical replicates each time (n=9). The statistical significance was calculated using an unpaired t test, p value of <0.0001 is indicated as (***).

The GH20 domain of EF0114 is responsible for degrading β1,4-$GlcNAc_2$ into GlcNAc monomers

EF0114 possesses two catalytic domains, an N-terminal GH18 domain and a C-terminal GH20 domain (Figure 2C). The GH18 domain of EF0114 has been previously characterized for deglycosylating complex glycoproteins, such as IgG and lactoferrin, by hydrolyzing the Asn-attached chitobiose (β-1,4-$GlcNAc_2$) (34, 40). On the other hand, glycosyl hydrolases that possesses a GH20 catalytic domain are predicted to cleave either non-reducing β-1,4- or β-1,6-glycosidic bonds between two adjacent N-acetylglucosamine moieties (41-43). Because EF0114 possess both a GH18 and a GH20 catalytic domain, we assessed individual recombinant domain constructs as well as two site-directed mutants for their ability to cleave the fluorogenic β1,4-$GlcNAc_2$ analogue, 4MU-GlcNAc. The GH18 domain of EF0114 is referred as EF0114 α, whereas the GH20 domain is referred to as EF0114 γ (34) (Figure 2C). The central linker domain was termed EF0114 β, due to its secondary structure and therefore was evaluated to determine if it contributed to overall enzymatic activity (34) (Figure 2C). Enzymatic activity of recombinant EF0114 domains against the fluorogenic 4MU-GlcNAc substrate shows that protein constructs containing the GH20 catalytic domain (EF0114 γ or EF0114 β+γ) possess glycosidase activity against the β1,4-$GlcNAc_2$ analogue (Figure 2D). In contrast, EF0114 domain variants possessing the GH18 domain did not result in glycosidase activity against 4MU-GlcNAc (Figure 2D). Additionally, the replacement of a key glutamate residue involved in the proton transfer during hydrolysis within the GH20 domain of EF0114 to a glutamine (EF0114 E662Q) results in the elimination of glycosidase activity against the 4MU-GlcNAc substrate relative to native EF0114 (Figure 2D), highlighting the important role of the GH20 domain in the enzymatic activity to degrade $GlcNAc_2$ into GlcNAc monomers. In contrast, the replacement of a key enzymatic residue

in the GH18 domain (EF0114 E186Q) retained glycosidase activity towards the 4MU-GlcNAc substrate (Figure 2D).

Importation of GlcNAc is mediated through the Mpt PTS complex and EF1516

The uptake of N-acetylglucosamine has previously been studied in various Gram-positive bacteria, such as *Bacillus subtilis, Streptococcus mutans,* and *Streptococcus pneumoniae* (9, 10, 12, 44, 45). In *S. mutans* and *S. pneumoniae*, the glucose/mannose-specific EII permease (ManLMN) is capable of transporting a variety of carbohydrates, including glucose and mannose, but also has shown specificity for galactose, N-acetylglucosamine, and glucosamine (12, 44, 45), however NagP (PTS EIICB) has been shown to be the main transporter of N-acetylglucosamine in *B. subtilis* (9, 10). It was of interest to identify the homologs of both the ManLMN PTS system and NagP in *E. faecalis* V583. The MptBACD PTS system in *E. faecalis* shares extensive sequence similarity with ManLMN in *S. mutans* (12, 44) and has been characterized as the primary glucose transporter and sole mannose transporter in *E. faecalis* (35, 46). In *E. faecalis*, *ef1516* encodes a IICBA PTS system and shares approximately 41% amino acid sequence identity and 55% sequence similarity with NagE (PTS IICBA) from *Escherichia coli* (47). EF1516 also shares 41% sequence identity and 60% sequence similarity with NagP (EIICB) in *B. subtilis* (9, 10). The major difference between EF1516 and NagP from *B. subtilis* is the presence of a PTS EIIA domain in EF1516 that is absent from NagP.

To address whether the enterococcal Mpt PTS and/or EF1516 are responsible for the importation of N-acetylglucosamine, single in-frame deletions of the *mptBACD* operon and *ef1516*, as well as the Δ*mptBACD*Δ*ef1516* double deletion mutant were grown in CDM supplemented with N-acetylglucosamine (10mM) as the sole carbon source (Figure 3A). As shown in figure 3A, the deletion of either *mptBACD* or *ef1516* does not impede the overall growth relative to the parental

strain in CDM with N-acetylglucosamine as the principal carbon source. However, a double deletion mutant of *mptBACD* and *ef1516* results in a significant attenuation in growth relative to that of the parental or single transporter deletion mutants. Individual gene complements from the double deletion background (Δ*mptBACD*Δ*ef1516*::*mptBACD* and Δ*mptBACD*Δ*ef1516*::*ef1516*) fully restored growth demonstrating that either PTS system can functionally transport GlcNAc.

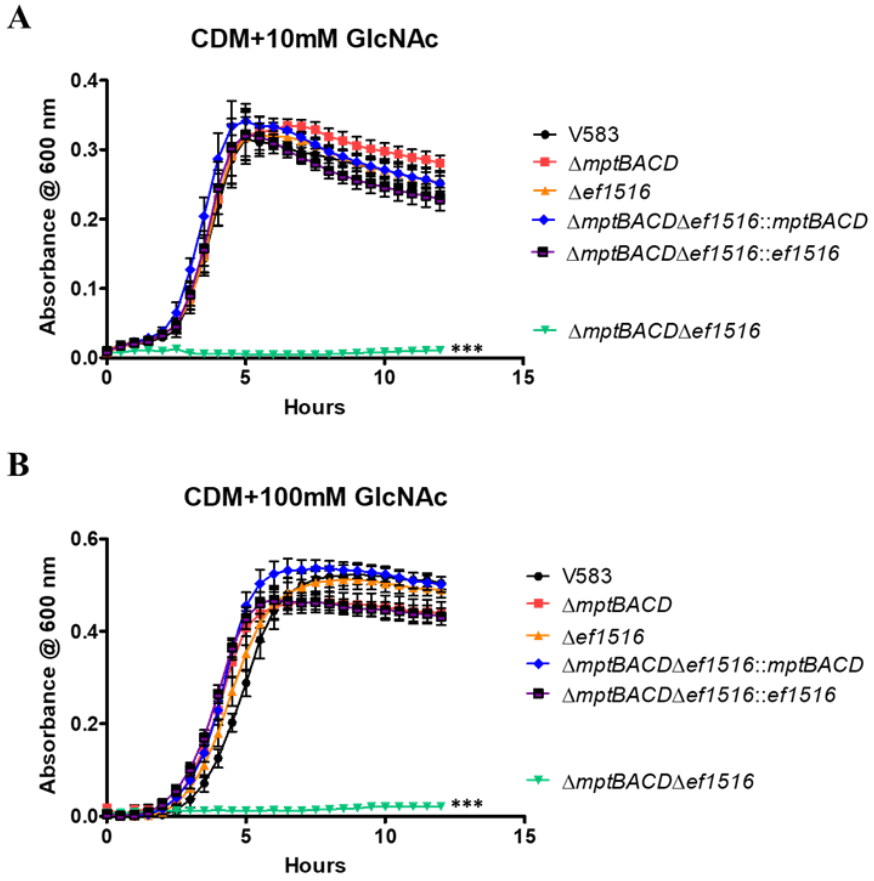

Figure 3: Growth of *E. faecalis* in CDM supplemented with (A) 10mM GlcNAc or (B) 100mM GlcNAc. Each graph is the average of three biological replicates, with three technical replicates each time (n=9). The statistical significance was calculated using a two-way ANOVA test, p value of <0.0001 is indicated as (***). The growth curves are shown in black (V583), red (Δ*mptBACD*), orange (Δ*ef1516*), green (Δ*mptBACD*Δ*ef1516*), blue (Δ*mptBACD*Δ*ef1516*::*mptBACD*), and purple (Δ*mptBACD*Δ*ef1516*::*ef1516*).

To ascertain that the poor growth of the Δ*mptBACD*Δ*ef1516* mutant cannot be rescued by increasing the concentration of N-acetylglucosamine, we also grew cells in CDM with 100mM GlcNAc. Figure 3B illustrates that increasing the concentration of N-acetylglucosamine does not

rescue the growth defect of the Δ*mptBACD*Δ*ef1516* mutant. Collectively, this indicates that *E. faecalis* is capable of importing N-acetylglucosamine via two separate PTS systems, the Mpt PTS complex and EF1516. Hereafter, EF1516 is referred to as NagE, based on the full-length sequence similarity with the *E. coli* NagE homolog.

The Mpt PTS system is the primary glucosamine (GlcN) transporter in *E. faecalis*

It was of interest to determine the transport machinery for the uptake of glucosamine (GlcN) in *E. faecalis*. Because the enterococcal NagE and Mpt PTS systems are responsible for importing N-acetylglucosamine into the bacterial cell, we hypothesized that they also play a role in the uptake of glucosamine. To assess this hypothesis, the Δ*mptBACD* mutant, the Δ*ef1516* mutant, and the Δ*mptBACD*Δ*ef1516* double mutant were grown in CDM supplemented with 10mM glucosamine. Figure 4A illustrates that the deletion of the *mptBACD* PTS operon eliminates growth with 10mM glucosamine as the sole carbon source relative to the growth of the parental strain and the *mptBACD* genetic revertant strain. There was no significant difference in growth between the Δ*ef1516* mutant relative to the parental strain in CDM with 10mM glucosamine (Figure 4A). In contrast to the growth assessment in 10mM GlcN, the growth defect of the *mptBACD* mutant is partially rescued by increasing the concentration of glucosamine to 100mM (Figure 4B), suggesting that an additional transporter contributes to GlcN uptake at high concentrations. This partial rescue is lost in the double deletion mutant of *mptBACD* and *ef1516* (*nagE*). Complementation of the double mutant with *nagE* partially restores growth to levels similar to that observed in the *mptBACD* mutant (Figure 4B). The growth defect associated with the double mutant (Δ*mptBACD*Δ*ef1516*) in CDM with 100mM GlcN is fully complementable with *mptBACD* as the Δ*mptBACD*Δ*ef1516*::*mptBACD* strain grew similarly to that of the parental strain. Collectively, these results indicate that although NagE has some specificity for importing

glucosamine at high concentrations, the Mpt PTS complex is the primary transport system for the uptake of glucosamine in *E. faecalis*.

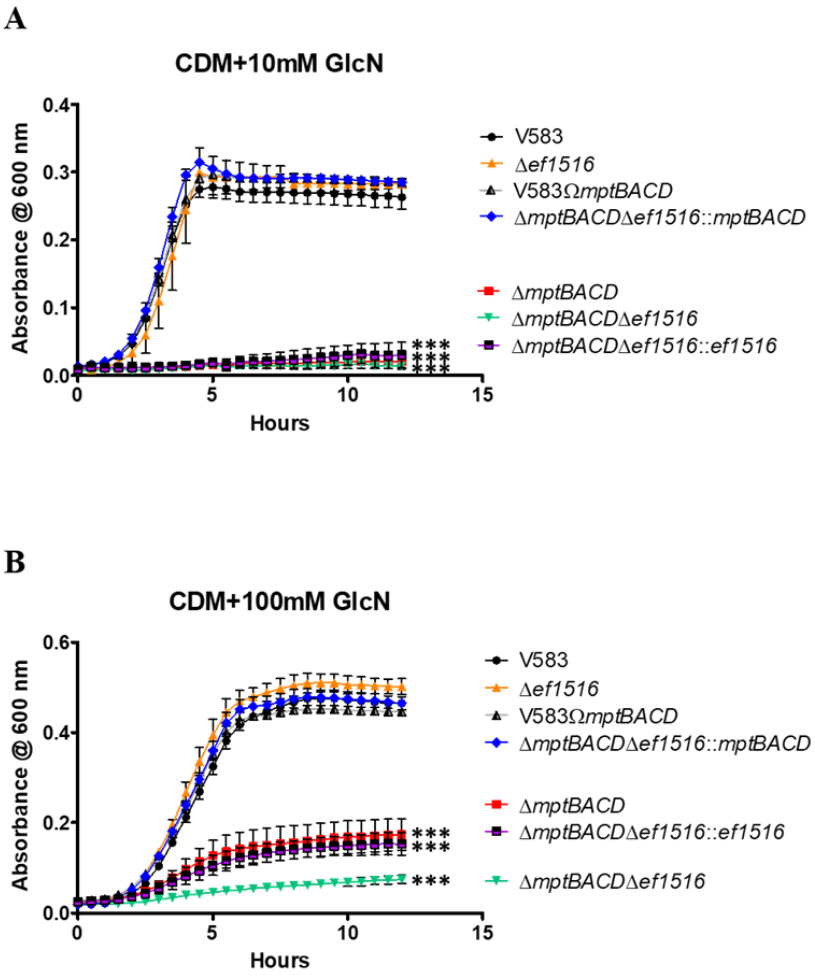

Figure 4: Growth of *E. faecalis* in CDM supplemented with (A) 10mM GlcN or (B) 100mM GlcN. Each graph is the average of three biological replicates, with three technical replicates each time (n=9). The statistical significance was calculated using a two-way ANOVA test, p value of <0.0001 is indicated as (***). The growth curves are shown in black (V583), red (Δ*mptBACD*), orange (Δ*ef1516*), green (Δ*mptBACD*Δ*ef1516*), gray (V583Ω*mptBACD* revertant), blue (Δ*mptBACD*Δ*ef1516*::*mptBACD*), and purple (Δ*mptBACD*Δ*ef1516*::*ef1516*).

Growth on N-acetylglucosamine is dependent on EF1317, an N-acetylglucosamine-6-phosphate deacetylase (NagA) homolog

After PTS-mediated importation of GlcNAc into the cell via either the Mpt PTS complex or NagE, deacetylation of the phosphorylated sugar (GlcNAc-6-P) would be required prior to the conversion

into fructose-6-phosphate (Fru-6-P). As observed in numerous bacteria, the enzyme responsible for deacetylating N-acetylglucosamine-6-phosphate is the N-acetylglucosamine-6-phosphate deacetylase (GlcNAc-6-P deacetylase), also referred to as NagA (7, 48-50). A predicted homolog of NagA in *E. faecalis* is encoded by *ef1317* and shares approximately 63% amino acid sequence identity and 77% sequence similarity with NagA in *S. pneumoniae* (7). We therefore constructed a deletion mutant of *ef1317* and assessed its growth in CDM supplemented with N-acetylglucosamine (10mM). Figure 5A shows that the deletion of *ef1317* eliminated the ability of *E. faecalis* to grow in CDM supplemented with 10mM GlcNAc, and that this phenotype is complementable, as the *ef1317* complement strain restored growth equivalent to that of the parental strain. The growth of the *ef1317* mutant can also be experimentally rescued by growing this mutant in CDM supplemented with glucosamine (Figure 5B).

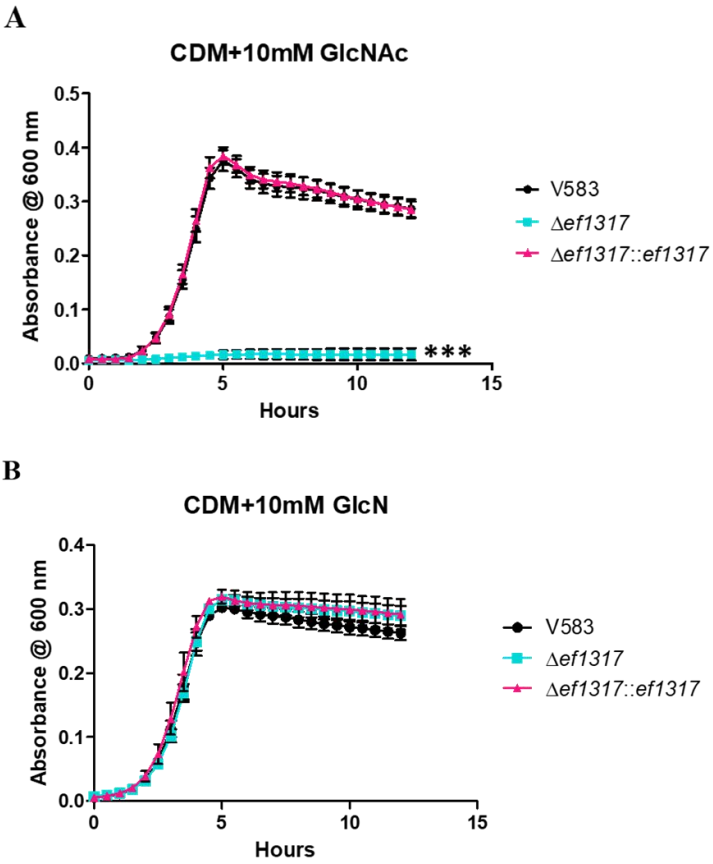

Figure 5: Growth of *E. faecalis* in CDM supplemented with (A) 10mM GlcNAc or (B) 10mM GlcN. Each graph is the average of three biological replicates, with six technical replicates each time (n=18). The statistical significance was calculated using a two-way ANOVA test, p value of <0.0001 is indicated as (***). The growth curves are shown in black (V583), aqua (Δ*ef1317*), and pink (Δ*ef1317*::*ef1317*).

Growth on glucosamine is dependent on the activity of EF0466, a glucosamine-6-phosphate deaminase (NagB) homolog

Following deacetylation of GlcNAc-6-P into GlcN-6-P, an additional reaction is required before the amino sugar is funneled into the glycolysis pathway. This reaction entails the conversion of GlcN-6-P to fructose-6-phosphate (Fru-6-P) by the glucosamine-6-phosphate deaminase (GlcN-6-P deaminase), referred to as NagB (7, 48, 51). The NagB homolog in *E. faecalis* was identified as EF0466, as it shares 60% amino acid sequence identity and 78% sequence similarity with NagB

of *S. pneumoniae* (7). When grown in CDM supplemented with glucosamine (10mM), the deletion of *ef0466* results in a significant decrease in growth relative to the parental and complement strains (Figure 6A). The growth defect associated with the *ef0466* mutant when grown in glucosamine can be restored by growing this mutant in CDM supplemented with fructose (Figure 6B), highlighting that pathways downstream of the glucosamine to fructose-6-phosphate remain undisturbed.

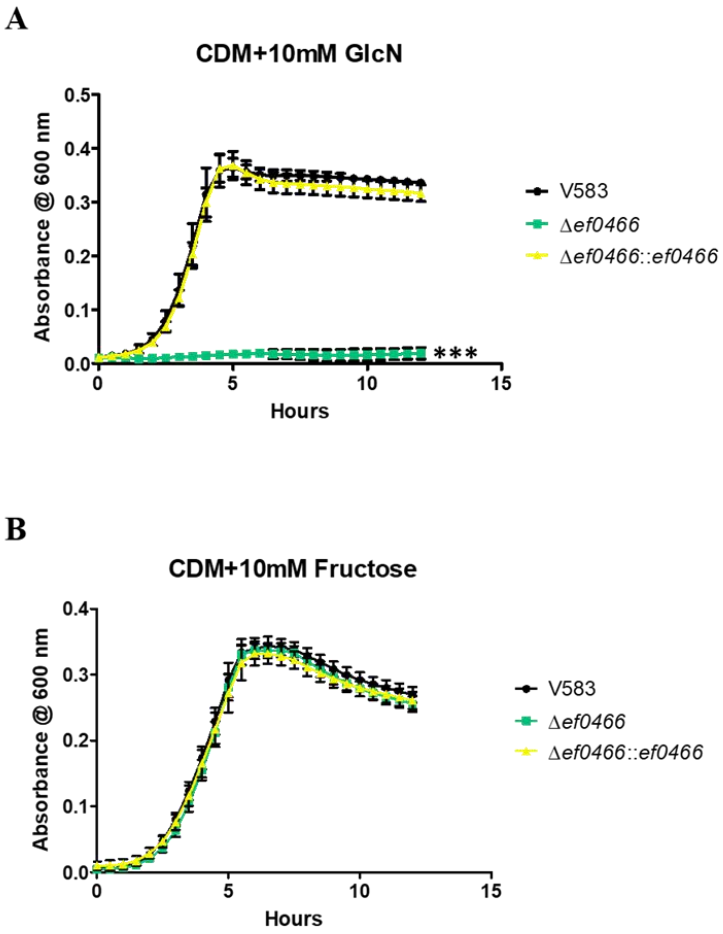

Figure 6: Growth of *E. faecalis* in CDM supplemented with (A) 10mM GlcN or (B) 10mM Fructose. Each graph is the average of three biological replicates, with six technical replicates each time (n=18). The statistical significance was calculated using a one-way ANOVA test, p value of <0.0001 is indicated as (***). The growth curves are shown in black (V583), green (Δ*ef0466*), and yellow (Δ*ef0466*::*ef0466*).

Discussion

The plethora of functionally encoded sugar transport systems in the *E. faecalis* genome emphasizes the importance of carbohydrate utilization and confers an advantage to survive in nutrient varying host environments. Although glucose is the preferred carbon source for bacteria, this carbohydrate is often present at concentrations that are growth limiting for most bacteria, including enterococci (52, 53). Extensive studies have been performed regarding the regulation of secondary nutrient acquisition systems that allow *E. faecalis* to survive in glucose-limiting environments (35, 54, 55). In Gram-positive bacteria, the transcriptional regulator CcpA plays a key role in regulating the expression of alternative nutrient acquisition systems via carbon catabolite repression (CCR) (35, 56, 57). Previously, the GH18 containing enterococcal glycosyl hydrolases (EF0114 (EndoE), EF0361 (EfChi18A), and EF2863 (EfEndo18A)) and the enterococcal chitin-binding protein/lytic polysaccharide monooxygenase (EF0362 (EfCBM33A)) were not only found to be significantly expressed in the absence of glucose and secreted (35), but also found to be negatively regulated by CcpA (34). Their enzymatic activity was also previously assessed and these studies revealed that they have enzymatic specificity towards the β1,4-linked N-acetylglucosamine glycosidic bond present in chitinous substrates (30) and glycoproteins (high-mannose and complex-type glycoproteins) (34, 39, 40), suggesting that they are involved in acquiring alternative carbon sources under glucose-limiting conditions. The genes encoding these enzymes have also been shown to be induced when *E. faecalis* is grown in blood or urine (54, 55), consistent with glucose-limited host environments.

Previous observations show that the enterococcal chitinase (EF0361; EfChi18A) is capable of degrading of poly-β1,4-linked GlcNAc substrates (i.e. chitin (poly-β1,4-GlcNAc), chitohexaose ($GlcNAc_6$), chitopentaose ($GlcNAc_5$), chitotetraose ($GlcNAc_4$), or chitotriose ($GlcNAc_3$) (30). However, in the presence of its cognate chitin binding protein/lytic polysaccharide

monooxygenase (EF0362; EfCBM33A), EfChi18A degrades chitin five-times more efficiently relative to chitin degradation by the chitinase alone (30). Therefore, EF0362-61 act synergistically to catalyze the degradation of poly-β1,4-linked GlcNAc substrates. The previous analyses were conducted with recombinant protein and not in the context of other enterococcal glycosyl hydrolases that have specificity towards the β-1,4-linked glycosidic bond between two adjoining N-acetylglucosamine moieties. Using genetic mutants of *ef0362-61* and the other GH18 containing glycosyl hydrolases present in the enterococcal genome (*ef0114* and *ef2863*), our analysis suggests that EF0362-61 and EF0114 are required for growth on poly-β-1,4-linked GlcNAc substrates. It is noteworthy that Vaaje-Kolstad et al. found that EF0362-61 can only synergistically degrade poly-β-1,4-GlcNAc substrates into dimers of β-1,4-linked N-acetylglucosamine, indicating that an additional enzyme(s) is required for fully degrading these poly-β-1,4-GlcNAc substrates into monomers of N-acetylglucosamine prior to uptake into the bacterial cell. Since EF0114 and EF2863 target β1,4-linked GlcNAc (34, 38, 39), these glycosidases are good candidates for hydrolyzing extracellular $GlcNAc_2$ into GlcNAc prior to importation into the bacterial cell. Based on our analysis using both genetic mutants and purified recombinant protein, this study revealed that the GH20 catalytic domain of EF0114 is responsible for cleaving the β1,4-linked glycosidic bond of extracellular chitobiose (β1,4-linked $GlcNAc_2$). To our knowledge, this would be the first instance in which a precise enzymatic function has been determined for the GH20 catalytic domain of EF0114. Collectively, these observations indicate that the degradation of extracellular poly-β1,4-linked GlcNAc containing substrates is dependent on the enzymatic activity of CcpA-regulated enzymes, EF0362-61 and EF0114.

Recent evidence indicates that chitinases and CBPs secreted by bacterial pathogens, such as *Listeria monocytogenes* (25, 26) and *Legionella pneumophila* (27), serve as virulence factors during infection of mammalian hosts (23, 24). Although chitin is not naturally present in

mammalian hosts, the biological role of bacterial chitinases during infection suggests that additional substrates for chitinases likely exist in mammalian hosts. Recent observations indicate that chitinases produced by *Salmonella* and *Listeria* also have specificity towards LacNac (Galβ1–4GlcNAc) and LacdiNAc (GalNAcβ1–4GlcNAc) sugar linkages present in mammalian N and O-linked glycans, glycolipids and glycosaminoglycans (24, 28). These LacNAc and LacdiNAc containing substrates present in a mammalian host are likely an additional substrate for bacterial chitinases and chitinolytic cleavage of these substrates may contribute to bacterial pathogenesis in a host. *L. monocytogenes* produces two chitinases annotated as ChiA and ChiB. Chaudhuri et al. observed that the deletion of *chiB* resulted in an approximate 8-fold and 14-fold decrease in bacterial burden in the liver and spleen of infected mice (25). However, the *chiA* deletion mutant exhibited a more dramatic virulence defect as bacterial recovery from the liver and spleen of infected mice were reduced 19-fold and 45-fold, respectively (25). Using NCBI BLAST, the ChiA chitinase of *L. monocytogenes* shares approximately 65% sequence identity and 77% sequence similarity with EF0361 (EfChi18A) produced by *E. faecalis*. In contrast, there is no apparent enterococcal homolog of the listerial ChiB chitinase or the chitinase produced by *L. pneumophila*. Determining a functional role for EF0362-61 in the context of mammalian infection by *E. faecalis* will be a component of ongoing studies.

Although evidence indicates that *E. faecalis* can utilize N-acetylglucosamine and glucosamine as a carbon source (6), little is known of the uptake machinery and cytosolic enzymes required for the importation and metabolism of these amino sugars. The uptake of N-acetylglucosamine has previously been studied in various Gram-positive bacteria, such as *Bacillus subtilis* (9, 10), *Streptococcus mutans* (12, 44), and *Streptococcus pneumoniae* (45). In *S. mutans* and *S. pneumoniae*, the glucose/mannose-specific EII permease (ManLMN) is capable of transporting a variety of carbohydrates, including glucose and mannose, but also has shown specificity for

galactose, N-acetylglucosamine, and glucosamine (12, 44, 45), however NagP (PTS EIICB) has been shown to be the main transporter of N-acetylglucosamine in *B. subtilis* (9, 10). Our study indicates that *E. faecalis* encodes two PTS systems that are involved in the uptake of N-acetylglucosamine, as single deletions of either the *mpt* PTS operon or *ef1516* did not display a significant change in growth; however, deletion of *ef1516* in the *mptBACD* mutant background resulted in complete attenuation of growth in CDM with either 10mM or 100mM N-acetylglucosamine. With respect to glucosamine uptake, the Mpt PTS system is the primary transporter for importing glucosamine into the cell, as the deletion of *mptBACD* resulted in an attenuation in growth with 10mM glucosamine as the sole carbon source. However, the PTS system encoded by *nagE* (*ef1516*) does have a low affinity towards importing glucosamine into the cell, as increasing the concentration of glucosamine to 100mM partially rescued the growth of the *mptBACD* mutant and growth of the Δ*mptBACD*Δ*ef1516* double mutant was significantly impaired relative to that of the Δ*mptBACD* mutant alone.

The functional redundancy of two GlcNAc/GlcN transporters in *E. faecalis* may be attributed to the fact that components of the Mpt PTS complex are known cellular receptors for class IIa and IIc bacteriocins (58). In complex human ecologies such as the oral cavity and gastrointestinal tract, *E. faecalis* is likely exposed to such bacteriocins that may inactivate sugar transport through the Mpt system (59) and therefore limit its metabolic capacity. The Mpt PTS system is the principal glucose transporter and the sole mannose transporter in *E. faecalis* (35); additionally here we have shown it to be the primary transporter of glucosamine and a major contributor to GlcNAc uptake. The ability of *E. faecalis* to take advantage of a dysbiotic intestinal microflora may stem from the ability to efficiently transport multiple key host sugars via the Mpt PTS system. The presence of a complex intestinal microflora is known to limit the growth of *E. faecalis* (33, 60), and highlights that maintaining this competitive microflora is a key aspect of disease prevention.

Furthermore, we have recently shown that the alternative sigma factor, RpoN, is required for *mptBACD* expression and significantly contributes to infection outcome in both endocarditis and urinary tract infection models (35), highlighting an important role for sugar metabolism during infection.

For catabolic processing of GlcNAc, the enzymatic function of NagA (N-acetylglucosamine-6-phosphate deacetylase), followed by the activity of NagB (glucosamine-6-phosphate deaminase) is required to metabolize GlcNAc via glycolysis (7, 48-51). Our study shows that EF1317 (NagA) and EF0466 (NagB) are essential for *E. faecalis* to utilize N-acetylglucosamine as a carbon source. A review on enterococcal physiology and metabolism (61) identified two potential NagA homologs in the *E. faecalis* genome, encoded by *ef1317* and *ef3044*, but our analysis provides direct evidence that EF1317 serves the primary activity of deacetylating GlcNAc.

N-acetylglucosamine has a dual purpose in bacterial catabolism. When supplied exogenously the catabolism of N-acetylglucosamine or glucosamine by NagB generates fructose-6-phosphate to provide a valuable source of energy to the cell and ammonia is liberated to assist with cellular nitrogen needs (51). N-acetylglucosamine is also an essential component of bacterial peptidoglycan (13, 62). Throughout the bacterial growth cycle, peptidoglycan is continuously made and degraded to accommodate cell growth and division into daughter cells (13, 62, 63). The involvement of GlcNAc for both metabolism and peptidoglycan synthesis requires regulatory circuit(s) for this dual utilization, and in related Gram-positive bacteria, such as *B. subtilis* and *S. mutans*, this regulatory control is governed by NagR (64). NagR belongs to the GntR family of transcriptional regulators and directly regulates the expression of *nagA*, *nagB*, and *glmS* in *S. mutans* (65). However, in *B. subiltis*, the expression of colocalized *nagAB* is regulated by NagR, while the regulation of *glmS* expression is independent of NagR (48). In both *S. mutans* and *B. subtilis*, NagR is encoded distantly from *nagA*, *nagB*, or *glmS*. Currently, there are 11 annotated

GntR regulators in the *E. faecalis* V583 genome with similar sequence identity and similarity to NagR in *S. mutans*, none of which are in close proximity to *ef1317* (*nagA*) or *ef0466* (*nagB*). Elucidating which GntR homolog is responsible for regulating the expression of *nagA* and *nagB* in *E. faecalis* will require further assessment and will be an area of future research interest.

We present here a model of the metabolic pathway by which *E. faecalis* utilizes poly-β1,4-linked N-acetylglucosamine as a carbon source (Figure 7). Extracellular polymers of β1,4-linked GlcNAc are hydrolyzed into β1,4-linked GlcNAc dimers by the combined activity of the chitin-binding protein, EF0362 (EfCBM33A), and the chitinase, EF0361 (EfChi18A). Subsequently, the GH20 catalytic domain of EF0114 (EndoE) is responsible for degrading β-1,4 linked $GlcNAc_2$ into monomers of N-acetylglucosamine. The monomeric form of this amino sugar can be imported into the bacterial cell and simultaneously phosphorylated via either the Mpt PTS complex or NagE (EF1516). Once inside the bacterial cell, prior to downstream glycolytic processing, phosphorylated GlcNAc (GlcNAc-6-P) is deacetylated by NagA (EF1317), followed by deamination by NagB (EF0466) converting glucosamine-6-P into fructose-6-P and ammonia. It is noteworthy that as a result of catabolizing GlcNAc or GlcN, ammonia is generated and can be utilized in amino acid synthesis or other essential components (12). The accumulation of cytosolic ammonia can increase the difference in pH inside relative to outside the cell (i.e. ΔpH) and therefore contributes to acid tolerance (12).

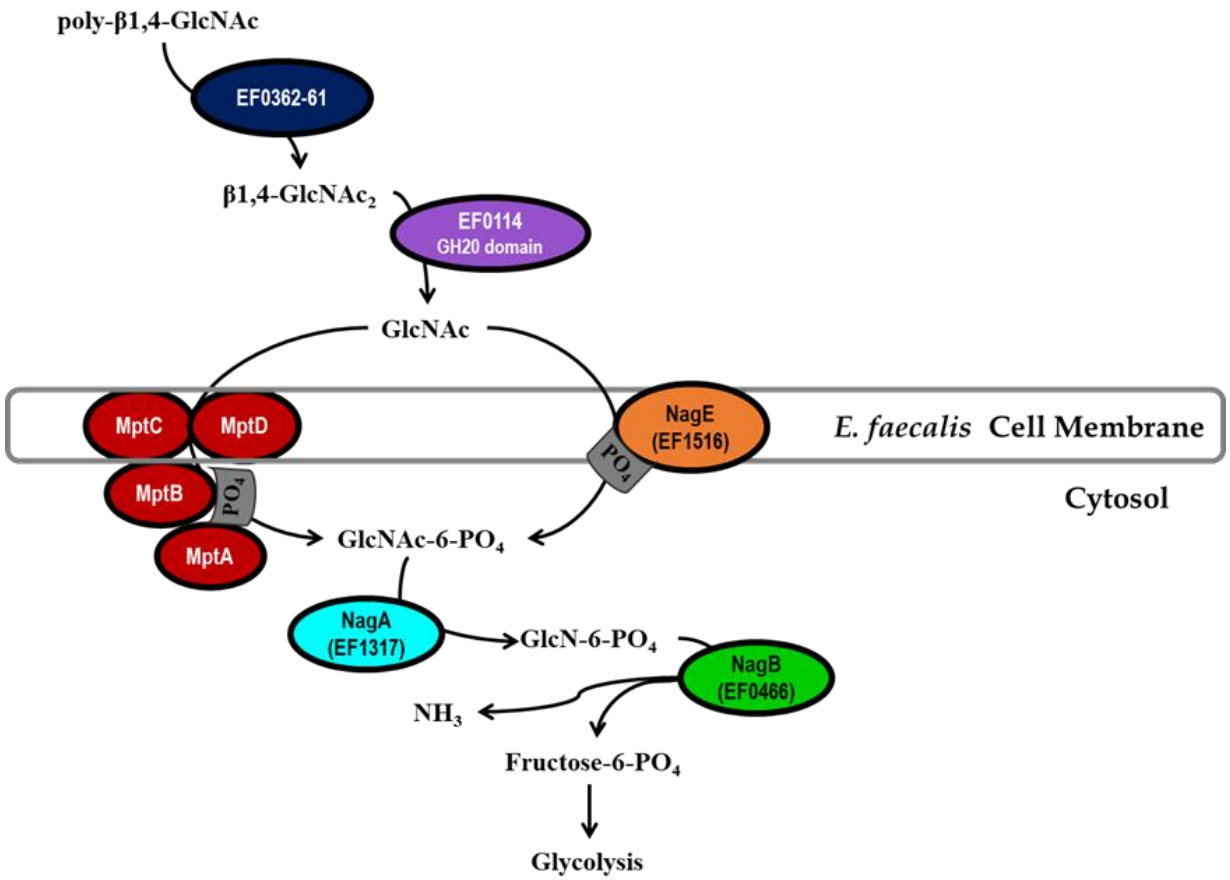

Figure 7: Model for poly-β1,4-GlcNAc degradation and GlcNAc uptake and metabolism in *Enterococcus faecalis*

Extracellular poly-β1,4-N-acetylglucosamine substrates (β1,4-GlcNAc$_{3-n}$) are hydrolyzed by EF0362-61 into dimers of β1,4-N-acetylglucosamine (β1,4-GlcNAc$_2$), followed by hydrolysis into monomeric GlcNAc by the GH20 catalytic domain of EF0114. N-acetylglucosamine is transported into the cell and simultaneously phosphorylated upon uptake by two PTS systems, the Mpt PTS complex (MptBACD) and EF1516 (NagE). For the phosphorylated amino sugar to be metabolized via glycolysis, it first requires deacetylation by EF1317 (NagA), followed by conversion into fructose-6-PO$_4$ by EF0466 (NagB) with ammonia generation (NH$_3$).

Although our study identified the chitinolytic machinery, the GlcNAc and GlcN-specific uptake systems, and cytosolic enzymes that are required for enterococcal metabolism of β-1,4 linked N-acetylglucosamine substrates, how they contribute to overall enterococcal pathogenesis will be an area of future research interest.

References

1. Lebreton F, Willems RJL, Gilmore MS. 2014. Enterococcus Diversity, Origins in Nature, and Gut Colonization. *In* Gilmore MS, Clewell DB, Ike Y, Shankar N (ed), Enterococci: From Commensals to Leading Causes of Drug Resistant Infection, Boston.
2. Garcia-Solache M, Rice LB. 2019. The Enterococcus: a Model of Adaptability to Its Environment. Clin Microbiol Rev 32.
3. Van Tyne D, Gilmore MS. 2014. Friend turned foe: evolution of enterococcal virulence and antibiotic resistance. Annu Rev Microbiol 68:337-56.
4. Weiner-Lastinger LM, Abner S, Edwards JR, Kallen AJ, Karlsson M, Magill SS, Pollock D, See I, Soe MM, Walters MS, Dudeck MA. 2020. Antimicrobial-resistant pathogens associated with adult healthcare-associated infections: Summary of data reported to the National Healthcare Safety Network, 2015-2017. Infect Control Hosp Epidemiol 41:1-18.
5. Fiore E, Van Tyne D, Gilmore MS. 2019. Pathogenicity of Enterococci. Microbiol Spectr 7.
6. Lebreton F, Manson AL, Saavedra JT, Straub TJ, Earl AM, Gilmore MS. 2017. Tracing the Enterococci from Paleozoic Origins to the Hospital. Cell 169:849-861 e13.
7. Afzal M, Shafeeq S, Manzoor I, Henriques-Normark B, Kuipers OP. 2016. N-acetylglucosamine-Mediated Expression of nagA and nagB in Streptococcus pneumoniae. Front Cell Infect Microbiol 6:158.
8. Dobrogosz WJ. 1968. Effect of amino sugars on catabolite repression in Escherichia coli. J Bacteriol 95:578-84.
9. Gaugue I, Oberto J, Plumbridge J. 2014. Regulation of amino sugar utilization in Bacillus subtilis by the GntR family regulators, NagR and GamR. Mol Microbiol 92:100-15.
10. Gaugue I, Oberto J, Putzer H, Plumbridge J. 2013. The use of amino sugars by Bacillus subtilis: presence of a unique operon for the catabolism of glucosamine. PLoS One 8:e63025.
11. Mobley HL, Doyle RJ, Streips UN, Langemeier SO. 1982. Transport and incorporation of N-acetyl-D-glucosamine in Bacillus subtilis. J Bacteriol 150:8-15.
12. Moye ZD, Burne RA, Zeng L. 2014. Uptake and metabolism of N-acetylglucosamine and glucosamine by Streptococcus mutans. Appl Environ Microbiol 80:5053-67.
13. Park JT, Uehara T. 2008. How bacteria consume their own exoskeletons (turnover and recycling of cell wall peptidoglycan). Microbiol Mol Biol Rev 72:211-27, table of contents.
14. Wheeler R, Chevalier G, Eberl G, Gomperts Boneca I. 2014. The biology of bacterial peptidoglycans and their impact on host immunity and physiology. Cell Microbiol 16:1014-23.
15. Garcia-Rubio R, de Oliveira HC, Rivera J, Trevijano-Contador N. 2019. The Fungal Cell Wall: Candida, Cryptococcus, and Aspergillus Species. Front Microbiol 10:2993.
16. Liu X, Zhang J, Zhu KY. 2019. Chitin in Arthropods: Biosynthesis, Modification, and Metabolism. Adv Exp Med Biol 1142:169-207.
17. Chen JK, Shen CR, Liu CL. 2010. N-acetylglucosamine: production and applications. Mar Drugs 8:2493-516.
18. Liao C, Rigali S, Cassani CL, Marcellin E, Nielsen LK, Ye BC. 2014. Control of chitin and N-acetylglucosamine utilization in Saccharopolyspora erythraea. Microbiology (Reading) 160:1914-1928.
19. Ismail SA, El-Sayed HS, Fayed B. 2020. Production of prebiotic chitooligosaccharide and its nano/microencapsulation for the production of functional yoghurt. Carbohydr Polym 234:115941.
20. van Huis A. 2020. Nutrition and health of edible insects. Curr Opin Clin Nutr Metab Care 23:228-231.
21. Verkhnyatskaya S, Ferrari M, de Vos P, Walvoort MTC. 2019. Shaping the Infant Microbiome With Non-digestible Carbohydrates. Front Microbiol 10:343.
22. Forsberg Z, Sørlie M, Petrović D, Courtade G, Aachmann FL, Vaaje-Kolstad G, Bissaro B, Røhr Å K, Eijsink VG. 2019. Polysaccharide degradation by lytic polysaccharide monooxygenases. Curr Opin Struct Biol 59:54-64.

23. Bhattacharya D, Nagpure A, Gupta RK. 2007. Bacterial chitinases: properties and potential. Crit Rev Biotechnol 27:21-8.
24. Frederiksen RF, Paspaliari DK, Larsen T, Storgaard BG, Larsen MH, Ingmer H, Palcic MM, Leisner JJ. 2013. Bacterial chitinases and chitin-binding proteins as virulence factors. Microbiology (Reading) 159:833-847.
25. Chaudhuri S, Bruno JC, Alonzo F, 3rd, Xayarath B, Cianciotto NP, Freitag NE. 2010. Contribution of chitinases to Listeria monocytogenes pathogenesis. Appl Environ Microbiol 76:7302-5.
26. Larsen MH, Leisner JJ, Ingmer H. 2010. The chitinolytic activity of Listeria monocytogenes EGD is regulated by carbohydrates but also by the virulence regulator PrfA. Appl Environ Microbiol 76:6470-6.
27. DebRoy S, Dao J, Soderberg M, Rossier O, Cianciotto NP. 2006. Legionella pneumophila type II secretome reveals unique exoproteins and a chitinase that promotes bacterial persistence in the lung. Proc Natl Acad Sci U S A 103:19146-51.
28. Frederiksen RF, Yoshimura Y, Storgaard BG, Paspaliari DK, Petersen BO, Chen K, Larsen T, Duus J, Ingmer H, Bovin NV, Westerlind U, Blixt O, Palcic MM, Leisner JJ. 2015. A diverse range of bacterial and eukaryotic chitinases hydrolyzes the LacNAc (Galβ1-4GlcNAc) and LacdiNAc (GalNAcβ1-4GlcNAc) motifs found on vertebrate and insect cells. J Biol Chem 290:5354-66.
29. Leisner JJ, Larsen MH, Ingmer H, Petersen BO, Duus JO, Palcic MM. 2009. Cloning and comparison of phylogenetically related chitinases from Listeria monocytogenes EGD and Enterococcus faecalis V583. J Appl Microbiol 107:2080-7.
30. Vaaje-Kolstad G, Bohle LA, Gaseidnes S, Dalhus B, Bjoras M, Mathiesen G, Eijsink VG. 2012. Characterization of the chitinolytic machinery of Enterococcus faecalis V583 and high-resolution structure of its oxidative CBM33 enzyme. J Mol Biol 416:239-54.
31. Thurlow LR, Thomas VC, Fleming SD, Hancock LE. 2009. *Enterococcus faecalis* capsular polysaccharide serotypes C and D and their contributions to host innate immune evasion. Infection and Immunity 77.
32. Flannagan SE, Clewell DB. 2002. Identification and characterization of genes encoding sex pheromone cAM373 activity in Enterococcus faecalis and Staphylococcus aureus. Mol Microbiol 44:803-17.
33. Gilmore MS, Rauch M, Ramsey MM, Himes PR, Varahan S, Manson JM, Lebreton F, Hancock LE. 2015. Pheromone killing of multidrug-resistant Enterococcus faecalis V583 by native commensal strains. Proc Natl Acad Sci U S A 112:7273-8.
34. Keffeler EC, Iyer VS, Henderson AJ, Huck IL, Schwarting N, Cortez A, Hancock LE. 2021. Activity of CcpA-regulated GH18 family glycosyl hydrolases that contribute to nutrient acquisition and fitness in Enterococcus faecalis Infection and Immunity (*in press*).
35. Keffeler EC, Iyer VS, Parthasarathy S, Ramsey MM, Gorman MJ, Barke TL, Varahan S, Olson S, Gilmore MS, Abdullahi ZH, Hancock EN, Hancock LE. 2021. Influence of the Alternative Sigma Factor RpoN on Global Gene Expression and Carbon Catabolism in Enterococcus faecalis V583. mBio 12.
36. Brown SA, Whiteley M. 2007. A novel exclusion mechanism for carbon resource partitioning in Aggregatibacter actinomycetemcomitans. J Bacteriol 189:6407-14.
37. Socransky SS, Dzink JL, Smith CM. 1985. Chemically defined medium for oral microorganisms. J Clin Microbiol 22:303-5.
38. Bohle LA, Mathiesen G, Vaaje-Kolstad G, Eijsink VG. 2011. An endo-beta-N-acetylglucosaminidase from Enterococcus faecalis V583 responsible for the hydrolysis of high-mannose and hybrid-type N-linked glycans. FEMS Microbiol Lett 325:123-9.
39. Collin M, Fischetti VA. 2004. A novel secreted endoglycosidase from Enterococcus faecalis with activity on human immunoglobulin G and ribonuclease B. J Biol Chem 279:22558-70.
40. Garbe J, Sjogren J, Cosgrave EF, Struwe WB, Bober M, Olin AI, Rudd PM, Collin M. 2014. EndoE from Enterococcus faecalis hydrolyzes the glycans of the biofilm inhibiting protein lactoferrin and mediates growth. PLoS One 9:e91035.

41. Jiang YL, Yu WL, Zhang JW, Frolet C, Di Guilmi AM, Zhou CZ, Vernet T, Chen Y. 2011. Structural basis for the substrate specificity of a novel beta-N-acetylhexosaminidase StrH protein from Streptococcus pneumoniae R6. J Biol Chem 286:43004-12.
42. Ramasubbu N, Thomas LM, Ragunath C, Kaplan JB. 2005. Structural analysis of dispersin B, a biofilm-releasing glycoside hydrolase from the periodontopathogen Actinobacillus actinomycetemcomitans. J Mol Biol 349:475-86.
43. Val-Cid C, Biarnes X, Faijes M, Planas A. 2015. Structural-Functional Analysis Reveals a Specific Domain Organization in Family GH20 Hexosaminidases. PLoS One 10:e0128075.
44. Abranches J, Chen YY, Burne RA. 2003. Characterization of Streptococcus mutans strains deficient in EIIAB Man of the sugar phosphotransferase system. Appl Environ Microbiol 69:4760-9.
45. Bidossi A, Mulas L, Decorosi F, Colomba L, Ricci S, Pozzi G, Deutscher J, Viti C, Oggioni MR. 2012. A functional genomics approach to establish the complement of carbohydrate transporters in Streptococcus pneumoniae. PLoS One 7:e33320.
46. Opsata M, Nes IF, Holo H. 2010. Class IIa bacteriocin resistance in Enterococcus faecalis V583: the mannose PTS operon mediates global transcriptional responses. BMC Microbiol 10:224.
47. Rogers MJ, Ohgi T, Plumbridge J, Söll D. 1988. Nucleotide sequences of the Escherichia coli nagE and nagB genes: the structural genes for the N-acetylglucosamine transport protein of the bacterial phosphoenolpyruvate: sugar phosphotransferase system and for glucosamine-6-phosphate deaminase. Gene 62:197-207.
48. Bertram R, Rigali S, Wood N, Lulko AT, Kuipers OP, Titgemeyer F. 2011. Regulon of the N-acetylglucosamine utilization regulator NagR in Bacillus subtilis. J Bacteriol 193:3525-36.
49. Kanehisa M, Goto S, Sato Y, Kawashima M, Furumichi M, Tanabe M. 2014. Data, information, knowledge and principle: back to metabolism in KEGG. Nucleic Acids Res 42:D199-205.
50. Vincent F, Yates D, Garman E, Davies GJ, Brannigan JA. 2004. The three-dimensional structure of the N-acetylglucosamine-6-phosphate deacetylase, NagA, from Bacillus subtilis: a member of the urease superfamily. J Biol Chem 279:2809-16.
51. Vincent F, Davies GJ, Brannigan JA. 2005. Structure and kinetics of a monomeric glucosamine 6-phosphate deaminase: missing link of the NagB superfamily? J Biol Chem 280:19649-55.
52. Shepard BD, Gilmore MS. 2002. Differential expression of virulence-related genes in Enterococcus faecalis in response to biological cues in serum and urine. Infect Immun 70:4344-52.
53. Wright EM, Hirayama BA, Loo DF. 2007. Active sugar transport in health and disease. J Intern Med 261:32-43.
54. Vebo HC, Snipen L, Nes IF, Brede DA. 2009. The transcriptome of the nosocomial pathogen Enterococcus faecalis V583 reveals adaptive responses to growth in blood. PLoS One 4:e7660.
55. Vebo HC, Solheim M, Snipen L, Nes IF, Brede DA. 2010. Comparative genomic analysis of pathogenic and probiotic Enterococcus faecalis isolates, and their transcriptional responses to growth in human urine. PLoS One 5:e12489.
56. Fujita Y. 2009. Carbon catabolite control of the metabolic network in Bacillus subtilis. Biosci Biotechnol Biochem 73:245-59.
57. Warner JB, Lolkema JS. 2003. CcpA-dependent carbon catabolite repression in bacteria. Microbiol Mol Biol Rev 67:475-90.
58. Miwa Y, Nakata A, Ogiwara A, Yamamoto M, Fujita Y. 2000. Evaluation and characterization of catabolite-responsive elements (cre) of Bacillus subtilis. Nucleic Acids Res 28:1206-10.
59. Sedgley CM, Clewell DB, Flannagan SE. 2009. Plasmid pAMS1-encoded, bacteriocin-related "Siblicide" in Enterococcus faecalis. J Bacteriol 191:3183-8.
60. Ubeda C, Taur Y, Jenq RR, Equinda MJ, Son T, Samstein M, Viale A, Socci ND, van den Brink MR, Kamboj M, Pamer EG. 2010. Vancomycin-resistant Enterococcus domination of intestinal microbiota is enabled by antibiotic treatment in mice and precedes bloodstream invasion in humans. J Clin Invest 120:4332-41.

61. Ramsey M, Hartke A, Huycke M. 2014. The Physiology and Metabolism of Enterococci. *In* Gilmore MS, Clewell DB, Ike Y, Shankar N (ed), Enterococci: From Commensals to Leading Causes of Drug Resistant Infection, Boston.
62. Plumbridge J. 2015. Regulation of the Utilization of Amino Sugars by Escherichia coli and Bacillus subtilis: Same Genes, Different Control. J Mol Microbiol Biotechnol 25:154-67.
63. Reith J, Mayer C. 2011. Peptidoglycan turnover and recycling in Gram-positive bacteria. Appl Microbiol Biotechnol 92:1-11.
64. Kawada-Matsuo M, Oogai Y, Komatsuzawa H. 2016. Sugar Allocation to Metabolic Pathways is Tightly Regulated and Affects the Virulence of Streptococcus mutans. Genes (Basel) 8.
65. Zeng L, Burne RA. 2015. NagR Differentially Regulates the Expression of the glmS and nagAB Genes Required for Amino Sugar Metabolism by Streptococcus mutans. J Bacteriol 197:3533-44.

Chapter 5: Concluding Remarks and Future Directions

Enterococcus faecalis is among the most prevalent bacteria found in mammalian gastrointestinal (GI) tracts, colonizing 60-80% of infants within the first week of life and 80% of adults (1, 2). *E. faecalis* is also a member of the human oral cavity, colonizing approximately 20% of healthy individuals (3). The beneficial effects of *E. faecalis* as a commensal include, modulating the host immune responses, preventing intestinal epithelial barrier leakage, and preventing the colonization and invasion of intestinal pathogens (4, 5). Specifically, native commensal strains of *E. faecalis* produce a bacteriocin capable of killing pathogenic *E. faecalis* V583 (6), therefore competing for the biological niche and preventing colonization of pathogenic *E. faecalis* V583.

Despite its beneficial roles in the GI tracts of the host, *E. faecalis* can transition into an opportunistic pathogen, often as a consequence of antibiotic treatment (7). Overgrowth in the intestinal tract can lead to subsequent translocation to other host anatomic sites and is often associated with diseases such as peritonitis, ulcerative colitis, and Crohn's disease (8-10). All of the studies reported in this dissertation were conducted using the pathogenic *E. faecalis* V583 strain. The *E. faecalis* V583 strain was originally isolated in 1989 from patients at the Barnes Hospital located in St. Louis, Missouri (11). V583 possesses a plethora of horizontally-acquired genetic elements, which accounts for approximately 25% of the entire V583 genetic content (12). These horizontally-acquired genetic elements include the capsular polysaccharide locus that limits opsonization (13, 14), an adhesin, referred to as Ace, that is involved in adherence to host collagen (15), a pathogenicity island that spans gene loci *ef0479-ef0648* (16), an endocarditis and biofilm-associated pili (17), 38 insertion sequence (IS) elements (12), and seven prophage elements (18). Additionally, V583 possesses three pathogenic plasmids: pTEF1, pTEF2, and pTEF3 (19).

E. faecalis can also rapidly fine-tune its metabolism in response to new environments, thus enhancing its survival under nutrient-varying conditions. This concept of alternative carbon

metabolism is the unifying theme of this dissertation. The alternative sigma factor 54 (RpoN) has previously been shown to regulate a variety of cellular processes, including PTS-mediated sugar uptake in both Gram-negative and Gram-positive bacteria (20). Therefore, RpoN-dependent sugar uptake is one regulatory mechanism certain bacteria can employ to modulate carbon metabolism in response to nutrient-varying environments. In the *E. faecalis* genome, binding sites for RpoN have previously been identified upstream of genes predicted to encode sugar PTS systems (Mpt, Mpo, Lpo, Lpt, Mph, and Xpo). Each PTS system is thought to be regulated by a bacterial enhancer binding protein (bEBP). bEBPs are required to elicit open complex formation upon association with RpoN and target DNA and do so in response to a specific environmental signal. bEBPs typically consist of three domains: a DNA-binding domain, an AAA+ ATPase/transcriptional activation domain, and a regulatory domain (21-23). The regulatory domain is responsive to cellular signals and has been shown to function as response-regulator domains of (a) two-component systems, (b) ligand-binding domains, or (c) phosphotransferase regulation domains (PRDs) (21, 22, 24). bEBPs whose activation is triggered by signal sensing through PRDs are members of the LevR-like family of regulators and have been described in both Gram-positive and Gram-negative bacteria (21, 22, 24). The activity of LevR-like regulators is controlled by the PTS enzymes that the bEBP in-turn regulates, via phosphorylation of the bEBP regulatory domain (22, 24, 25). All bEBPs encoded in the *E. faecalis* genome belong to the LevR-like family of regulators. The regulatory domain of LevR-like bEBPs contain two unique PRDs, one undergoes HPr-mediated phosphorylation at a key histidine amino acid residue that leads to the activation of the bEBP (PRD1), while PRD2 undergoes EII-mediated phosphorylation at a secondary histidine residue, that is inhibitory (22, 24, 25). These key histidine residues involved in HPr- or EII-mediated PRD phosphorylation are unidentified in all of the bEBPs encoded in the *E. faecalis* genome and could be a component of ongoing studies.

Of the six predicted RpoN-dependent PTS systems, only three (*mptBACD, lptBAC*, and *xpoABCD*) were found to be differentially expressed under CDM plus glucose growth conditions. Of these three differentially expressed RpoN-dependent PTS systems, only the Mpt system plays a significant role in glucose- and mannose-dependent growth, as the *mptR* mutant and the *mptBACD* mutant phenocopy the *rpoN* mutant for growth in CDM supplemented with glucose or mannose. In contrast, neither the other known bEBPs (MphR, MpoR, and LpoR) nor the XpoABCD PTS system contribute to glucose-dependent growth. Previously, it was hypothesized that the Xpo PTS complex was inactive in *E. faecalis* V583 due to disruption by an IS256 insertion element (23). In fact, this IS256 insertion element is annotated as *ef3215* in the *E. faecalis* V583 genome and splits the *xpoR* gene almost exactly in half, where the N-terminal AAA+ ATPase and DNA binding domains are annotated as *ef3214,* and the C-terminal regulatory domain is annotated as *ef3216*. Interestingly, the insertion element introduced an in-frame stop codon directly at the end of *ef3214* (AAA+ ATPase/DNA binding domain portion of XpoR). Our results indicate that the expression of the *xpoABCD* PTS system is dependent on RpoN, suggesting that the truncated XpoR may still be functional. Others have shown that a bEBP that only possesses its AAA+ ATPase domain is capable of stimulating transcription of RpoN-dependent promoters in *Salmonella enterica* subsp. *enterica* serovar Typhimurium LT2 (26), suggesting that, in some instances, bEBPs may activate transcription of its RpoN-dependent genes without possessing regulatory and/or DNA binding domains. Presumably, *ef3214* possesses all essential promoter elements, as the IS256 element did not disrupt the upstream promoter sequence of *ef3214*. Identification of the transcriptional start site (TSS; +1) by 5' RACE analysis would aid in the identification of putative *ef3214* promoter elements. Because the XpoR AAA+ ATPase/DNA-binding domain is encoded by *ef3214* and *ef3214* has an in-frame stop codon, I hypothesize that the truncated XpoR (EF3214), possessing only the AAA+ ATPase and DNA-binding domains, is capable of activating the expression of the

xpoABCD PTS system. This could be examined by creating an *ef3214* deletion mutant and measuring differences in *xpoABCD* expression between the Δ*ef3214* mutant and parental V583 strain via qRT-PCR. To ascertain that the disrupted XpoR regulatory domain encoded by *ef3216* does not contribute to the expression of *xpoABCD*, a Δ*ef3216* deletion mutant could be created and assessed under similar qRT-PCR assay conditions.

All of the bEBPs discussed in this dissertation are encoded in the genomes of a variety of *E. faecalis* strains (NCBI BLAST). Homologs of these bEBPs present in *E. faecalis* are present in a variety of other bacterial species, however these bacterial species are restricted to the phylum of Firmicutes (NCBI BLAST). As for the PTS systems that possess RpoN binding sites within their promoter regions (Mpt, Mpo, Mph, Lpo, Lpt, and Xpo), homologs of these PTS operons are present in additional enterococcal species as well as species beyond the genus of *Enterococcus*, however restricted to the phylum of Firmicutes (NCBI BLAST).

In chapter two of this dissertation, we also show that RpoN influences a larger regulatory network when RpoN-dependent glucose uptake is disrupted. The majority of the differentially affected genes in the *rpoN* mutant encode transport/transport binding proteins and proteins involved in energy metabolism, which can be correlated to gene products that may enable the bacterium to cope in glucose-limited host environments. In conjunction with RpoN contributing to enterococcal *in vivo* fitness, this also provides important evidence that links central carbon metabolism with *in vivo* growth and provides the rationale for several distinct pathways that could be targeted as a potential therapeutic for treating enterococcal infections.

Among the genes that were significantly upregulated in the *rpoN* mutant, a novel PTS system encoded by *ef0552-55* resides within a known pathogenicity island (PAI) in the *E. faecalis* V583 genome (Figure 1). Also encoded in the same operon is a cytosolic glycosyl hydrolase family 31

(GH31) enzyme, encoded by *ef0551* (Figure 1). The cytosolic nature of EF0551 was predicted using the SignalP 5.0 software (http://www.cbs.dtu.dk/services/SignalP/) (data not shown).

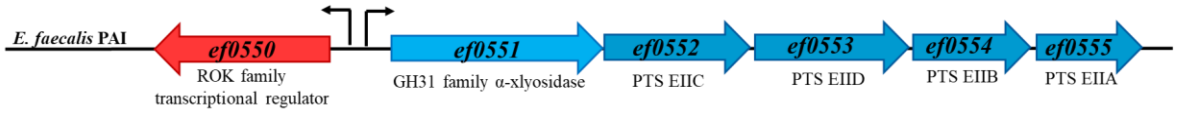

Figure 1: Genetic organization of PTS EIICDBA system encoded by *ef0552-55* residing within the *E. faecalis* V583 pathogenicity island (PAI). *ef0551* encodes for a putative glycosyl hydrolase family 31 (GH31) α-xylosidase. Encoded divergently upstream from the *ef0551-55* operon is a transcriptional regulator belonging to the ROK family of regulators.

The GH31 family of glycosidases is a diverse group of enzymes with a range of different hydrolytic activities (27). Members of this family include α-glucosidases, α-xylosidases, α-galactosidases, α-mannosidases, 6-α-glucosyltransferases, and 3-α-isomaltosyltransferases (27). The GH31 enzyme encoded by *ef0551* possesses a catalytic domain belonging to the XylS-like family of GH31 α-xylosidases, which are enzymes that catalyze the release of α-xylose from xyloglucan oligosaccharides (27). Xyloglucan is a polysaccharide present in the cell wall of plants and possesses a backbone of β1,4-linked glucose residues, most of which are substituted with α1,6-linked xylose sidechains (28). Additionally, the xylose residues are sometimes capped with a galactose moiety (29). The GH31 α-xylosidase encoded by *ef0551* shares homology the α-xylosidases (Xyl31A) characterized in the Gram-positive bacterium, *Ruminiclostridium cellulolyticum* (28, 29), and also shares homology with the α-xylosidase (*Bo*GH32A) produced by the human gut commensal, *Bacteroides ovatus* (30). The human genome does not encode enzymes responsible for xyloglucan degradation, therefore humans must rely on their resident microbiota for digestion of this polysaccharide. *Bacteroides* secretes enzymes that specifically degrades xyloglucan into xyloglucan dextrins of various lengths (30), which can subsequently be imported into the bacterial cell. Once transported into the bacterial cell, xyloglucan dextrins are

depolymerized into the respective simple sugars (i.e. galactose, xylose, and glucose) by sequential activity of a β-galactosidase, an α-xylosidase, and a β-glucosidase (28-30). It is uncertain whether secreted xyloglucan degrading enzyme(s) are encoded in the *E. faecalis* genome, however in complex microbial intestinal ecologies, *E. faecalis* could scavenge xyloglucan dextrins from the environment by simply expressing a xyloglucan dextrin-specific transport system(s). With an α-xylosidase encoded in the same operon as a PTS system in the *E. faecalis* PAI, I hypothesize that the PTS system encoded by *ef0552-55* is responsible for importing xyloglucan dextrins, followed by subsequent depolymerization by the α-xylosidase encoded by *ef0551*, along with a currently unknown β-galactosidase and β-glucosidase. Intriguingly, divergently upstream from the *ef0551-55* operon is a putative ROK family transcriptional regulator (EF0550) (Figure 1), which could possibly regulate the expression of the GH31/PTS system operon (*ef0551-55*).

One of the common themes observed with the transcriptional profile of the *rpoN* mutant was the significant upregulation of genes that possessed predicted catabolite responsive element (*cre*) sites within their promoter regions, representing 42.74% of the upregulated genes in the *rpoN* mutant. The presence of a *cre* site is suggestive of an involvement with the major transcriptional regulator, catabolite control protein A (CcpA). In Gram-positive bacteria, CcpA plays a key role in regulating the expression of alternative nutrient acquisition systems via carbon catabolite repression (CCR) (31, 32), therefore this is another example of a regulatory mechanism for which certain bacteria can use to modulate its metabolism. Because our analysis showed that RpoN directly regulates the expression of the primary glucose transporter and sole mannose transporter (MptBACD), I infer that the inability of the Δ*rpoN* mutant to efficiently import glucose or mannose into the cell via the Mpt PTS complex influences the rate of carbon catabolite derepression. This interpretation is depicted in a proposed model regarding how RpoN and CcpA interface in the cell to regulate

central carbon metabolism (Chapter 2, Figure 10). The expression seen in the array data with respect to *cre* site containing genes is consistent with this interpretation.

As previously stated, CcpA is known to play a critical role in secondary carbon metabolism by repressing secondary catabolite genes when preferred carbon sources are readily available. However, CcpA can also act as a positive regulator and activate the expression of genes known to be involved in central glycolytic pathways and overflow metabolism (33, 34). For example, when *Bacillus subtilis* is grown under high glucose conditions, CcpA positively regulates the expression of genes to convert excess glucose into acetate or lactate, among other organic acids as products of overflow metabolism (34), which can later be utilized as a carbon source under glucose-limiting conditions. Upon assessing the *ccpA* mutant in the murine catheter urinary tract infection (CAUTI) model (Chapter 2, Figure 9), this mutant perplexingly has a significant decrease of *in vivo* fitness despite secondary nutrient acquisition systems being overexpressed in this mutant. The dysregulation of normal metabolism and inability to elicit overflow metabolism, which would occur in a *ccpA* mutant, likely explains its attenuated *in vivo* phenotype and is consistent with a growing body of evidence for the role of CcpA in Gram-positive bacterial pathogenesis (35-37). Of note, one of the lactate dehydrogenase genes encoded by *ef0255* in *E. faecalis* possesses a *cre* site within its promoter region. Lactate dehydrogenase is responsible for catalyzing the conversion of lactate into pyruvate, and vice versa (38). The location of the *cre* site within the promoter region of *ef0255* is indicative of CcpA acting as an activator of *ldh-1* expression and we have confirmed such regulation by qRT-PCR (Chapter 3, Figure S4). Since two lactate dehydrogenases are encoded in the *E. faecalis* genome, it would be of interest to determine the contribution of each *ldh* gene. Because *ldh-1* expression is activated by CcpA, I hypothesize that Ldh-1 is the primary contributor for converting excess glucose into lactate as a mechanism of overflow metabolism.

Measuring the amount of lactate produced by single deletion strains of each lactate dehydrogenase genes grown under glucose-replete conditions would likely address this hypothesis.

Among the putatively secreted, *cre* site-containing genes that were upregulated in the *rpoN* mutant, three endoglycosyl hydrolases (*ef0114*, *ef0361*, and *ef2863*) and the cognate chitin-binding protein/lytic polysaccharide monooxygenase (*ef0362*) of EF0361 were pursued as these secreted enzymes likely contribute to the survival of *E. faecalis* in nutrient limited environments. These enterococcal enzymes were also significantly upregulated in other transcriptomic studies conducted in human urine, blood, and an *in vivo* subdermal abscess model (39-41), indicating biological host colonization relevance. Chapter 3 of this dissertation highlights that *E. faecalis* has evolved two CcpA-regulated endoglycosyl hydrolases that have a specific effectiveness towards certain N-linked glycoprotein types. Our analysis indicates that EF2863 is required for the utilization of N-linked high-mannose type glycoproteins as a carbon source by cleaving the Asn-attached chitobiose (Asn-GlcNAc-β1,4-GlcNAc), as the deletion of *ef2863* eliminated growth on the model high-mannose type glycoprotein, RNase B (Chapter 3, Figure 7A). In contrast, the activity of EF0114 is required to deglycosylate N-linked complex type glycoproteins, such as IgG (Chapter 3, Figure 9A-D) and lactoferrin (42), by cleaving the Asn-attached chitobiose (Asn-GlcNAc-β1,4-GlcNAc). The dose-dependence analysis with RNase B revealed that although EF0114 can deglycosylate RNase B, EF2863 is far more efficient at deglycosylating RNase B; the reverse observation was seen regarding IgG deglycosylation, where EF0114 is principally responsible for deglycosylating IgG. Although both EF0114 and EF2863 target the same glycosidic linkage (GlcNAc-β14-GlcNAc) of N-linked glycoproteins, the subtle differences in the glycan sugar decorations may explain why the two glycosyl hydrolases evolved their substrate specificities. Of note is the presence of a fucose moiety that is attached to the first GlcNAc residue

of the Asn-attached chitobiose of complex glycoproteins, including IgG and lactoferrin. N-linked high-mannose glycoproteins do not possess this fucose decoration. It will be of interest to elucidate how the presence or absence of the fucose decoration impacts the binding and/or enzymatic activity of EF2863 relative to EF0114. Comparative co-crystallization studies with various glycosyl hydrolase/substrate combinations (EF0114+RNase B, EF2863+RNase B, EF0114+IgG, and EF2863+IgG) may reveal the key contacts between the glycoprotein type and corresponding glycosidase that influences the substrate specificities of these two GH18 ENGases. This analysis would likely provide insight into why *E. faecalis* evolved to secrete two CcpA-regulated glycosyl hydrolases that target the same glycosidic linkage present in N-linked glycan. For the co-crystallization studies, I would propose to utilize the site-directed variants of EF0114 and EF2863, as these glycosyl hydrolase variants are catalytically inactive, but theoretically are still capable of binding to their target glycoprotein.

With the observation of EF2863 being the primary glycosidase of high-mannose type glycoproteins, I hypothesize that once EF2863 removes the glycans from these glycoproteins, additional α-mannosidases would be responsible for further liberation of the mannose residues that could be imported into the cell via the *E. faecalis* Mpt PTS complex (43). This is consistent with observations reported by both Roberts (44) and Li (45), who demonstrated α-mannosidase activity in *E. faecalis* culture filtrates only after pre-treatment of RNase B with either EndoH (44) or PNGase F (45). The analysis conducted in chapter 3 of this dissertation shows that the Mpt PTS system is required for importation of mannose residues from the released glycans of high-mannose type glycoproteins, as the *mptBACD* mutant had a significant growth defect when grown on RNase B as a carbon source (Chapter 3, Figure 7B). Three α-mannosidases are annotated in the *E. faecalis* V583 genome, *ef1708-07* and *ef2217*. EF1708 is a putative family 125 glycosyl hydrolase that

putatively targets the α-1,6-linked non-reducing terminal mannose residues of N-glycans (46). EF1707 is a putative family 38 glycosyl hydrolase that is thought to target α-1,3-mannosidic linkages (47), whereas EF2217 belongs to the family 92 glycosyl hydrolase family and has been shown to cleave α-1,2-linked mannose residues of liberated N-linked glycans of RNase B (RNase B treated with PNGase F) (45). This suggests that EF2863, the Mpt PTS complex, EF1708-07 and EF2217 likely act in a coordinated fashion to metabolize the sugar moieties of N-linked high-mannose host glycoproteins. To preliminarily address whether *ef1707*, *ef1708,* and/or *ef2217* are involved in utilizing high-mannose type glycoproteins as a carbon source, single deletions of these three α-mannosidases were constructed, as well as a triple α-mannosidase mutant (Δ*ef2217*Δ*ef1708-07*) and all were assessed for growth in CDM supplemented with RNase B as the sole carbon source. For this particular assay, a 10mg/mL concentration of RNase B was used (instead of 5 mg/mL in all other CDM+RNase B assays in this dissertation) because this source of RNase B was purchased from Alfa Aesar. At the concentration of 5 mg/mL, RNase B from Alfa Aesar doesn't support growth to the equivalent level of RNase B purchased from Sigma Aldrich (data not shown), therefore 10 mg/mL of Alfa Aesar RNase B must be used to assess growth of *E. faecalis* on this substrate. As shown in figure 2, the deletion of Δ*ef2217* results in a significant decrease in growth relative to the parental strain, but still grew to an optical density of approximately 0.06. As for the single deletions of Δ*ef1707* and Δ*ef1708* and the triple α-mannosidase mutant, these mutants exhibited a significant growth defect when grown in CDM+10mg/mL RNase B (Figure 2).

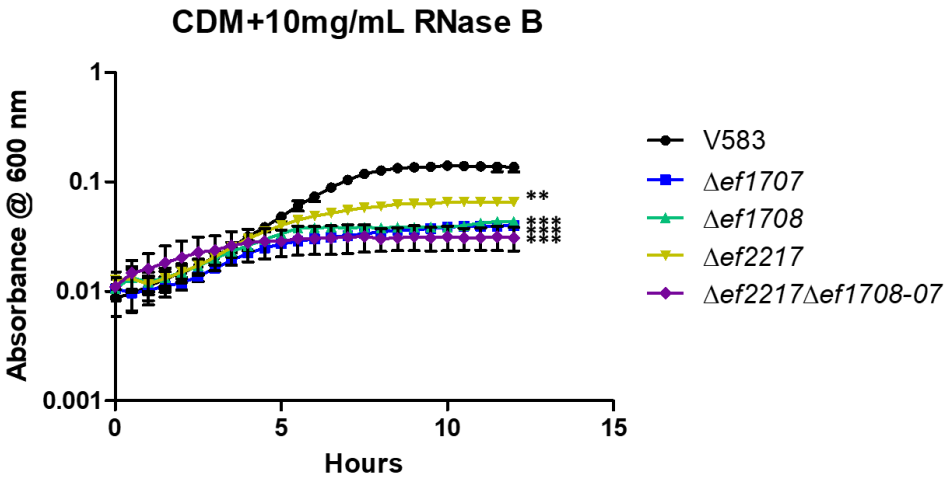

Figure 2: Growth of *E. faecalis* in CDM supplemented with 10 mg/mL RNase B purchased from Alfa Aesar. Each graph is the average of three biological replicates, with three technical replicates each time (n=9). The statistical significance was calculated using a one-way ANOVA test, p value of <0.001 is indicated as (**), p value of <0.0001 is indicated as (***). The growth curves are shown in black (V583), blue (Δ*ef1707*), green (Δ*ef1708*), gold (Δ*ef2217*), and purple (Δ*ef2217*Δ*ef1708-07*).

The intermediate growth of the Δ*ef2217* mutant is likely attributed to this α-mannosidase targeting the α-1,2-mannosidic linkage within the glycans of RNase B. It is noteworthy that RNase B is glycosylated with a range of high-mannose glycan lengths, meaning that the mannose moieties of this glycan structure range from five up to nine mannose sugars (Figure 3). Therefore, the core glycan structure of RNase B is Asn-GlcNAc$_2$-Man$_5$ (Figure 3).

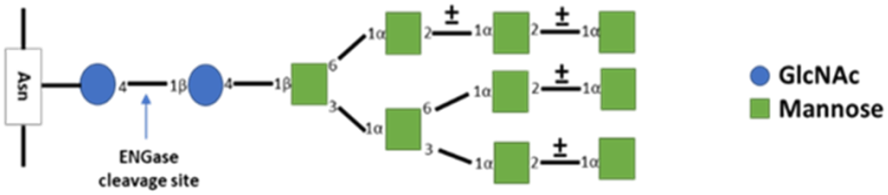

Figure 3: Representation of RNase B glycan structure. The blue arrow depicts deglycosylation site of RNase B by GH18 ENGases. The glycoforms of RNase B range from five to nine mannose moieties attached to chitobiose (β-1,4-GlcNAc$_2$).

The source of RNase B is likely a mixture of these varied glycans lengths, therefore EF2217 is not always required to degrade RNase B glycans when the glycoprotein only possess the core glycan

structure. To improve the rigor of the observation depicted in figure 2 of this chapter, the α-mannosidase deletion mutants would need to be complemented and could be a component of future studies.

It is noteworthy that in the *Streptococcus pneumoniae* N-glycan degradation model proposed by Robb et al. (48), the streptococcal GH92 α-mannosidase trims high-mannose glycans into the $GlcNAc_2$-Man_5 core structure, which this high-mannose core is subsequently transported into the bacterial cell by an ABC transporter. Their model implies that the GH92 α-mannosidase is cell wall-associated despite the absence of any known secretion signal (48). Similarly, the enterococcal GH92 α-mannosidase (EF2217) does not possess a signal peptide sequence (SignalP 5.0, data not shown). There is evidence that *S. pneumoniae* is capable of non-classically translocating various proteins to the cell surface or extracellularly by an unknown mechanism (49-51). It would be of interest to conduct a cellular fractionation study to determine whether the enterococcal GH92 α-mannosidase is cell-wall associated. If EF2217 is indeed cell-wall associated, this would suggest that a non-classical secretion mechanism would exist in *E. faecalis* as well. Identification of the transport system responsible for importing the liberated high-mannose glycan core structure (GlcNAc-Man_5) in *E. faecalis* would support the hypothesis that EF2217 is cell-wall associated. Our lab has hypothesized that this transport system is the ABC transporter encoded by *ef2223-21*, as EF2223-21 shares significant homology to the streptococcal $GlcNAc_2$-Man_5 ABC transporter (48). Interestingly, this ABC transport system encoded by *ef2223-21* was found to be the most abundantly expressed genes in the *rpoN* mutant microarray study (Chapter 2, Table S4) and possesses a low affinity towards the uptake of glucose (Chapter 2, Figure 6). Recent observations in the Hancock lab indicates that a novel three-component system, YesLMN, encoded by *ef2220-18*, activates the transcription of the EF2223-21 ABC transporter. These genes were also found to

be significantly upregulated in the *rpoN* mutant microarray study (Chapter 2, Table S4). Our lab hypothesizes that $GlcNAcMan_5$ is recognized by the single transmembrane sensor, YesL, and histidine kinase, YesM, leading to the phosphorylation of the response regulator, YesN, thus activating the expression of the EF2223-21 ABC transporter for the uptake of $GlcNAcMan_5$ into the bacterial cell. Additionally, it is possible that YesN autoregulates the three-component system operon (*ef2220-18*) and regulates the expression of *ef2217*, which encodes the GH92 α-mannosidase. The contribution of EF2223-21 and the YesLMN three-component system in the metabolism of N-linked high-mannose glycans is a current component of on-going studies. Illustrated in figure 4 of this chapter is the proposed model for N-linked high-mannose glycoprotein metabolism in *E. faecalis*.

While designing primers to create the deletion constructs of *ef1707* and *ef1708*, I noticed that a GntR transcriptional regulator encoded by *ef1709* is divergently located upstream from the *ef1708-07* α-mannosidases operon. In bacteria, the GntR family of transcriptional regulators is one of the most widespread families of transcription factors that regulate the transcription of effector genes via allosteric binding to metabolites (52, 53). I hypothesize that EF1709 directly regulates the expression of *ef1708-07*. To determine which type of transcriptional regulation EF1709 employs on the downstream α-mannosidase operon, transcript abundance of either *ef1708* or *ef1707* could be compared between parental and a Δ*ef1709* deletion strain using qRT-PCR or an *ef1708-07* promoter fusion to the *lacZ* reporter gene could be created and the promoter activity could be assessed in either strain (V583 vs Δ*ef1709*) using the β-galactosidase/Miller assay method.

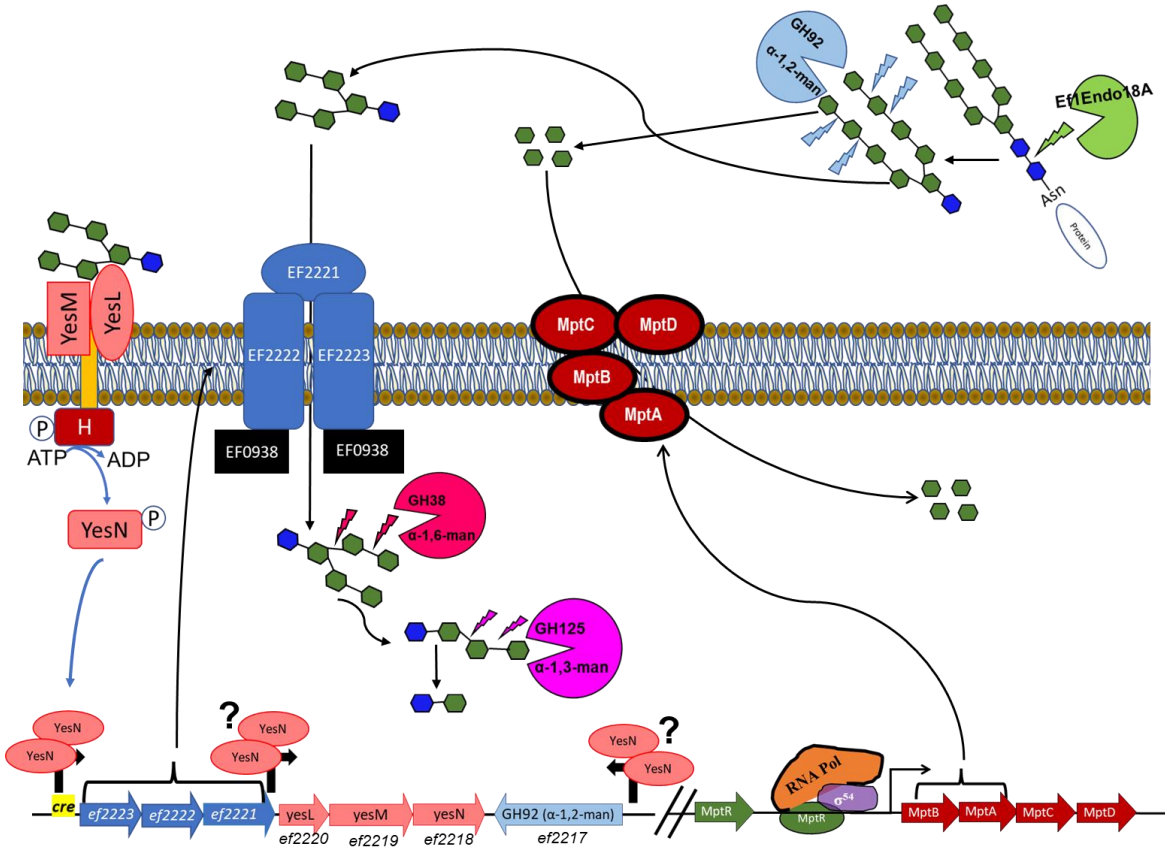

Figure 4: Proposed model for N-linked high-mannose glycan metabolism in *E. faecalis*. High-mannose N-linked glycoproteins are acted on by EfEndo18A (EF2863) to release the glycan from the protein backbone. The released high-mannose glycan is acted on by the GH92 α-mannosidase (EF2217) to produce $Man_5GlcNAc$. $Man_5GlcNAc$ is recognized by the YesLMN three-component system (YesL=single transmembrane sensor ; YesM=sensor histidine kinase ; YesN=response regulator) leading to the activation of the EF2223-21 ABC transporter. The EF2223-21 ABC transporter in conjunction with the ABC transporter ATP-binding protein (EF0938) imports $Man_5GlcNAc$ into the cytoplasm, where further depolymerization is carried out by the GH38 α-mannosidase (EF1707) and GH125 α-mannosidase (EF1708).

In a biological host, bacteria will encounter a more hostile environment as preferable nutrient sources are often host limited and the organism is subject to attack from the host immune system. Potential alternative host nutrient sources are high-mannose and complex type glycoproteins, which are prevalent on host epithelial cells lining the gastrointestinal tract and urinary tract (54, 55). For example, uroplakin is an abundant cell-surface associated protein complex in the urinary tract epithelium, and is comprised of four major proteins, termed uroplakin Ia, Ib, II and IIIa.

Proteins Ia, Ib and IIIa are modified with N-linked glycans, specifically Ia possesses high-mannose glycans, whereas Ib is exclusively comprised of complex type glycosylation (56). Uromodulin or Tamm-Horsfall glycoprotein is the most abundant protein in urine, and possesses high-mannose glycosylation (57). Additionally, a bacterial chitinase, which shares homology to EF0361, targets LacNac (Galβ1–4GlcNAc) and LacdiNAc (GalNAcβ1–4GlcNAc) sugar linkages present in mammalian N and O-linked glycans, glycolipids and glycosaminoglycans (58-60). These LacNAc and LacdiNAc containing substrates present in a mammalian host are likely an additional substrate for bacterial chitinases and chitinolytic cleavage of these substrates may contribute to bacterial pathogenesis in a host.

N-glycosylation at the conserved asparagine residue at position 297 within the heavy chain of the Fc region of IgG has been discovered as an essential player in Fc effector functions such as antibody-dependent cellular cytotoxicity and optimal activation of the classical complement pathway (61, 62). Alterations of glycan composition or removal of the glycan can severely impact the effector functions due to conformational changes of the Fc domain, ultimately affecting the binding affinity to Fcγ receptors (62-64) and complement C1q binding to activate the classical complement pathway (65). The loss of deglycosylation of IgG in the absence of the streptococcal EndoS glycosidase resulted in a decrease of *S. pyogenes* resistance to phagocytic killing, *in vitro* and decreased virulence, *in vivo* (66, 67). These observations link bacterial glycosidase-dependent IgG glycan hydrolysis to immune evasion. This also suggests that EF0114 likely plays a similar role in enterococcal immune evasion, as our study identified EF0114 as the primary glycosidase against IgG. Although the mice used in our study, described in chapter 3 of this dissertation, were not immunized with enterococci prior to infection, the presence of natural IgGs have been found to provide innate protection against bacteria (66, 68) and would be subject to deglycosylation by

EF0114. It will be of interest to elucidate whether enterococcal EF0114-dependent deglycosylation of IgG is an immune evasion mechanism. This could be assessed using an *in vitro* C1q uptake assay (65, 69), an *in vitro* neutrophil or monocyte killing assay (67, 70), and/or assessed for an overall *in vivo* fitness contribution using the *in vivo* murine catheter-associated urinary tract infection (CAUTI) model (71). The C1q uptake assay would provide insight into whether EF0114-dependent deglycosylation of IgG disrupts the IgG glycan-dependent Fc effector activation of the classical complement pathway, whereas the neutrophil or monocyte killing assay would elucidate whether EF0114 disrupts Fc glycan-dependent cellular cytotoxicity. Determining the contribution of EF0114 in enterococcal pathogenesis using the *in vivo* murine CAUTI model is an upmost priority, especially since the GH18 glycosyl hydrolase triple mutant (Δ*ef0114*Δ*ef0362-61*Δ*ef2863*) had a significant attenuated *in vivo* phenotype. This triple mutant was assessed because of the potential functional redundancy of the GH18 domain containing proteins in V583 and now that an *in vivo* fitness defect was observed, a major interest is to assess single and double deletions of the glycosyl hydrolases EF2863, EF0114 and EF0361 for their individual or combined contribution to *in vivo* fitness. I hypothesize that individual deletions of the GH18 domain containing glycosyl hydrolases would result in a significant *in vivo* colonization defect, as (a) the loss of *ef2863* would inhibit the bacterium's ability to utilize the glycans from N-linked high-mannose glycoproteins as an alternative carbon source, (b) the loss of *ef0114* would result in an increased susceptibility to IgG effector functions including complement activation and phagocytic clearance, as well as inhibit the ability to utilize complex glycans of N-linked glycoprotein as a nutrient source, and (c) the loss of *ef0361* would hinder the ability to utilize the sugar moieties of N and O-linked glycans, glycolipids and glycosaminoglycans, based on bacterial chitinases targeting the LacNAc and LacdiNAc linkage within these mammalian substrates.

The GH18 containing glycosyl hydrolases (EF0114, EF0361, and EF2863) and the chitin-binding protein/lytic monooxygenase (EF0362) under study are encoded in the genomes of nearly all *E. faecalis* strains (NCBI BLAST), and are considered part of the core genome. Of the aforementioned enzymes, homologs of EF0362 are present in additional enterococcal species, such as, *Enterococcus caccae*, *Enterococcus rotai*, *Enterococcus termitis*, *Enterococcus moraviensis*, and *Enterococcus durans* (NCBI BLAST). Homologs of EF0114, EF0362, EF0361, and EF2863 are present in a variety of other bacterial species, however these bacterial species are restricted to the phylum of Firmicutes (NCBI BLAST). The best studied homologs of EF0114 and EF0361 in other bacterial species are EndoS of *Streptococcus pyogenes* (66, 67) and ChiA of *Listeria monocytogenes* (58), respectively. To my knowledge, homologs of EF0362 and EF2863 have not been identified in bacterial species beyond *E. faecalis*, which may increase its overall fitness in the context of varying host microbial ecologies.

Previous observations have shown that EF0114 (EndoE) of *E. faecalis* is also capable of deglycosylating the N-linked complex glycoprotein, lactoferrin (42). Lactoferrin is an abundant multifunctional glycoprotein of the innate immune system found circulating in the blood and present in secreted fluids (72). Lactoferrin is primarily thought of as an iron-binding protein; however, it also carries many important biological functions, including anti-bacterial properties (73). The iron-chelating property of lactoferrin is considered its primary mechanism of its antimicrobial activity as it sequesters the iron in the environment (73). Lactoferrin has also been shown to inhibit bacterial biofilm formation (42, 74), decrease bacterial adherence to mammalian epithelial cells (75-77), and increases bacterial lysozyme susceptibility (78). The inhibition of biofilm formation by lactoferrin is thought to be caused by its iron-chelating property, as iron is an essential nutrient for biofilm development and growth (74, 79); however, this may not be the

only mode of action lactoferrin possesses to inhibit biofilm formation. In contrast, the hindrance of bacterial adhesion to host epithelial cells and increased lysozyme susceptibility in the presence of lactoferrin is attributed to lactoferrin having large cationic patches on its surface that binds to the negatively charged cell surface molecules of bacteria (75-78). Specifically for bacterial lysozyme susceptibility, lactoferrin binds to the anionic lipoteichoic acids on the bacterial cell surface, thus decreasing the net negative cell wall charge, enabling greater access for lysozyme to penetrate the peptidoglycan (78). Although lysozyme susceptibility has been observed in *E. faecalis*, the cooperative effect of lactoferrin and lysozyme has not been elucidated against this pathogen. This could be assessed by comparing the susceptibility of *E. faecalis* to lysozyme in the presence and absence of lactoferrin.

Although lactoferrin possesses these anti-bacterial properties, little is known of how the glycan moieties in lactoferrin contribute to its antimicrobial activities. Glycans play a critical role in many biological processes; therefore, it is likely that the glycans of lactoferrin play a significant role in the biological properties of lactoferrin. Since lactoferrin increases the efficacy of lysozyme activity, it would be of interest to determine whether the glycans of lactoferrin contributes to the synergistic antimicrobial activity of lactoferrin and lysozyme. It is intriguing that *E. faecalis* secretes a glycosyl hydrolase (EF0114) that is capable of deglycosylating lactoferrin (42); therefore, deglycosylation of lactoferrin by EF0114 could be an additional mechanism for bacterial resistance to lysozyme. I hypothesize that the addition of EF0114 would decrease the bacterial susceptibility (in other words, increase bacterial resistance) to lysozyme due to its glycosidase activity against lactoferrin. This could be assessed by growing various species of bacteria, including *E. faecalis*, in media supplemented with an inhibitory concentration of lysozyme +

lactoferrin and comparing the growth phenotypes to those also grown in the presence of purified recombinant EF0114 (EndoE).

As EF0114 possesses an additional GH20 family glycosyl hydrolase domain, it was of interest to explore the function of this catalytic domain. GH20 glycosyl hydrolases are reported to possess the ability to hydrolyze the β1,4 linked terminal non-reducing *N*-acetyl-D-hexosamine residues and/or the β-1,6-glycosidic linkage between two adjoining N-acetylglucosamine moieties (80-83). Based on the NCBI Conserved Domain Database, the GH20 domain of *E. faecalis* V583 EF0114 possesses Dispersin B-like GH20 catalytic domain sharing homology with the well-studied Dispersin B (DspB) produced by the oral pathogen, *Aggregatibacter actinomycetemcomitans* (81, 84-87). A number of studies have shown that Dispersin B disaggregates self-produced biofilms, as well as biofilms produced by several bacterial species including *Staphylococcus epidermidis*, *Escherichia coli*, *Yersinia pestis*, and *Pseudomonas fluorescens* (81, 84, 86, 88). The mode of action of DspB is to disaggregate the aforementioned biofilms by cleaving the β-1,6-linkage between N-acetylglucosamine residues, a major component of the extracellular polysaccharide matrix produced by many bacterial species (81, 84-86, 88). Based on the sequence conservation between EF0114 GH20 domain and Dispersin B, I hypothesized that EF0114 would possesses substrate specificity towards substrates containing β-1,6-linked N-acetylglucosamine. One such substrate is the staphylococcal intercellular adhesion, Ica, and this repeat polymer of β-1,6-linked N-acetylglucosamine is responsible for polysaccharide-dependent biofilm formation in *S. epidermidis* (89). I did assess whether EF0114 can function as a biofilm dispersing enzyme by growing *S. epidermidis* in a 96-well microtiter plate and quantified its biofilm formation in the presence and absence of purified recombinant EF0114 using the crystal violet staining method (90). Based on the results depicted in figure S3 of chapter 3 of this dissertation, EF0114 does not

appear to function as a biofilm dispersing enzyme, as EF0114 had no significant effect on *S. epidermidis* biofilms. This result also suggests that the GH20 catalytic domain of EFF0114 likely doesn't target the β-1,6-glycosidic bond between two adjoining N-acetylglucosamine moieties.

Nonetheless, described in chapter 4 of this dissertation, a precise enzymatic function for the GH20 catalytic domain of EF0114 has been determined. The analysis described in chapter 4 of this dissertation revealed that the GH20 domain of EF0114 is responsible for cleaving the β-1,4-linked glycosidic bond of extracellular chitobiose (GlcNAc-β-1,4-GlcNAc; β-1,4-$GlcNAc_2$). Collectively, chapter 4 of this dissertation shows the metabolic pathway for which *E. faecalis* utilizes poly-β-1,4-linked N-acetylglucosamine as a carbon source. As depicted in our model (Chapter 4, Figure 7), extracellular polymers of β-1,4-linked GlcNAc are degraded into β-1,4-linked GlcNAc dimers by the combined activity of the chitin-binding protein, EF0362 (EfCBM33A), and the cognate chitinase, EF0361 (EfChi18A). This is based on previous observations by Vaaje-Kolstad et al. that show EF0361 and EF0362 synergistically degrading poly-β1,4-linked GlcNAc substrates (i.e. chitin (poly-β1,4-GlcNAc), chitohexaose ($GlcNAc_6$), chitopentaose ($GlcNAc_5$), chitotetraose ($GlcNAc_4$), or chitotriose ($GlcNAc_3$) (91). Our observation that the deletion of *ef0362-61* results in a severe growth defect when grown on chitopentaose ($GlcNAc_5$) supports their findings (Chapter 4, Figure 1). It is noteworthy that Vaaje-Kolstad et al. found that EF0362-61 can only synergistically degrade poly-β-1,4-GlcNAc substrates into dimers of β-1,4-linked N-acetylglucosamine, indicating that an additional enzyme is required for fully degrading these poly-β-1,4-GlcNAc substrates into monomers of N-acetylglucosamine prior to uptake into the bacterial cell. We determined this enzyme to be EF0114 and its GH20 domain is responsible for degrading β-1,4-GlcNAc dimers into monomers of N-acetylglucosamine. Once in its monomeric form, this amino sugar is imported into the bacterial

cell and simultaneously phosphorylated via either the Mpt PTS system or NagE (EF1516), as only the deletion of *ef1516* in the *mptBACD* mutant background resulted in complete attenuation of growth in CDM with either 10mM or 100mM N-acetylglucosamine (Chapter 4, Figure 3). Once inside the bacterial cell, prior to downstream glycolytic processing, phosphorylated GlcNAc (GlcNAc-6-P) is deacetylated by NagA (EF1317), as the Δ*ef1317* mutant failed to grow on N-acetylglucosamine as the sole carbon source (Chapter 4, Figure 5). Deamination of glucosamine to fructose-6-phosphate is required for entry into glycolysis and we show that growth on glucosamine is dependent on EF0466 (a glucosamine-6-phosphate deaminase; NagB homolog).

As observed in other related Gram-positive bacteria, the transcriptional regulator, NagR directly regulates the expression of *nagA* and *nagB* in *Streptococcus mutans* and *Bacillus subtilis* (92-94). In both *S. mutans* and *B. subtilis*, NagR is encoded distantly from *nagA* and *nagB*. Currently, there are 7 annotated GntR regulators in the *E. faecalis* V583 genome that share homology to NagR in *S. mutans* UA159 (95), none of which are in close proximity to *ef1317* (*nagA*) or *ef0466* (*nagB*) (Table 1). Elucidating which GntR homolog is responsible for regulating the expression of *nagA* and *nagB* in *E. faecalis* will require further assessment and could be an area of future research interest. I propose to first assess whether EF1328 is responsible for directly regulating the expression of *nagA* and *nagB* in *E. faecalis*, as this GntR transcriptional regulator has the highest sequence identity, sequence similarity, and query cover percentages relative to the NagR encoded by *S. mutans* UA159 (Table 1).

Table 1: NagR homologs in *E. faecalis*

Gene loci	Sequence identity to NagR in *S. mutans* UA159	Sequence similarity to NagR in *S. mutans* UA159	Query Cover relative to NagR in *S. mutans* UA159
EF1328	59%	75%	98%
EF1156	30%	51%	96%

EF3034	29%	50%	94%
EF1242	25%	51%	96%
EF1809	28%	50%	87%
EF0814	29%	54%	63%
EF1709	35%	69%	29%

Additionally, observed in *S. mutans* and *B. subtilis*, the expression of *nagA* and *nagB* are induced in the presence of N-acetylglucosamine (92, 95). I hypothesize that this too is likely the case in *E. faecalis*, where the presence of N-acetylglucosamine would increase the expression of *nagA* (*ef1317*) and *nagB* (*ef0466*). This could be assessed by measuring transcript abundance of *ef1317* and *ef0466* and compare the transcription levels in the wildtype V583 strain in the presence and absence of N-acetylglucosamine using qRT-PCR or *ef1317* and *ef0466* promoter fusions to the *lacZ* reporter gene could be created and their promoter activities could be assessed in the wildtype strain with and without N-acetylglucosamine in the culture medium using the β-galactosidase/Miller assay method.

Collectively, this dissertation provides insight into the regulation of central carbon metabolism in *E. faecalis* and highlight alternative nutrient acquisition mechanisms that may facilitate this bacterium's survival in nutrient-limiting host environments. Beyond the content of this dissertation, an area of research interest would be to characterize the functional role(s) and regulon of the other alternative sigma factors encoded in the *E. faecalis* V583 genome. Table 1 of the introductory chapter is a summation of the gene loci that encode these additional alternative sigma factors. Thus far, the Hancock lab has extensively contributed to the characterization of the enterococcal alternative sigma factor 54 (RpoN) (this dissertation and (96)) and the alternative sigma factor/anti-sigma factor pair, SigV and RsiV. The alternative sigma factor, SigV has been shown to play a role in the heat shock response, ethanol tolerance, acid stress response, and tolerance to lysozyme (97, 98). Recently, the lab has constructed single deletions of *ef1850* and

ef2244 and began assessing these mutants under a variety of stress conditions. One alternative sigma factor that I find of interest to characterize is EF3020, as this is the only other alternative sigma factor encoded in the *E. faecalis* genome that is paired with an anti-sigma factor. Without first knowing the environmental signal that induces the activity of the alternative sigma factor, it would be difficult to identify the associated regulon, as most genes regulated by alternative sigma factors are activated in the presence of a particular environmental signal. With EF3020 having a cognate anti-sigma factor (EF3019), it is possible to identify the regulon of EF3020, even if the activating stimulus is undetermined, by conducting a RNAseq study comparing the transcriptome of a Δ*ef3019* deletion mutant to that of a Δ*ef3020* and/or the parental V583 strain. The function of an anti-sigma factor is to prevent their cognate sigma factor from binding to the core RNA polymerase, therefore inhibiting the expression of the alternative sigma factor's target genes (99, 100). I hypothesize that by deleting the anti-sigma factor, EF3019, the inhibition of the EF3020 regulon is alleviated, leading to an increase in expression of EF3020 effector genes relative to that of the parental V583 strain.

References

1. Azad MB, Konya T, Maughan H, Guttman DS, Field CJ, Chari RS, Sears MR, Becker AB, Scott JA, Kozyrskyj AL, Investigators CS. 2013. Gut microbiota of healthy Canadian infants: profiles by mode of delivery and infant diet at 4 months. CMAJ 185:385-94.
2. Qin J, Li R, Raes J, Arumugam M, Burgdorf KS, Manichanh C, Nielsen T, Pons N, Levenez F, Yamada T, Mende DR, Li J, Xu J, Li S, Li D, Cao J, Wang B, Liang H, Zheng H, Xie Y, Tap J, Lepage P, Bertalan M, Batto JM, Hansen T, Le Paslier D, Linneberg A, Nielsen HB, Pelletier E, Renault P, Sicheritz-Ponten T, Turner K, Zhu H, Yu C, Li S, Jian M, Zhou Y, Li Y, Zhang X, Li S, Qin N, Yang H, Wang J, Brunak S, Dore J, Guarner F, Kristiansen K, Pedersen O, Parkhill J, Weissenbach J, et al. 2010. A human gut microbial gene catalogue established by metagenomic sequencing. Nature 464:59-65.
3. Portenier I, Waltimo TMT, Haapasalo M. 2003. Enterococcus faecalis– the root canal survivor and 'star' in post-treatment disease. Endodontic Topics 6:135-159.
4. Kao PHN, Kline KA. 2019. Dr. Jekyll and Mr. Hide: How Enterococcus faecalis Subverts the Host Immune Response to Cause Infection. J Mol Biol 431:2932-2945.
5. Martin R, Miquel S, Ulmer J, Kechaou N, Langella P, Bermudez-Humaran LG. 2013. Role of commensal and probiotic bacteria in human health: a focus on inflammatory bowel disease. Microb Cell Fact 12:71.
6. Gilmore MS, Rauch M, Ramsey MM, Himes PR, Varahan S, Manson JM, Lebreton F, Hancock LE. 2015. Pheromone killing of multidrug-resistant Enterococcus faecalis V583 by native commensal strains. Proc Natl Acad Sci U S A 112:7273-8.
7. Arias CA, Murray BE. 2012. The rise of the Enterococcus: beyond vancomycin resistance. Nat Rev Microbiol 10:266-78.
8. Chang CS, Chen GH, Lien HC, Yeh HZ. 1998. Small intestine dysmotility and bacterial overgrowth in cirrhotic patients with spontaneous bacterial peritonitis. Hepatology 28:1187-90.
9. Lin HC. 2004. Small intestinal bacterial overgrowth: a framework for understanding irritable bowel syndrome. JAMA 292:852-8.
10. Zhou Y, Chen H, He H, Du Y, Hu J, Li Y, Li Y, Zhou Y, Wang H, Chen Y, Nie Y. 2016. Increased Enterococcus faecalis infection is associated with clinically active Crohn disease. Medicine (Baltimore) 95:e5019.
11. Sahm DF, Kissinger J, Gilmore MS, Murray PR, Mulder R, Solliday J, Clarke B. 1989. In vitro susceptibility studies of vancomycin-resistant Enterococcus faecalis. Antimicrob Agents Chemother 33:1588-91.
12. Paulsen IT, Banerjei L, Myers GS, Nelson KE, Seshadri R, Read TD, Fouts DE, Eisen JA, Gill SR, Heidelberg JF, Tettelin H, Dodson RJ, Umayam L, Brinkac L, Beanan M, Daugherty S, DeBoy RT, Durkin S, Kolonay J, Madupu R, Nelson W, Vamathevan J, Tran B, Upton J, Hansen T, Shetty J, Khouri H, Utterback T, Radune D, Ketchum KA, Dougherty BA, Fraser CM. 2003. Role of mobile DNA in the evolution of vancomycin-resistant Enterococcus faecalis. Science 299:2071-4.
13. Bourgogne A, Garsin DA, Qin X, Singh KV, Sillanpaa J, Yerrapragada S, Ding Y, Dugan-Rocha S, Buhay C, Shen H, Chen G, Williams G, Muzny D, Maadani A, Fox KA, Gioia J, Chen L, Shang Y, Arias CA, Nallapareddy SR, Zhao M, Prakash VP, Chowdhury S, Jiang H, Gibbs RA, Murray BE, Highlander SK, Weinstock GM. 2008. Large scale variation in Enterococcus faecalis illustrated by the genome analysis of strain OG1RF. Genome Biol 9:R110.
14. Hancock LE, Gilmore MS. 2002. The capsular polysaccharide of Enterococcus faecalis and its relationship to other polysaccharides in the cell wall. Proc Natl Acad Sci U S A 99:1574-9.
15. Nallapareddy SR, Qin X, Weinstock GM, Hook M, Murray BE. 2000. Enterococcus faecalis adhesin, ace, mediates attachment to extracellular matrix proteins collagen type IV and laminin as well as collagen type I. Infect Immun 68:5218-24.
16. Coburn PS, Baghdayan AS, Dolan GT, Shankar N. 2007. Horizontal transfer of virulence genes encoded on the Enterococcus faecalis pathogenicity island. Mol Microbiol 63:530-44.

17. Nallapareddy SR, Singh KV, Sillanpaa J, Garsin DA, Hook M, Erlandsen SL, Murray BE. 2006. Endocarditis and biofilm-associated pili of Enterococcus faecalis. J Clin Invest 116:2799-807.
18. Matos RC, Lapaque N, Rigottier-Gois L, Debarbieux L, Meylheuc T, Gonzalez-Zorn B, Repoila F, Lopes Mde F, Serror P. 2013. Enterococcus faecalis prophage dynamics and contributions to pathogenic traits. PLoS Genet 9:e1003539.
19. Aakra A, Nyquist OL, Snipen L, Reiersen TS, Nes IF. 2007. Survey of genomic diversity among Enterococcus faecalis strains by microarray-based comparative genomic hybridization. Appl Environ Microbiol 73:2207-17.
20. Deutscher J, Francke C, Postma PW. 2006. How phosphotransferase system-related protein phosphorylation regulates carbohydrate metabolism in bacteria. Microbiol Mol Biol Rev 70:939-1031.
21. Bush M, Dixon R. 2012. The role of bacterial enhancer binding proteins as specialized activators of sigma54-dependent transcription. Microbiol Mol Biol Rev 76:497-529.
22. Deutscher J, Ake FM, Derkaoui M, Zebre AC, Cao TN, Bouraoui H, Kentache T, Mokhtari A, Milohanic E, Joyet P. 2014. The bacterial phosphoenolpyruvate:carbohydrate phosphotransferase system: regulation by protein phosphorylation and phosphorylation-dependent protein-protein interactions. Microbiol Mol Biol Rev 78:231-56.
23. Hechard Y, Pelletier C, Cenatiempo Y, Frere J. 2001. Analysis of sigma(54)-dependent genes in Enterococcus faecalis: a mannose PTS permease (EII(Man)) is involved in sensitivity to a bacteriocin, mesentericin Y105. Microbiology (Reading) 147:1575-1580.
24. Hartman CE, Samuels DJ, Karls AC. 2016. Modulating Salmonella Typhimurium's Response to a Changing Environment through Bacterial Enhancer-Binding Proteins and the RpoN Regulon. Front Mol Biosci 3:41.
25. Martin-Verstraete I, Charrier V, Stulke J, Galinier A, Erni B, Rapoport G, Deutscher J. 1998. Antagonistic effects of dual PTS-catalysed phosphorylation on the Bacillus subtilis transcriptional activator LevR. Mol Microbiol 28:293-303.
26. Samuels DJ, Frye JG, Porwollik S, McClelland M, Mrazek J, Hoover TR, Karls AC. 2013. Use of a promiscuous, constitutively-active bacterial enhancer-binding protein to define the sigma(5)(4) (RpoN) regulon of Salmonella Typhimurium LT2. BMC Genomics 14:602.
27. Okuyama M. 2011. Function and structure studies of GH family 31 and 97 alpha-glycosidases. Biosci Biotechnol Biochem 75:2269-77.
28. Kampik C, Denis Y, Pages S, Perret S, Tardif C, Fierobe HP, de Philip P. 2020. A Novel Two-Component System, XygS/XygR, Positively Regulates Xyloglucan Degradation, Import, and Catabolism in Ruminiclostridium cellulolyticum. Appl Environ Microbiol 86.
29. Ravachol J, de Philip P, Borne R, Mansuelle P, Mate MJ, Perret S, Fierobe HP. 2016. Mechanisms involved in xyloglucan catabolism by the cellulosome-producing bacterium Ruminiclostridium cellulolyticum. Sci Rep 6:22770.
30. Larsbrink J, Rogers TE, Hemsworth GR, McKee LS, Tauzin AS, Spadiut O, Klinter S, Pudlo NA, Urs K, Koropatkin NM, Creagh AL, Haynes CA, Kelly AG, Cederholm SN, Davies GJ, Martens EC, Brumer H. 2014. A discrete genetic locus confers xyloglucan metabolism in select human gut Bacteroidetes. Nature 506:498-502.
31. Fujita Y. 2009. Carbon catabolite control of the metabolic network in Bacillus subtilis. Biosci Biotechnol Biochem 73:245-59.
32. Warner JB, Lolkema JS. 2003. CcpA-dependent carbon catabolite repression in bacteria. Microbiol Mol Biol Rev 67:475-90.
33. Dauner M, Storni T, Sauer U. 2001. Bacillus subtilis metabolism and energetics in carbon-limited and excess-carbon chemostat culture. J Bacteriol 183:7308-17.
34. Tobisch S, Zuhlke D, Bernhardt J, Stulke J, Hecker M. 1999. Role of CcpA in regulation of the central pathways of carbon catabolism in Bacillus subtilis. J Bacteriol 181:6996-7004.
35. Iyer R, Baliga NS, Camilli A. 2005. Catabolite control protein A (CcpA) contributes to virulence and regulation of sugar metabolism in Streptococcus pneumoniae. J Bacteriol 187:8340-9.

36. Li C, Sun F, Cho H, Yelavarthi V, Sohn C, He C, Schneewind O, Bae T. 2010. CcpA mediates proline auxotrophy and is required for Staphylococcus aureus pathogenesis. J Bacteriol 192:3883-92.
37. Watson ME, Jr., Nielsen HV, Hultgren SJ, Caparon MG. 2013. Murine vaginal colonization model for investigating asymptomatic mucosal carriage of Streptococcus pyogenes. Infect Immun 81:1606-17.
38. Garvie EI. 1980. Bacterial lactate dehydrogenases. Microbiol Rev 44:106-39.
39. Frank KL, Colomer-Winter C, Grindle SM, Lemos JA, Schlievert PM, Dunny GM. 2014. Transcriptome analysis of Enterococcus faecalis during mammalian infection shows cells undergo adaptation and exist in a stringent response state. PLoS One 9:e115839.
40. Vebo HC, Snipen L, Nes IF, Brede DA. 2009. The transcriptome of the nosocomial pathogen Enterococcus faecalis V583 reveals adaptive responses to growth in blood. PLoS One 4:e7660.
41. Vebo HC, Solheim M, Snipen L, Nes IF, Brede DA. 2010. Comparative genomic analysis of pathogenic and probiotic Enterococcus faecalis isolates, and their transcriptional responses to growth in human urine. PLoS One 5:e12489.
42. Garbe J, Sjogren J, Cosgrave EF, Struwe WB, Bober M, Olin AI, Rudd PM, Collin M. 2014. EndoE from Enterococcus faecalis hydrolyzes the glycans of the biofilm inhibiting protein lactoferrin and mediates growth. PLoS One 9:e91035.
43. Keffeler EC, Iyer VS, Parthasarathy S, Ramsey MM, Gorman MJ, Barke TL, Varahan S, Olson S, Gilmore MS, Abdullahi ZH, Hancock EN, Hancock LE. 2021. Influence of the Alternative Sigma Factor RpoN on Global Gene Expression and Carbon Catabolism in Enterococcus faecalis V583. mBio 12.
44. Roberts G, Tarelli E, Homer KA, Philpott-Howard J, Beighton D. 2000. Production of an endo-beta-N-acetylglucosaminidase activity mediates growth of Enterococcus faecalis on a high-mannose-type glycoprotein. J Bacteriol 182:882-90.
45. Li Y, Li R, Yu H, Sheng X, Wang J, Fisher AJ, Chen X. 2020. Enterococcus faecalis alpha1-2-mannosidase (EfMan-I): an efficient catalyst for glycoprotein N-glycan modification. FEBS Lett 594:439-451.
46. Gregg KJ, Zandberg WF, Hehemann JH, Whitworth GE, Deng L, Vocadlo DJ, Boraston AB. 2011. Analysis of a new family of widely distributed metal-independent alpha-mannosidases provides unique insight into the processing of N-linked glycans. J Biol Chem 286:15586-96.
47. Suits MD, Zhu Y, Taylor EJ, Walton J, Zechel DL, Gilbert HJ, Davies GJ. 2010. Structure and kinetic investigation of Streptococcus pyogenes family GH38 alpha-mannosidase. PLoS One 5:e9006.
48. Robb M, Hobbs JK, Woodiga SA, Shapiro-Ward S, Suits MD, McGregor N, Brumer H, Yesilkaya H, King SJ, Boraston AB. 2017. Molecular Characterization of N-glycan Degradation and Transport in Streptococcus pneumoniae and Its Contribution to Virulence. PLoS Pathog 13:e1006090.
49. Bergmann S, Rohde M, Hammerschmidt S. 2004. Glyceraldehyde-3-phosphate dehydrogenase of Streptococcus pneumoniae is a surface-displayed plasminogen-binding protein. Infect Immun 72:2416-9.
50. Jeong JK, Kwon O, Lee YM, Oh DB, Lee JM, Kim S, Kim EH, Le TN, Rhee DK, Kang HA. 2009. Characterization of the Streptococcus pneumoniae BgaC protein as a novel surface beta-galactosidase with specific hydrolysis activity for the Galbeta1-3GlcNAc moiety of oligosaccharides. J Bacteriol 191:3011-23.
51. Perez-Dorado I, Galan-Bartual S, Hermoso JA. 2012. Pneumococcal surface proteins: when the whole is greater than the sum of its parts. Mol Oral Microbiol 27:221-45.
52. Jain D. 2015. Allosteric control of transcription in GntR family of transcription regulators: A structural overview. IUBMB Life 67:556-63.
53. Liu GF, Wang XX, Su HZ, Lu GT. 2021. Progress on the GntR family transcription regulators in bacteria. Yi Chuan 43:66-73.

54. Park D, Brune KA, Mitra A, Marusina AI, Maverakis E, Lebrilla CB. 2015. Characteristic Changes in Cell Surface Glycosylation Accompany Intestinal Epithelial Cell (IEC) Differentiation: High Mannose Structures Dominate the Cell Surface Glycome of Undifferentiated Enterocytes. Mol Cell Proteomics 14:2910-21.
55. Sherblom AP, Smagula RM. 1993. High-mannose chains of mammalian glycoproteins. Methods Mol Biol 14:143-9.
56. Xie B, Zhou G, Chan SY, Shapiro E, Kong XP, Wu XR, Sun TT, Costello CE. 2006. Distinct glycan structures of uroplakins Ia and Ib: structural basis for the selective binding of FimH adhesin to uroplakin Ia. J Biol Chem 281:14644-53.
57. Cavallone D, Malagolini N, Monti A, Wu XR, Serafini-Cessi F. 2004. Variation of high mannose chains of Tamm-Horsfall glycoprotein confers differential binding to type 1-fimbriated Escherichia coli. J Biol Chem 279:216-22.
58. Chaudhuri S, Bruno JC, Alonzo F, 3rd, Xayarath B, Cianciotto NP, Freitag NE. 2010. Contribution of chitinases to Listeria monocytogenes pathogenesis. Appl Environ Microbiol 76:7302-5.
59. Frederiksen RF, Paspaliari DK, Larsen T, Storgaard BG, Larsen MH, Ingmer H, Palcic MM, Leisner JJ. 2013. Bacterial chitinases and chitin-binding proteins as virulence factors. Microbiology (Reading) 159:833-847.
60. Frederiksen RF, Yoshimura Y, Storgaard BG, Paspaliari DK, Petersen BO, Chen K, Larsen T, Duus JO, Ingmer H, Bovin NV, Westerlind U, Blixt O, Palcic MM, Leisner JJ. 2015. A diverse range of bacterial and eukaryotic chitinases hydrolyzes the LacNAc (Galbeta1-4GlcNAc) and LacdiNAc (GalNAcbeta1-4GlcNAc) motifs found on vertebrate and insect cells. J Biol Chem 290:5354-66.
61. Boune S, Hu P, Epstein AL, Khawli LA. 2020. Principles of N-Linked Glycosylation Variations of IgG-Based Therapeutics: Pharmacokinetic and Functional Considerations. Antibodies (Basel) 9.
62. Li W, Zhu Z, Chen W, Feng Y, Dimitrov DS. 2017. Crystallizable Fragment Glycoengineering for Therapeutic Antibodies Development. Front Immunol 8:1554.
63. Liu L. 2015. Antibody glycosylation and its impact on the pharmacokinetics and pharmacodynamics of monoclonal antibodies and Fc-fusion proteins. J Pharm Sci 104:1866-1884.
64. Mimura Y, Katoh T, Saldova R, O'Flaherty R, Izumi T, Mimura-Kimura Y, Utsunomiya T, Mizukami Y, Yamamoto K, Matsumoto T, Rudd PM. 2018. Glycosylation engineering of therapeutic IgG antibodies: challenges for the safety, functionality and efficacy. Protein Cell 9:47-62.
65. Allhorn M, Briceno JG, Baudino L, Lood C, Olsson ML, Izui S, Collin M. 2010. The IgG-specific endoglycosidase EndoS inhibits both cellular and complement-mediated autoimmune hemolysis. Blood 115:5080-8.
66. Naegeli A, Bratanis E, Karlsson C, Shannon O, Kalluru R, Linder A, Malmstrom J, Collin M. 2019. Streptococcus pyogenes evades adaptive immunity through specific IgG glycan hydrolysis. J Exp Med 216:1615-1629.
67. Sjogren J, Okumura CY, Collin M, Nizet V, Hollands A. 2011. Study of the IgG endoglycosidase EndoS in group A streptococcal phagocyte resistance and virulence. BMC Microbiol 11:120.
68. Panda S, Zhang J, Tan NS, Ho B, Ding JL. 2013. Natural IgG antibodies provide innate protection against ficolin-opsonized bacteria. EMBO J 32:2905-19.
69. Basta M, Fries LF, Frank MM. 1991. High doses of intravenous immunoglobulin do not affect the recognition phase of the classical complement pathway. Blood 78:700-2.
70. Kristian SA, Datta V, Weidenmaier C, Kansal R, Fedtke I, Peschel A, Gallo RL, Nizet V. 2005. D-alanylation of teichoic acids promotes group a streptococcus antimicrobial peptide resistance, neutrophil survival, and epithelial cell invasion. J Bacteriol 187:6719-25.
71. Guiton PS, Hung CS, Hancock LE, Caparon MG, Hultgren SJ. 2010. Enterococcal biofilm formation and virulence in an optimized murine model of foreign body-associated urinary tract infections. Infect Immun 78:4166-75.

72. Karav S, German JB, Rouquie C, Le Parc A, Barile D. 2017. Studying Lactoferrin N-Glycosylation. Int J Mol Sci 18.
73. Jenssen H, Hancock RE. 2009. Antimicrobial properties of lactoferrin. Biochimie 91:19-29.
74. Ammons MC, Copie V. 2013. Mini-review: Lactoferrin: a bioinspired, anti-biofilm therapeutic. Biofouling 29:443-55.
75. Alugupalli KR, Kalfas S. 1995. Inhibitory effect of lactoferrin on the adhesion of Actinobacillus actinomycetemcomitans and Prevotella intermedia to fibroblasts and epithelial cells. APMIS 103:154-60.
76. Kawasaki Y, Tazume S, Shimizu K, Matsuzawa H, Dosako S, Isoda H, Tsukiji M, Fujimura R, Muranaka Y, Isihida H. 2000. Inhibitory effects of bovine lactoferrin on the adherence of enterotoxigenic Escherichia coli to host cells. Biosci Biotechnol Biochem 64:348-54.
77. Quintero-Villegas MI, Wittke A, Hutkins R. 2014. Adherence inhibition of Cronobacter sakazakii to intestinal epithelial cells by lactoferrin. Curr Microbiol 69:574-9.
78. Leitch EC, Willcox MDP. 1999. Elucidation of the antistaphylococcal action of lactoferrin and lysozyme. J Med Microbiol 48:867-871.
79. Latorre M, Quenti D, Travisany D, Singh KV, Murray BE, Maass A, Cambiazo V. 2018. The Role of Fur in the Transcriptional and Iron Homeostatic Response of Enterococcus faecalis. Front Microbiol 9:1580.
80. Jiang YL, Yu WL, Zhang JW, Frolet C, Di Guilmi AM, Zhou CZ, Vernet T, Chen Y. 2011. Structural basis for the substrate specificity of a novel beta-N-acetylhexosaminidase StrH protein from Streptococcus pneumoniae R6. J Biol Chem 286:43004-12.
81. Ramasubbu N, Thomas LM, Ragunath C, Kaplan JB. 2005. Structural analysis of dispersin B, a biofilm-releasing glycoside hydrolase from the periodontopathogen Actinobacillus actinomycetemcomitans. J Mol Biol 349:475-86.
82. Robb M, Robb CS, Higgins MA, Hobbs JK, Paton JC, Boraston AB. 2015. A Second beta-Hexosaminidase Encoded in the Streptococcus pneumoniae Genome Provides an Expanded Biochemical Ability to Degrade Host Glycans. J Biol Chem 290:30888-900.
83. Val-Cid C, Biarnes X, Faijes M, Planas A. 2015. Structural-Functional Analysis Reveals a Specific Domain Organization in Family GH20 Hexosaminidases. PLoS One 10:e0128075.
84. Itoh Y, Wang X, Hinnebusch BJ, Preston JF, 3rd, Romeo T. 2005. Depolymerization of beta-1,6-N-acetyl-D-glucosamine disrupts the integrity of diverse bacterial biofilms. J Bacteriol 187:382-7.
85. Kaplan JB, Ragunath C, Ramasubbu N, Fine DH. 2003. Detachment of Actinobacillus actinomycetemcomitans biofilm cells by an endogenous beta-hexosaminidase activity. J Bacteriol 185:4693-8.
86. Kaplan JB, Ragunath C, Velliyagounder K, Fine DH, Ramasubbu N. 2004. Enzymatic detachment of Staphylococcus epidermidis biofilms. Antimicrob Agents Chemother 48:2633-6.
87. Stacy A, Abraham N, Jorth P, Whiteley M. 2016. Microbial Community Composition Impacts Pathogen Iron Availability during Polymicrobial Infection. PLoS Pathog 12:e1006084.
88. Kaplan JB, Velliyagounder K, Ragunath C, Rohde H, Mack D, Knobloch JK, Ramasubbu N. 2004. Genes involved in the synthesis and degradation of matrix polysaccharide in Actinobacillus actinomycetemcomitans and Actinobacillus pleuropneumoniae biofilms. J Bacteriol 186:8213-20.
89. Handke LD, Slater SR, Conlon KM, O'Donnell ST, Olson ME, Bryant KA, Rupp ME, O'Gara JP, Fey PD. 2007. SigmaB and SarA independently regulate polysaccharide intercellular adhesin production in Staphylococcus epidermidis. Can J Microbiol 53:82-91.
90. Toledo-Arana A, Valle J, Solano C, Arrizubieta MJ, Cucarella C, Lamata M, Amorena B, Leiva J, Penades JR, Lasa I. 2001. The enterococcal surface protein, Esp, is involved in Enterococcus faecalis biofilm formation. Appl Environ Microbiol 67:4538-45.
91. Vaaje-Kolstad G, Bohle LA, Gaseidnes S, Dalhus B, Bjoras M, Mathiesen G, Eijsink VG. 2012. Characterization of the chitinolytic machinery of Enterococcus faecalis V583 and high-resolution structure of its oxidative CBM33 enzyme. J Mol Biol 416:239-54.

92. Bertram R, Rigali S, Wood N, Lulko AT, Kuipers OP, Titgemeyer F. 2011. Regulon of the N-acetylglucosamine utilization regulator NagR in Bacillus subtilis. J Bacteriol 193:3525-36.
93. Kawada-Matsuo M, Oogai Y, Komatsuzawa H. 2016. Sugar Allocation to Metabolic Pathways is Tightly Regulated and Affects the Virulence of Streptococcus mutans. Genes (Basel) 8.
94. Zeng L, Burne RA. 2015. NagR Differentially Regulates the Expression of the glmS and nagAB Genes Required for Amino Sugar Metabolism by Streptococcus mutans. J Bacteriol 197:3533-44.
95. Moye ZD, Burne RA, Zeng L. 2014. Uptake and metabolism of N-acetylglucosamine and glucosamine by Streptococcus mutans. Appl Environ Microbiol 80:5053-67.
96. Iyer VS, Hancock LE. 2012. Deletion of sigma(54) (rpoN) alters the rate of autolysis and biofilm formation in Enterococcus faecalis. J Bacteriol 194:368-75.
97. Parthasarathy S, Wang X, Carr K, Varahan S, Hancock EB, Hancock LE. 2021. SigV mediates lysozyme resistance in Enterococcus faecalis via RsiV and PgdA. Journal of Bacteriology *accepted*.
98. Varahan S, Iyer VS, Moore WT, Hancock LE. 2013. Eep confers lysozyme resistance to enterococcus faecalis via the activation of the extracytoplasmic function sigma factor SigV. J Bacteriol 195:3125-34.
99. Paget MS. 2015. Bacterial Sigma Factors and Anti-Sigma Factors: Structure, Function and Distribution. Biomolecules 5:1245-65.
100. Souza BM, Castro TL, Carvalho RD, Seyffert N, Silva A, Miyoshi A, Azevedo V. 2014. sigma(ECF) factors of gram-positive bacteria: a focus on Bacillus subtilis and the CMNR group. Virulence 5:587-600.